

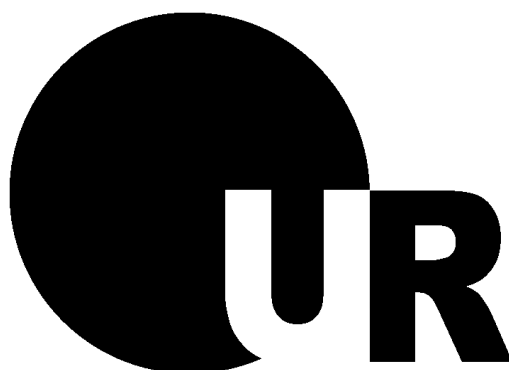
# **Scavengers, Reagents, and Catalysts Supported on Recyclable Magnetic Nanoparticles**

**Dissertation**

**Zur Erlangung des Doktorgrades**

**Dr. rer. nat.**

**an der Fakultät für Chemie und Pharmazie  
der Universität Regensburg**



vorgelegt von

**Quirin Kainz**

aus Scheyern

**Regensburg 2013**

Die Arbeit wurde angeleitet von: Prof. Dr. O. Reiser

Promotionsgesuch eingereicht am: 18. September 2013

Promotionskolloquium am: 31. Oktober 2013

Prüfungsausschuss:      Vorsitz: Prof. Dr. J. Wegener

1. Gutachter: Prof. Dr. O. Reiser

2. Gutachter: Prof. Dr. A. J. von Wangelin

3. Gutachter: Prof. Dr. M. Scheer

Der experimentelle Teil der vorliegenden Arbeit wurde in der Zeit von Oktober 2010 bis September 2013 unter der Gesamtleitung von Prof. Dr. O. Reiser am Lehrstuhl für Organische Chemie der Universität Regensburg angefertigt. Zusätzliche Betreuer waren von Oktober 2010 bis Dezember 2010 Prof. Dr. P. R. Hanson an der University of Kansas (USA) und von Oktober 2011 bis Dezember 2013 Prof. Dr. W. J. Stark an der ETH Zürich (Schweiz).

Besonders bedanken möchte ich mich bei Herrn Prof. Dr. O. Reiser für die Aufnahme in seinen Arbeitskreis, die Überlassung des äußerst interessanten Themas, die anregenden Diskussionen und die stete Unterstützung.



*Meiner Familie*

*“An expert is a person who has made all the mistakes that can be made in a very narrow field.” - Niels Bohr*



# Table of Contents

<b>A</b>	<b>Summary</b>	<b>1</b>
<b>B</b>	<b>Zusammenfassung</b>	<b>4</b>
<b>C</b>	<b>Introduction</b>	<b>7</b>
1.	Magnetic Supports: Synthesis and Surface Functionalization	8
2.	Dendrimer-coated Magnetic Nanoparticles	11
3.	Polymer-functionalized Magnetic Nanoparticles	15
4.	Conclusion and Perspectives	22
5.	References	23
<b>D</b>	<b>Main Part</b>	<b>25</b>
1.	Intramolecular Monomer-on-Monomer (MoM) Mitsunobu Cyclization for the Synthesis of Benzo-fused Thiadiazepine-dioxides	25
1.1	Introduction	26
1.2	Results and Discussion	26
1.3	Conclusion	29
1.4	Experimental Section	31
1.5	References	49
2.	Magnetic Nanobeads as Support for Zinc(II)–Cyclen Complexes: Selective and Reversible Extraction of Riboflavin	51
2.1	Introduction	52
2.2	Results and Discussion	52
2.3	Conclusion	59
2.4	Addendum	60
2.5	Experimental Section	62
2.6	References	73
3.	Ring-Opening Metathesis Polymerization-based Recyclable Magnetic Acylation Reagents	75
3.1	Introduction	76
3.2	Results and Discussion	76

3.3	Conclusion	88
3.4	Experimental Section	89
3.5	References	96
4.	Synthesis of Trisubstituted Ureas by a Multistep Sequence Utilizing Recyclable Magnetic Reagents and Scavengers	99
4.1	Introduction	100
4.2	Results and Discussion	101
4.3	Conclusion	113
4.4	Addendum	115
4.5	Experimental Section	119
4.6	References	134
5.	Palladium Nanoparticles Supported on Magnetic Carbon-Coated Cobalt Nanobeads – Highly Active and Recyclable Catalysts for Alkene Hydrogena- tion	137
5.1	Introduction	138
5.2	Results and Discussion	139
5.3	Conclusion	154
5.4	Experimental Section	156
5.5	References	162
6.	Towards Magnetic Dendrimer- and Polymer-Encapsulated Palladium Nanoparticles	165
6.1	Introduction	166
6.2	Magnetic Dendrimer-Encapsulated Nanoparticles	169
6.3	Magnetic Polymer-Encapsulated Nanoparticles	173
6.4	Conclusion and Outlook	176
6.5	Experimental Section	178
6.6	References	183
<b>E</b>	<b>List of Abbreviations</b>	<b>185</b>
<b>F</b>	<b>Curriculum Vitae</b>	<b>187</b>
<b>G</b>	<b>Acknowledgement</b>	<b>193</b>



## A Summary

The present dissertation deals with the immobilization of scavenging groups, reagents, chelating ligands, and catalysts on highly magnetic carbon-coated iron (Fe/C) or cobalt (Co/C) nanoparticles (Figure 1). To improve the dispersion stabilities of the nanoparticles and likewise the loading with functional groups, polymers were introduced by surface-initiated polymerization. The extraordinary high magnetization of the metal core allowed for rapid separation of the hybrid materials enabling convenient purification of reaction mixtures by magnetic decantation (Figure 2).

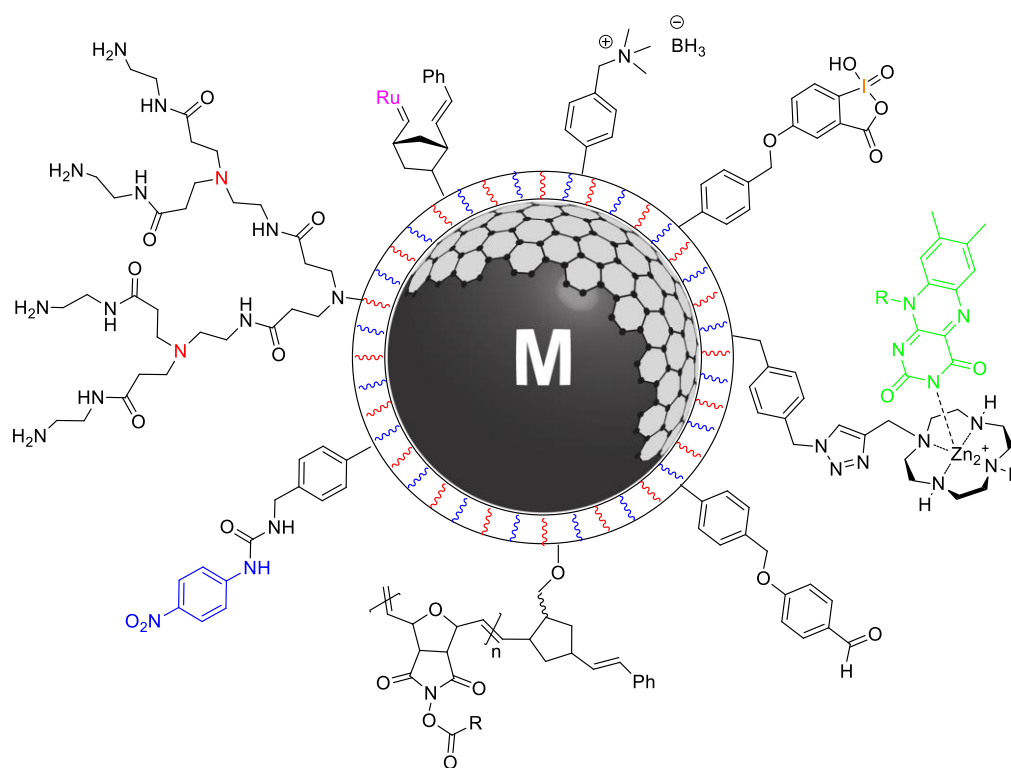


**Figure 1.** Tethering scavengers, reagents, chelators, and catalysts to the surface of (polymer-coated) Co/C and Fe/C nanoparticles.

In the introduction carbon-coated metal nanoparticles are compared to conventional iron oxide nanoparticles and the synthesis, stabilization, and surface functionalization of both is described. Furthermore, it is discussed, how the stabilities and loadings can be increased by the grafting of dendrimers or the synthesis of dendrimers on the surface. The second part of the introduction is focused on several different methods for coating nanoparticles with polymers, which have different pros and cons when compared to dendrimers.

The first chapter of the main part deals with the purification of intramolecular Mitsunobu cyclization reactions utilizing reagents tagged with norbornene moieties. After completion of the reaction, the excess and spent reagents were sequestered by the addition of either free metathesis catalyst, or by Co/C nanoparticles or silica pre-activated with metathesis catalyst. Benzofused thiadiazepine-dioxides were obtained in excellent yields and purities after filtration or magnetic decantation, respectively.

In chapter 2 polystyrene-coated Fe/C beads are highlighted as supports for zinc(II)–cyclen complexes. These nanocarriers were successfully applied for the quantitative extraction of riboflavin (vitamin B<sub>2</sub>) from aqueous solutions and a vitamin tablet. The polymer significantly enhanced the capacity and efficiently blocked the carbon-surface preventing unspecific adsorption. The extracted riboflavin was released upon washing with aqueous HCl enabling recycling of the nanomaterial.

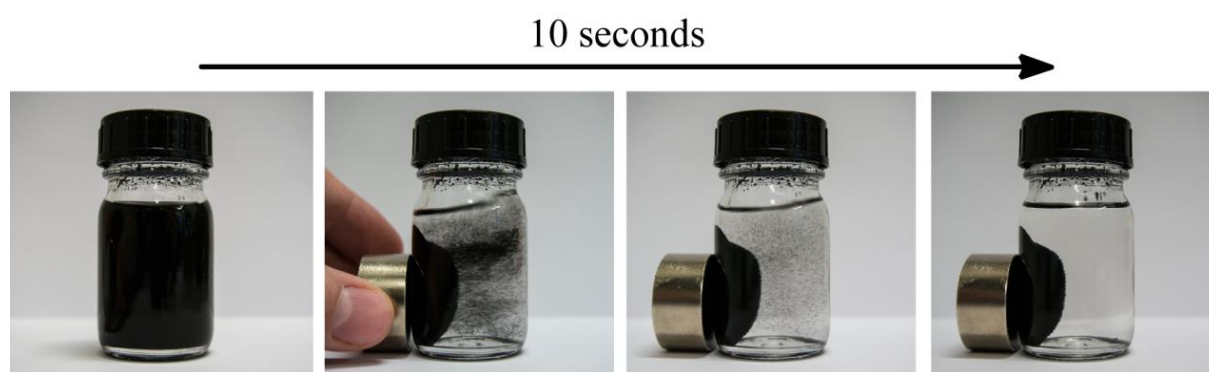


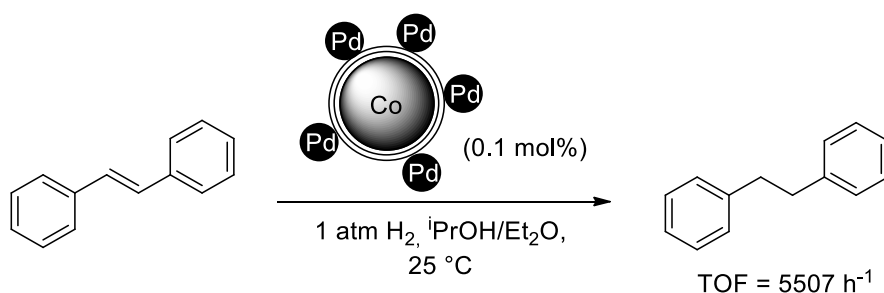
**Figure 2.** Rapid magnetic recovery of polymer-coated nanobeads from a CH<sub>2</sub>Cl<sub>2</sub> solution.

The third chapter is devoted to an operationally simple concept for the acylation of primary and secondary amines. Norbornene-tags were covalently introduced to Co/C and Fe/C nanomagnets and subsequently activated with metathesis catalyst. The activated particles were then examined as scaffolds for the preparation of acylated *N*-hydroxysuccinimide ROMPgels (ROMP=ring-opening metathesis polymerization). The novel high loading hybrid materials fostered the synthesis of amides in high yields and purities and allowed for subsequent re-acylation by acid chlorides, anhydrides, and carboxylic acids.

The synthesis of an entire library of ureas and thioureas exclusively applying magnetic scavengers and reagents is presented in chapter 4 demonstrating the broad applicability of these novel nano-tools. For this project polystyrene-coated nanoparticles were functionalized in a microwave oven exploiting the susceptibility of

the metal core for microwave adsorption. Magnetic borohydride exchange, magnetic Wang aldehyde, and magnetic amine resins with high loadings (up to 3.0 mmol/g) were prepared by this technique in short reaction times. After the concerted application of these synergistic reagents and scavengers the pure (thio)ureas were isolated using magnetic decantation as the sole purification step. Also, a hypervalent iodine complex (IBX) was probed as recyclable resin for the oxidation of alcohols.

In chapter 5 the first controlled synthesis of transition-metal nanoparticles on the surface of Co/C nanobeads is described in detail. In contrast to the established synthesis of Pd nanoparticles via reduction of Pd(II) precursors, the microwave decomposition of a Pd(0) source led to a material with an extraordinary high activity in the hydrogenation of alkenes (Scheme 1). Interestingly, the catalytic activity was further improved upon addition of 10 vol% diethyl ether and by lowering the Pd loading. The obtained turn over frequencies (TOFs) exceeded all reported Pd nanocatalysts as well as commercial Pd/C by far without the need for elaborate filtration or centrifugation. Although the catalytic activity was found to decrease slightly from run to run, leaching of Pd stayed below the limits for heavy metal contamination set by the industry. Additional stabilization was provided by the introduction of functional groups to the surface.



**Scheme 1.** Hydrogenation of *trans*-stilbene using Pd@Co/C nanocatalyst.

Finally, chapter 6 extends the concept introduced in chapter 5. Here, strategies for the introduction of poly(amidoamine) (PAMAM) dendrimers and polyethylene imine (PEI) polymers to the surface of the magnetic nanoparticles are discussed. These coatings considerably promote the dispersion stability of the magnetic nanoparticles in polar solvents and are known to be ideal templates for the deposition of transition-metal nanoparticles.

## B Zusammenfassung

Die vorliegende Dissertation beschäftigt sich mit der Immobilisierung von “Abfang-Gruppen”, Reagenzien, chelatisierenden Liganden und Katalysatoren auf hoch magnetischen, Kohlenstoff-beschichteten Eisen (Fe/C) und Cobalt (Co/C) Nanopartikeln (Abbildung 1). Um die Dispersionsstabilität der Nanopartikel sowie die Beladung mit funktionellen Gruppen zu verbessern, wurden Polymere auf die Oberfläche aufgebracht. Die außergewöhnlich hohe Magnetisierung des Metallkerns ermöglichte eine rasche Abtrennung der Hybridmaterialien und dadurch eine bequeme Aufreinigung von Reaktionsgemischen durch magnetisches Dekantieren (Abbildung 2).

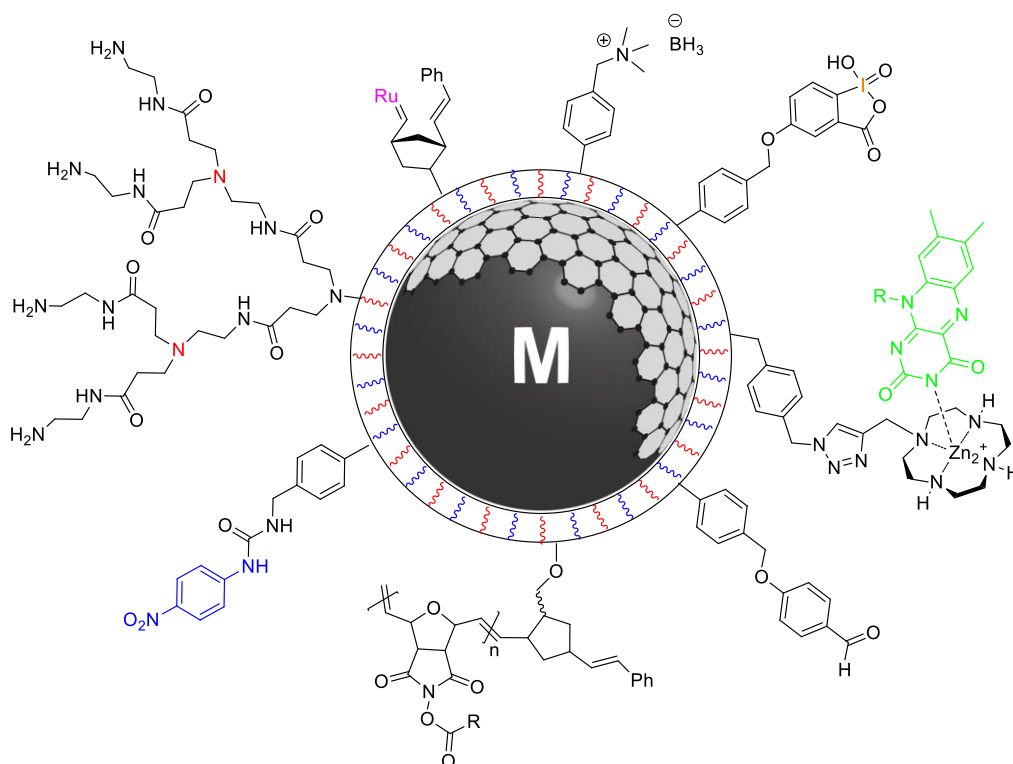


**Abbildung 1.** Reagenzien, chelatisierende Liganden und Katalysatoren auf der Oberfläche von (Polymer-beschichteten) Co/C und Fe/C Nanopartikeln.

In der Einleitung werden Co/C Partikel mit konventionellen Eisenoxid Partikeln verglichen und die Synthese, Stabilisierung, sowie Oberflächenfunktionalisierung von beiden beschrieben. Außerdem wird diskutiert, wie die Stabilitäten und Beladungen durch das Anbringen von Dendrimeren auf der Oberfläche gesteigert werden können. Der darauffolgende Abschnitt bespricht verschiedene Techniken zur Beschichtung

von Nanopartikeln mit Polymeren und deren Vor- und Nachteile gegenüber Dendrimern.

Das erste Kapitel des Hauptteils beschäftigt sich mit der Aufreinigung von intramolekularen Mitsunobu-Reaktionen unter Verwendung von Norbornen-markierten Reagenzien. Nach Beendigung der Reaktion wurde der Überschuss an Reagenzien durch Zugabe von Metathese-Katalysator, oder von Co/C Nanopartikeln bzw. Kieselgel aktiviert mit Katalysator, abgetrennt. Nach Filtration oder magnetischem Dekantieren blieben Thiadiazepin-Dioxide in exzellenten Ausbeuten und Reinheitsgraden zurück.

In Kapitel 2 werden mit Polystyrol beschichtete Fe/C Partikel als Trägermaterialien für Zink(II)-Cyclen Komplexe beschrieben. Diese Nanotransporter wurden erfolgreich für die quantitative Extraktion von Riboflavin (Vitamin B2) aus wässrigen Lösungen sowie aus einer Vitamintablette eingesetzt. Dabei wurde die Kapazität durch das Polymer signifikant erhöht sowie die Oberfläche erfolgreich vor unspezifischer Adsorption abgeschirmt. Das extrahierte Riboflavin wurde anschließend durch eine HCl-Lösung ausgewaschen, was ein Recycling des Nanomaterials ermöglichte.

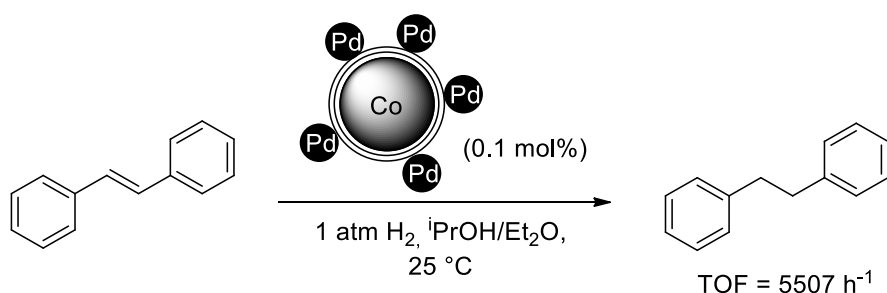


**Abbildung 2.** Magnetische Abtrennung von Polymer-beschichteten Nanopartikeln aus  $\text{CH}_2\text{Cl}_2$ .

Das dritte Kapitel ist einem Konzept für die operativ einfache Acylierung von primären und sekundären Aminen gewidmet. Norbornen-Gruppen wurden kovalent an Co/C und Fe/C Nanopartikel gebunden und daraufhin mit Metathese-Katalysator aktiviert. Die aktivierten Partikel wurden anschließend für die Herstellung von acylierten *N*-Hydroxysuccinimid ROMP-Gelen (ROMP = ring-opening metathesis polymerization) verwendet. Diese neuartigen und hoch beladenen Hybridmaterialien ermöglichten anschließend die Synthese von Amiden in hohen Ausbeuten und wurden mit Säurechloriden, Anhydriden und Carbonsäuren erfolgreich regeneriert.

In Kapitel 4 wird die breite Anwendbarkeit dieser neuen Nano-Werkzeuge anhand der Synthese einer Bibliothek von Harnstoffen unter ausschließlicher Verwendung magnetischer Reagenzien demonstriert. Dafür wurden magnetische Borhydrid, Wang-Aldehyd und Amin Partikel mit hohen Beladungen (bis zu 3.0 mmol/g) in sehr kurzen Zeiten durch Verwendung einer Mikrowelle hergestellt. (Thio)-Harnstoffe wurden durch eine sukzessive Anwendung dieser Reagenzien hergestellt mit magnetischer Separation als einzigen Aufreinigungsschritt. Zusätzlich wurde ein wiederverwendbarer hyper-valenter Iod Komplex (IBX) in der Oxidation von Alkoholen erprobt.

In Kapitel 5 wird die erstmalige kontrollierte Synthese von Übergangsmetallkomplexen auf der Oberfläche der Co/C Partikeln beschrieben. Im Gegensatz zur üblichen Synthese durch Reduktion von Pd(II)-Verbindungen ergab die Zersetzung einer Pd(0)-Quelle in der Mikrowelle ein sehr aktives Material. Interessanterweise konnte die Aktivität in der Hydrierung von Alkenen durch Zusatz von 10 vol% Diethylether und durch Absenkung der Beladung mit Pd noch weiter erhöht werden. Die gemessenen turn over frequencies (TOFs) übertrafen alle bisherigen Palladium Nanokatalysatoren und kommerzielles Pd/C bei weitem. Die katalytische Aktivität sank leicht von Lauf zu Lauf, jedoch blieb die Kontamination der Produkte mit Pd jederzeit unter den kritischen Grenzwerten der Industrie. Zusätzliche Stabilisierung konnte durch das Einführen von funktionellen Gruppen auf der Oberfläche erzielt werden.



**Schema 1.** Hydrierung von *trans*-Stilben durch Pd@Co/C Nanopartikel.

Darauf aufbauend wurden in Kapitel 6 abschließend Strategien für die Einführung von Poly(amidoamin) (PAMAM) Dendrimeren und Polyethylenimin (PEI) Polymeren auf die Oberfläche von magnetischen Nanopartikeln diskutiert. Diese Beschichtungen erhöhen die Dispersionsstabilität der Nanopartikel in polaren Lösungsmitteln deutlich und sind bekannt als ideale Template für die Abscheidung von Übergangsmetallnanopartikeln.

## C Introduction

In modern organic chemistry with countless reagents and catalysts developed for synthesis the purification of products often turns out to be the most problematic and tedious step within the whole process. Especially transition-metal catalysts are generally expensive and, more problematic, highly toxic. Therefore, sophisticated purification methods have often to be applied to remove these catalysts - particularly in the pharmaceutical industry, where only low limits of heavy metal concentrations are allowed in the final drug molecules.<sup>[1]</sup> Common purification techniques include column chromatography, liquid-liquid extraction, and filtration. However, all of them have some drawbacks, for example high amounts of solvents needed in order to pump the reaction mixture through packed columns or filters, the energy requirements to remove the solvents from the product, and the auxiliary materials, which often cannot be recycled.

Moreover, the purification process of reaction mixtures has to be reconsidered and evaluated by the principles of green and sustainable chemistry established by Anastas and Warner in 1991.<sup>[2]</sup> The key concept is to prevent the formation of chemical waste rather than cleaning up accumulated waste. Since catalysts and reagents are inevitable for most chemical transformations, one strategy for their recovery and subsequent recycling is the heterogenization by grafting them to insoluble supports, e.g. silica, alumina, ceria, or carbon.<sup>[3]</sup> However, depending on the nature of the support, the active sites might be buried inside pores or cavities limiting the accessibility for substrates, which results in a reduced activity. In addition, rapid filtration from the support can be energy and resource intensive and also difficult from a practical point of view since filters tend to clog.

Within the last few years magnetic nanoparticles emerged as a new class of semi-heterogeneous supports for catalysts.<sup>[4–6]</sup> The excellent surface-to-volume ratio enables a high loading of catalyst accompanied by a high catalytic activity, which is usually the prerogative of homogeneous systems. Moreover, the intrinsic magnetic properties of the support allow for operationally convenient separation (e.g. via magnetic decantation) dispensing from the need of centrifugation or flocculation generally required for the recovery of non-magnetic nanomaterials.

In this account we describe the key features of magnetic supports and compare magnetic nanobeads comprising of different compositions highlighting carbon

coated metal particles. Furthermore, the surface functionalization of these nanomaterials is discussed aiming at high functional group loading and dispersibility in solvents, which is essential for the attachment of ligands, catalysts, scavengers, and reagents and their subsequent application.

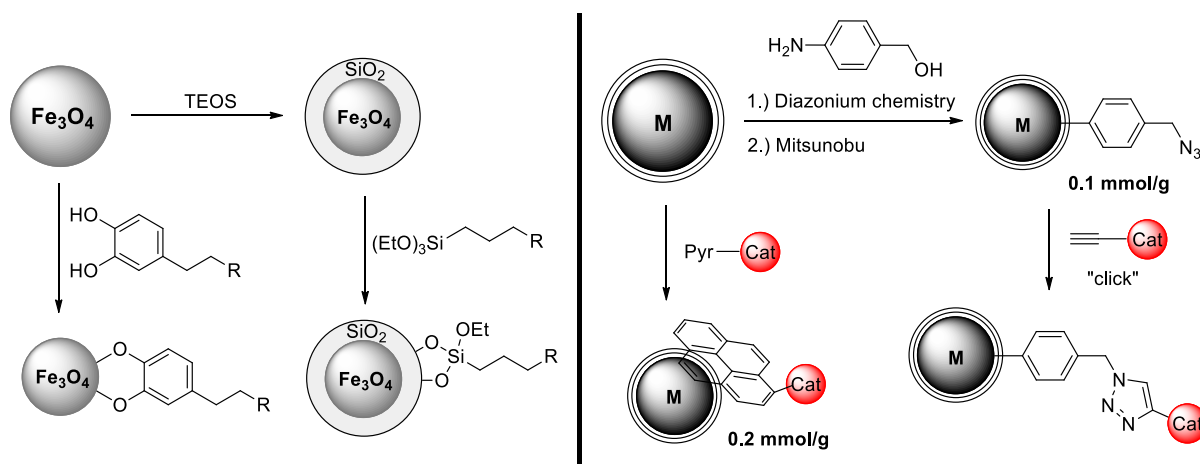
## 1. Magnetic Supports: Synthesis and Surface Functionalization

Nowadays a plethora of magnetic nanoparticles derived from metals (Fe, Co, Ni), alloys (FePt, CoPt), metal oxides (FeO, Fe<sub>2</sub>O<sub>3</sub>, Fe<sub>3</sub>O<sub>4</sub>), or ferrites (CoFe<sub>2</sub>O<sub>4</sub>, MnFe<sub>2</sub>O<sub>4</sub>) with a manifold of characteristics and applications are known. A comprehensive discussion of the synthesis and functionalization of these magnetic nanoparticles is beyond the scope of this account.<sup>[5,7]</sup> Instead, we highlight magnetic nanoparticles that are especially suitable as supports for catalysts, scavengers, or reagents. Consequently, what are the key features of an ideal magnetic support in such applications? Desirable properties should include: (i) inexpensive and easily accessible starting materials, (ii) a reproducible and sustainable large-scale synthesis, (iii) a nano-sized core with high magnetization and low toxicity, (iv) protection of the core by an impenetrable inert shell for reactions under forcing conditions ( $\Delta T$ , H<sup>+</sup>, OH<sup>-</sup>), and (v) an efficient method to introduce functional groups to the surface.

Magnetic nanoparticles derived from iron oxide, e.g. magnetite (Fe<sub>3</sub>O<sub>4</sub>) and maghemite ( $\gamma$ -Fe<sub>2</sub>O<sub>3</sub>), fulfill most of these requirements after some modifications, and recent advances in their synthesis give access to size-controlled, monodisperse particles.<sup>[8],[9]</sup> Superparamagnetic iron oxide nanoparticles (SPIONs) show a negligible remanent magnetization and therefore reduced agglomeration.<sup>[7]</sup> This, and their toxicologically uncritical constituents, renders SPIONs ideal for a broad range of biomedical applications like magnetic drug targeting, magnetic fluid hyperthermia, and magnetic resonance imaging.<sup>[10]</sup> For the same reasons SPIONs are also attractive as recyclable supports for catalysts. A protective coating of the surface has to be introduced in order to guarantee the stability of SPIONs under demanding reaction conditions. Usually, during their synthesis long-chain alkyl surfactants, e.g. oleic acid or oleylamine, are added to prevent agglomeration of the magnetic beads by steric shielding.<sup>[9]</sup> Recently, also phosphonic acid<sup>[11]</sup> and dopamine<sup>[12]</sup> (Scheme 1) derivatives were attached to the surface of iron oxide beads to provide functional groups for the immobilization of catalysts. A silica shell protects the magnetic core even more efficiently and eliminates unwanted interactions between the core and attached



agents. The deposition of silica shells with a thickness between 2 and 100 nm can be achieved via the Stöber method by hydrolyzing a sol-gel precursor such as tetraethoxysilane (TEOS).<sup>[13]</sup> No additional primer is required due to the strong affinity of iron oxide surfaces to silica and the silanol groups on the surface allow simple surface functionalization with various silanes (Scheme 1).



**Scheme 1.** Common functionalization strategies for magnetite (left) or carbon-coated metal nanoparticles (right). M = Co, Fe.

Nanoparticles derived from pure metals or metal alloys exceed the saturation magnetization of iron oxides, e.g. magnetite ( $M_{\text{S,bulk}} \leq 92 \text{ emu/g}$ ), by far (Co:  $M_{\text{S,bulk}} \leq 163 \text{ emu/g}$ ; Fe:  $M_{\text{S,bulk}} \leq 222 \text{ emu/g}$ ). However, unprotected metal nanoparticles are highly sensitive to air, which renders them potentially pyrophoric. Hence, a strong protective shell has to be introduced to exploit metal nanoparticles as supports. The deposition of a silica shell is more difficult due to the lack of OH groups on the metal nanoparticle surface requiring the addition of a primer. Moreover, silica shells do not completely block the diffusion of oxygen.<sup>[4]</sup> Carbon shells offer an alternative due to their superior chemical and thermal stabilities over all aforementioned organic and inorganic coatings.<sup>[7],[14]</sup> However, the controlled synthesis of carbon-coated metal nanoparticles is, however, challenging and was initially limited to small scale operations ( $< 1 \text{ g h}^{-1}$ ) using arc discharge techniques<sup>[15]</sup> or chemical vapor deposition (CVD).<sup>[16]</sup> In 2007, Stark *et al.*<sup>[17]</sup> reported a large scale ( $> 30 \text{ g h}^{-1}$ ) synthesis of carbon-coated ferromagnetic cobalt nanoparticles (Co/C) via reducing flame-spray pyrolysis, a process related to from flame-aerosol synthesis which is used in industry on ton-scale for the production of carbon, silica, and titania nanomaterials.<sup>[18]</sup> The deposition of

roughly three carbon layers with a thickness of about 1 nm leads to a remarkable stability under acidic and basic conditions as well as at elevated temperatures (up to 190 °C). However, with a mean particle size of 25 nm Co/C beads are considerably larger than carbon coated metal nanoparticles synthesized via CVD.<sup>[16]</sup> The very high magnetization of 158 emu/g, which is equivalent to that of bulk cobalt, allows for rapid magnetic separation. The synthesis via flame spray pyrolysis was later extended to the production of iron and iron carbide nanoparticles with similar properties.<sup>[19]</sup>

In order to implement a plentitude of functional groups on the surface of the carbon-coated metal nanoparticles covalent functionalization via diazonium chemistry proved to be a very effective method.<sup>[17]</sup> We extended this strategy by introducing azide groups, allowing the efficient covalent immobilization of complex acetylene-tagged molecules via Cu(I)-catalyzed “click”-reaction (Scheme 1), for example of TEMPO (2,2,6,6-tetramethylpiperidin-1-yl)oxidanyl resulting in a robust catalyst for the oxidation of alcohols.<sup>[20]</sup> More recently, a Cu(II)-azabis(oxazoline) complex was immobilized by a similar procedure and subsequently applied to the kinetic resolution of racemic 1,2-diphenylethane-1,2-diol via asymmetric monobenzylation.<sup>[21]</sup> The high magnetization of the carbon coated nanoparticles made agitation and containment in a reactor by adverse rotating magnets possible, opening the way to a continuous flow setup (Figure 1). Complementary non-covalent functionalization was achieved via  $\pi$ - $\pi$  stacking interactions.<sup>[22]</sup> For example, a pyrene-tagged palladium *N*-heterocyclic carbene (NHC) complex was used as a “boomerang-catalyst”: at 100 °C the catalyst was desorbed in large part into the aqueous phase to perform the hydroxycarbonylation of aryl halides, while upon cooling to room temperature, it was re-adsorbed onto the carbon surface enabling convenient separation and recycling. While in all these examples the catalysts were recovered completely within seconds by magnetic decantation and recycled for several runs, the effective loading with functional molecules was limited to a moderate level of 0.1 - 0.2 mmol/g. This is sufficient for the immobilization of highly active catalysts but not for the development of magnetic reagents that have to be employed in stoichiometric amounts.

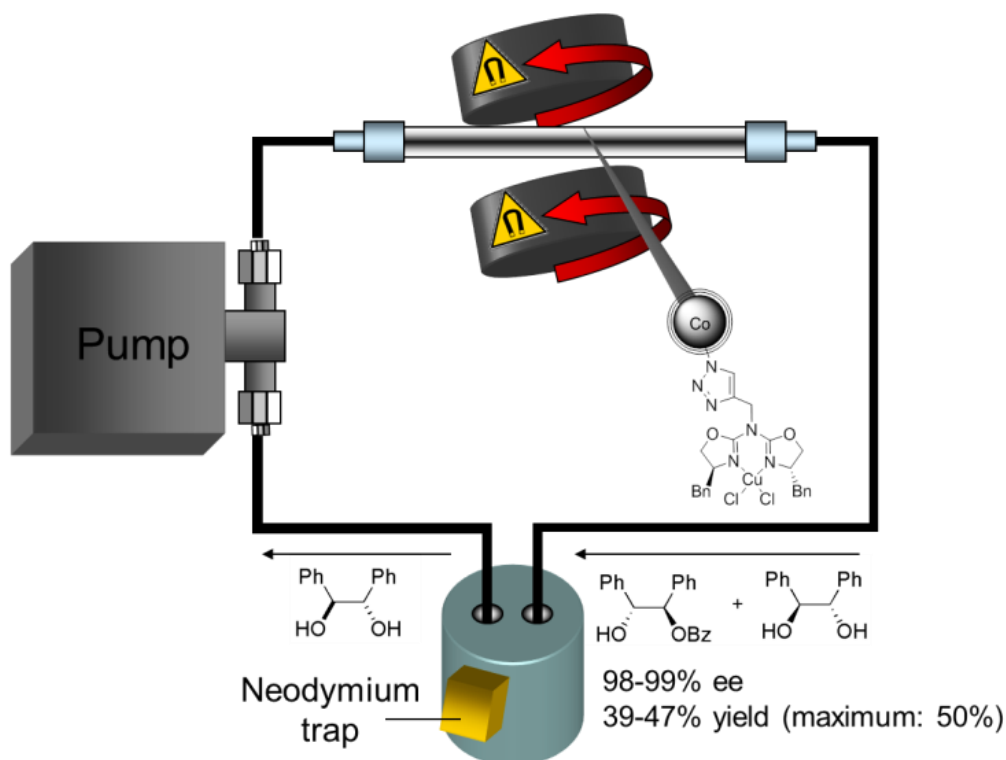
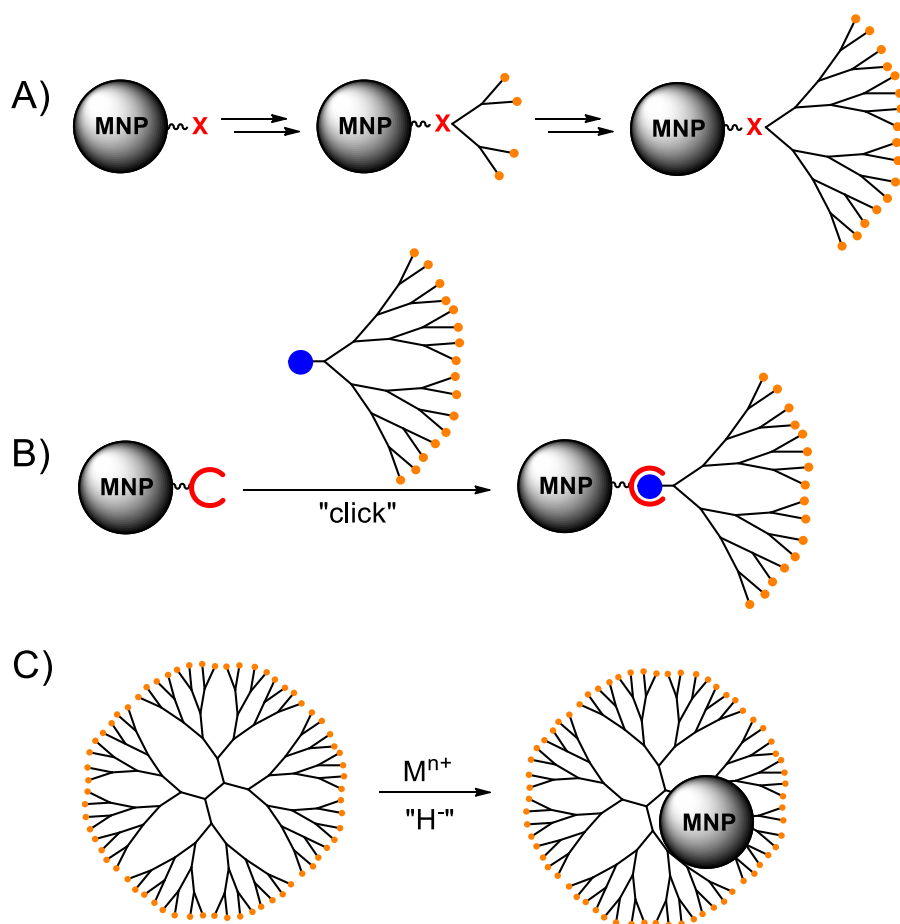


**Figure 1.** Cu(II)-azabis(oxazoline) complexes immobilized on magnetic Co/C nanoparticles for continuous-flow kinetic resolutions. Figure adapted with permission from ref [21]. Copyright 2006, American Chemical Society.

## 2. Dendrimer-coated Magnetic Nanoparticles

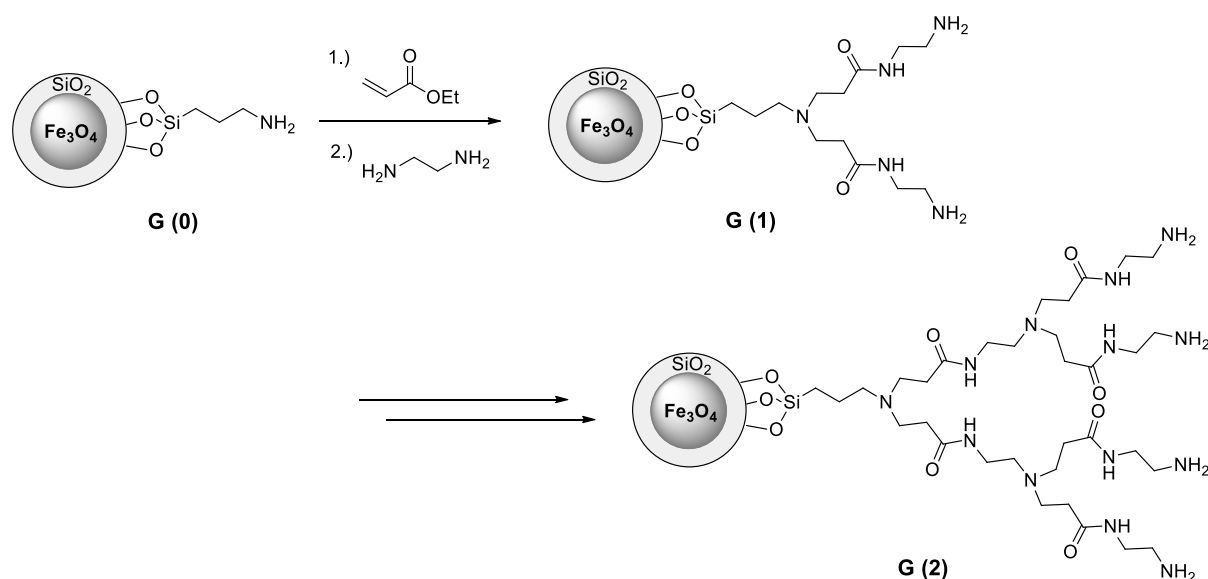
By introducing a shell of dendrimers or polymers to the surface of the nanoparticles, however, the loading with functional groups can be considerably increased. Initiated by the pioneering work of Tomalia<sup>[23]</sup> and Newkome<sup>[24]</sup> dendrimers have gained considerable attention as well-defined highly branched structures. One of the intriguing properties of the starburst dendritic architecture is the high number of functional end groups contrasting linear polymers. There are basically three strategies for the functionalization of solid supports with dendrimers: The divergent synthesis of dendrimers on the surface of the support after the introduction of a linker, the grafting of pre-synthesized dendrimers of various generations, and the synthesis of nanoparticles within the boundaries of preformed dendrimers (Scheme 2). While the solution phase synthesis of dendrimers and subsequent grafting might offer a better control of the synthesis allowing routine analytics, the synthesis on the magnetic support can lead to a denser decoration with functional groups and enables a more convenient separation after each coupling step.



**Scheme 2.** Synthesis of dendrimer-coated magnetic nanoparticles via step-wise divergent synthesis (A), grafting of complete dendrons (B), or synthesis of magnetic nanoparticles (MNP) inside globular dendrimers (C).

In the last decade dendrimers were introduced onto magnetic nanobeads to improve the dispersion of the latter in organic solvents due to increased steric repulsion and to multiply functional groups on the surface. Alper and coworkers grew poly(amidoamine) (PAMAM) dendrimers on the surface of silica coated magnetite nanoparticles.<sup>[25]</sup> In order to introduce an amino group as initiator to the surface, the magnetic core-shell particles with an approximate size of 60 nm were functionalized with (3-aminopropyl)triethoxysilane (APTMS). PAMAM dendrons up to generation three were synthesized on the particles by Michael-type addition of methyl acrylate followed by subsequent amide formation with ethylenediamine (Scheme 3). However, long reaction times of up to 5 days and reduced yields for the functionalization might limit the applicability of this method. Nevertheless, supported Rh complexes were formed by phosphonation and the addition of  $[Rh(cod)Cl]_2$ . The resulting magnetic

catalyst was applied in the hydroformylation of styrene derivatives giving rise to excellent selectivities and reactivities for five runs.



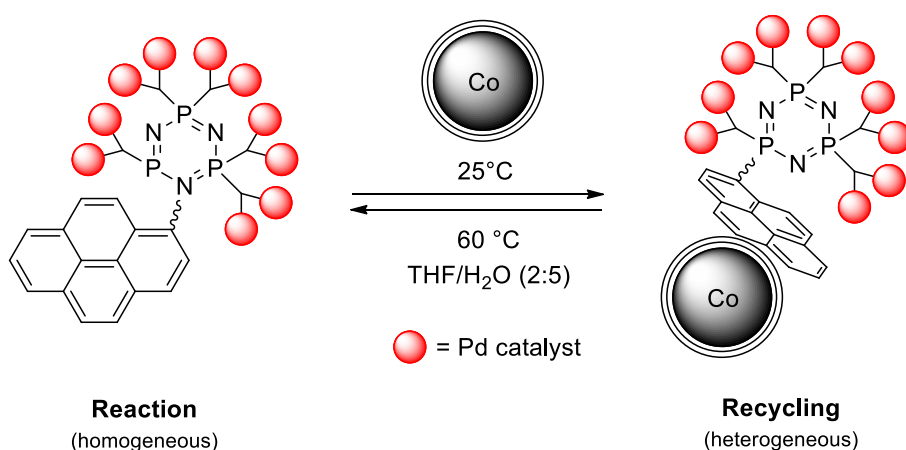
**Scheme 3.** Growing PAMAM dendrimers on the surface of silica-coated magnetite beads. Scheme adapted from ref [25].

Magnetite nanoparticles were directly functionalized with APTMS by Toprak et al.<sup>[26]</sup> for the surface-initiated PAMAM synthesis, omitting the extended silica shell. VSM measurements of particles bearing G5 PAMAM dendrimers showed a saturation magnetization of 55 emu/g. Invertase was subsequently attached via glutaraldehyde linkers leading to a 2.5 times higher loading when compared to analog particles lacking the dendrimer shell. Also, the storage stability of the enzyme was improved upon immobilization. PAMAM coated magnetite particles proved their high adsorption capacities of heavy metals in the reversible extraction of Zn(II) from aqueous solutions.<sup>[27]</sup> pH induced desorption was triggered by washing with diluted HCl allowing for ten consecutive cycles at full efficiency.

Entire fourth generation PAMAM dendrimers were grafted on the surface of magnetite beads pre-activated with cyano moieties. Again, glutaraldehyde linkers were used to immobilize an antibody and the hybrid material was applied as a magnetic-controlled potentiometric immunosensor.<sup>[28]</sup> In another study, PAMAM dendrons of various generations comprising a thiol group at the focal point were grafted on maleimide-functionalized magnetite beads.<sup>[29]</sup> However, a reduced degree of immobilization was observed for G3-G6 dendrons when compared to analogous materials syn-

thesized by the divergent approach. The magnetic hybrid material was applied for the recovery of  $\lambda$ DNA with modest success. A significant improvement (96% of DNA recovered) was achieved by integrating phospholipid bilayers between the magnetic beads and the dendrimers, hence increasing the flexibility of the support.

The grafting approach was also exploited by our group to functionalize Co/C nanobeads with polyester dendrons.<sup>[30]</sup> First, azide moieties were introduced covalently followed by “click”-reaction with dendrons bearing alkyne groups at the focal point and either hydroxy or ammonium groups at the periphery. The loading with functional groups was increased by a factor of three to 0.32 mmol/g and the stability of particle dispersions in water improved considerably. Next to the covalently grafted dendrons, an orthogonal and reversible non-covalent functionalization with pyrene-tagged boradiazaindacene (BODIPY) fluorescent dye was achieved through  $\pi$ - $\pi$  stacking on the carbon surface. Fluorescence quenching, a problem typical for fluorescent dyes on  $sp^2$ -hybridized carbon materials, e.g. CNTs, was not observed. Majoral and coworkers subsequently exploited the  $\pi$ - $\pi$  interactions for a thermally-triggered catch and release system of catalyst-loaded dendrimers (Scheme 4).<sup>[31]</sup> Phosphorous dendrimers with a pyrene-tagged phosphazene core and phosphine end groups were added to Pd-catalyzed Suzuki-Miyaura cross-coupling reactions of aryl halides with phenylboronic acids. Efficient recovery of the catalyst system was achieved by cooling to room temperature inducing the non-covalent attachment of the pyrene-tagged complexes to the surface of the Co/C beads and subsequent magnetic decantation. Upon heating at the reaction temperature (60 °C) the catalyst was desorbed again and the system was reused for up to twelve iterative runs without significant loss of activity.



**Scheme 4.** A thermally-triggered catalyst catch and release system.<sup>[31]</sup>

A completely different approach is based on the synthesis of metal nanoparticles within the core area of globular dendrimers. The variation of the dendrimer generation allows size-tuning of incorporated metal nanoparticles and therefore their properties. Crooks reported the synthesis of dendrimer-encapsulated Ni nanoparticles containing < 150 Ni atoms.<sup>[32]</sup> The Ni nanoparticles entrapped in G6 PAMAM dendrimers functionalized with alkyl groups on their periphery were found to have diameters of 1.5 nm and a rather low magnetic saturation of <4 emu/g. However, despite the stabilization within the dendrimers, the Ni nanoparticles are prone to oxidation when exposed to air, so far restricting their application in catalysis.

### **3. Polymer-functionalized Magnetic Nanoparticles**

While dendrimers can efficiently multiply functional groups on the surface of magnetic nanoparticles, polymers offer some additional advantages: They usually require less synthetic effort and high molecular weight analogues are easily accessible, which expedites dispersion stabilities of the particles due to increased steric repulsion. Also, the polarity and solubility of polymers can be easily tuned by varying monomers and method of polymerization. However, polymer-coatings deal with an inherent limitation: Within dense polymers diffusion, and as a consequence thereof access to active sites, can be hampered. This is not the case for dendrimers, which usually exhibit all active sites on the surface. The synthesis of magnetic colloids in polymer matrices as surfactants as well as the self-assembly of polymer layers onto magnetic nanoparticles are known for decades and have been extensively reviewed.<sup>[33],[34]</sup> In this account, however, we focus on advanced methods generating stable polymer - nanoparticle interactions which can withstand conditions applied for typical organic reactions (e.g. elevated temperatures).

One straightforward method to covalently link polyacrylic acid to the surface of as-prepared magnetite nanoparticles was reported by Chen.<sup>[35]</sup> Carbodiimide activation of acid groups within the polymer was used to form ester linkages with free hydroxyl groups present on the surface of the iron oxide beads. The hybrid beads showed a high ion exchange capacity and were used for the extraction of lysozyme, which was quantitatively released by washing with a NaSCN solution. Another recent publication demonstrated the successful grafting of polyethylene imine (PEI) on citrate-capped magnetite beads via amide bonds.<sup>[36]</sup> The formation of stable amide linkages was proven by infrared spectroscopy and Pd nanoparticles were synthe-

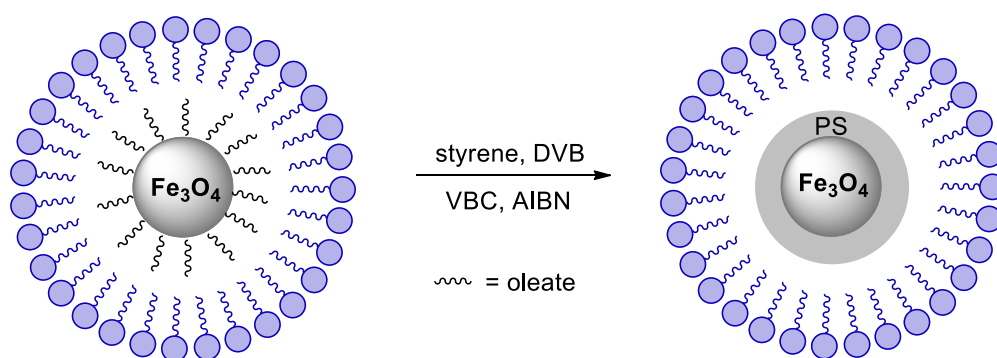
sized inside the PEI shell by impregnation with a Pd(II)-precursor and subsequent reduction to Pd(0). The amine groups within the PEI effectively stabilized the Pd nanoparticles for more than ten consecutive runs of ligand-free Suzuki-Miyaura couplings.

Emulsion polymerization was examined by Gao and coworkers as an alternative route to core/shell polymer-coated iron oxide nanoparticles.<sup>[37]</sup> As-prepared  $\gamma$ -Fe<sub>2</sub>O<sub>3</sub> nanocrystals coated with a layer of oleate were trapped in micelles by vigorously stirring with an amphiphilic surfactant in an aqueous medium (Scheme 5). 4-Vinylbenzene chloride (VBC), and 1,4-divinylbenzene (DVB) were embedded into the hydrophobic micellar cores and polymerized upon addition of a radical initiator forming very thin (~ 2 nm) polymer shells around the magnetic nanoparticles. *N*-heterocyclic carbenes were subsequently introduced by nucleophilic substitution followed by the formation of Pd-complexes. The supported Pd-NHC catalyst was subsequently applied in Suzuki-Miyaura reactions using very low catalyst loadings (0.015 mol%). However, additional stabilizing layers, e.g. silica shells, as well as extended polymers gradually diminish the magnetization levels of the hybrid materials. For example, Fe<sub>3</sub>O<sub>4</sub>/Si particles coated with polypyrrole exhibited a saturation magnetization of less than 11 emu/g requiring strong magnets for acceptable recovery times.<sup>[38]</sup> Therefore, the highest potential for the polymer-encapsulated SPIONs might be found in biomedical applications due to reduced agglomeration,<sup>[10]</sup> while magnetic resins featuring stronger magnetic metal cores have more potential as recyclable tools for organic chemistry.

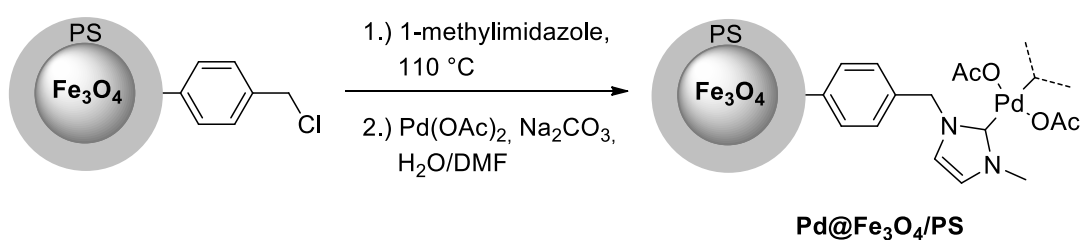
Arguably the easiest way to introduce a polymer shell to the surface of carbon-coated metal nanoparticles is the non-covalent grafting by stirring with an appropriate polymer solution. Stark and coworkers adsorbed PEI onto Fe/C nanomagnets and demonstrated the stability of this coating by several washing steps with acetate buffer (pH 3.5).<sup>[39]</sup> This can be explained by the high energy needed to simultaneously disrupt all binding interactions between the first layer of the high molecular weight polymer and the carbon surface. The amino groups within the immobilized PEI were used as linkers to tether an ethylenediaminetetraacetic acid (EDTA)-like ligand to the polymer-coated supports (Scheme 6). The magnetic EDTA analogue was subsequently applied for the rapid removal of heavy metals from contaminated water<sup>[39]</sup> and blood<sup>[40]</sup> efficiently recycling the metal chelators after each extraction. This method was later transferred to the pilot scale level, allowing continuous magnetic extractions



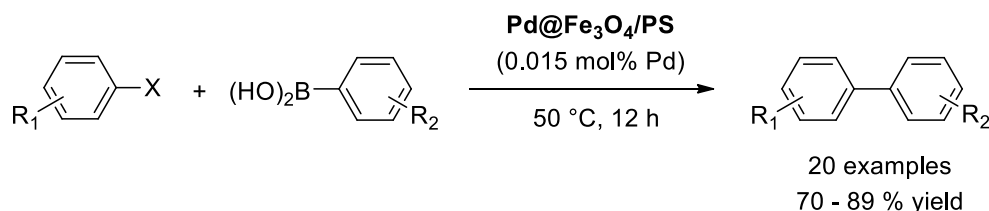
### Polymer-coating



### Functionalization



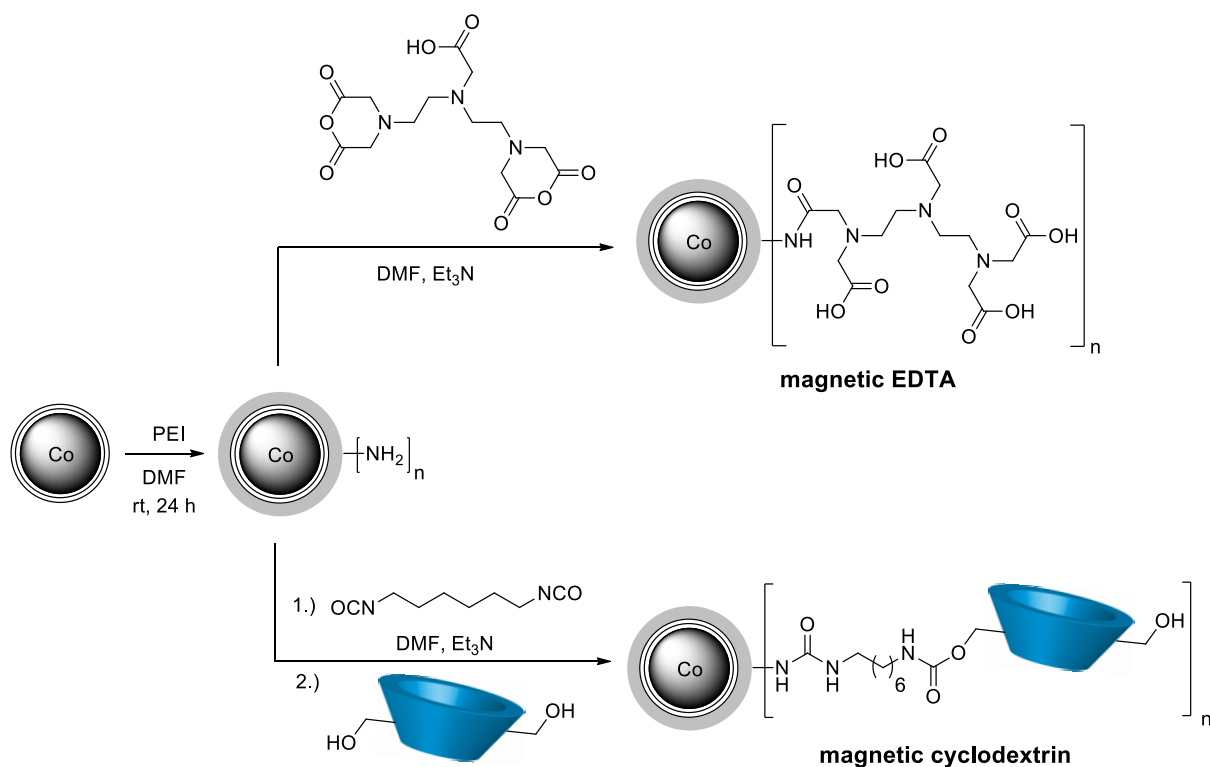
### Catalysis



**Scheme 5.** Synthesis of polymer-coated iron oxide nanoparticles via emulsion polymerization, subsequent functionalization with Pd-NHC complexes, and the application in Suzuki couplings. AIBN = azobisisobutyronitrile. Scheme adapted from ref [37].

and subsequent filtration at  $1\text{ m}^3\text{ h}^{-1}$  while circumventing pressure drops common with conventional large-scale solid phase extraction systems.<sup>[41]</sup> Also, an efficient removal of organic contaminants was achieved by covalently linking  $\beta$ -cyclodextrin to the PEI coated nanoparticles (Scheme 6).<sup>[42]</sup> The trapped molecules were completely released by filling the cyclodextrin cavity with microbiologically well accepted benzyl alcohol and experiments at ultra-low concentrations of 160 ppb showed the potential of this hybrid system as enrichment tool for trace analysis.

In order to covalently attach polymers to carbon-coated magnetic nanobeads, which is arguably more stable than simple physisorption, linkers on the surface are essential. Norbornene-tags were introduced to Co/C nanobeads via diazonium



**Scheme 6.** Physisorption of PEI on Co/C nanobeads for the synthesis of magnetic extractors. Scheme adapted from refs [39] and [42].

chemistry and subsequent “click”-reaction (Figure 3).<sup>[43]</sup> After activation with Grubbs 2<sup>nd</sup> generation catalyst, surface-initiated ring opening metathesis polymerization (ROMP) with norbornene-modified triphenylphosphine was carried out followed by complexation with Pd acetate. The saturation magnetization of the resulting magnetic hybrid material (34 emu/g) was consistent with the mass percentage of cobalt in the sample and the magnetic catalyst was applied in iterative Suzuki-Miyaura reactions without loss of activity or material. Hanson and coworkers applied the Co/C nanoparticles pre-activated with metathesis catalyst in the purification of intermolecular<sup>[44]</sup> as well as intramolecular<sup>[45]</sup> Mitsunobu reactions. Rapid sequestration of excess and depleted norbornene-tagged reagents was achieved by surface-initiated ROM polymerization on the magnetic supports. Simple magnetic decantation completely removed the reagents together with the magnetic beads giving rise to pure esters and thiadiazepine-dioxides. However, it was not possible to recycle the magnetic auxiliaries due to irreversibly bound polymer. Recently, we extended this methodology to the synthesis of high loading and recyclable magnetic acylation reagents.<sup>[46]</sup> Active esters derived from *N*-hydroxysuccinimide (NHS) were polymerized via surface-initiated ROMP on Co/C and Fe/C nanobeads (Figure 2). A high loading of up to

2.6 mmol/g was achieved, which is 25-times higher than for nanoparticles lacking the polymer layer. The NHS ROMPgel was successfully applied for the acylation of primary and secondary amines. After isolation of the products in excellent yields and purities, the magnetic resin was readily re-acylated by various acid chlorides, anhydrides, and carboxylic acids.

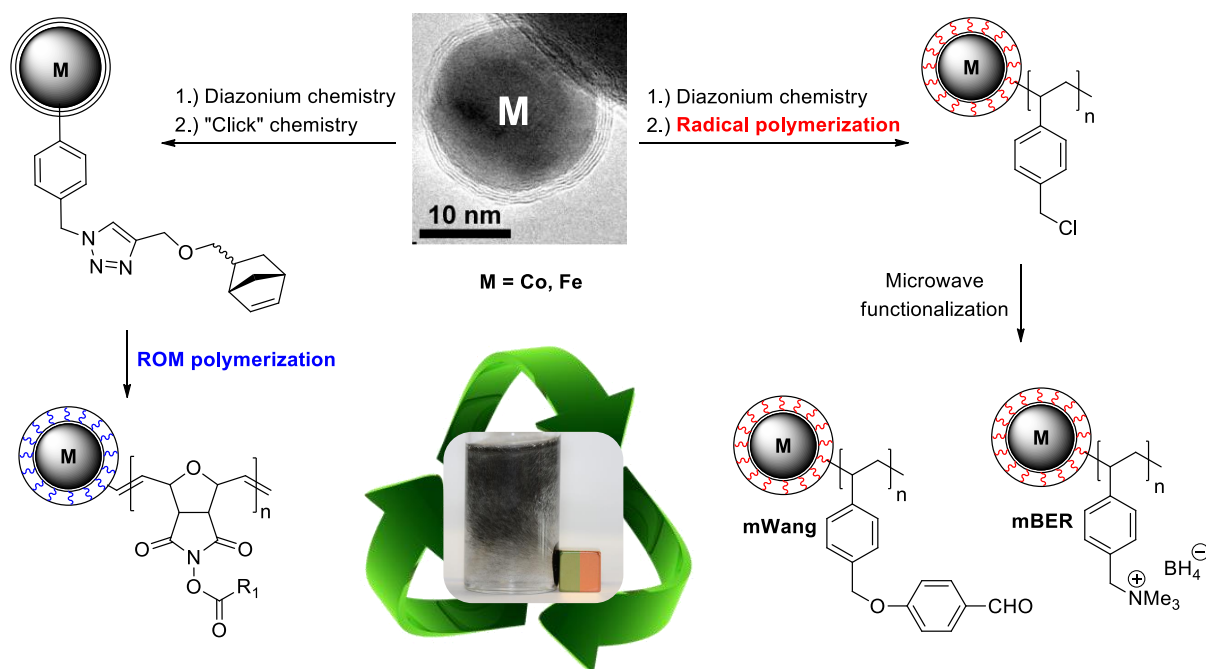


**Figure 2.** Preparation of polymer-coated magnetic nanoparticles via ROMP or free radical polymerization leading to highly magnetic as well as high loading reagents and scavengers.

Radical polymerization is an alternative approach to synthesize polymer shells around carbon-coated nanoparticles deaggregating the formerly densely packed ferromagnetic nanoparticles (Figure 3). Stark *et al.*<sup>[14]</sup> reported the surface-initiated grafting polymerization of 4-chloromethylstyrene onto vinyl-functionalized Co/C scaffolds. Optimization of the reaction conditions resulted in a nearly complete incorporation of the monomer into the hybrid material leading to high loadings of up to 3 mmol/g at magnetization levels ( $M_s = 33$  emu/g) typical for lower loading (< 1.1 mmol/g) magnetite materials. The functionalization with a trialkylsilane reagent allowed the application as "magnetic silyl protecting group" for various primary and secondary alcohols. In this case, the exceptional durability of the scaffold was a prerequisite to withstand the harsh acidic cleavage conditions applied in the recycling process. Also, magnetic amine (mAmine), borohydride exchange (mBER), and Wang

aldehyde (mWang) resins were conveniently prepared from the magnetic poly(benzylchloride) resin by rapid microwave functionalization exploiting the strong microwave absorbing properties of the metal cores (Figure 2).<sup>[47]</sup> A small library of (thio)ureas was prepared in a multi-step sequence exclusively applying these high loading magnetic scavengers and reagents. Excellent purities of the products were obtained with convenient magnetic decantation as the sole purification step and the magnetic resins were efficiently regenerated.

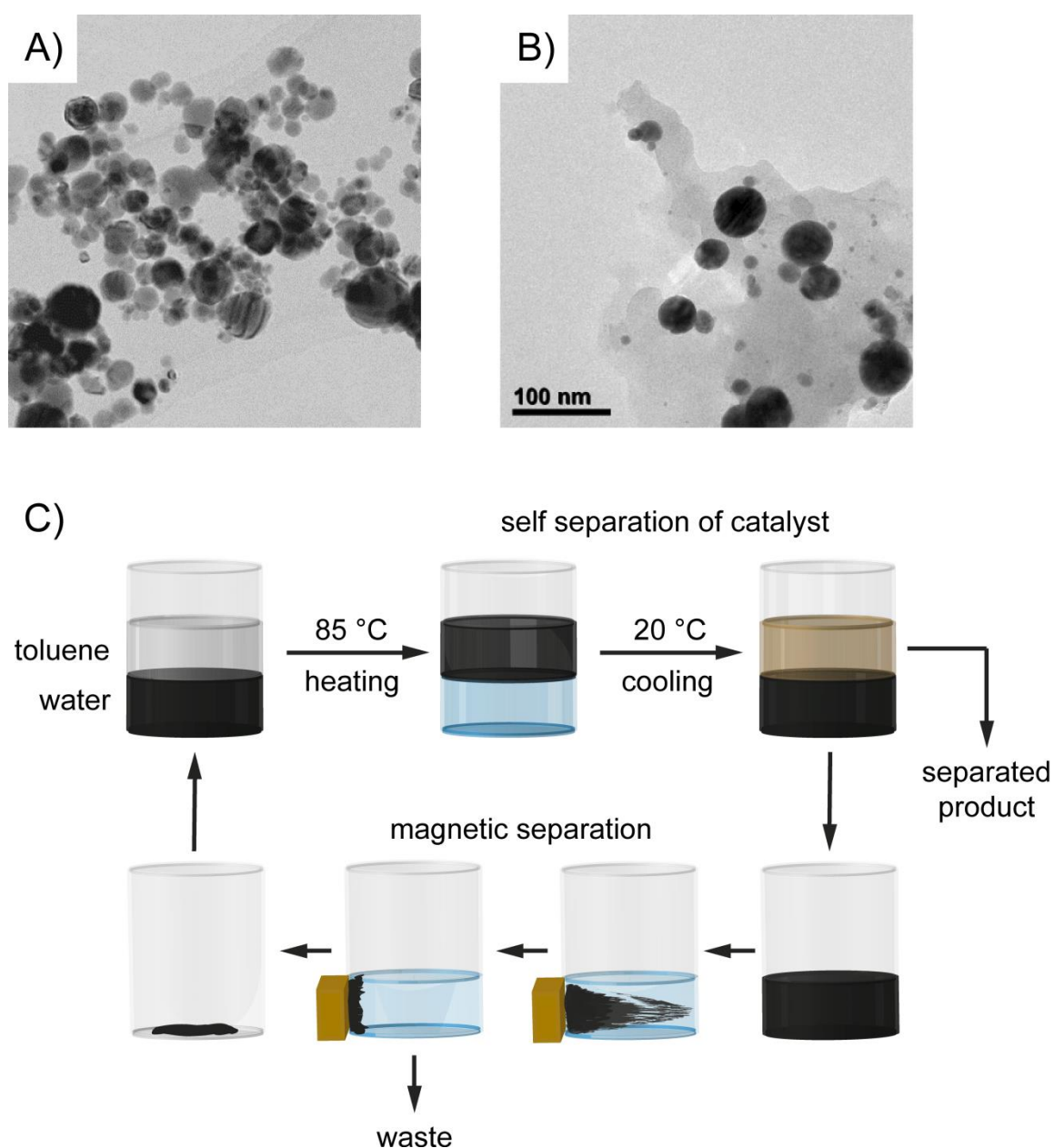


**Figure 3.** Transmission electron micrographs (TEM) of non-functionalized Fe/C (A) and particles with covalently attached polystyrene (B). (C) shows the concept of a self-separating magnetic catalyst. (A), (B) reproduced with permission from ref [48] and (C) adapted from ref [49].

Apart from the preparation of high loading reagents and scavengers, the polystyrene-coated Co/C and Fe/C nanoparticles also proved to be suitable for the immobilization of a Jørgensen–Hayashi organocatalyst<sup>[48]</sup> or palladium NHC complexes.<sup>[49]</sup> Likewise, the extraction of organic compounds and heavy metals particularly profits from high magnetizations (rapid separations) as well as high loadings of immobilized chelators (low material input). This was demonstrated with the covalent immobilization of zinc(II)–cyclen complexes on polystyrene-coated Fe/C beads that allowed the rapid quantitative extraction of riboflavin (vitamin B<sub>2</sub>) from a vitamin tablet.<sup>[50]</sup> Washing of the isolated particles with aqueous hydrochloric acid efficiently released the riboflavin allowing for recycling of the magnetic scaffolds in six consecutive extractions. A similar concept was used by Stark et al. for the pH-dependent reversible extraction of As(IV) using polystyrene-coated nanoparticles functionalized with N-methyl-d-glucamine (NMDG) as chelating ligand in a moving bed reactor system.<sup>[51]</sup>

The properties of polymer-coated magnetic nanoparticles cannot only be tuned by late-stage functionalization but also by using different monomers. For example, amphiphilic *N*-isopropylacrylamide (NIPAM) was polymerized on vinyl-tagged Co/C nanoparticles.<sup>[52]</sup> The incorporation of N-acryloxysuccinimide monomers allowed the tethering of Pd-phosphine complexes. The novel “smart” material was applied for Suzuki–Miyaura cross-coupling reactions in a biphasic toluene-water mixture (Figure 3C). At elevated temperatures, the thermoresponsive part of the polymer collapses and the particles translocate into the organic phase where the reaction takes place. Upon cooling to room temperature, the catalyst returns to the aqueous phase resulting in a self-separating catalyst, which can be completely removed by applying an external magnet.

## 4. Conclusion and Perspectives

Current synthetic advances facilitated the preparation of well-defined superparamagnetic iron oxide nanoparticles and the large scale production of ferromagnetic carbon-coated metal nanoparticles. Both types of nanomaterial have specific benefits, such as diminished agglomeration for SPIONs and high stabilities and magnetization levels for Co/C and Fe/C nanoparticles. The introduction of dendrimers and polymers to the surface of the nanomagnets boosts the loading capacity with functional groups considerably, either by ligation with pre-synthesized dendrimers or polymers or by surface-initiated synthesis. While the ligation allows for the attachment of well-defined and possibly commercial material, the synthesis on the particles enables a denser functionalization and an easy tuning of the properties. The resulting core-shell hybrid materials were extensively used as recyclable platforms for organic chemistry, for example in the extraction of analytes or contaminants, as supports for metal- and organocatalysts, and in the preparation of magnetic scavengers and reagents. All these applications have in common, that a high loading magnetic hybrid material was used that allowed for convenient magnetic separation and, whenever possible, recycling for further runs. It has also been shown, that a full multi-step synthesis can be performed exclusively by applying magnetic reagents and scavengers.

Further work is required to bring these multi-functional materials closer to industrial applications: Synthetic methods have to be pushed to the multi-kg scale at reasonable costs, the particle size and size distributions need to be fully controlled, and state of the art polymerization techniques have to be applied in order to yield site isolated particles with a well-defined shell. First examples of continuous-flow synthesis using catalysts and reagents immobilized on highly magnetic supports which are contained in the system exclusively by external magnets needs further exploration. Furthermore, the automation of the recycling by magnetic decantation has to be investigated in detail in order to establish magnetic nanoparticles as useful supports for highly parallelized as well as high throughput syntheses.

## 5. References

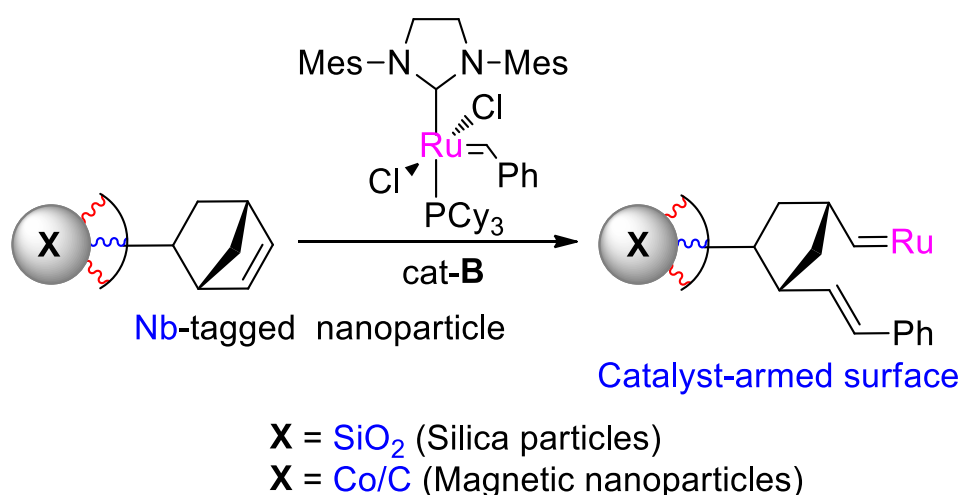
- [1] C. E. Garrett, K. Prasad, *Adv. Synth. Catal.* **2004**, *346*, 889–900.
- [2] P. T. Anastas, J. C. Warner, *Green chemistry. Theory and practice*, Oxford University Press, Oxford, New York, **1998**.
- [3] R. A. Sheldon, H. van Bekkum, *Fine chemicals through heterogeneous catalysis*, Wiley-VCH, Weinheim, New York, **2001**.
- [4] A. Schätz, O. Reiser, W. J. Stark, *Chem. Eur. J.* **2010**, *16*, 8950–8967.
- [5] S. Shylesh, V. Schünemann, W. R. Thiel, *Angew. Chem. Int. Ed.* **2010**, *49*, 3428–3459.
- [6] V. Polshettiwar, R. Luque, A. Fihri, H. Zhu, M. Bouhrara, J.-M. Basset, *Chem. Rev.* **2011**, *111*, 3036–3075.
- [7] A.-H. Lu, E. L. Salabas, F. Schüth, *Angew. Chem. Int. Ed.* **2007**, *46*, 1222–1244.
- [8] T. Hyeon, S. S. Lee, J. Park, Y. Chung, H. B. Na, *J. Am. Chem. Soc.* **2001**, *123*, 12798–12801.
- [9] S. Sun, H. Zeng, *J. Am. Chem. Soc.* **2002**, *124*, 8204–8205.
- [10] A. K. Gupta, R. R. Naregalkar, V. D. Vaidya, M. Gupta, *Nanomedicine* **2007**, *2*, 23–39.
- [11] A. Hu, G. T. Yee, W. Lin, *J. Am. Chem. Soc.* **2005**, *127*, 12486–12487.
- [12] C. Xu, K. Xu, H. Gu, R. Zheng, H. Liu, X. Zhang, Z. Guo, B. Xu, *J. Am. Chem. Soc.* **2004**, *126*, 9938–9939.
- [13] Y. Lu, Y. Yin, B. T. Mayers, Y. Xia, *Nano Lett.* **2002**, *2*, 183–186.
- [14] A. Schätz, M. Zeltner, T. D. Michl, M. Rossier, R. Fuhrer, W. J. Stark, *Chem. Eur. J.* **2011**, *17*, 10566–10573.
- [15] Y. Saito, *Carbon* **1995**, *33*, 979–988.
- [16] W. S. Seo, J. H. Lee, X. Sun, Y. Suzuki, D. Mann, Z. Liu, M. Terashima, P. C. Yang, M. V. McConnell, D. G. Nishimura, H. Dai, *Nat Mater* **2006**, *5*, 971–976.
- [17] R. N. Grass, E. K. Athanassiou, W. J. Stark, *Angew. Chem. Int. Ed.* **2007**, *46*, 4909–4912.
- [18] E. K. Athanassiou, R. N. Grass, W. J. Stark, *Aerosol. Sci. Technol.* **2010**, *44*, 161–172.
- [19] I. K. Herrmann, R. N. Grass, D. Mazunin, W. J. Stark, *Chem. Mater.* **2009**, *21*, 3275–3281.
- [20] A. Schätz, R. N. Grass, W. J. Stark, O. Reiser, *Chem. Eur. J.* **2008**, *14*, 8262–8266.
- [21] A. Schätz, R. N. Grass, Q. Kainz, W. J. Stark, O. Reiser, *Chem. Mater.* **2010**, *22*, 305–310.
- [22] S. Wittmann, A. Schätz, R. N. Grass, W. J. Stark, O. Reiser, *Angew. Chem. Int. Ed.* **2010**, *49*, 1867–1870.
- [23] D. A. Tomalia, H. Baker, J. Dewald, M. Hall, Kallos, *Polym. J.* **1985**, *17*, 117–132.
- [24] G. R. Newkome, Z. Yao, G. R. Baker, V. K. Gupta, *J. Org. Chem.* **1985**, *50*, 2003–2004.
- [25] R. Abu-Reziq, H. Alper, D. Wang, M. L. Post, *J. Am. Chem. Soc.* **2006**, *128*, 5279–5282.
- [26] K. Uzun, E. Çevik, M. Şenel, H. Sözeri, A. Baykal, M. F. Abasıyanık, M. S. Toprak, *J. Nanopart. Res.* **2010**, *12*, 3057–3067.
- [27] C.-M. Chou, H.-L. Lien, *J. Nanopart. Res.* **2011**, *13*, 2099–2107.
- [28] X.-H. Fu, *Anal. Lett.* **2010**, *43*, 455–465.
- [29] T. Tanaka, K. Shibata, M. Hosokawa, K. Hatakeyama, A. Arakaki, H. Gomyo, T. Mogi, T. Taguchi, H. Wake, T. Tanaami et al., *J. Colloid. Inf. Sci.* **2012**, *377*, 469–475.
- [30] Q. M. Kainz, A. Schätz, A. Zöpfl, W. J. Stark, O. Reiser, *Chem. Mater.* **2011**, *23*, 3606–3613.
- [31] M. Keller, V. Collière, O. Reiser, A.-M. Caminade, J.-P. Majoral, A. Ouali, *Angew. Chem. Int. Ed.* **2013**, *52*, 3626–3629.
- [32] M. R. Knecht, J. C. Garcia-Martinez, R. M. Crooks, *Chem. Mater.* **2006**, *18*, 5039–5044.
- [33] J. Pyun, *Polym. Rev.* **2007**, *47*, 231–263.
- [34] F. Caruso, *Adv. Mater.* **2001**, *13*, 11–22.
- [35] M.-H. Liao, D.-H. Chen, *Biotechnol. Lett.* **2002**, *24*, 1913–1917.
- [36] A. J. Amali, R. K. Rana, *Green Chem.* **2009**, *11*, 1781.
- [37] P. D. Stevens, J. Fan, H. M. R. Gardimalla, M. Yen, Y. Gao, *Org. Lett.* **2005**, *7*, 2085–2088.
- [38] M. Butterworth, S. Bell, S. Armes, A. Simpson, *J. Colloid. Inf. Sci.* **1996**, *183*, 91–99.
- [39] F. M. Koehler, M. Rossier, M. Waelle, E. K. Athanassiou, L. K. Limbach, R. N. Grass, D. Günther, W. J. Stark, *Chem. Commun.* **2009**, 4862–4864.

- [40] I. K. Herrmann, M. Urner, F. M. Koehler, M. Hasler, B. Roth-Z'Graggen, R. N. Grass, U. Ziegler, B. Beck-Schimmer, W. J. Stark, *Small* **2010**, *6*, 1388–1392.
- [41] M. Rossier, M. Schreier, U. Krebs, B. Aeschlimann, R. Fuhrer, M. Zeltner, R. N. Grass, D. Günther, W. J. Stark, *Sep. Purif. Technol.* **2012**, *96*, 68–74.
- [42] R. Fuhrer, I. K. Herrmann, E. K. Athanassiou, R. N. Grass, W. J. Stark, *Langmuir* **2011**, *27*, 1924–1929.
- [43] A. Schätz, T. R. Long, R. N. Grass, W. J. Stark, P. R. Hanson, O. Reiser, *Adv. Funct. Mater.* **2010**, *20*, 4323–4328.
- [44] P. K. Maity, A. Rolfe, T. B. Samarakoon, S. Faisal, R. D. Kurtz, T. R. Long, A. Schätz, D. L. Flynn, R. N. Grass, W. J. Stark et al., *Org. Lett.* **2011**, *13*, 8–10.
- [45] P. K. Maity, Q. M. Kainz, S. Faisal, A. Rolfe, T. B. Samarakoon, F. Z. Basha, O. Reiser, P. R. Hanson, *Chem. Commun.* **2011**, *47*, 12524–12526.
- [46] Q. M. Kainz, R. Linhardt, P. K. Maity, P. R. Hanson, O. Reiser, *ChemSusChem* **2013**, *6*, 721–729.
- [47] Q. M. Kainz, M. Zeltner, M. Rossier, W. J. Stark, O. Reiser, *Chem. Eur. J.* **2013**, *19*, 10038–10045.
- [48] M. Keller, A. Perrier, R. Linhardt, L. Travers, S. Wittmann, A.-M. Caminade, J.-P. Majoral, O. Reiser, A. Ouali, *Adv. Synth. Catal.* **2013**, *355*, 1748–1754.
- [49] S. Wittmann, J.-P. Majoral, R. N. Grass, W. J. Stark, O. Reiser, *Green Proc. Synth.* **2012**, *1*, 275–279.
- [50] Q. M. Kainz, A. Späth, S. Weiss, T. D. Michl, A. Schätz, W. J. Stark, B. König, O. Reiser, *ChemistryOpen* **2012**, *1*, 125–129.
- [51] M. Rossier, A. Schaetz, E. K. Athanassiou, R. N. Grass, W. J. Stark, *Chem. Eng. J.* **2011**, *175*, 244–250.
- [52] M. Zeltner, A. Schätz, M. L. Hefti, W. J. Stark, *J. Mat. Chem.* **2011**, *21*, 2991–2996.



## D Main Part

### 1. Intramolecular Monomer-on-Monomer (MoM) Mitsunobu Cyclization for the Synthesis of Benzo-fused Thiadiazepine-dioxides<sup>i</sup>



The utilization of a monomer-on-monomer (MoM) intramolecular-Mitsunobu cyclization reaction employing norbornenyl-tagged (Nb-tagged) reagents is reported for the synthesis of benzofused thiadiazepine-dioxides. Facile purification was achieved via ringopening metathesis (ROM) polymerization initiated by one of three metathesis catalyst methods: (i) free metathesis catalyst, (ii) surface-initiated catalyst-armed silica, or (iii) surface-initiated catalyst-armed Co/C magnetic nanoparticles.<sup>ii</sup>

<sup>i</sup> Reproduced with permission from: P. K. Maity, Q. M. Kainz, S. Faisal, A. Rolfe, T. B. Samarakoon, F. Z. Basha, O. Reiser, P. R. Hanson, *Chem. Commun.* **2011**, 47, 12524-12526. Copyright 2011 The Royal Society of Chemistry.

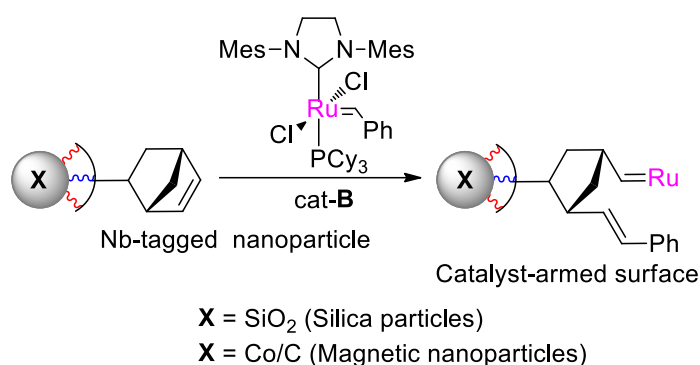
<sup>ii</sup> Compounds **2a**, **2g**, **2n**, **3a**, **3g-j** were prepared by Q. M. Kainz, compounds **2a-d**; **2h**, **2j**, **2l**, **3a-d** by P. K. Maity, compounds **2e**, **2f**, **2i**, **2k**, **2m**, **3e**, **3f**, by S. Faisal, and compounds **3k-n** by A. Rolfe.

## 1.1 Introduction

The ongoing effort in the search for new pharmacophores and small molecular probes is a key feature of modern drug discovery. The Mitsunobu reaction and its variants<sup>[1]</sup> represent versatile synthetic methods which are pivotal to accessing small molecules for drug discovery.<sup>[2]</sup> The Mitsunobu reaction is a mild and effective method for the conversion of alcohols into a variety of functionality through the formation of C–C, C–O, C–N and C–S bonds, including the ability to invert the stereochemistry of stereogenic carbinol-bearing centers. A formal “redox” reaction, the Mitsunobu reaction is promoted under relatively mild conditions by a combination of a tertiary phosphine, usually triphenyl-phosphine (PPh<sub>3</sub>) and an azodicarboxylate, usually diethyl or diisopropyl ester (DEAD or DIAD). Such is the scope of the Mitsunobu reaction, its application has played a pivotal role in the synthesis of natural products,<sup>[3]</sup> and bioactive small molecules.<sup>[4]</sup> Despite these powerful attributes, the Mitsunobu reaction suffers from the need for tedious purifications to isolate the desired product, an operational disadvantage in both high-throughput chemistry and natural product synthesis. Addressing this issue, several variants of the Mitsunobu reaction have been developed which include tagged, immobilized and water-soluble reagents that allow for facile separation of the desired product from unwanted Mitsunobu by-products.<sup>[5]</sup>

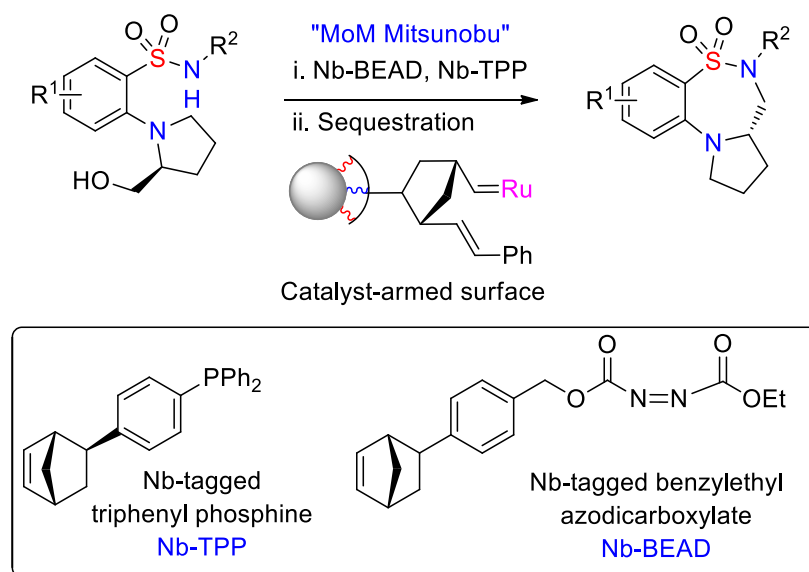
## 1.2 Results and Discussion

Methods developed within our group for facile purification-free Mitsunobu protocols have focused on the application of a polymer-on-polymer (PoP) Mitsunobu protocol, employing ROMP-derived oligomeric triphenylphosphine (OTPP) and oligomeric benzylethyl azodicarboxylate (OBEAD) reagents,<sup>[6]</sup> as well as a monomer-on-monomer (MoM) Mitsunobu protocol, utilizing norbornenyl-tagged (Nb-tagged) PPh<sub>3</sub> and BEAD reagents.<sup>[7]</sup> In the latter case, facile sequestration of the excess and spent reagents was achieved *via* ring-opening metathesis (ROM) polymerization initiated by any one of three methods utilizing Grubbs catalyst [(IMesH<sub>2</sub>)(PCy<sub>3</sub>)(Cl)<sub>2</sub>Ru=CHPh, cat-**B**]:<sup>[8]</sup> (i) free catalyst in solution, (ii) surface-initiated catalyst-armed silica,<sup>[9,10]</sup> or (iii) surface-initiated catalyst-armed carbon-coated (Co/C) magnetic nanoparticles (Nps) (Scheme 1).<sup>[7,11]</sup>



**Scheme 1.** Catalyst-armed Silica and Co/C magnetic nanoparticles.

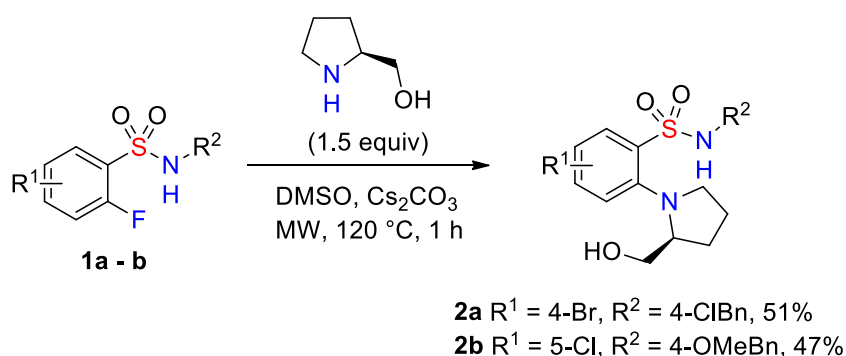
The intramolecular Mitsunobu reaction has been widely utilized as a cyclization protocol for the synthesis of heterocyclic molecules.<sup>[12]</sup> Building on these reports, we herein report the synthesis of benzofused thiadiazepine-dioxides *via* an intramolecular 7-membered MoM Mitsunobu cyclization reaction, whereby facile purification was achieved utilizing ROMP sequestration initiated by free metathesis catalyst or catalyst-armed particle surfaces (Scheme 2).



**Scheme 2.** Synthesis of benzofused thiadiazepine-dioxides via a intramolecular MoM Mitsunobu cyclization.

The synthesis of benzofused thiadiazepine-dioxides **3a** and **3b** was investigated utilizing the intramolecular MoM Mitsunobu cyclization with the readily prepared Nb-tagged  $\text{PPh}_3$  (Nb-TPP) and DEAD (Nb-BEAD) reagents.<sup>[6]</sup> The correspond-

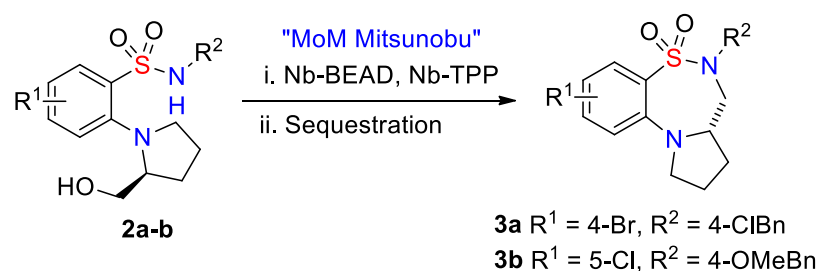
ing hydroxy-benzylsulfonamide starting materials **2a** and **2b** were rapidly generated via a microwave-assisted  $S_NAr$  protocol (Scheme 3).<sup>[13]</sup>



**Scheme 3.** Synthesis of hydroxy-benzylsulfonamides **2a-b** via microwave-assisted  $S_NAr$ .

With sulfonamides **2a-b** in hand, the application of MoM cyclization reaction was investigated utilizing Nb-TPP and Nb-BEAD (Table 1). Initially, purification was achieved by phase switching of all Nb-tagged species in solution (monomeric reagents and spent reagents) by addition of free metathesis catalyst [(IMesH<sub>2</sub>)(PCy<sub>3</sub>)(Cl)<sub>2</sub>Ru=CHPh, cat-**B**] (Method **A**) to induce ROM polymerization. The ROM polymerization event was followed by precipitation to produce the desired benzofused thiadiazepine-dioxides **3a** and **3b** in good yield and excellent crude purity (Table 1, entries 1–2). Purification was followed by TLC analysis, whereby the typical Mitsunobu multispot crude reaction mixture was reduced to a single spot after utilizing this polymerization sequestration protocol. Despite this success, the need for precipitation of the crude reaction mixture to remove the polymerized reagents/spent reagents was deemed not ideal for a high-throughput approach. Therefore, alternative syntheses of benzofused thiadiazepine-dioxides **3a** and **3b** were investigated utilizing a catalyst-armed surface generated from either Nb-tagged Co/C magnetic particles, or Nb-tagged silica particles.

After polymerization sequestration of excess reagents/spent reagents on the surface of the magnetic Co/C beads [Method **B**], **3a** and **3b** could be obtained in reasonable crude purity by collecting the nanobeads with an external magnet, decanting the solution and evaporating the solvent (Table 1, entries 3-4). Noteworthy, this work-up procedure is carried out within a few seconds, being an operational advantage to conventional filtration techniques. However, to further improve the product purity the solution was filtered over a silica SPE. As an alternative method, the sequestration

**Table 1.** Intramolecular MoM Mitsunobu-Sequestration.

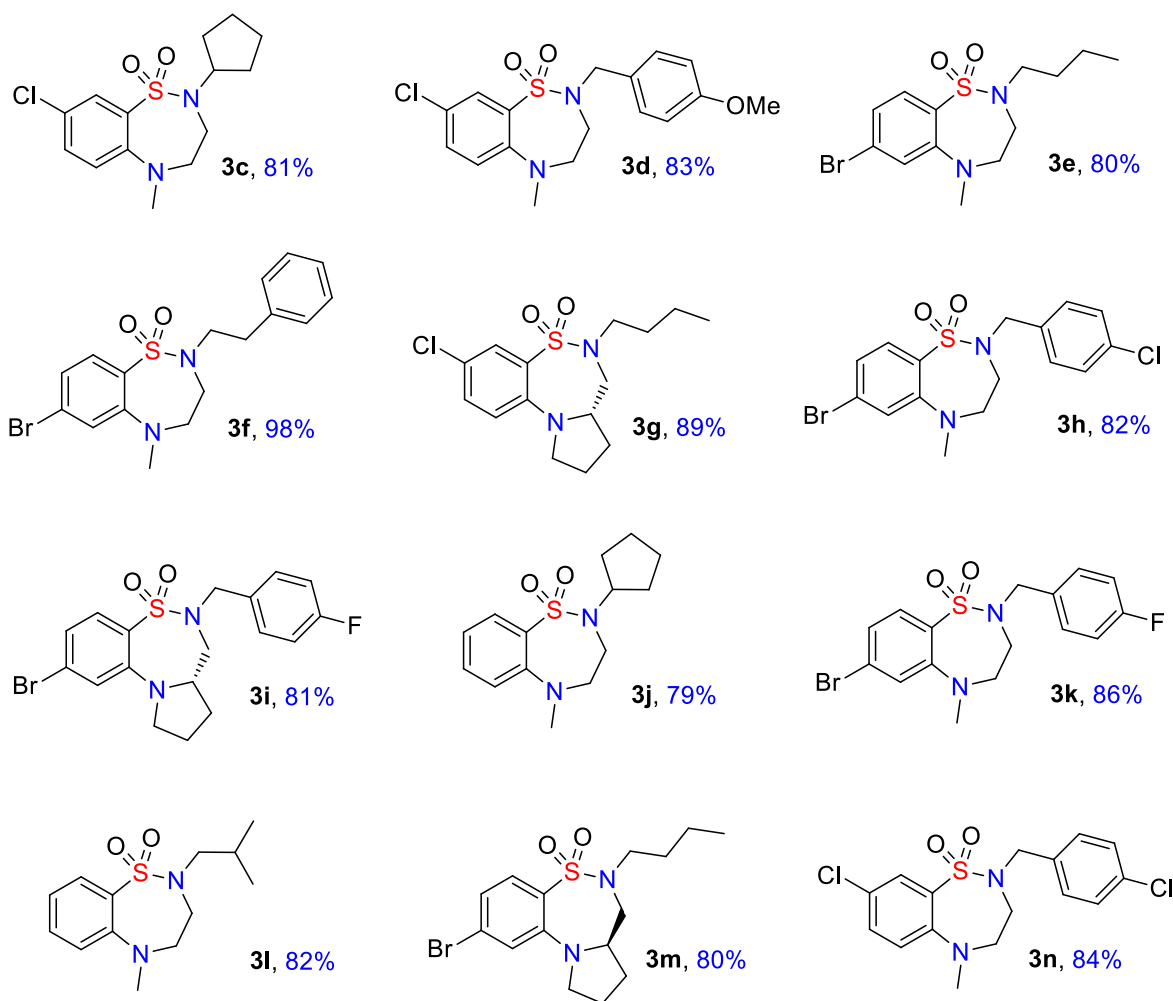
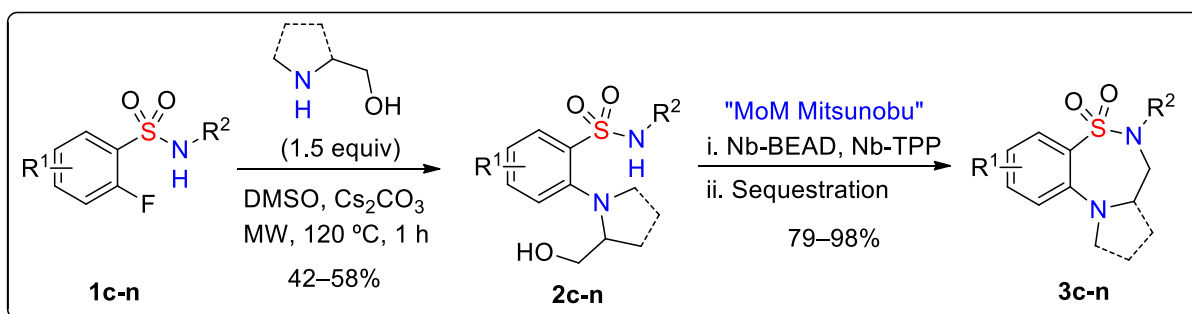
Entry	Sequestration	Comp.	Method	Yield [%]	Crude [%] <sup>[a]</sup>	Purity
1 <sup>[b]</sup>	Cat- <b>B</b>	<b>3a</b>	A	85	> 95	
2 <sup>[b]</sup>	Cat- <b>B</b>	<b>3b</b>	A	88	> 95	
3 <sup>[c]</sup>	Co/C Nb-tagged	<b>3a</b>	B	87	> 95	
4 <sup>[c]</sup>	Co/C Nb-tagged	<b>3b</b>	B	81	> 95	
5 <sup>[d]</sup>	Si Nb-tagged	<b>3a</b>	C	89	> 95	
6 <sup>[d]</sup>	Si Nb-tagged	<b>3b</b>	C	84	> 95	

[a] Purity determined by <sup>1</sup>H NMR. [b] Isolated via precipitation in Et<sub>2</sub>O. [c] Isolated via magnetic decantation and filtration through Silica SPE. [d] Isolated via filtration through Celite® SPE

by Nb-tagged silicaparticles (Method **C**) was applied to generate **3a** and **3b** in comparable yields and purities with simple filtration through Celite® SPE to isolate the desired product, avoiding the need for precipitation (Table 1, entries 5–6). Building on these results, substrate scope was evaluated across all three purificationsequestration protocols **A–C** for the synthesis of **3c–3n** via MoM Mitsunobu cyclization (Scheme 4). Thus, benzofused thiadiazepine-dioxides **3c–3f** were generated with free cat-**B** (Method **A**), compounds **3g–3j** via Nb-tagged Co/C magnetic particles [Method **B**] and benzofused thiadiazepine-dioxides **3k–3n** utilizing Nb-tagged SiO<sub>2</sub> particles (Method **C**).

### 1.3 Conclusion

In conclusion, we have demonstrated the application of a MoM intramolecular Mitsunobu cyclization for the synthesis of bi- and tri-cyclic benzofused thiadiazepine-dioxides. Facile purification of crude reaction mixtures was achieved via ROM polymerization sequestration of excess reagents/spent reagents. This was



**Scheme 4.** Synthesis of benzofused thiadiazepine-dioxides. (**3c-3f**: Method A; **3g-3j**: Method B; **3k-3n**: Method C).<sup>iii</sup>

accomplished initially utilizing free metathesis catalyst Cat-B, followed by precipitation. The method was further optimized utilizing catalyst-armed surfaces generated from either Nb-tagged Si-particles or Nb-tagged Co/C magnetic nanoparticles.

<sup>iii</sup> Modified to fit on page.

## 1.4 Experimental Section

### Methods and materials

All air and moisture sensitive reactions were carried out in flame- or oven-dried glassware under argon atmosphere using standard gastight syringes, cannulas and septa. CH<sub>2</sub>Cl<sub>2</sub> and toluene were purified by passage through a Solv-Tek ([www.solvtek.com](http://www.solvtek.com)) purification system employing activated Al<sub>2</sub>O<sub>3</sub> and degassed with argon. Flash column chromatography was performed with SiO<sub>2</sub> (Sorbent Technologies 30930M-25, Silica Gel 60 Å, 40-63 µm). Thin layer chromatography was performed on silica gel 60F 254 plates. Visualization of TLC spots was effected using KMnO<sub>4</sub> stain. <sup>1</sup>H and <sup>13</sup>C NMR spectra were recorded in CDCl<sub>3</sub> (unless otherwise mentioned) on a Bruker DRX-400 spectrometer operating at 400 MHz, and 100 MHz respectively as well as Bruker DRX-500 spectrometer operating at 500 MHz, and 125 MHz, respectively and calibrated to the solvent peak. High-resolution mass spectrometry (HRMS) was recorded on a LCT Premier Spectrometer (Micromass UK Limited) operating on ESI (MeOH). The nanoparticles were analyzed by scanning electron microscopy (Hitachi S-2700 equipped with a quartz PCI digital capture) and FTIR Perkin Elmer Spectrum 100 FT-IR spectrometer. All other commercially available compounds were used as received. metathesis catalyst [(IMesH<sub>2</sub>)(PCy<sub>3</sub>)(Cl)<sub>2</sub>Ru=CHPh; cat-**B**] was provided by Materia Inc. and used without further purification. Deuterated solvents were purchased from Cambridge Isotope laboratories.

### General Procedure A: Synthesis of the benzofused sulfonamides

To a 25 mL round-bottom flask was added sulfonyl chloride (1 equiv) followed by CH<sub>2</sub>Cl<sub>2</sub> (0.4 M), amine (2.0 equiv) and a solution of NaHCO<sub>3</sub> (3.0 equiv) in H<sub>2</sub>O (0.8 M). The reaction was stirred at room temperature for 12 h, after which time the reaction mixture was quenched with H<sub>2</sub>O (30 mL) and extracted with CH<sub>2</sub>Cl<sub>2</sub> (3x30 mL). The combined organic layers were dried over Na<sub>2</sub>SO<sub>4</sub>, filtered, concentrated *in vacuo* and purification by column chromatography eluting with hexanes/EtOAc 4:1.

### General Procedure B: Synthesis of 2a-2n via SNAr

To a microwave vial was added sulfonamide (1 equiv) under argon atmosphere followed by the addition of dry DMSO (0.8 M), amine (1.5 equiv) and Cs<sub>2</sub>CO<sub>3</sub> (3.0

equiv). The mixture was heated in the microwave at 120 °C for 60 mins, after which time the mixture was quenched with H<sub>2</sub>O (30 mL), and extracted with EtOAc (2x30 mL). The combined organic layer separated, washed with H<sub>2</sub>O (30 mL), dried over Na<sub>2</sub>SO<sub>4</sub> and concentrated *in vacuo*. Thereafter, the crude mixture was purified by column chromatography eluting with hexanes/EtOAc 3:1.

**General Procedure C: Intramolecular monomer-on-monomer (MoM) Mitsunobu reaction utilizing [(IMesH<sub>2</sub>)(PCy<sub>3</sub>)(Cl)<sub>2</sub>Ru=CHPh, cat-B] [Sequestration Method A]**

To a round-bottom under argon atmosphere was added benzenesulfonamide alcohol **2c-2f** (1 equiv) in dry THF (0.1 M). The reaction was cooled to 0 °C, stirred for 15 min, after which Nb-TPP (3 equiv) and Nb-BEAD (3 equiv) were added to the reaction mixture and stirred at room temperature for 2-12 hrs (TLC monitoring). The reaction was concentrated and resolvated in degassed CH<sub>2</sub>Cl<sub>2</sub> (0.1 M), cat-**B** (0.05 equiv) [(IMesH<sub>2</sub>)(PCy<sub>3</sub>)(Cl)<sub>2</sub>Ru=CHPh, cat-**B**] was added and reaction heated at 50 °C for 30 mins to 1 hr (TLC monitoring). Upon completion, the reaction was cooled to room temperature, quenched with ethyl vinyl ether (4 equiv) and stirred for an additional 30 mins. After such time was added Na<sub>2</sub>CO<sub>3</sub> (10 equiv) followed by dropwise addition of tetrakis(hydroxymethyl) phosphonium chloride (THPC) 80% in water (10 equiv) while stirring and was refluxed for 4 h. The reaction mixture was cooled to room temperature, extracted with dichloromethane (2x20 mL), washed with water and brine. The organic layer was dried over MgSO<sub>4</sub>, filtered through a celite plug and concentrated *in vacuo*. The resulting solution was filtered through a plug of silica, eluting with 2:1-Hexane/EtOAc. The resulting eluent was then concentrated *in vacuo* to yield the desired products in good to excellent yields and purities.

**General Procedure D: Intramolecular monomer-on-monomer (MoM) Mitsunobu reaction utilizing catalyst-armed Nb-tagged Co/C magnetic nanoparticles [Sequestration Method B]**

To a round-bottom flask under argon atmosphere was added benzenesulfonamide alcohol **2g-2j** ( $2.92 \times 10^{-4}$  mol, 1 equiv) solvated in dry THF (0.1 M). The reaction was cooled to 0 °C, stirred for 20 minutes, after which was added Nb-TPP (3.0 equiv.) and Nb-BEAD (3.0 equiv.) and the reaction warmed to room temperature and stirred

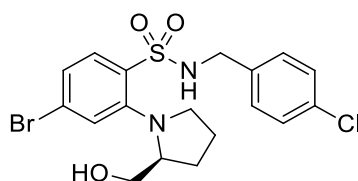


for 2–12 h (TLC monitoring). Upon completion of the reaction, the solvent was removed, the crude mixture was dissolved in degassed  $\text{CH}_2\text{Cl}_2$  (0.1 M) and added to a pressure tube containing a mixture of Co/CNp (3 mol%) and Grubbs catalyst [3 mol%,  $(\text{IMesH}_2)(\text{PCy}_3)(\text{Cl})_2\text{Ru}=\text{CHPh}$ , cat-**B**] in dry degassed  $\text{CH}_2\text{Cl}_2$  (0.05 M), that had been sonicated at 60 °C for 30 min. After additional sonication for 1–5 h at 60 °C (TLC monitoring), a neodymium-based magnet was attached to the side of the tube and the crude reaction mixture was decanted, filtered through a silica SPE and concentrated *in vacuo*, yielding the desired products in good purities.

**General Procedure E: Intramolecular monomer-on-monomer (MoM) Mitsunobu reaction utilizing catalyst-armed Nb-tagged silica particles [Sequestration Method C]**

Into a vial was added benzenesulfonamide alcohol **2k-2l** ( $1.28 \times 10^{-4}$  mol, 1 equiv), dry THF (0.1 mL) and Nb-TPP ( $2.04 \times 10^{-4}$  mol, 1.6 equiv) under an argon atmosphere. After stirring for 5 mins, a solution of Nb-BEAD ( $2.04 \times 10^{-4}$  mol, 1.6 equiv) in dry THF (0.16 mL) was added dropwise and the reaction was stirred at room temperature for 2–12 h (TLC monitoring). After evaporation of the solvent, Nb-tagged silica ( $6.12 \times 10^{-4}$  mol, 3 mol%) was added followed by the addition of a solution of cat-**B** [3 mol%,  $(\text{IMesH}_2)(\text{PCy}_3)(\text{Cl})_2\text{Ru}=\text{CHPh}$ ] in dry Ar degassed  $\text{CH}_2\text{Cl}_2$  (2 mL). The reaction was heated at 50 °C for 30 mins (TLC monitoring), after which the crude reaction was diluted with EtOAc, filtered through a silica SPE washing the SPE and residual Si-ROMP gel with EtOAc, concentrated, yielding the desired products in good purities.

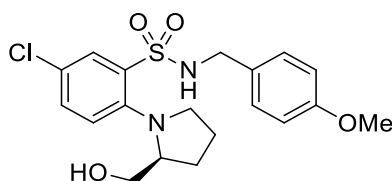
**(S)-4-Bromo-N-(4-chlorobenzyl)-2-(2-(hydroxymethyl)pyrrolidin-1-yl)benzenesulfonamide (2a)**



Utilizing general procedure B, **2a** (0.186 g, 0.405 mmol, 51%) was isolated as a brown thick liquid.

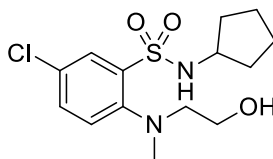
$[\alpha]_D^{20} = -28.6^\circ$  ( $c = 0.99$ ,  $\text{CHCl}_3$ ); **IR** (neat,  $\bar{\nu}/\text{cm}^{-1}$ ): 3502, 3204, 2947, 2874, 1574, 1553, 1454, 1389, 1161, 1086, 1014;  **$^1\text{H}$  NMR** (500 MHz,  $\text{CDCl}_3$ ):  $\delta = 7.74$  (d,  $J = 8.4$  Hz, 1H), 7.37 (d,  $J = 1.7$  Hz, 1H), 7.32 (dd,  $J = 8.4, 1.8$  Hz, 1H), 7.17–7.11 (m, 4H), 6.91 (t,  $J = 6.4$  Hz, 1H), 3.99 (dd,  $J = 14.4, 7.1$  Hz, 1H), 3.76 (dd,  $J = 14.4, 5.8$  Hz, 1H), 3.60–3.50 (m, 2H), 3.39 (s, 2H), 2.75 (dt,  $J = 10.3, 7.0$  Hz, 1H), 2.10 (s, 1H), 2.02–1.93 (m, 1H), 1.83–1.71 (m, 3H);  **$^{13}\text{C}$  NMR** (126 MHz,  $\text{CDCl}_3$ ):  $\delta = 151.3, 136.7, 135.8, 133.3, 131.1, 129.2, 128.6, 128.3, 128.2, 127.9, 64.7, 62.3, 58.4, 46.9, 26.5, 24.1$ ; **HRMS** calculated for  $\text{C}_{18}\text{H}_{20}\text{BrClN}_2\text{NaO}_3\text{S}$  ( $\text{M}+\text{Na}$ ) $^+$  480.9964; found 480.9965 (TOF MS).

**(S)-5-Chloro-2-(2-(hydroxymethyl)pyrrolidin-1-yl)-N-(4-methoxybenzyl) benzene-sulfonamide (2b)**



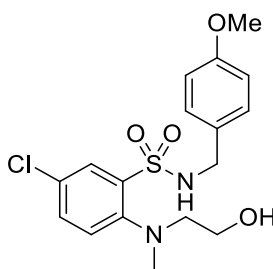
Utilizing general procedure B, **2b** (0.915 g, 2.22 mmol, 47%) was isolated as a brown thick liquid.

$[\alpha]_D^{20} = +27.2^\circ$  ( $c = 1.05$ ,  $\text{CHCl}_3$ ); **IR** (neat,  $\bar{\nu}/\text{cm}^{-1}$ ): 3511, 2952, 1610, 1512, 1458, 1319, 1249, 1161, 1031;  **$^1\text{H}$  NMR** (500 MHz,  $\text{CDCl}_3$ ):  $\delta = 7.98$  (t,  $J = 4.6$  Hz, 1H), 7.50 (dd,  $J = 8.6, 2.6$  Hz, 1H), 7.29 (d,  $J = 8.5$  Hz, 1H), 7.19 (d,  $J = 8.6$  Hz, 2H), 6.83–6.79 (m, 2H), 6.67 (t,  $J = 5.7$  Hz, 1H), 4.11 (dd,  $J = 13.7, 6.2$  Hz, 1H), 3.99–3.92 (m, 1H), 3.81 (s, 3H), 3.61–3.56 (m, 1H), 3.50 (ddd,  $J = 16.2, 10.2, 4.8$  Hz, 1H), 3.46–3.42 (m, 2H), 2.84–2.73 (m, 1H), 2.17 (t,  $J = 5.4$  Hz, 1H), 2.08–1.98 (m, 2H), 1.88–1.82 (m, 2H);  **$^{13}\text{C}$  NMR** (126 MHz,  $\text{CDCl}_3$ ):  $\delta = 159.1, 148.6, 139.4, 133.6, 130.7, 129.6, 129.3, 128.8, 126.5, 113.9, 65.4, 62.3, 58.3, 55.3, 47.4, 26.5, 24.1$ ; **HRMS** calculated for  $\text{C}_{19}\text{H}_{23}\text{ClN}_2\text{NaO}_4\text{S}$  ( $\text{M}+\text{Na}$ ) $^+$  433.0965; found 433.0970 (TOF MS).

**5-Chloro-*N*-cyclopentyl-2-((2-hydroxyethyl)(methyl)amino)benzenesulfon-amide (2c)**

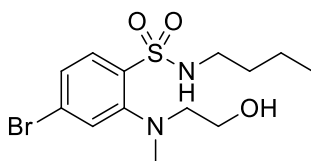
Utilizing general procedure B, **2c** (0.210 g, 0.631 mmol, 58%) was isolated as a white solid.

**IR** (neat,  $\bar{\nu}/\text{cm}^{-1}$ ): 3498, 2956, 1558, 1506, 1471, 1456, 1323, 1157, 1058;  **$^1\text{H}$  NMR** (400 MHz,  $\text{CDCl}_3$ ):  $\delta$  = 8.02 (d,  $J$  = 2.5 Hz, 1H), 7.54 (dd,  $J$  = 8.5, 2.5 Hz, 1H), 7.33 (d,  $J$  = 8.5 Hz, 1H), 6.61 (d,  $J$  = 6.6 Hz, 1H), 3.85 (dd,  $J$  = 10.2, 5.1 Hz, 2H), 3.52 (m, 1H), 3.16–3.03 (m, 2H), 2.77 (s, 3H), 2.56 (t,  $J$  = 5.1 Hz, 1H), 1.75–1.69 (m, 2H), 1.66–1.56 (m, 2H), 1.50–1.44 (m, 2H), 1.43–1.33 (m, 2H);  **$^{13}\text{C}$  NMR** (126 MHz,  $\text{CDCl}_3$ ):  $\delta$  = 150.9, 138.7, 133.5, 130.9, 129.7, 125.8, 59.8, 59.1, 55.5, 41.8, 32.9, 23.1; **HRMS** calculated for  $\text{C}_{14}\text{H}_{21}\text{ClN}_2\text{NaO}_3\text{S}$  ( $\text{M}+\text{Na}$ ) $^+$  355.0859; found 355.0857 (TOF MS ES+).

**5-Chloro-2-((2-hydroxyethyl)(methyl)amino)-*N*-(4-methoxybenzyl) benzenesulfonamide (2d)**

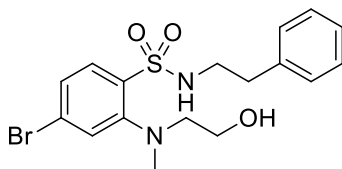
Utilizing general procedure B, **2d** (0.196 g, 0.51 mmol, 55%) was isolated as a colourless thick liquid.

**IR** (neat,  $\bar{\nu}/\text{cm}^{-1}$ ): 3521, 3182, 2358, 1575, 1552, 1454, 1323, 1159, 1137, 1074;  **$^1\text{H}$  NMR** (400 MHz,  $\text{CDCl}_3$ ):  $\delta$  = 7.95 (d,  $J$  = 2.5 Hz, 1H), 7.48 (dd,  $J$  = 8.5, 2.6 Hz, 1H), 7.25 (d,  $J$  = 6.3 Hz, 1H), 7.21 (d,  $J$  = 8.5 Hz, 1H), 7.13–7.02 (m, 2H), 6.80–6.71 (m, 2H), 4.04 (d,  $J$  = 6.3 Hz, 2H), 3.77–3.74 (m, 5H), 3.01–2.95 (m, 2H), 2.60 (s, 3H), 2.42 (t,  $J$  = 4.6 Hz, 1H);  **$^{13}\text{C}$  NMR** (126 MHz,  $\text{CDCl}_3$ ):  $\delta$  = 159.0, 150.8, 138.4, 133.4, 130.9, 129.7, 129.6, 128.6, 125.8, 113.7, 59.2, 59.0, 55.3, 47.3, 42.6; **HRMS** calculated for  $\text{C}_{17}\text{H}_{21}\text{ClN}_2\text{NaO}_4\text{S}$  ( $\text{M}+\text{Na}$ ) $^+$  407.0808; found 407.0806 (TOF MS ES+).

**4-Bromo-*N*-butyl-2-((2-hydroxyethyl)(methyl)amino)benzenesulfonamide (2e)**

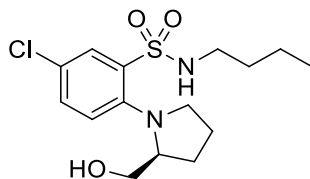
Utilizing general procedure B, **2e** (0.166 g, 0.454 mmol, 56%) was isolated as a brown solid.

**IR** (neat,  $\bar{\nu}/\text{cm}^{-1}$ ): 3301, 2958, 1583, 1454, 1406, 1319, 1159, 1130, 1081;  **$^1\text{H}$  NMR** (400 MHz,  $\text{CDCl}_3$ ):  $\delta$  = 7.86 (d,  $J$  = 8.4 Hz, 1H), 7.49 (d,  $J$  = 1.8 Hz, 1H), 7.44 (dd,  $J$  = 8.4, 1.9 Hz, 1H), 6.83 (t,  $J$  = 4.9 Hz, 1H), 3.87–3.79 (m, 2H), 3.14–3.05 (m, 2H), 2.95 (t,  $J$  = 7.1 Hz, 1H), 2.75 (s, 5H), 1.51–1.40 (m, 2H), 1.33–1.24 (m, 2H), 0.85 (t,  $J$  = 7.5 Hz, 3H);  **$^{13}\text{C}$  NMR** (126 MHz,  $\text{CDCl}_3$ ):  $\delta$  = 155.7, 129.4, 129.2, 123.9, 122.0, 121.6, 52.2, 48.5, 42.8, 31.4, 30.8, 19.6, 13.5; **HRMS** calculated for  $\text{C}_{13}\text{H}_{21}\text{BrN}_2\text{NaO}_3\text{S}$  ( $\text{M}+\text{Na}$ ) $^+$  387.0354; found 387.0323 (TOF MS ES+).

**4-Bromo-2-((2-hydroxyethyl)(methyl)amino)-*N*-phenethylbenzenesulfon-amide (2f)**

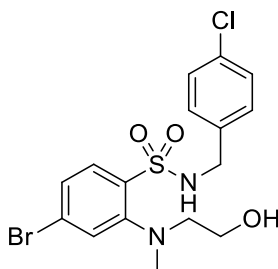
Utilizing general procedure B, **2f** (0.282 g, 0.682 mmol, 49%) was isolated as a brown thick liquid.

**IR** (neat,  $\bar{\nu}/\text{cm}^{-1}$ ): 3496, 3197, 1573, 1454, 1386, 1321, 1159, 1074;  **$^1\text{H}$  NMR** (400 MHz,  $\text{CDCl}_3$ ):  $\delta$  = 7.88–7.84 (m, 1H), 7.45–7.43 (m, 2H), 7.29–7.19 (m, 3H), 7.13–7.11 (m, 2H), 6.94 (t,  $J$  = 6.3 Hz, 1H), 3.71 (t,  $J$  = 4.9 Hz, 2H), 3.06–2.97 (m, 4H), 2.79 (t,  $J$  = 7.3 Hz, 2H), 2.56 (s, 3H), 2.35 (brs, 1H);  **$^{13}\text{C}$  NMR** (126 MHz,  $\text{CDCl}_3$ ):  $\delta$  = 153.5, 138.5, 135.3, 131.3, 128.9, 128.9, 128.7, 128.7, 128.6, 128.1, 127.8, 126.6, 59.5, 59.0, 44.9, 42.1, 36.2; **HRMS** calculated for  $\text{C}_{17}\text{H}_{21}\text{BrN}_2\text{NaO}_3\text{S}$  ( $\text{M}+\text{Na}$ ) $^+$  435.0354; found 435.0338 (TOF MS).

**(S)-N-Butyl-5-chloro-2-(2-(hydroxymethyl)pyrrolidin-1-yl)benzenesulfonamide (2g)**

Utilizing general procedure B, **2g** (0.311 g, 0.898 mmol, 48%) was isolated as a yellow oil.

$[\alpha]_D^{20} = +28.4^\circ$  ( $c = 1.1$ ,  $\text{CHCl}_3$ ); **IR** (neat,  $\bar{\nu}/\text{cm}^{-1}$ ): 3502, 3215, 2959, 2872, 1464, 1319, 1163, 1105, 895;  **$^1\text{H}$  NMR** (500 MHz,  $\text{CDCl}_3$ ):  $\delta = 7.94$  (d,  $J = 2.5$  Hz, 1H), 7.49 (dd,  $J = 8.6, 2.6$  Hz, 1H), 7.33 (d,  $J = 8.6$  Hz, 1H), 6.16 (t,  $J = 6.2$  Hz, 1H), 3.60–3.49 (m, 2H), 3.47 (t,  $J = 4.0$  Hz, 2H), 2.89–2.78 (m, 4H), 2.10–2.02 (m, 1H), 1.95–1.87 (m, 3H), 1.51–1.43 (m, 2H), 1.36–1.26 (m, 2H), 0.87 (t,  $J = 7.4$  Hz, 3H);  **$^{13}\text{C}$  NMR** (126 MHz,  $\text{CDCl}_3$ ):  $\delta = 148.6, 139.3, 133.7, 130.8, 129.6, 126.8, 65.8, 62.3, 58.5, 43.6, 32.0, 26.5, 24.3, 19.8, 13.7$ ; **HRMS** calculated for  $\text{C}_{15}\text{H}_{24}\text{ClN}_2\text{O}_3\text{S}$  ( $\text{M}+\text{H}^+$ ) 347.1196; found 347.1190 (TOF MS).

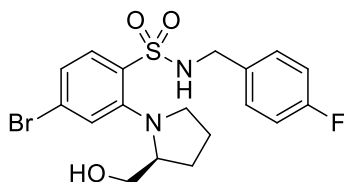
**4-Bromo-N-(4-chlorobenzyl)-2-((2-hydroxyethyl)(methyl)amino)benzenesulfonamide (2h)**

Utilizing general procedure B, **2a** (0.220 g, 0.507 mmol, 49%) was isolated as a white solid.

**IR** (neat,  $\bar{\nu}/\text{cm}^{-1}$ ): 3475, 3132, 1575, 1524, 1384, 1327, 1245, 1154, 1074;  **$^1\text{H}$  NMR** (400 MHz,  $\text{CDCl}_3$ ):  $\delta = 7.86$  (d,  $J = 8.4$  Hz, 1H), 7.48–7.42 (m, 2H), 7.37 (t,  $J = 6.5$  Hz, 1H), 7.24–7.20 (m, 2H), 7.15 (d,  $J = 8.5$  Hz, 2H), 3.96 (d,  $J = 6.5$  Hz, 2H), 3.79 (dd,  $J = 9.8, 4.6$  Hz, 2H), 3.09–3.02 (m, 2H), 2.67 (s, 3H), 2.19 (t,  $J = 4.4$  Hz, 1H).  **$^{13}\text{C}$  NMR** (126 MHz,  $\text{CDCl}_3$ ):  $\delta = 153.4, 135.6, 135.4, 133.4, 131.3, 129.4, 128.7, 128.5,$

128.0, 127.9, 59.1, 59.0, 46.9, 42.7; **HRMS** calculated for  $C_{16}H_{18}BrClN_2O_3S$  ( $M+H$ )<sup>+</sup> 432.9988; found 432.9966 (TOF MS ES<sup>+</sup>).

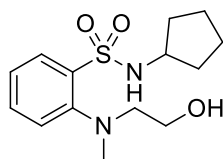
**(S)-4-Bromo-N-(4-fluorobenzyl)-2-(2-(hydroxymethyl)pyrrolidin-1-yl) benzenesulfonamide (2i)**



Utilizing general procedure B, **2i** (0.368 g, 0.831 mmol, 43%) was isolated as a brown thick liquid.

**IR** (neat,  $\bar{\nu}/\text{cm}^{-1}$ ): 3502, 3209, 2947, 1573, 1552, 1510, 1456, 1388, 1321, 1220, 1161; **<sup>1</sup>H NMR** (400 MHz,  $\text{CDCl}_3$ ):  $\delta$  = 7.84 (d,  $J$  = 8.4 Hz, 1H), 7.47–7.36 (m, 2H), 7.26–7.21 (m, 2H), 6.99–6.90 (m, 2H), 6.87 (t,  $J$  = 6.4 Hz, 1H), 4.08 (dd,  $J$  = 14.2, 7.0 Hz, 1H), 3.87 (dd,  $J$  = 14.2, 5.9 Hz, 1H), 3.64–3.57 (m, 2H), 3.49–3.44 (m, 2H), 2.87–2.76 (m, 1H), 2.15 (t,  $J$  = 5.3 Hz, 1H), 2.09–1.97 (m, 1H), 1.89–1.80 (m, 3H); **<sup>13</sup>C NMR** (126 MHz,  $\text{CDCl}_3$ ):  $\delta$  = 163.2, 161.2, 151.3, 136.7, 133.0, 132.9, 131.1, 129.5, 129.5, 128.4, 128.3, 127.9, 115.4, 115.3, 64.9, 62.4, 58.4, 46.9, 26.5, 24.2; **HRMS** calculated for  $C_{19}H_{21}BrFN_2O_3S$  ( $M+H$ )<sup>+</sup> 443.0440; found 443.0403 (TOF MS).

**N-Cyclopentyl-2-((2-hydroxyethyl)(methyl)amino)benzenesulfonamide (2j)**

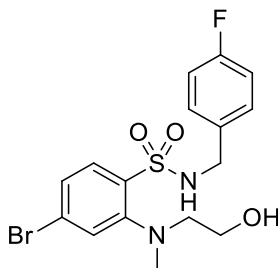


Utilizing general procedure B, **2j** (0.130 g, 0.434 mmol, 42%) was isolated as a white solid.

**IR** (neat,  $\bar{\nu}/\text{cm}^{-1}$ ): 3489, 3120, 2958, 1574, 1532, 1453, 1396, 1332, 1255, 1064; **<sup>1</sup>H NMR** (400 MHz,  $\text{CDCl}_3$ ):  $\delta$  = 8.03 (dd,  $J$  = 7.9, 1.6 Hz, 1H), 7.59 (dt,  $J$  = 7.9, 1.6 Hz, 1H), 7.41 (dd,  $J$  = 8.0, 1.0 Hz, 1H), 7.30 (dt,  $J$  = 7.8, 1.1 Hz, 1H), 6.53 (brs, 1H), 3.84 (dd,  $J$  = 10.2, 5.1 Hz, 2H), 3.54–3.45 (m, 1H), 3.18–3.09 (m, 2H), 2.84–2.76 (m, 4H), 1.76–1.57 (m, 4H), 1.50–1.32 (m, 4H); **<sup>13</sup>C NMR** (126 MHz,  $\text{CDCl}_3$ ):  $\delta$  = 152.4, 137.1,

133.6, 129.8, 125.4, 124.3, 60.1, 59.2, 55.5, 41.8, 33.0, 23.1; **HRMS** calculated for  $C_{14}H_{22}N_2NaO_3S$  ( $M+Na$ )<sup>+</sup> 321.1249; found 321.1254 (TOF MS ES<sup>+</sup>).

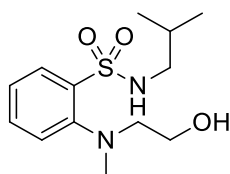
**4-Bromo-*N*-(4-fluorobenzyl)-2-((2-hydroxyethyl)(methyl)amino)benzenesulfonamide (2k)**



Utilizing general procedure B, **2k** (0.150 g, 0.360 mmol, 52%) was isolated as a white solid.

**IR** (neat,  $\bar{\nu}/\text{cm}^{-1}$ ): 3494, 2958, 1571, 1523, 1453, 1386, 1342, 1321, 1259, 1060; **<sup>1</sup>H NMR** (400 MHz,  $CDCl_3$ ):  $\delta$  = 7.87 (d,  $J$  = 8.4 Hz, 1H), 7.45 (dd,  $J$  = 8.4, 1.8 Hz, 1H), 7.41 (d,  $J$  = 1.8 Hz, 1H), 7.34–7.29 (m, 1H), 7.16 (dd,  $J$  = 8.5, 5.4 Hz, 2H), 6.94–6.89 (m, 2H), 3.96 (d,  $J$  = 6.4 Hz, 2H), 3.77 (brs, 2H), 3.04–3.01 (m, 2H), 2.64 (s, 3H), 2.28–2.16 (m, 1H); **<sup>13</sup>C NMR** (126 MHz,  $CDCl_3$ ):  $\delta$  = 163.2, 161.2, 153.5, 135.7, 132.6, 131.2, 129.9, 129.8, 128.6, 128.1, 128.0, 127.8, 115.3, 115.1, 59.2, 46.8, 42.6; **HRMS** calculated for  $C_{16}H_{18}BrFN_2NaO_3S$  ( $M+Na$ )<sup>+</sup> 439.0103; found 439.0071 (TOF MS).

**2-((2-Hydroxyethyl)(methyl)amino)-*N*-isobutylbenzenesulfonamide (2l)**

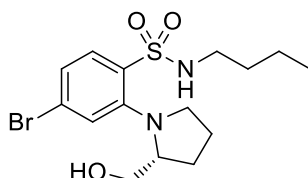


Utilizing general procedure B, **2l** (0.201 g, 0.701 mmol, 54%) was isolated as a white solid.

**IR** (neat,  $\bar{\nu}/\text{cm}^{-1}$ ): 3501, 3296, 2958, 2358, 1558, 1521, 1473, 1419, 1319, 1163, 1068  $\text{cm}^{-1}$ ; **<sup>1</sup>H NMR** (400 MHz,  $CDCl_3$ ):  $\delta$  = 8.03 (dd,  $J$  = 7.9, 1.6 Hz, 1H), 7.59 (dt,  $J$  = 7.9, 1.6 Hz, 1H), 7.42 (dd,  $J$  = 8.0, 1.0 Hz, 1H), 7.33 (dt,  $J$  = 7.9, 1.1 Hz, 1H), 6.65 (t,  $J$  = 6.2 Hz, 1H), 3.82 (q,  $J$  = 4.6 Hz, 2H), 3.12 (t,  $J$  = 4.6 Hz, 2H), 2.79 (s, 3H), 2.71 (brs, 1H), 2.57 (t,  $J$  = 6.7 Hz, 2H), 1.82–1.76 (m, 1H), 0.91 (d,  $J$  = 6.7 Hz, 6H); **<sup>13</sup>C NMR**

**NMR** (126 MHz, CDCl<sub>3</sub>):  $\delta$  = 152.2, 135.9, 133.7, 130.2, 125.5, 124.3, 60.3, 59.2, 50.8, 42.1, 28.7, 20.1; **HRMS** calculated for C<sub>13</sub>H<sub>22</sub>N<sub>2</sub>NaO<sub>3</sub>S (M+Na)<sup>+</sup> 309.1249; found 309.1234 (TOF MS ES+).

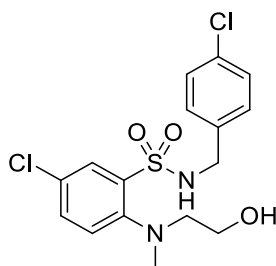
**(*R*)-4-Bromo-*N*-butyl-2-(2-(hydroxymethyl)pyrrolidin-1-yl)benzenesulfon-amide (2m)**



Utilizing general procedure B, **2m** (0.111 g, 0.284 mmol, 44%) was isolated as a brown thick liquid.

$[\alpha]_D^{20}$  = +3.4° (*c* = 1.0, CHCl<sub>3</sub>); **IR** (neat,  $\bar{\nu}$ /cm<sup>-1</sup>): 3498, 3220, 2956, 1573, 1529, 1388, 1319, 1163, 1083; **<sup>1</sup>H NMR** (400 MHz, CDCl<sub>3</sub>):  $\delta$  = 7.83 (d, *J* = 8.4 Hz, 1H), 7.49 (s, 1H), 7.40 (d, *J* = 8.4 Hz, 1H), 6.09 (s, 1H), 3.61–3.56 (m, 2H), 3.50 (s, 2H), 2.93–2.76 (m, 4H), 2.09–2.04 (m, 1H), 1.93 (s, 3H), 1.53–1.42 (m, 2H), 1.34–1.27 (m, 3H), 0.87 (t, *J* = 6.5 Hz, 2H); **<sup>13</sup>C NMR** (126 MHz, CDCl<sub>3</sub>):  $\delta$  = 151.3, 136.8, 131.1, 128.8, 128.4, 127.8, 65.7, 62.4, 58.4, 43.5, 32.0, 26.5, 24.4, 19.8, 13.7; **HRMS** calculated for C<sub>15</sub>H<sub>23</sub>BrN<sub>2</sub>NaO<sub>3</sub>S (M+Na)<sup>+</sup> 413.0510; found 413.0519 (TOF MS).

**5-Chloro-*N*-(4-chlorobenzyl)-2-((2-hydroxyethyl)(methyl)amino)benzenesulfon-amide (2n)**



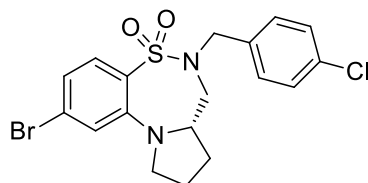
Utilizing general procedure B, **2n** (0.180 g, 0.462 mmol, 46%) was isolated as a brown solid.

**IR** (neat,  $\bar{\nu}$ /cm<sup>-1</sup>): 3502, 2358, 2331, 1490, 1471, 1325, 1161; **<sup>1</sup>H NMR** (400 MHz, CDCl<sub>3</sub>):  $\delta$  = 7.95 (d, *J* = 2.5 Hz, 1H), 7.51 (dt, *J* = 8.1, 4.1 Hz, 2H), 7.24 (d, *J* = 8.5 Hz, 1H), 7.22–7.14 (m, 4H), 4.01 (d, *J* = 6.5 Hz, 2H), 3.78 (m, 2H), 3.05–2.99 (m, 2H), 2.64 (s, 3H), 2.32 (m, 1H); **<sup>13</sup>C NMR** (126 MHz, CDCl<sub>3</sub>):  $\delta$  = 150.8, 138.2, 135.3,



133.6, 133.4, 131.1, 129.7, 129.5, 128.5, 125.9, 59.1, 59.0, 46.9, 42.9; **HRMS** calculated for  $C_{16}H_{18}Cl_2N_2NaO_3S$  ( $M+Na$ )<sup>+</sup> 411.0313; found 411.0310 (TOF MS ES+).

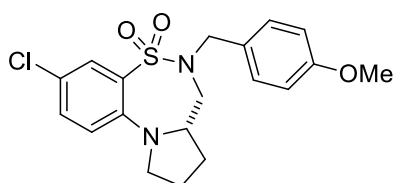
**(S)-2-Bromo-6-(4-chlorobenzyl)-6,7,7a,8,9,10-hexahydrobenzo[*f*] pyrrolo-[2,1-*d*] [1,2,5]thiadiazepine 5,5-dioxide (3a)**



Utilizing general procedure C, **3a** (0.086 g, 0.195 mmol, 85%) was isolated as a brown thick liquid.

$[\alpha]_D^{20} = -65.6^\circ$  ( $c = 1.0$ ,  $CHCl_3$ ); **IR** (neat,  $\bar{\nu}/cm^{-1}$ ): 2961, 2937, 1578, 1539, 1467, 1410, 1338, 1155, 1095; **<sup>1</sup>H NMR** (500 MHz,  $CDCl_3$ ):  $\delta = 7.72$  (d,  $J = 8.5$  Hz, 1H), 7.33–7.28 (m, 2H), 7.23 (d,  $J = 8.4$  Hz, 2H), 7.04 (dd,  $J = 8.4, 1.4$  Hz, 1H), 6.96 (s, 1H), 4.40–4.22 (m, 3H), 3.40–3.29 (m, 3H), 2.86 (brs, 1H), 2.14–1.99 (m, 2H), 1.98–1.83 (m, 1H), 1.63–1.60 (m, 1H); **<sup>13</sup>C NMR** (126 MHz,  $CDCl_3$ ):  $\delta = 146.6, 134.5, 133.8, 130.8, 129.7$  (2C), 128.8 (2C), 127.6, 127.1, 121.9, 118.5, 59.6, 54.3, 53.2, 51.2, 29.7, 23.5; **HRMS** calculated for  $C_{18}H_{19}BrClN_2O_2S$  ( $M+H$ )<sup>+</sup> 441.0039; found 441.0040 (TOF MS).

**(S)-3-Chloro-6-(4-methoxybenzyl)-6,7,7a,8,9,10-hexahydrobenzo[*f*]pyrrolo-[2,1-*d*] [1,2,5]thiadiazepine 5,5-dioxide (3b)**

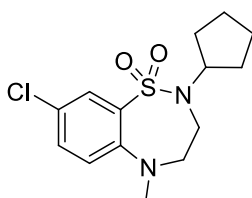


Utilizing general procedure C, **3b** (0.101 g, 0.257 mmol, 88%) was isolated as a brown thick liquid.

$[\alpha]_D^{20} = -106.5^\circ$  ( $c = 1.05$ ,  $CHCl_3$ ); **IR** (neat,  $\bar{\nu}/cm^{-1}$ ): 2952, 1733, 1591, 1512, 1471, 1338, 1245, 1153, 1058; **<sup>1</sup>H NMR** (500 MHz,  $CDCl_3$ ):  $\delta = 7.88$  (d,  $J = 2.4$  Hz, 1H), 7.31 (dd,  $J = 8.9, 2.5$  Hz, 1H), 7.22 (d,  $J = 8.6$  Hz, 2H), 6.89–6.85 (m, 2H), 6.79 (brs, 1H), 4.27 (brs, 2H), 3.82 (s, 3H), 3.33–3.28 (m, 4H), 3.04 (brs, 1H), 2.15–2.02 (m, 2H), 2.01–1.91 (m, 1H), 1.63–1.58 (m, 1H); **<sup>13</sup>C NMR** (126 MHz,  $CDCl_3$ ):  $\delta = 159.4,$

144.3, 132.6, 129.8 (2C), 129.4, 128.9, 127.7, 123.8, 116.9, 114.0 (2C), 59.3, 55.3, 53.6, 53.1, 51.3, 29.8, 23.6; **HRMS** calculated for  $C_{19}H_{21}ClN_2NaO_3S$  ( $M+Na$ )<sup>+</sup> 415.0859; found 415.0864 (TOF MS).

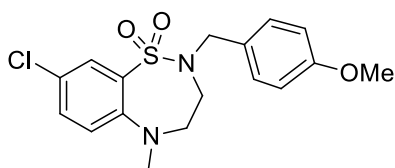
**8-Chloro-2-cyclopentyl-5-methyl-2,3,4,5-tetrahydrobenzo[*f*][1,2,5] thiadiazepine 1,1-dioxide (3c)**



Utilizing general procedure C, **3c** (0.054 g, 0.172 mmol, 81%) was isolated as a brown solid.

**IR** (neat,  $\bar{\nu}/\text{cm}^{-1}$ ): 2952, 1733, 1716, 1558, 1490, 1394, 1323, 1151, 1054; **<sup>1</sup>H NMR** (400 MHz,  $\text{CDCl}_3$ ):  $\delta$  = 7.84 (d,  $J$  = 2.6 Hz, 1H), 7.32–7.27 (m, 1H), 6.83 (d,  $J$  = 8.9 Hz, 1H), 4.24–4.14 (m, 1H), 3.63–3.56 (m, 2H), 3.51–3.44 (m, 2H), 3.06 (s, 3H), 1.77–1.74 (m, 2H), 1.66–1.61 (m, 2H), 1.57–1.41 (m, 4H); **<sup>13</sup>C NMR** (126 MHz,  $\text{CDCl}_3$ ):  $\delta$  = 146.7, 132.4, 132.2, 128.6, 124.3, 117.7, 59.5, 54.3, 44.3, 41.7, 29.5, 22.8; **HRMS** calculated for  $C_{14}H_{19}ClN_2O_2S$  ( $M+H$ )<sup>+</sup> 315.0934; found 315.0949 (TOF MS ES<sup>+</sup>).

**8-Chloro-2-(4-methoxybenzyl)-5-methyl-2,3,4,5-tetrahydrobenzo[*f*][1,2,5] thiadiazepine 1,1-dioxide (3d)**

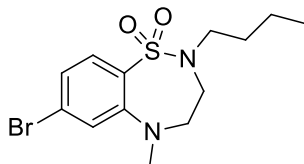


Utilizing general procedure C, **3d** (0.087 g, 0.237 mmol, 83%) was isolated as colorless oil.

**IR** (neat,  $\bar{\nu}/\text{cm}^{-1}$ ): 2952, 1733, 1591, 1512, 1471, 1338, 1245, 1153, 1058; **<sup>1</sup>H NMR** (400 MHz,  $\text{CDCl}_3$ ):  $\delta$  = 7.95 (d,  $J$  = 2.6 Hz, 1H), 7.40 (dd,  $J$  = 8.8, 2.6 Hz, 1H), 7.27–7.23 (m, 2H), 6.99 (d,  $J$  = 8.8 Hz, 1H), 6.91–6.86 (m, 2H), 4.19 (s, 2H), 3.82 (s, 3H), 3.43–3.37 (m, 2H), 3.32–3.25 (m, 2H), 3.03 (s, 3H); **<sup>13</sup>C NMR** (126 MHz,  $\text{CDCl}_3$ ):  $\delta$  = 159.4, 147.2, 132.9, 131.9, 129.8, 129.4, 127.4, 125.8, 119.5, 114.1, 55.3, 51.5,

51.3, 46.9, 42.6; **HRMS** calculated for  $C_{17}H_{20}ClN_2O_3S$  ( $M+H$ )<sup>+</sup> 367.8703; found 367.8732 (TOF MS ES<sup>+</sup>).

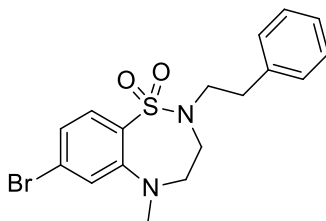
**7-Bromo-2-butyl-5-methyl-2,3,4,5-tetrahydrobenzo[*f*][1,2,5]thiadiazepine 1,1-dioxide (3e)**



Utilizing general procedure C, **3e** (0.05 g, 0.144 mmol, 80%) was isolated as a colorless thick liquid.

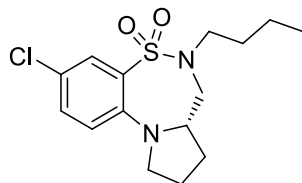
**IR** (neat,  $\bar{\nu}/\text{cm}^{-1}$ ): 2956, 1577, 1542, 1481, 1373, 1326, 1153, 1093; **<sup>1</sup>H NMR** (400 MHz,  $\text{CDCl}_3$ ):  $\delta$  = 7.73 (d,  $J$  = 8.3 Hz, 1H), 7.15–7.10 (m, 2H), 3.54–3.47 (m, 2H), 3.36–3.31 (m, 2H), 3.06 (s, 3H), 2.99 (t,  $J$  = 7.2 Hz, 2H), 1.61–1.51 (m, 2H), 1.38–1.31 (m, 2H), 0.92 (t,  $J$  = 7.3 Hz, 3H); **<sup>13</sup>C NMR** (126 MHz,  $\text{CDCl}_3$ ):  $\delta$  = 148.5, 130.2, 128.5, 126.4, 122.4, 119.9, 75.7, 51.2, 47.4, 41.5, 29.7, 18.7, 12.7; **HRMS** calculated for  $C_{13}H_{19}BrN_2NaO_2S$  ( $M+Na$ )<sup>+</sup> 369.0248; found 369.0251 (TOF MS ES<sup>+</sup>).

**7-Bromo-5-methyl-2-phenethyl-2,3,4,5-tetrahydrobenzo[*f*][1,2,5]thiadiazepine 1,1-dioxide (3f)**



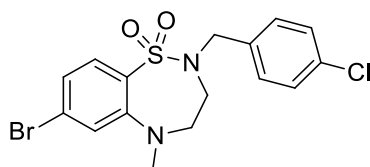
Utilizing general procedure C, **3f** (0.046 g, 0.116 mmol, 98%) was isolated as a colorless thick liquid.

**IR** (neat,  $\bar{\nu}/\text{cm}^{-1}$ ): 2925, 1577, 1541, 1481, 1436, 1328, 1153, 1091; **<sup>1</sup>H NMR** (400 MHz,  $\text{CDCl}_3$ ):  $\delta$  = 7.76–7.72 (m, 1H), 7.34–7.27 (m, 2H), 7.24–7.18 (m, 3H), 7.14–7.10 (m, 2H), 3.42–3.40 (m, 2H), 3.34–3.28 (m, 2H), 3.26–3.20 (m, 2H), 3.03 (s, 3H), 2.95–2.91 (m, 2H); **<sup>13</sup>C NMR** (126 MHz,  $\text{CDCl}_3$ ):  $\delta$  = 149.5, 138.3, 131.2, 129.4, 128.9, 128.6, 127.5, 126.6, 123.4, 120.9, 52.5, 51.1, 49.8, 42.4, 36.2; **HRMS** calculated for  $C_{17}H_{19}BrN_2NaO_2S$  ( $M+Na$ )<sup>+</sup> 417.0248; found 417.0247 (TOF MS).

**(S)-6-Butyl-3-chloro-6,7,7a,8,9,10-hexahydrobenzo[*f*]pyrrolo[2,1-*d*][1,2,5] thiadiazepine 5,5-dioxide (3g)**

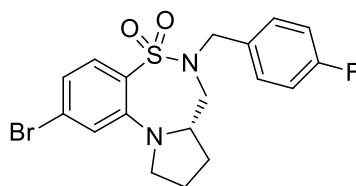
Utilizing general procedure C, **3a** (0.085 g, 0.260 mmol, 89%) was isolated as a yellow oil.

$[\alpha]_D^{20} = -120.0^\circ$  ( $c = 0.6$ ,  $\text{CHCl}_3$ ); **IR** (neat,  $\bar{\nu}/\text{cm}^{-1}$ ): 2957, 2932, 2872, 1591, 1472, 1396, 1337, 1150, 1057, 808;  **$^1\text{H}$  NMR** (400 MHz,  $\text{CDCl}_3$ ):  $\delta = 7.81$  (d,  $J = 2.5$  Hz, 1H), 7.30–7.24 (m, 1H), 6.78 (d,  $J = 8.4$  Hz, 1H), 4.19 (bs, 1H), 3.54–3.40 (m, 1H), 3.40–3.25 (m, 2H), 3.09 (bs, 3H), 2.18–1.94 (m, 3H), 1.72–1.65 (m, 1H), 1.59–1.48 (m, 2H), 1.33 (dq,  $J = 15.0, 7.3$  Hz, 2H), 0.90 (t,  $J = 7.3$  Hz, 3H);  **$^{13}\text{C}$  NMR** (126 MHz,  $\text{CDCl}_3$ ):  $\delta = 144.3, 132.5, 129.1, 123.9, 117.0, 59.2, 55.1, 51.4, 49.8, 30.8, 29.8, 23.6, 19.7, 13.7$ ; **HRMS** calculated for  $\text{C}_{15}\text{H}_{22}\text{ClN}_2\text{O}_2\text{S}$  ( $\text{M}+\text{H}^+$ ) 329.1091; found 329.1096 (TOF MS).

**7-Bromo-2-(4-chlorobenzyl)-5-methyl-2,3,4,5-tetrahydrobenzo[*f*][1,2,5]thia-diazepine 1,1-dioxide (3h)**

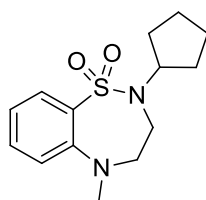
Utilizing general procedure C, **3a** (0.099 g, 0.239 mmol, 82%) was isolated as a yellow oil.

**IR** (neat,  $\bar{\nu}/\text{cm}^{-1}$ ): 2947, 2883, 1578, 1489, 1327, 1277, 1155, 1092, 976;  **$^1\text{H}$  NMR** (500 MHz,  $\text{CDCl}_3$ ):  $\delta = 7.80$ –7.75 (m, 1H), 7.33–7.29 (m, 2H), 7.27–7.24 (m, 2H), 7.16–7.14 (m, 2H), 4.19 (s, 2H), 3.37 (s, 4H), 3.03 (s, 3H);  **$^{13}\text{C}$  NMR** (126 MHz,  $\text{CDCl}_3$ ):  $\delta = 149.5, 134.3, 133.9, 131.1, 129.7, 129.3, 128.9, 127.8, 123.6, 121.0, 51.9, 51.6, 47.5, 42.4, 29.7$ ; **HRMS** calculated for  $\text{C}_{16}\text{H}_{17}\text{BrClN}_2\text{O}_2\text{S}$  ( $\text{M}+\text{H}^+$ ) 414.9882; found 414.9870 (TOF MS).

**(S)-2-bromo-6-(4-fluorobenzyl)-6,7,7a,8,9,10-hexahydrobenzo[*f*]pyrrolo[2,1-*d*][1,2,5]thiadiazepine 5,5-dioxide (3i)**

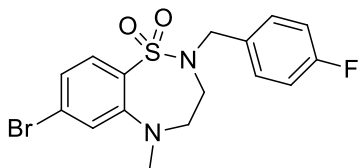
Utilizing general procedure C, **3i** (0.100 g, 0.235 mmol, 81%) was isolated as a colourless thick liquid.

$[\alpha]_D^{20} = -60.2^\circ$  ( $c = 1.05$ ,  $\text{CHCl}_3$ ); **IR** (neat,  $\bar{\nu}/\text{cm}^{-1}$ ): 2957, 2872, 1578, 1508, 1468, 1412, 1337, 1221, 1155, 781;  **$^1\text{H NMR}$**  (500 MHz,  $\text{CDCl}_3$ ):  $\delta = 7.72$  (d,  $J = 8.5$  Hz, 1H), 7.28–7.23 (m, 2H), 7.06–6.98 (m, 3H), 6.95 (s, 1H), 4.50–4.15 (m, 3H), 3.40–3.25 (m, 3H), 2.95 (brs, 1H), 2.03 (dt,  $J = 6.5, 5.7$  Hz, 2H), 1.98–1.86 (m, 1H), 1.61 (dd,  $J = 11.4, 6.4$  Hz, 1H);  **$^{13}\text{C NMR}$**  (126 MHz,  $\text{CDCl}_3$ ):  $\delta = 163.6, 161.6, 146.7, 131.8, 130.9, 130.2, 130.1, 127.7, 122.0, 118.6, 115.7, 115.6, 59.8, 54.2, 53.3, 51.3, 29.9, 23.6$ ; **HRMS** calculated for  $\text{C}_{18}\text{H}_{19}\text{BrFN}_2\text{O}_2\text{S}$  ( $\text{M}+\text{H}^+$ ) 425.0335; found 425.0331 (TOF MS).

**2-Cyclopentyl-5-methyl-2,3,4,5-tetrahydrobenzo[*f*][1,2,5]thiadiazepine 1,1-dioxide (3j)**

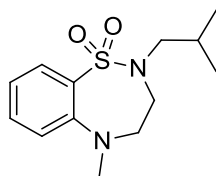
Utilizing general procedure D, **3j** (0.065 g, 0.23 mol, 79%) was isolated as a yellow oil.

**IR** (neat,  $\bar{\nu}/\text{cm}^{-1}$ ): 2953, 2872, 1593, 1491, 1321, 1148, 754, 588;  **$^1\text{H NMR}$**  (500 MHz,  $\text{CDCl}_3$ ):  $\delta = 7.85$  (dd,  $J = 7.9, 1.6$  Hz, 1H), 7.34 (ddd,  $J = 8.6, 7.3, 1.6$  Hz, 1H), 6.93–6.86 (m, 2H), 4.16 (ddd,  $J = 17.3, 9.2, 7.8$  Hz, 1H), 3.61–3.54 (m, 2H), 3.49–3.43 (m, 2H), 3.05 (s, 3H), 1.77–1.69 (m, 2H), 1.66–1.57 (m, 2H), 1.52–1.43 (m, 4H);  **$^{13}\text{C NMR}$**  (126 MHz,  $\text{CDCl}_3$ ):  $\delta = 148.2, 132.5, 131.4, 129.1, 119.4, 116.5, 59.6, 54.4, 44.5, 41.7, 29.7, 22.9$ ; **HRMS** calculated for  $\text{C}_{14}\text{H}_{21}\text{N}_2\text{O}_2\text{S}$  ( $\text{M}+\text{H}^+$ ) 281.1323; found 281.1313 (TOF MS).

**7-Bromo-2-(4-fluorobenzyl)-5-methyl-2,3,4,5-tetrahydrobenzo[f][1,2,5]thia-diazepine 1,1-dioxide (3k)**

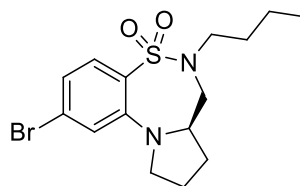
Utilizing general procedure E, **3k** (0.044 g, 0.11 mmol, 86%) was isolated as a clear oil.

**IR** (neat,  $\bar{\nu}/\text{cm}^{-1}$ ): 1577, 1467, 1409, 1321, 1155;  **$^1\text{H}$  NMR** (500 MHz,  $\text{CDCl}_3$ ):  $\delta$  = 7.79–7.77 (d,  $J$  = 8.6 Hz, 1H), 7.30–7.27 (m, 2H), 7.15 (dt,  $J$  = 4.7, 1.8 Hz, 2H), 7.04–7.00 (m, 2H), 4.19 (s, 2H), 3.37 (s, 4H), 3.02 (s, 3H);  **$^{13}\text{C}$  NMR** (126 MHz,  $\text{CDCl}_3$ ):  $\delta$  = 162.5 (d,  $^1J_{\text{C-F}}$  = 244.2 Hz), 149.5, 131.4, 131.1, 130.0 (d,  $^2J_{\text{C-F}}$  = 10.2 Hz), 129.3, 127.7, 123.5, 121.0, 115.6 (d,  $^2J_{\text{C-F}}$  = 22.0 Hz), 51.4, 47.3, 42.4; **HRMS** calculated for  $\text{C}_{16}\text{H}_{16}\text{BrFN}_2\text{NaO}_2\text{S}$  ( $\text{M}+\text{Na}$ ) $^+$  420.9998; found 420.9987 (TOF MS ES+).

**2-Isobutyl-5-methyl-2,3,4,5-tetrahydrobenzo[f][1,2,5]thiadiazepine 1,1-di-oxide (3l)**

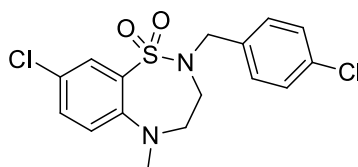
Utilizing general procedure E, **3l** (0.028 g, 0.105 mmol, 82%) was isolated as a light yellow oil.

**IR** (neat,  $\bar{\nu}/\text{cm}^{-1}$ ): 1577, 1467, 1409, 1321, 1155;  **$^1\text{H}$  NMR** (500 MHz,  $\text{CDCl}_3$ ):  $\delta$  = 7.89 (dd,  $J$  = 7.9, 1.6 Hz, 1H), 7.41 (ddd,  $J$  = 8.6, 7.3, 1.7 Hz, 1H), 7.04 (d,  $J$  = 8.3 Hz, 1H), 7.02–6.99 (m, 1H), 3.50 (t,  $J$  = 7.8 Hz, 2H), 3.29–3.25 (m, 2H), 3.06 (s, 3H), 2.74 (d,  $J$  = 7.4 Hz, 2H), 1.90 (dq,  $J$  = 13.8, 6.9 Hz, 1H), 0.94 (d,  $J$  = 6.7 Hz, 6H);  **$^{13}\text{C}$  NMR** (126 MHz,  $\text{CDCl}_3$ ):  $\delta$  = 148.6, 132.9, 130.7, 130.1, 120.6, 118.1, 55.5, 52.0, 49.4, 42.6, 27.9, 20.0; **HRMS** calculated for  $\text{C}_{13}\text{H}_{21}\text{N}_2\text{O}_2\text{S}$  ( $\text{M}+\text{H}$ ) $^+$  269.1324; found 269.1326 (TOF MS ES+).

**(R)-2-Bromo-6-butyl-6,7,7a,8,9,10-hexahydrobenzo[f]pyrrolo[2,1-d][1,2,5] thiadiazepine 5,5-dioxide (3m)**

Utilizing general procedure E, **3m** (0.038 g, 0.102 mmol, 80%) was isolated as a light yellow oil.

$[\alpha]_D^{20} = +69.0^\circ$  ( $c = 1.5$ ,  $\text{CHCl}_3$ ); **IR** (neat,  $\bar{\nu}/\text{cm}^{-1}$ ): 1577, 1467, 1409, 1321, 1155;  **$^1\text{H}$  NMR** (500 MHz,  $\text{CDCl}_3$ ):  $\delta = 7.68$  (d,  $J = 8.4$  Hz, 1H), 7.01 (dd,  $J = 8.4$ , 1.3 Hz, 1H), 6.96 (s, 1H), 3.48 (dd,  $J = 14.0$ , 6.9 Hz, 1H), 3.37 (dd,  $J = 9.9$ , 4.9 Hz, 1H), 3.31 (dt,  $J = 14.5$ , 7.4 Hz, 1H), 3.15–2.99 (m, 3H), 2.14–1.97 (m, 4H), 1.70 (dd,  $J = 11.9$ , 4.6 Hz, 1H), 1.59–1.50 (m, 2H), 1.37–1.27 (m, 2H), 0.90 (t,  $J = 7.4$  Hz, 3H);  **$^{13}\text{C}$  NMR** (126 MHz,  $\text{CDCl}_3$ ):  $\delta = 146.6$ , 130.9, 127.3, 121.8, 118.5, 55.2, 51.2, 30.8, 29.8, 23.5, 19.7, 13.7; **HRMS** calculated for  $\text{C}_{15}\text{H}_{22}\text{BrN}_2\text{O}_2\text{S}$  ( $\text{M}+\text{H}$ ) $^+$  373.0585; found 373.0585 (TOF MS ES+).

**8-Chloro-2-(4-chlorobenzyl)-5-methyl-2,3,4,5-tetrahydrobenzo[f][1,2,5]thiadiazepine 1,1-dioxide (3n)**

Utilizing general procedure E, **3n** (0.040 g, 0.107 mmol, 84%) was isolated as a light yellow oil.

**IR** (neat,  $\bar{\nu}/\text{cm}^{-1}$ ): 1577, 1467, 1409, 1321, 1155;  **$^1\text{H}$  NMR** (500 MHz,  $\text{CDCl}_3$ ):  $\delta = 7.91$  (d,  $J = 2.6$  Hz, 1H), 7.38 (dd,  $J = 8.8$ , 2.6 Hz, 1H), 7.30 (d,  $J = 8.5$  Hz, 2H), 7.26 (d,  $J = 8.5$  Hz, 2H), 6.98 (d,  $J = 8.8$  Hz, 1H), 4.19 (s, 2H), 3.38 (m, 2H), 3.32–3.28 (m, 2H), 3.02 (s, 3H);  **$^{13}\text{C}$  NMR** (126 MHz,  $\text{CDCl}_3$ ):  $\delta = 147.2$ , 134.2, 133.9, 133.1, 131.7, 129.7, 129.4, 128.9, 125.8, 119.5, 51.6, 50.8, 46.5, 43.1; **HRMS** calculated for  $\text{C}_{16}\text{H}_{17}\text{Cl}_2\text{N}_2\text{O}_2\text{S}$  ( $\text{M}+\text{H}$ ) $^+$  371.0388; found 371.0396 (TOF MS ES+).

→ Please find supporting information including  $^1\text{H}$ - and  $^{13}\text{C}$ -NMR spectra on the enclosed CD.

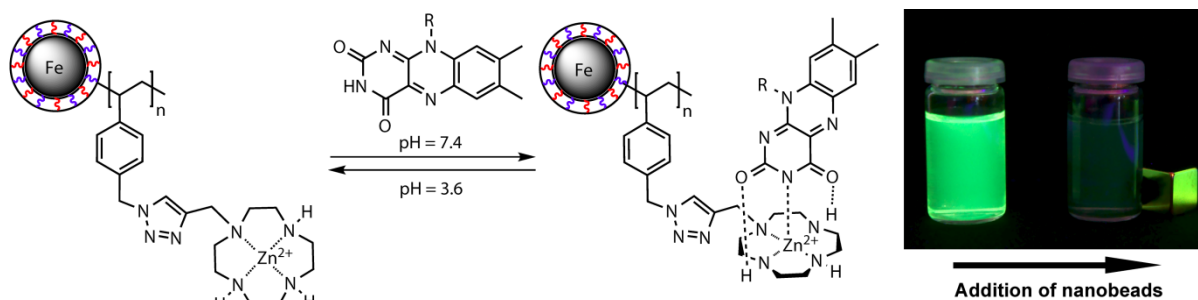


## 1.5 References

- [1] For leading reviews on the Mitsunobu reaction, see: a) O. Mitsunobu, *Synthesis* **1981**, 1–28; b) D. L. Hughes, *Org. Prep. Proced. Int.* **1996**, 28, 127–164; c) N.-H. Nam, S. Sardari, K. Parang, *J. Comb. Chem.* **2003**, 5, 479–546; d) S. Dandapani, D. P. Curran, *Chem. Eur. J.* **2004**, 10, 3130–3138; e) R. Dembinski, *Eur. J. Org. Chem.* **2004**, 2763–2772; f) T. Y. S. But, P. H. Toy, *Chem. Asian J.* **2007**, 2, 1340–1355; g) A. J. Reynolds, M. Kassiou, *Curr. Org. Chem.* **2009**, 13, 1610–1632; (h) K. C. K. Swamy, N. N. B. Kumar, E. Balaraman, K. V. P. P. Kumar, *Chem. Rev.* **2009**, 109, 2551–2651; and references cited therein.
- [2] a) M. A. Abero, N.-H. Lin, D. S. Garvey, D. E. Gunn, A.-M. Hettinger, J. T. Wasicak, P. A. Pavlik, Y. C. Martin, D. L. Donnelly-Roberts, J. P. Sullivan, M. Williams, S. P. Arneric, M. W. Holladay, *J. Med. Chem.* **1996**, 39, 817–825; b) A.-Y. Park, H. R. Moon, K. R. Kim, M. W. Chun, L. S. Jeong, *Org. Biomol. Chem.* **2006**, 22, 4065–4067; c) C. W. Zapf, J. R. Del Valle, M. Goodman, *Bioorg. Med. Chem. Lett.* **2005**, 15, 4033–4036.
- [3] a) T. Toma, Y. Kita, T. Fukuyama, *J. Am. Chem. Soc.* **2010**, 132, 10233–10235; b) M. Bruder, S. J. Smith, A. J. Blake, C. J. Moody, *Org. Biomol. Chem.* **2009**, 7, 2127–2134; c) K. G. Poul-lennec, D. Romo, *J. Am. Chem. Soc.* **2003**, 125, 6344–6345; d) P. K. M. Venukadasula, R. Chegondi, S. Maitra, P. R. Hanson, *Org. Lett.* **2010**, 12, 1556–1559.
- [4] a) J. K. Mishra, G. Panda, *J. Comb. Chem.* **2007**, 9, 321–338; b) K. Samanta, B. Chakravarti, J. K. Mishra, S. K. D. Dwivedi, L. V. Nayak, P. Choudhry, H. K. Bid, R. Konwar, N. Chattopadhyay, G. Panda, *Bioorg. Med. Chem. Lett.* **2010**, 20, 283–287.
- [5] a) Q. Chu, C. Henry, D. P. Curran, *Org. Lett.* **2008**, 10, 2453–2456; b) P. Lan, J. A. Porco Jr., M. S. South, J. J. Parlow, *J. Comb. Chem.* **2003**, 5, 660–669; c) G. W. Starkey, J. J. Parlow, D. L. Flynn, *Bioorg. Med. Chem. Lett.* **1998**, 8, 2385–2390; d) S. Danapani, J. J. Newsome, D. P. Curran, *Tetrahedron Lett.* **2004**, 45, 6653–6656; e) T. Y. S. But, P. H. Toy, *J. Am. Chem. Soc.* **2006**, 128, 9636–9637; f) B. R. Taft, E. C. Swift, B. H. Lipshutz, *Synthesis* **2009**, 2, 332–334; g) J. Yang, L. Dai, X. Wang, Y. Chen, *Tetrahedron* **2011**, 67, 1456–1462; h) M. Figlus, A. C. Tar-ruella, A. Messer, S. L. Sollis, R. C. Hartley, *Chem. Commun.* **2010**, 46, 4405–4407; i) M. Figlus, N. Wellaway, A. W. J. Cooper, S. L. Sollis, R. C. Hartley, *ACS Comb. Sci.* **2011**, 13, 280–285; j) D. E. Bergbreiter, Y.-C. Yang, C. E. Hobbs, *J. Org. Chem.* **2011**, 76, 6912–6917.
- [6] a) A. M. Harned, H. S. Song He, P. H. Toy, D. L. Flynn, P. R. Hanson, *J. Am. Chem. Soc.* **2005**, 127, 52–53; b) Of notable importance is the seminal advances made by Barrett and co-workers demonstrating the concept of reagent annihilation (norbornenyl-tagged DEAD), see; c) A. G. M. Barrett, R. S. Roberts, J. Schröder, *Org. Lett.* **2000**, 2, 2999–3001; For additional examples of in situ scavenging, see: d) J. D. Moore, A. M. Harned, J. Henle, D. L. Flynn, P. R. Hanson, *Org. Lett.* **2002**, 4, 1847–1849.
- [7] P. K. Maity, A. Rolfe, T. B. Samarakoon, S. Faisal, R. Kurtz, T. R. Long, A. Schätz, D. Flynn, R. N. Grass, W. J. Stark, O. Reiser, P. R. Hanson, *Org. Lett.* **2011**, 1, 8–10.
- [8] Cat-B: a) M. Scholl, S. Ding, C. W. Lee, R. H. Grubbs, *Org. Lett.* **1999**, 1, 953–956. It should be noted that the Grubbs first generation catalyst (PCy<sub>3</sub>)<sub>2</sub>(Cl)<sub>2</sub>Ru=CHPh [Cat-A] is deactivated in the presence of Ph<sub>3</sub>P=O; b) P. Schwab, R. H. Grubbs, J. W. Ziller, *J. Am. Chem. Soc.* **1996**, 118, 100–110; c) P. Schwab, M. B. France, J. W. Ziller, R. H. Grubbs, *Angew. Chem., Int. Ed. Engl.* **1995**, 34, 2039–2041.
- [9] a) M. R. Buchmeiser, F. Sinner, M. Mupa, K. Wurst, *Macromolecules* **2000**, 33, 32–39; b) J. O. Krause, S. Lubbad, O. Nuyken, M. R. Buchmeiser, *Adv. Synth. Catal.* **2003**, 345, 996–1004; c) N. Y. Kim, N. L. Jeon, I. S. Choi, S. Takami, Y. Harada, K. R. Finnie, G. S. Girolami, R. G. Nuz-zo, G. S. Whitesides, P. E. Laibinis, *Macromolecules* **2000**, 33, 2793–2795.
- [10] A. Rolfe, J. K. Loh, P. K. Maity, P. R. Hanson, *Org. Lett.* **2011**, 13, 4–7.
- [11] a) A. Schätz, T. R. Long, R. N. Grass, W. J. Stark, P. R. Hanson, O. Reiser, *Adv. Funct. Mater.* **2010**, 20, 4323–4328; b) R. N. Grass, E. K. Athanassiou, W. J. Stark, *Angew. Chem.* **2007**, 119, 4996–4999; c) A. Schätz, R. N. Grass, W. J. Stark, O. Reiser, *Chem. Eur. J.* **2008**, 14, 8262–8266; d) A. Schätz, R. N. Grass, Q. Kainz, W. J. Stark, O. Reiser, *Chem. Mater.* **2010**, 22, 305–310; e) S. Wittmann, A. Schätz, R. N. Grass, W. J. Stark, O. Reiser, *Angew. Chem. Int. Ed.* **2010**, 49, 1867–1870.

- [12] a) L. K. Ottesen, C. A. Olsen, M. Witt, J. W. Jaroszewski, H. Franzyk, *Chem. Eur. J.* **2009**, *15*, 2966–2978; b) P. Arya, C.-Q. Wei, M. L. Barnes, M. Daroszewska, *J. Comb. Chem.* **2004**, *6*, 65–72; c) P.-P. Kung, E. Swayze, *Tetrahedron Lett.* **1999**, *40*, 5651–5654; d) L. Banfi, A. Basso, L. Giardini, R. Riva, V. Rocca, G. Guanti, *Eur. J. Org. Chem.* **2011**, 100–109.
- [13] a) A. Rolfe, T. B. Samarakoon, P. R. Hanson, *Org. Lett.* **2010**, *12*, 1216–1219; b) A. Rolfe, T. B. Samarakoon, S. V. Klimberg, M. Brzozowski, B. Neuenswander, G. H. Lushington, P. R. Hanson, *J. Comb. Chem.* **2010**, *12*, 850–854; c) T. B. Samarakoon, M. Y. Hur, R. D. Kurtz, P. R. Hanson, *Org. Lett.* **2010**, *12*, 2182–2185; d) F. Ullah, T. B. Samarakoon, A. Rolfe, R. D. Kurtz, P. R. Hanson, M. G. Organ, *Chem. Eur. J.* **2010**, 10959–10962.

## 2. Magnetic Nanobeads as Support for Zinc(II)–Cyclen Complexes: Selective and Reversible Extraction of Riboflavin<sup>i</sup>



**Fishing for riboflavin:** Highly magnetic polymer-coated Fe/C nanoparticles are used as supports for zinc(II)–cyclen complexes. Quantitative and reversible extraction of riboflavin (vitamin B<sub>2</sub>) from aqueous solutions and a vitamin dietary supplement is achieved retaining high efficacy for six consecutive cycles. Applying an external magnetic field readily recycles the nanobeads.<sup>ii</sup>

<sup>i</sup> Reproduced with permission from: Q. M. Kainz, A. Späth, S. Weiss, A. Schätz, W. J. Stark, B. König, O. Reiser, *ChemistryOpen* **2012**, 1, 125–129. Copyright 2012 The Authors.

<sup>ii</sup> The functionalization of the nanoparticles and recycling experiments were carried out by Q. M. Kainz. The syntheses of propargylated cyclen and biscyclen as well as extraction experiments were performed by A. Späth.

## 2.1 Introduction

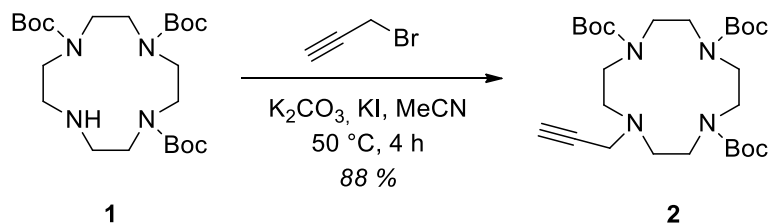
Riboflavin (vitamin B<sub>2</sub>) is essential for the health of humans and animals. Its structure is part of flavin adenine dinucleotide (FAD) and riboflavin-5'-phosphate (flavin mononucleotide, FMN), redox cofactors found among others in dehydrogenases, oxidases and photolyases.<sup>[1]</sup> A lack of vitamin B<sub>2</sub> can cause growth failure, seborrheic dermatitis or even cataracts and normocytic anemia.<sup>[2]</sup> Therefore, extraction and quantification of riboflavin in body fluids, like urine or blood plasma, or in nutrition supplements, for example vitamin tablets, is of analytical interest.<sup>[3]</sup>

It has been shown that artificial receptors containing zinc(II)-cyclen complexes can reversibly coordinate imide moieties, like thymine, uracil, and flavins.<sup>[4]</sup> Recent reviews outline the molecular interactions of zinc(II)-cyclen and its derivatives.<sup>[5]</sup> We previously reported on a zinc(II)-cyclen-functionalized polymer that reversibly and selectively binds flavins at physiological pH and enables the extraction of riboflavin from aqueous solutions.<sup>[6]</sup> A magnetic support would further improve this concept by allowing rapid agitation and separation by applying an external magnetic field. Various surface-modified magnetic nanoparticles<sup>[7]</sup> have been successfully employed for the extraction of histidine-tagged proteins,<sup>[8]</sup> DNA/RNA,<sup>[9]</sup> biotin-labeled antibodies,<sup>[10]</sup> or heavy metal ions<sup>[11]</sup> from aqueous media. We report here the immobilization of zinc(II)-cyclen complexes as binding motifs for the extraction and release of riboflavin from aqueous media on carbon-coated magnetic metal nanoparticles, featuring both high thermal and chemical stability, as well as high magnetization levels (158 emu/g).<sup>[12]</sup> This concept may be applied to the extraction of other target molecules by an exchange of the receptor molecules on the surface of the magnetic nanobeads. Previously, these nanobeads have been applied as supports for catalysts<sup>[13,14]</sup> or as magnetic scavengers.<sup>[15]</sup>

## 2.1 Results and Discussion

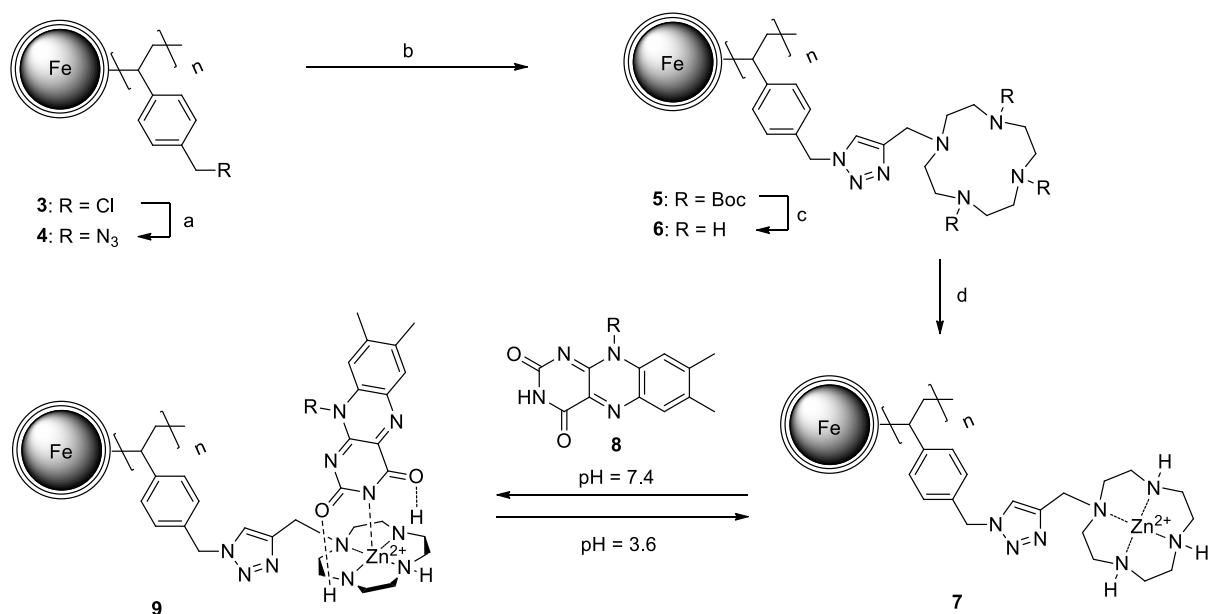
The synthesis of cyclen-functionalized nanobeads started from threefold *tert*-butoxycarbonyl (Boc)-protected cyclen **1**.<sup>[16]</sup> Propargylation applying standard conditions afforded **2** in good yields (Scheme 1). Polymer-coated magnetic support **3** was prepared by in situ grafting polymerization of 4-chloromethyl styrene on vinyl-functionalized Fe/C nanobeads following literature procedures.<sup>[17]</sup> A high loading of benzyl chloride functional groups (2.5 mmol/g) was determined for polymer-

encapsulated nanobeads **3** by elemental microanalysis. Despite their high loading, nanobeads **3** reach magnetization levels (33 emu/g) that are typical for low-loading magnetite particles ( $\sim 1$  mmol/g).<sup>[18]</sup>



**Scheme 1.** Synthesis of the propargylated and Boc-protected cyclen building block.

Exchange of chloride for azide in the polymer backbone of **3** yielded magnetic beads **4** being suitable for a “click”-reaction with propargylated cyclen **2** (Scheme 2). The reaction was monitored using attenuated total reflectance (ATR) IR spectroscopy. During the course of the reaction the benzyl chloride peak at  $1263\text{ cm}^{-1}$  decreased and a new peak at  $2093\text{ cm}^{-1}$  was detected corresponding to the introduced azide groups.<sup>[19]</sup> The azide loading calculated from nitrogen elemental analysis was 2.0 mmol/g (83% substitution). Subsequently, propargylated cyclen **2** was immobilized on **4** using copper-catalyzed azide-alkyne cycloaddition (CuAAC; Scheme 2).<sup>[20]</sup> To obtain a high degree of functionalization, 10 mol% copper(I) iodide was used and the nanoparticles were stirred for three days utilizing their intrinsic magnetic properties. Traces of copper and iron were removed by washing the particles with an ethylenediaminetetraacetic acid (EDTA) solution to prevent the formation of unwanted metal-cyclen complexes upon Boc deprotection in the later course of the synthesis. The completion of the reaction was conveniently monitored by IR-ATR spectroscopy, observing the decreasing azide peak at  $2100\text{ cm}^{-1}$  and the increasing peak of the carbonyl stretch at  $1677\text{ cm}^{-1}$ .<sup>[19]</sup> Based on the molar mass of protected cyclen **2** and the initial azide loading of particles **4**, the maximum theoretical loading for the resulting nanoparticles (**5**) functionalized with protected cyclen was calculated to be 1.0 mmol/g. In practice, owing to the high steric demand of **2** accompanied by limited penetration of the polymer shell, 0.67 mmol/g cyclen could be realized using CuAAC (67% functionalization). The cyclen loading could not be further improved by a second run. Nevertheless, this cyclen loading is about five times higher than loadings in comparable studies where conventional polymer beads were used.<sup>[6]</sup>



**Scheme 2.** Functionalization of polymer-coated Fe/C nanoparticles with a cyclen ligand using click reaction and subsequent complexation with zinc(II). Riboflavin is reversibly coordinated by these immobilized complexes. Reagents and conditions: a) NaN<sub>3</sub>, THF/H<sub>2</sub>O, 80 °C, 3 d; b) Boc-protected cyclen **2**, CuI (10 mol%), NEt<sub>3</sub>, CH<sub>2</sub>Cl<sub>2</sub>, RT, 3 d; c) TFA (25 %), CH<sub>2</sub>Cl<sub>2</sub>, RT, 6 h; then NaOH (1M), 1 h; d) Zn(ClO<sub>4</sub>)<sub>2</sub>·6H<sub>2</sub>O, NaHCO<sub>3</sub>, H<sub>2</sub>O, 80 °C, 18 h.<sup>iii</sup>

Deprotection of **5** by treatment with trifluoroacetic acid (TFA) in dichloromethane followed by deprotonation with aqueous sodium hydroxide gave polymer-coated Fe/C nanoparticles functionalized with free cyclen ligand **6**. Subsequently, the corresponding immobilized zinc(II)–cyclen complex **7** was generated by stirring **6** with zinc(II) perchlorate hexahydrate in water at pH 8. Heating to 80 °C was sufficient for this ligand to overcome the thermodynamic barrier of the complexation process.<sup>[21]</sup> Despite the high loading with polymer and the additional functionalization with cyclen and zinc(II), **7** was readily collected with a magnet within seconds. IR-ATR investigations revealed almost complete disappearance of the carbonyl peak and the appearance of a new strong peak at 1076 cm<sup>-1</sup>.<sup>[19]</sup> Inductively coupled plasma atomic emission spectroscopy (ICP-AES) was used to determine the amount of zinc(II) in **7**. The measured value of 0.65 mmol/g zinc(II) is in good agreement with the value of 0.67 mmol/g cyclen determined by elemental analysis for **5**, while the residual amount of copper was negligible (0.2 μmol/g). Transmission electron microscopy (TEM) analysis of **3** and **7** showed no substantial differences, indicating the successful and selective complexation, as zinc(II) ions coordinated by cyclen should

<sup>iii</sup> Modified to fit on page.

not be visible by this method in contrast to unselective deposition of zinc aggregates onto the nanoparticles.<sup>[19]</sup>

In order to determine the maximum loading of **7** with riboflavin (**8**), the nanoparticles were added to a stock solution of **8**. A concentration of 0.16 mmol/g could be extracted by the nanobeads as determined by UV/Vis and fluorescence measurements,<sup>[19]</sup> which is considerably lower than the calculated value if complexation of all zinc(II)–cyclen moieties would have occurred (0.52 mmol/g). It appears that not all of the binding sites can be accessed by the guest, most likely due to steric reasons.

Next, the potential application of nanocarriers **7** for the quantitative extraction of riboflavin from aqueous solutions and the recovery of riboflavin from the nanobeads by acidification was examined.<sup>[22]</sup> The typical absorption spectrum of flavin in buffer (10  $\mu$ M HEPES, pH 7.4)<sup>[23]</sup> disappeared entirely after stirring with a threefold excess of nanoparticles for 5 min indicating quantitative extraction (Figure 1A). By removing the particles via magnetic decantation and washing them with dilute hydrochloric acid (pH 3.6), almost all of the initial absorption was restored. These results were further reinforced by fluorescence measurements, also revealing full recovery of the fluorescence intensity and therefore perfect reversibility (Figure 1B). To ensure that the observed binding is not only caused by unspecific adsorption to the polymer-coated particles, a control experiment was conducted using unmodified polymer-coated nanoparticles **3**. No binding was detected by UV/Vis or fluorescence measurements.<sup>[19]</sup>

To address the question whether a polymer is necessary to shield the nanoparticle surface from unspecific adsorption of riboflavin, or if simple functionalization with the zinc(II)–cyclen complexes is sufficient, magnetic carbon-coated cobalt nanoparticles (Co/C) bearing azide groups at the surface were prepared according to literature procedures (0.1 mmol/g azide).<sup>[14,24]</sup> The Co/C nanobeads are identical to the previously described Fe/C nanobeads in magnetization, stability and functionalization. Cyclen **2** was immobilized via CuAAC, followed by its deprotection and complexation using similar conditions as for the synthesis of polymer-coated nanobeads **7**.<sup>[19]</sup> The amount of ligand immobilized on the surface was determined by elemental microanalysis as 0.06 mmol/g. The amount of zinc absorbed was again measured by ICP-AES. However, in this case, the observed zinc-loading was 0.38 mmol/g, a value about six times higher than expected for complete complexation. This indicates considerable unspecific absorption of zinc(II) onto the nanoparti

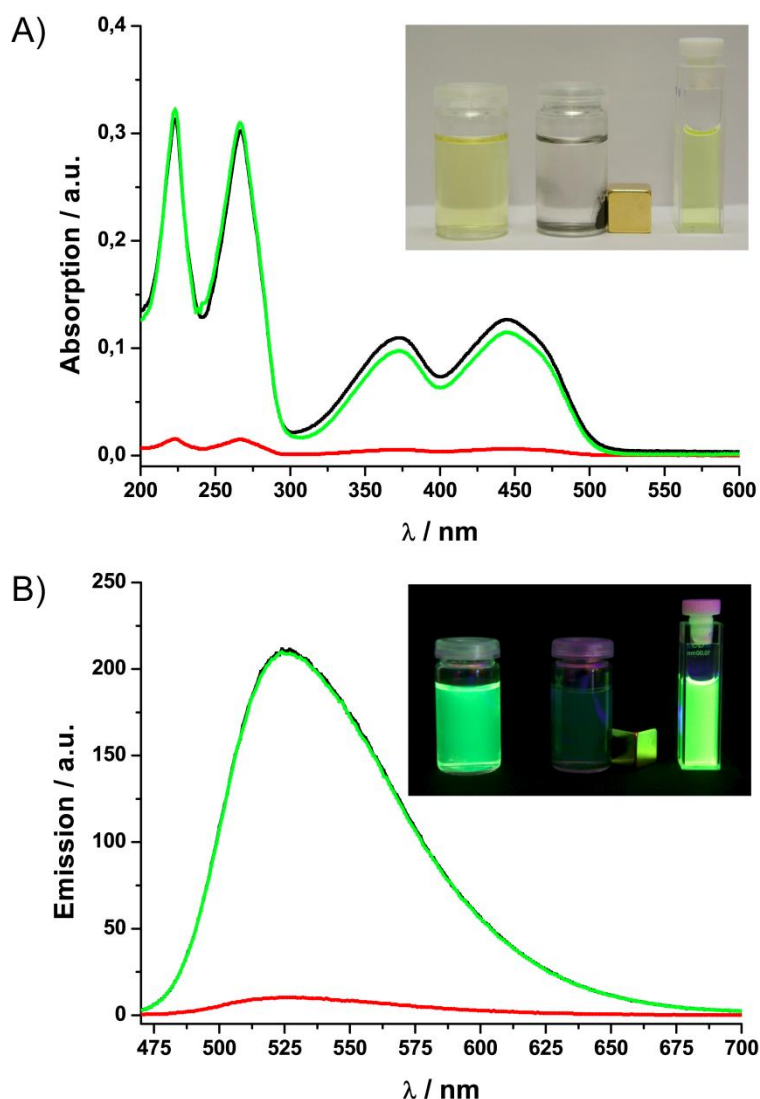


**Figure 1.** Quantitative and reversible extraction of riboflavin using polymer-coated nanobeads **7**. a) Absorption spectra and b) emission spectra. Solution of riboflavin (10  $\mu$ M, —), solution after treatment with **7** (—), recovery of riboflavin from **7** (—). The insets show photographs taken at normal daylight (a) and under UV light (b). The golden cube is a neodymium-based magnet.

cles despite the functionalization with zinc(II)–cyclen complexes.

Nevertheless, we examined the potential of the non-polymer-coated nanocarriers in the extraction and recovery of riboflavin from aqueous solutions. Although the particles were added in a sixfold excess, they were not able to remove riboflavin quantitatively from the sample solution. Moreover, not all bound riboflavin can be subsequently recovered by acidification. A control experiment using unfunctionalized Co/C nanoparticles indeed proved that particles lacking the polymer, irreversibly bind considerable amounts of riboflavin to the carbon surface.<sup>[19]</sup>



The reusability of polymer-coated iron nanoparticles **7** with immobilized zinc(II)–cyclen complex was investigated by repeating the binding and release process six times using a fresh aliquot of riboflavin in buffer for each cycle (Figure 2). The binding and release ability only slightly decreased with the number of cycles, presumably by minor loss of particles in each cycle. ICP-AES measurements of the recovered nanoparticles revealed almost complete retention of zinc loading after six cycles (0.64 mmol/g, >98%), underlining the good reusability of **7** despite repetitive washing with aqueous hydrochloric acid (pH 3.6).

Additionally, we conducted quantitative analysis of riboflavin in vitamin tablets containing various vitamins as well as other additives.<sup>[19]</sup> The tablet was dissolved in

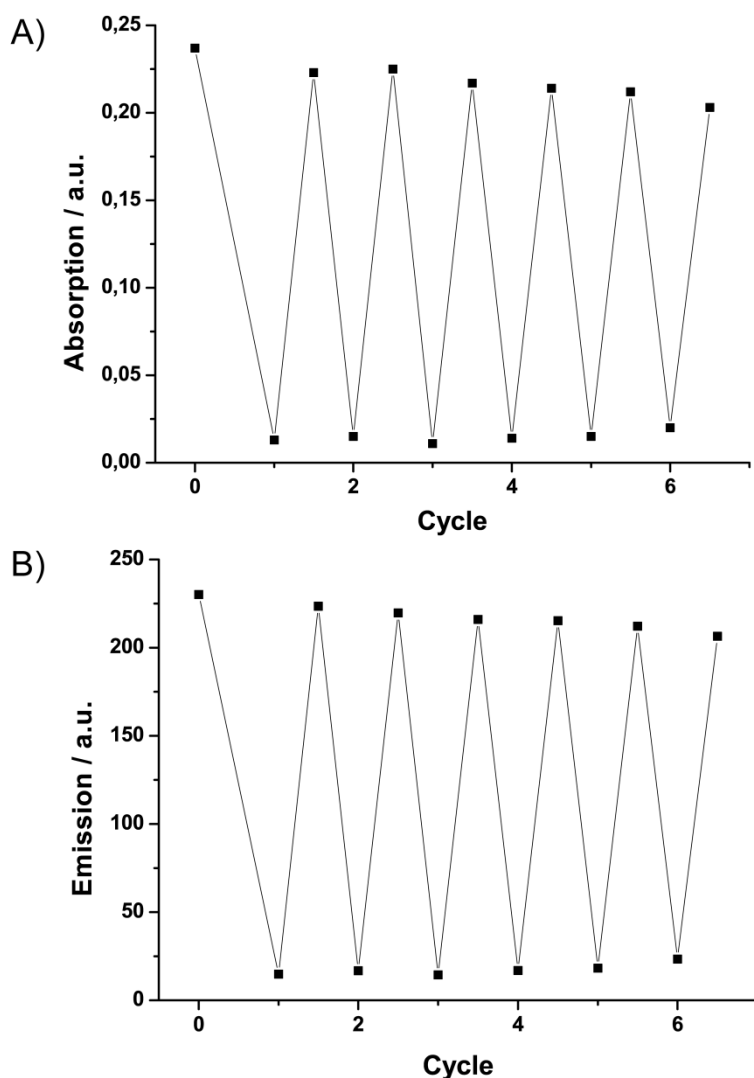


**Figure 2.** Recycling experiments using polymer-coated and zinc(II)–cyclen-functionalized nanobeads **7** (20 mg) and riboflavin-containing buffer (50 mL, 20  $\mu$ M). a) Absorption of riboflavin in solution at 445 nm and b) emission at 524 nm.

aqueous sodium hydroxide, and the solution was adjusted to pH 8. In the absorption spectrum of the vitamin-tablet solution (Figure 3), the characteristic peaks of riboflavin can be clearly identified. After treatment with **7**, these absorption bands disappear, indicating that contained flavin is completely bound to the magnetic nanoparticles. After subsequent washing of the isolated particles with aqueous hydrochloric acid (pH 3.6) and analysis of its absorption spectrum, only the typical peaks of riboflavin can be recognized in the spectrum of the washing solution. This result suggests that, of the variety of the vitamins and other substances in the tablet, only flavin was bound to the immobilized zinc(II)-cyclen complexes. The quantitative evaluation of the absorption spectrum of the washing solution resulted in a riboflavin content of

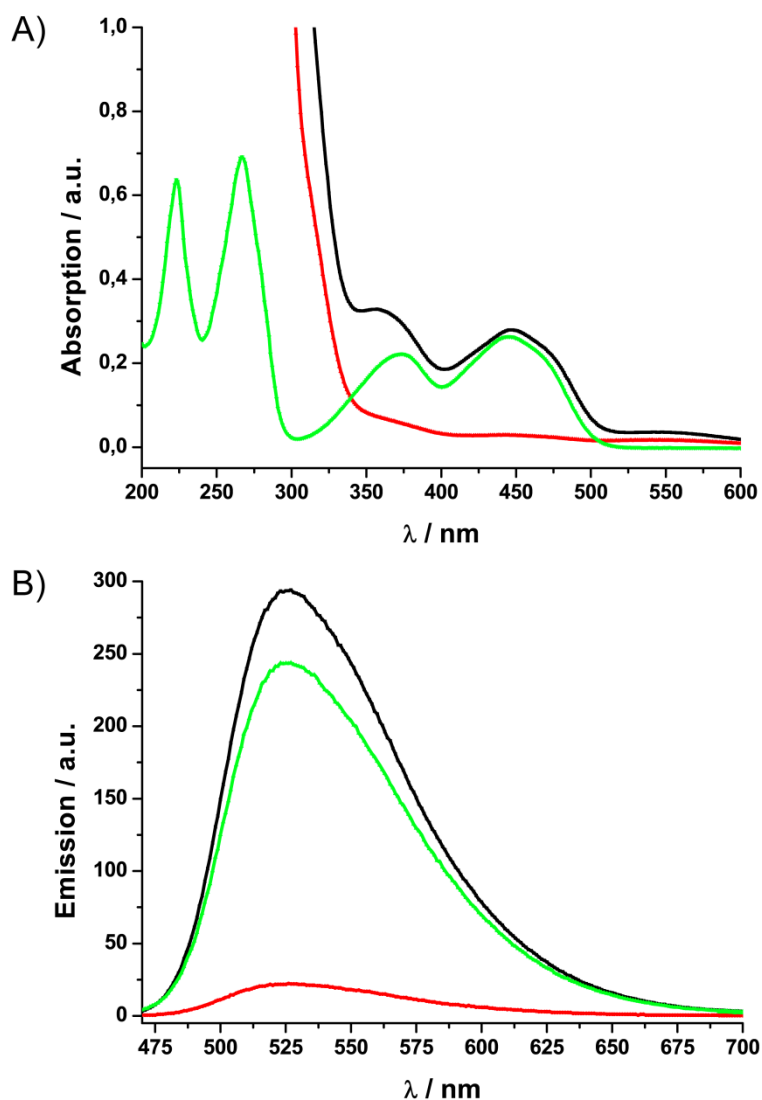


**Figure 3.** a) Absorption and b) emission spectra of riboflavin extracted from a vitamin tablet solution by zinc(II)-cyclen-functionalized nanoparticles **7**. Vitamin-tablet solution (20  $\mu$ M riboflavin, —), solution after treatment with **7** (—), recovery of riboflavin from **7** (—).

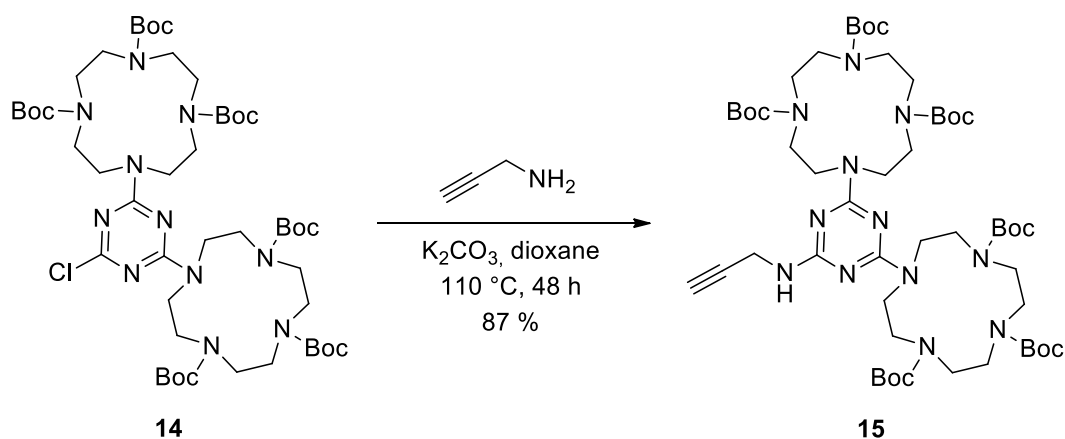
1.5 mg per tablet, which is in good accordance with the manufacturer's specifications (1.4 mg per tablet).

## 2.3 Conclusion

In conclusion, we demonstrated the successful functionalization of polymer-coated Fe/C nanobeads with zinc(II)-cyclen complexes. These nanocarriers were then applied for quantitative and reversible extraction of riboflavin from aqueous solutions. Additional experiments revealed that the polymer coating is essential to block the carbon surface of the nanobeads from unspecific adsorption of riboflavin, while simple covalent functionalization of the nanoparticles is not sufficient. The reusability of the nanobeads at high efficacy was demonstrated for six consecutive cycles. Moreover, the quantitative extraction of riboflavin from more complex matrices, for example a vitamin tablet, was also achieved. This concept could be further expanded to other important natural products by exchanging the zinc(II)-cyclen moieties on the surface of the magnetic nanobeads with other receptor molecules. Such studies are currently ongoing in our laboratories.

## 2.4 Addendum

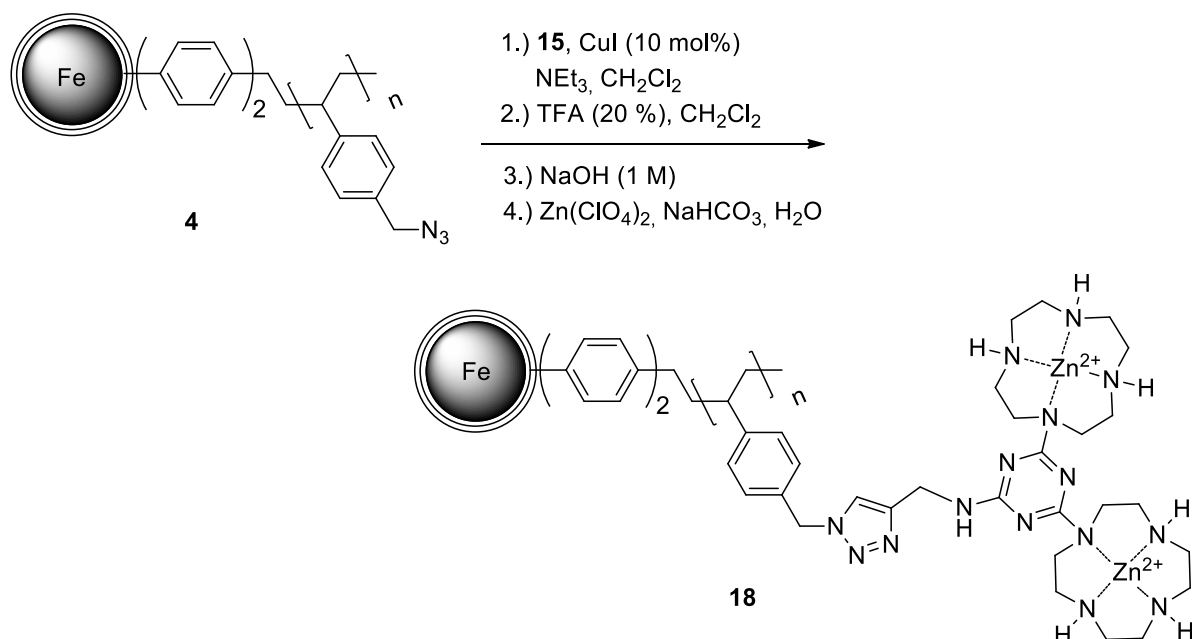
To elaborate the effects of two cyclen molecules attached to one binding site within the polymer on the efficiency of the extraction, propargylated biscyclen **15** was additionally prepared following literature procedures.<sup>[16]</sup> Stirring biscyclen chlorotriazine **14** with propargylamine under elevated temperatures for two days led to **15** in excellent yields (Scheme 3).



**Scheme 3.** Preparation of the propargylated biscyclen ligand.

The “click”-reaction between **15** and azide-tagged polymerbeads **4**, deprotection, and subsequent complexation with zinc(II) applying analogue conditions as for the cyclen immobilization resulted in zinc(II)-biscyclen functionalized nanobeads **18** (Scheme 4). The loading of the protected biscyclen **16** on the polymer beads was determined by elemental microanalysis as 0.13 mmol biscyclen/g, which results in 0.26 mmol cyclen moieties per gram of hybrid material. While this value is considerably higher as for Co/C-Cyclen (**13**), immobilizing mono-cyclen to the polymer-coated beads **4** an about 60% higher loading with cyclen moieties was achieved (0.67 mmol/g). After complexation with zinc(II) 0.24 mmol Zn/g was measured by ICP-AES for the complexed biscyclen beads **18** corresponding to more than 92% complexation. Despite this good result, the overall loading with zinc(II)cyclen moieties in **18** is only one third of the mono-cyclen functionalized beads **13** (Table 1).

The extraction and release experiments were repeated with the polymer-coated biscyclen particles **18**. Using the same amount of particles, the Fe/C-PS-Biscyclen beads (**18**) were less efficient as the Fe/C-PS-Cyclen beads (**7**) due to the lower loading.<sup>[19]</sup> Therefore, for quantitative extraction of riboflavin a higher amount of



**Scheme 4.** Loading of azide-tagged Fe/C nanobeads with zinc(II)-biscyclen complexes.

particles is required. Moreover, it can be assumed that the second binding site is not fully accessible by a second guest molecule due to steric hindrance. Taking the more elaborated synthesis for the biscyclen ligand into account, the cyclen-modified nanoparticles seem to be the superior nanomaterial for the extraction of riboflavin.

**Table 1.** Comparison of the loadings of different nanocarriers.

Entry	Particles	Loading of cyclen moieties [mmol/g] <sup>[a]</sup>	Loading of Zn [mmol/g] <sup>[b]</sup>
1	Co/C-Cyclen ( <b>13</b> )	0.06	0.38 <sup>[c]</sup>
2	Fe/C-PS-Cyclen ( <b>7</b> )	0.67	0.65
3	Fe/C-PS-Biscyclen ( <b>18</b> )	0.26	0.24

[a] Determined by nitrogen microanalysis. [b] Determined by ICP-AES; [c] Unspecific absorption of zinc onto the nanoparticle surface

## 2.5 Experimental section

### Materials and methods

Analytical characterization of the synthesized compounds was performed by common methods. IR Spectra were recorded with a Bio-Rad FT-IR Excalibur FTS 3000 equipped with a Specac *Golden Gate* Diamond Single Reflection ATR-System. Absorption spectra were recorded on a Varian Cary BIO 50 UV/VIS/NIR spectrometer with temperature control using 1 cm quartz cuvettes (Hellma) and Uvasol solvents (Merck, Baker or Acros). Fluorescence measurements were performed with UV-grade solvents (Baker or Merck) in 1 cm quartz cuvettes (Hellma) and recorded on a Varian 'Cary Eclipse' fluorescence spectrophotometer with temperature control. Electro spray mass spectra were performed on a Finnigan MAT TSQ 7000 ESI-spectrometer. NMR spectra were recorded in CDCl<sub>3</sub> on Bruker Avance 300 (<sup>1</sup>H: 300.1 MHz, <sup>13</sup>C: 75.5 MHz, T = 300 K) relative to external standards. Characterization of the signals: s = singlet, m = multiplet. Integration is determined as the relative number of atoms, the coupling constants are given in Hertz [Hz].

The carbon coated cobalt and iron nanomagnets (Co/C, Fe/C, 20.5 m<sup>2</sup>/g, mean particle size ≈ 25 nm) were purchased from Turbobeads LLC, Switzerland. Prior to use, they were washed in a concentrated HCl / water mixture (1:1) 5 times for 24 h. Acid residuals were removed by washing with millipore water (5x) and the particles were dried at 50°C in a vacuum oven.<sup>[11b]</sup> The magnetic nanobeads were dispersed using an ultrasound bath and recovered with the aid of a neodymium based magnet (15 x 30 mm). They were characterized by IR-ATR spectroscopy, elemental microanalysis (LECO CHN-900), transmission electron microscopy (Zeiss, LEO912AB, 100 kV) and ICP-AES (Spectro Analytical Instruments ICP Modula EOP). Poly(benzylchloride)styrene coated iron nanoparticles **3**<sup>[17]</sup> and azide functionalized cobalt nanoparticles **10**<sup>[13,24]</sup> and were prepared on the gram scale following previously reported procedures.

Cyclen-Boc<sub>3</sub> **1** was purchased from PolyPeptide Group. Biscyclen-Boc<sub>6</sub> **14** was prepared according to literature known procedures.<sup>[16]</sup> The vitamin pill (4.0 g) with orange flavor of TIP contains besides 1.4 mg riboflavin: Vitamin B1 (1.1 mg), vitamin B6 (1.4 mg), niacin (16 mg), folic acid (0.2 mg), Vitamin B12 (2.25 micrograms), biotin (0.05 mg), vitamin C (80 mg), vitamin E (12 mg), pantothenic acid (6.0 mg), carbohydrates (100 mg). Other ingredients are: citric acid, fructose, starch,

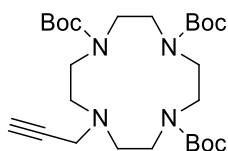
sodium bicarbonate, dye from beetroot, sodium cyclamate and sodium saccharin. All other solvents and chemicals were of reagent grade and were used without further purification.

## Nomenclature

The Nomenclature of the cyclen derivatives described in this work is as follows: Cyclen-Boc<sub>3</sub> [Tris(*tert*-butyl oxycarbonyl) 1, 4, 7, 10-tetraazacyclododecane] describes a cyclen azamacro-cycle with three *tert*-butoxycarbonyl protecting groups, whereas Biscyclen-Boc<sub>6</sub> denotes a biscyclen ligand protected with six *tert*-butoxycarbonyl groups. Acet-Cyclen-Boc<sub>3</sub> and Acet-Biscyclen-Boc<sub>3</sub> describe derivatives bearing an acetylene moiety.

For the nanoparticles the nomenclature is as follows: Co/C for magnetic nanoparticles with cobalt core and carbon shell and Fe/C for iron nanoparticles with carbon shell. Fe/C-PS-R for polystyrene coated iron nanoparticles, where R indicates the functional groups in the polymeric network: Cl for benzylchloride, N<sub>3</sub> for benzylazide, Cyclen-Boc<sub>3</sub> and Biscyclen-Boc<sub>6</sub> for *tert*-butoxycarbonyl protected cyclen as well as biscyclen, Cyclen and Biscyclen for unprotected cyclen as well as biscyclen, Cyclen-Zn and Biscyclen-Zn<sub>2</sub> for cyclen and biscyclen coordinating zinc(II).

## Synthesis of Boc-protected cyclen (Acet-Cyclen-Boc<sub>3</sub>, 2)<sup>[25]</sup>

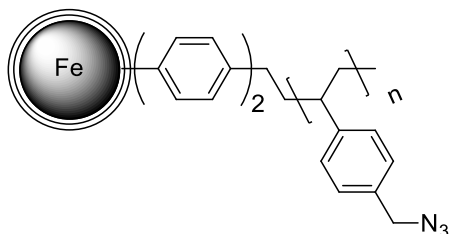


Cyclen-Boc<sub>3</sub> **1** (940 mg, 2.0 mmol) was dissolved in acetonitrile (10 ml), propargylbromide (80% in toluene, 484 mg, 0.4 mL), potassium carbonate (414 mg, 3.0 mmol) and potassium iodide (333 mg, 2.0 mmol) were added. The suspension was stirred for 2 h at room temperature and was then heated to 50°C for 4 h under light protection and nitrogen atmosphere. After cooling to room temperature a second portion of propargylbromide (80% in toluene, 484 mg, 0.4 mL) was added and the reaction mixture was kept at 50 °C under light protection and nitrogen atmosphere for 30 h. After cooling to room temperature ethyl acetate (20 mL) was added, the mixture was filtered over celite and the filter cake was washed with small amounts of ethyl acetate. The solvent was evaporated and the residue was purified by column chro-

matography with EtOAc / hexanes (1:2) to yield the product as colorless solid (900 mg, 1.76 mmol, 88%).

**Mp:** 103 - 105 °C; **<sup>1</sup>H-NMR** (300 MHz, CDCl<sub>3</sub>):  $\delta$  = 3.55 – 3.09 (m, 14 H), 2.78 – 2.60 (m, 4 H), 2.13 (s, 1 H), 1.39 (s, 27 H); **<sup>13</sup>C-NMR** (75 MHz, CDCl<sub>3</sub>, signal doubling due to rotamers):  $\delta$  = 155.99, 155.70, 155.25, 79.68, 79.45, 79.24, 73.68, 54.31, 53.19, 49.91, 47.86, 47.68, 47.05, 46.53, 39.08, 28.75, 28.49; **IR** (KBr,  $\bar{\nu}$ /cm<sup>-1</sup>): 3251, 2976, 2932, 2834, 1674, 1461, 1457, 1414, 1402, 1364, 1248, 1152, 1104, 1031, 980, 946, 917, 859, 772, 730, 647; **MS** (ESI-MS):  $m/z$  (%) = 511.2 (100, MH<sup>+</sup>), calc. 510.34.

#### Azide functionalized polymer coated iron nanoparticles (Fe/C-PS-N<sub>3</sub>, 4)

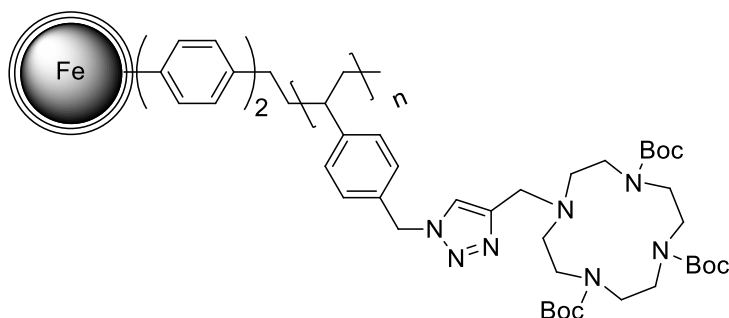


Poly(benzylchloride)styrene coated Fe/C nanoparticles **3** (1 g, 2.49 mmol) were dispersed in 10 mL of a THF / deionized water (Millipore) mixture (1:1) using an ultrasonic bath, 1.62 g (24.9 mmol) of sodium azide was added and the resulting slurry heated to 80 °C for 3 d. The particles were recovered by the aid of a magnet and washed with a THF / deionized water (Millipore) mixture (1:1, 5 x 10 mL) and acetone (3 x 10 mL). After evaporation of the solvent, 1.03 g of Fe/C-PS-N<sub>3</sub> were obtained.

**IR** ( $\bar{\nu}$ /cm<sup>-1</sup>): 2923, 2093, 1510, 1264, 813, 670; **elemental microanalysis** (%): C, 32.85; H, 2.49; N, 8.56; Cl, 2.83.



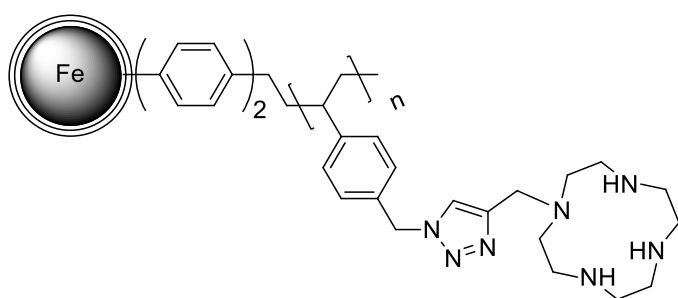
**“Click”-reaction to generate polymer coated iron nanoparticles functionalized with Boc-protected cyclen (Fe/C-PS-Cyclen-Boc<sub>3</sub>, 5)**



To 400 mg (0.82 mmol) of Fe/C-PS-N<sub>3</sub> dispersed in 10 mL of degassed dichloromethane 1.27 g (2.46 mmol) of Acet-Cyclen-Boc<sub>3</sub>, 29 mg (0.15 mmol) of copper(I) iodide and 208  $\mu$ L (1.5 mmol) triethylamine were added. The reaction mixture was stirred at room temperature for 3 d. Then, the particles were collected by a magnet and washed with dichloromethane (5 x 5 mL), aqueous EDTA (3 x 5 mL), water (3 x 5 mL) and acetone (3 x 5 mL). After drying in vacuum 805 mg of Fe/C-PS-Cyclen-Boc<sub>3</sub> were obtained.

**IR** ( $\bar{\nu}$ /cm<sup>-1</sup>): 2974, 2932, 1677, 1456, 1413, 1364, 1247, 1151, 942, 857, 822, 722, 731, 700; **elemental microanalysis** (%): C, 43.36; H, 5.55; N, 8.01; Cl, 2.45.

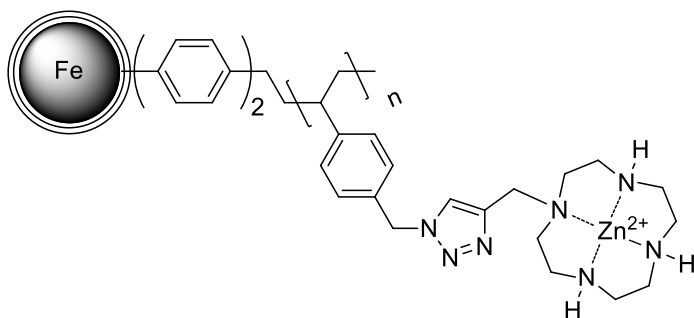
**Deprotection of the Fe/C-PS-Cyclen-Boc<sub>3</sub> to the corresponding free cyclen (Fe/C-PS-Cyclen, 6)**



Fe/C-PS-Cyclen-Boc<sub>3</sub> nanoparticles **5** (700 mg) were stirred in 10 mL of a trifluoroacetic acid / dichloromethane mixture (1:3) at ambient temperature for 6 h. After magnetic decantation the particles were washed with dichloromethane (3 x 10 mL). Deprotonation of the cyclen moieties was achieved by stirring the particles in 10 mL of aqueous NaOH (1M) for 3 h. Finally, the particles were collected by the aid of a magnet and washed with water (3 x 5 mL) and dichloromethane (5 x 10 mL). After evaporation 450 mg of Fe/C-PS-Cyclen **6** were yielded.

**IR** ( $\bar{\nu}/\text{cm}^{-1}$ ): 3252, 2917, 2811, 1685, 1510, 1439, 1345, 1196, 1110, 1042, 912, 782;  
**elemental microanalysis** (%): C, 38.04; H, 4.76; N, 10.73; Cl, 0.73.

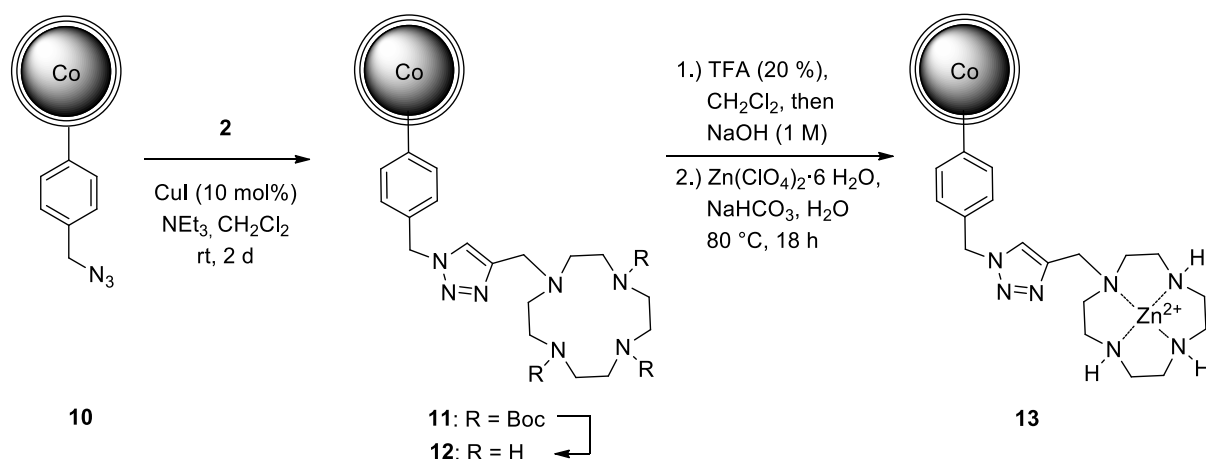
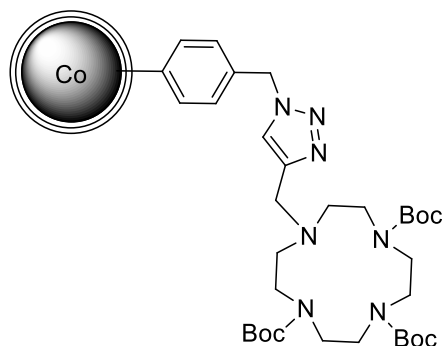
**Synthesis of zinc(II)-cyclen complexes at the surface of magnetic nanoparticles  
 (Fe/C-PS-Cyclen-Zn, 7)**



A suspension of 370 mg of Fe/C-PS-Cyclen **6** and 2.48 g (6.66 mmol) of  $\text{Zn}(\text{ClO}_4)_2 \cdot 6 \text{H}_2\text{O}$  in 10 mL of deionized water (Millipore) was prepared. The reaction mixture was buffered to pH 8 by the addition of  $\text{NaHCO}_3$  and stirred at 80 °C for 18 h. After cooling down to room temperature, the nanoparticles were recovered by a magnet and washed with water, methanol and acetone (5 x 5 mL each). 422 mg of Fe/C-PS-Cyclen-Zn **7** were obtained after drying.

**IR** ( $\bar{\nu}/\text{cm}^{-1}$ ): 3278, 2918, 2871, 1700, 1439, 1355, 1220 1076, 928, 788; **elemental microanalysis** (%): C, 33.26; H, 4.04; N, 9.23; Cl, 4.16; **ICP-AES**, Zn: 0.65 mmol/g.

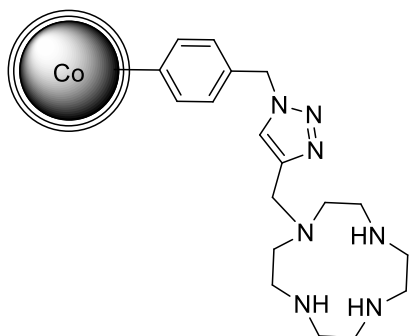
## Functionalization of Co/C nanoparticles with zinc(II)-cyclen complexes

Synthesis of cobalt nanoparticles functionalized with Boc-protected cyclen (Co/C-Cyclen-Boc<sub>3</sub>, 11)

Azide functionalized Co/C nanoparticles **10** (200 mg, 0.02 mmol) were pre-dispersed in 5 mL dichloromethane by the aid of an ultrasonic bath. Thereafter, 51 mg of Acet-Cyclen-Boc<sub>3</sub> (0.1 mmol), 2 mg of CuI (0.01 mmol) and 14  $\mu$ L of triethylamine (0.1 mmol) were added and the sonication continued for 1 h followed by stirring for 2 d at room temperature. The particles were collected by applying a magnet to the side of the reaction vessel and the supernatant was decanted. The particles were then washed with dichloromethane (5 x 5 mL), aqueous EDTA (3 x 5 mL), water (3 x 5 mL) and acetone (3 x 5 mL). After evaporation of the solvent, 201 mg of Co/C-Cyclen-Boc<sub>3</sub> **11** nanoparticles were obtained.

IR ( $\bar{\nu}$ /cm<sup>-1</sup>): 2980, 2927, 1687, 1600, 1458, 1417, 1367, 1251, 1175, 1108, 1016, 785; **elemental microanalysis** (%): C, 8.7; H, 0.24; N, 0.68.

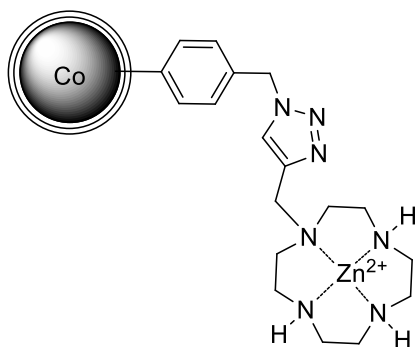
### Generation of the free cyclen tethered to the surface of magnetic cobalt nanoparticles (Co/C-Cyclen, 12)



Boc-protected particles **11** (130 mg) were stirred in a trifluoroacetic acid / dichloromethane mixture (1:4) for 3 h. After magnetic decantation and washing of the nanobeads with dichloromethane (3 x 5 mL), 5 mL of aqueous NaOH (1 M) were added and the stirring continued for 3 h. The particles were collected by a magnet and again washed with water (5 x 5 mL) and dichloromethane (5 x 5 mL). Drying under vacuum yielded 122 mg of Co/C-Cyclen nanobeads.

IR ( $\bar{\nu}/\text{cm}^{-1}$ ): 2917, 1647, 1593, 1381, 1217, 1011, 820; **elemental microanalysis** (%): C, 8.76; H, 0.18; N, 0.63.

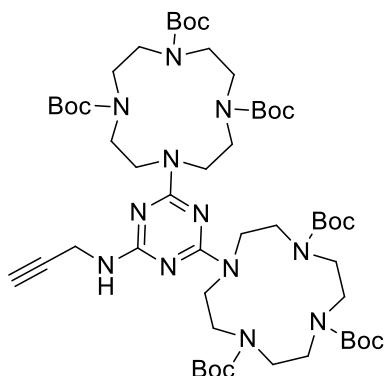
### Complexation of the free cyclen at the surface of magnetic cobalt nanoparticles with zinc(II) (Co/C-Cyclen-Zn, 13)



Nanoparticles **12** (100 mg) were dispersed in 5 mL water by sonication followed by addition of 45 mg (0.12 mmol)  $\text{Zn}(\text{ClO}_4)_2 \cdot 6 \text{H}_2\text{O}$  and  $\text{NaHCO}_3$  to buffer the solution to pH 8. The slurry was stirred at 80 °C for 18 h, cooled down to room temperature and the nanobeads recovered by magnetic decantation. After washing with water, methanol and acetone (5 x 5 mL each), the particles were dried in vacuum. 105 mg of Co/C-Cyclen-Zn nanoparticles **13** could be obtained.

**IR** ( $\bar{\nu}/\text{cm}^{-1}$ ): 2922, 2854, 1668, 1600, 1505, 1381, 1215, 1014, 963, 833; **elemental microanalysis** (%): C, 8.43; H, 0.16; N, 0.47; **ICP-AES**, Zn: 0.38 mmol/g.

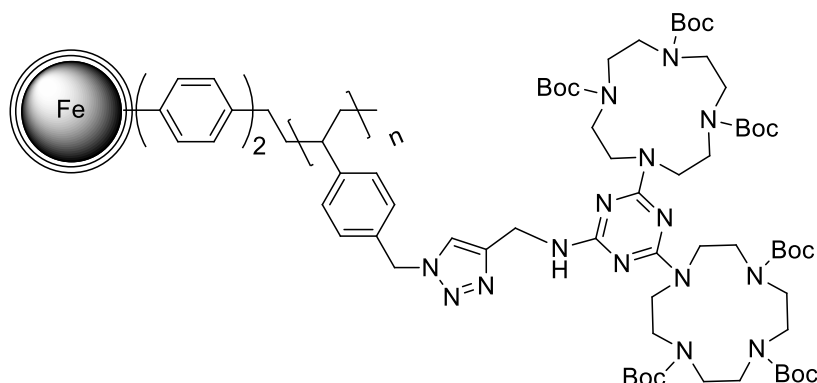
### Synthesis of Boc-protected biscyclen (Acet-Biscyclen-Boc<sub>6</sub>, **15**)<sup>[25]</sup>



Biscyclen-Boc<sub>6</sub> **14** (1.06 g, 1.0 mmol) was dissolved in 30 ml of dioxane. Potassium carbonate (690 mg, 5.0 mmol) and propargyl amine (320  $\mu\text{l}$ , 275 mg, 5.0 mmol) were added. The suspension was stirred at 110 °C in the dark under nitrogen atmosphere for 48 h. The suspension was filtered over celite and the filter cake was washed thoroughly with ethyl acetate. The solvent was evaporated under reduced pressure to obtain a brown oil, which was purified by column chromatography with ethyl acetate / petrol ether 1:2 and then again with  $\text{CH}_2\text{Cl}_2$  / MeOH 98:2. The alkyne **15** was obtained as a colorless solid in a yield of 930 mg (0.87 mmol, 87 %).

**Mp**: 149 °C; **<sup>1</sup>H-NMR** (300 MHz,  $\text{CDCl}_3$ ):  $\delta$  = 1.36 – 1.40 (m, 54 H), 2.09 (t,  $^4J$  = 2.3 Hz, 1 H), 3.21 – 3.56 (m, 32 H), 4.06 – 4.10 (m, 2 H), 4.86 (bs, 1 H); **<sup>13</sup>C-NMR** (75 MHz,  $\text{CDCl}_3$ ):  $\delta$  = 166.2, 165.4, 156.3, 81.2, 79.8, 79.7, 70.6, 50.2, 30.4, 28.5, 28.4; **IR** (KBr,  $\bar{\nu}/\text{cm}^{-1}$ ): 3403, 3313, 3256, 2978, 2933, 2103, 1681, 1539, 1478, 1412, 1368, 1249, 1177, 778; **MS** (ESI-MS):  $m/z$  (%) = 1075.8 (100,  $\text{MH}^+$ ), calc. 1075.36.

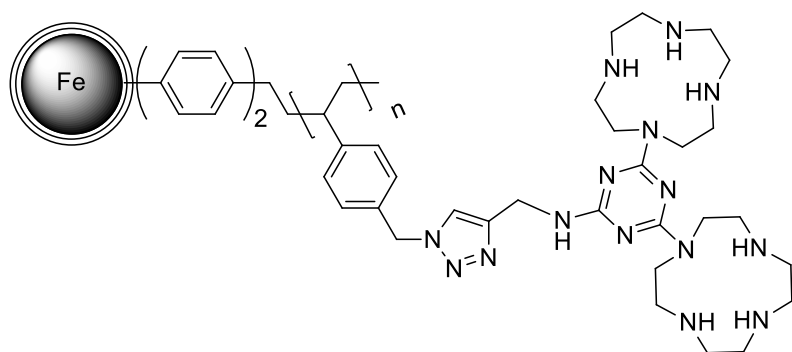
### Immobilization of Boc-protected biscyclen ligands onto polymer encapsulated iron nanoparticles via “click-reaction” (Fe/C-PS-Biscyclen-Boc<sub>6</sub>, 16)



25 mg (51  $\mu\text{mol}$ ) of Fe/C-PS-N<sub>3</sub> **4** were stirred with 201 mg (188  $\mu\text{mol}$ ) Acet-Biscyclen-Boc<sub>6</sub>, 1.8 mg (19  $\mu\text{mol}$ ) CuI and 13  $\mu\text{L}$  (188  $\mu\text{mol}$ ) Et<sub>3</sub>N in 2 mL of degassed dichloromethane for 3 d following the procedure for the synthesis of Fe/C-PS-Cyclen-Boc<sub>3</sub>. After washing with acetone (5 x 3 mL) and dichloromethane (5 x 3 mL), 65 mg of Fe/C-PS-Biscyclen-Boc<sub>6</sub> could be recovered.

**IR** ( $\bar{\nu}/\text{cm}^{-1}$ ): 3116, 2972, 2927, 1682, 1560, 1535, 1461, 1406, 1362, 1244, 1153, 811, 744; **elemental microanalysis** (%): C, 44.27; H, 5.68; N, 10.73.

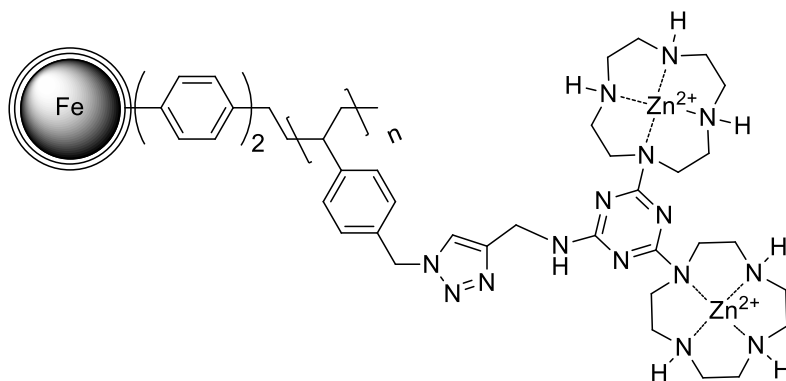
### Deprotection of Fe/C-PS-Biscyclen-Boc<sub>6</sub> to the corresponding free biscyclen (Fe/C-PS-Biscyclen-Boc<sub>6</sub>, 17)



50 mg of Fe/C-PS-Biscyclen-Boc<sub>6</sub> **16** were stirred in 3 mL of a trifluoroacetic acid / dichloro-methane mixture (1:1) at ambient temperature for 6 h analog to the procedure for the protected cyclen functionalized nanobeads. After deprotonation by stirring in 3 mL of aqueous NaOH (1 M) for 1 h, 39 mg of Fe/C-PS-Biscyclen were yielded.

IR ( $\bar{\nu}/\text{cm}^{-1}$ ): 3285, 2915, 2839, 2359, 1646, 1552, 1529, 1491, 1415, 1347, 1277, 1106, 1007, 806.

**Complexation of the free biscyclen ligand at the surface of polymer coated magnetic iron nanoparticles with zinc(II) (Fe/C-PS-Biscyclen-Zn<sub>2</sub>, 18)**



Following the procedure for cyclen functionalized iron nanoparticles, to 33 mg of Fe/C-PS-Biscyclen (**17**) 221 mg (594  $\mu\text{mol}$ ) of  $\text{Zn}(\text{ClO}_4)_2 \cdot 6 \text{H}_2\text{O}$  in 3 mL of deionized water (Millipore) were added, the mixture buffered to pH 8 by the addition of  $\text{NaHCO}_3$  and stirred at 80 °C for 18 h. 35 mg of Fe/C-PS-Biscyclen-Zn<sub>2</sub> were yielded after drying under high vacuum.

IR ( $\bar{\nu}/\text{cm}^{-1}$ ): 3356, 2913, 2847, 1645, 1532, 1484, 1417, 1349, 1065, 808; ICP-AES, Zn: 0.24 mmol/g.

**General procedure for the reversible extraction of riboflavin**

In a typical experiment the magnetic nanoparticles (10 mg) were added into a solution of riboflavin in HEPES-buffer (50 mL,  $c = 10^{-5} \text{ mol/l}$ , pH 7.6) and stirred vigorously for 5 min utilizing the intrinsic magnetic properties of the nanomagnets. Then, the nanoparticles were collected by an external magnet. A sample (1 mL) of the solution was filtered and the absorption- and emission-spectrum recorded. Subsequently, the nanoparticles were washed twice with deionized water and the riboflavin was subsequently released by stirring the particles in diluted hydrochloric acid (50 mL, pH 3.6) for 10 min. The particles were again washed twice with water and reused in the next cycle.

→ Please find supporting information including TEM pictures, IR spectra, as well as  $^1\text{H}$ - and  $^{13}\text{C}$ -NMR spectra on the enclosed CD.

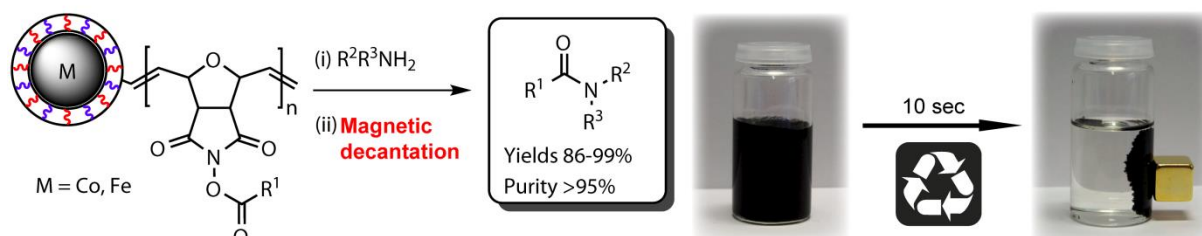


## 2.6 References

- [1] a) B. König, M. Pelka, R. Reichenbach-Klinke, J. Schelter, J. Daub, *Eur. J. Org. Chem.* **2001**, 2297–2303; b) R. Reichenbach-Klinke, M. Kruppa, B. König, *J. Am. Chem. Soc.* **2002**, 124, 12999–13007.
- [2] a) D. B. McCormick in *Modern Nutrition in Health and Disease* (Eds.: M. Shils, J. A. Olson, M. Shike, A. C. Ross), Williams & Wilkins, Baltimore, **1999**; b) H. J. Powers, *Am. J. Clin. Nutr.* **2003**, 77, 1352–1360.
- [3] a) G. Massolini, E. Lorenzi, E. Calleri, E. Tabolotti, G. Caccialanza, *J. Chromatogr. B: Biomed. Sci. Appl.* **2000**, 738, 343–355; b) S. Hustad, P. M. Ueland, J. Schneede, *Clin. Chem.* **1999**, 45, 862–868; c) C. C. Hardwick, T. R. Herivel, S. C. Hernandez, P. H. Ruane, R. P. Goodrich, *Photochem. Photobiol.* **2004**, 80, 609–615; d) A.-K. Su, C.-H. Lin, *J. Chromatogr. B* **2003**, 785, 39–46.
- [4] a) E. Kimura, T. Koike, *Chem. Commun.* **1998**, 1495–1500; b) E. Kikuta, M. Murata, N. Katsube, T. Koike, E. Kimura, *J. Am. Chem. Soc.* **1999**, 121, 5426–5436; c) B. König, M. Pelka, H. Zieg, T. Ritter, H. Bouas-Laurent, R. Bonneau, J.-P. Desvergne, *J. Am. Chem. Soc.* **1999**, 121, 1681–1687.
- [5] a) S. Aoki, E. Kimura, *Chem. Rev.* **2004**, 104, 769–787; b) M. Kruppa, B. König, *Chem. Rev.* **2006**, 106, 3520–3560.
- [6] B. König, H.-C. Gallmeier, R. Reichenbach-Klinke, *Chem. Commun.* **2001**, 2390.
- [7] a) A.-H. Lu, E. L. Salabas, F. Schüth, *Angew. Chem.* **2007**, 119, 1242–1266; *Angew. Chem. Int. Ed.* **2007**, 46, 1222–1244; b) S. Shylesh, V. Schünemann, W. R. Thiel, *Angew. Chem. Int. Ed.* **2010**, 49, 3428–3459; c) A. Schätz, O. Reiser, W. J. Stark, *Chem. Eur. J.* **2010**, 16, 8950–8967.
- [8] a) C. Xu, K. Xu, H. Gu, R. Zheng, H. Liu, X. Zhang, Z. Guo, B. Xu, *J. Am. Chem. Soc.* **2004**, 126, 9938–9939; b) C. Xu, K. Xu, H. Gu, X. Zhong, Z. Guo, R. Zheng, X. Zhang, B. Xu, *J. Am. Chem. Soc.* **2004**, 126, 3392–3393.
- [9] a) X. Zhao, R. Tapecc-Dytioco, K. Wang, W. Tan, *Anal. Chem.* **2003**, 75, 3476–3483; b) L. Wang, W. Zhao, W. Tan, *Nano Res.* **2008**, 1, 99–115.
- [10] I. K. Herrmann, M. Urner, F. M. Koehler, M. Hasler, B. Roth-Z'Graggen, R. N. Grass, U. Ziegler, B. Beck-Schimmer, W. J. Stark, *Small* **2010**, 6, 1388–1392.
- [11] a) F. M. Koehler, M. Rossier, M. Waelle, E. K. Athanassiou, L. K. Limbach, R. N. Grass, D. Günther, W. J. Stark, *Chem. Commun.* **2009**, 4862–4864; b) M. Rossier, F. M. Koehler, E. K. Athanassiou, R. N. Grass, B. Aeschlimann, D. Günther, W. J. Stark, *J. Mater. Chem.* **2009**, 19, 8239–8243; c) M. Rossier, F. M. Koehler, E. K. Athanassiou, R. N. Grass, M. Waelle, K. Birbaum, D. Günther, W. J. Stark, *Ind. Eng. Chem. Res.* **2010**, 49, 9355–9362.
- [12] a) R. N. Grass, E. K. Athanassiou, W. J. Stark, *Angew. Chem.* **2007**, 119, 4996–4999; *Angew. Chem. Int. Ed.* **2007**, 46, 4909–4912; b) I. K. Herrmann, R. N. Grass, D. Mazunin, W. J. Stark, *Chem. Mater.* **2009**, 21, 3275–3281.
- [13] a) S. Wittmann, A. Schätz, R. N. Grass, W. J. Stark, O. Reiser, *Angew. Chem.* **2010**, 122, 1911–1914; *Angew. Chem. Int. Ed.* **2010**, 49, 1867–1870; b) A. Schätz, T. R. Long, R. N. Grass, W. J. Stark, P. R. Hanson, O. Reiser, *Adv. Funct. Mater.* **2010**, 20, 4323–4328.
- [14] A. Schätz, R. N. Grass, Q. Kainz, W. J. Stark, O. Reiser, *Chem. Mater.* **2010**, 22, 305–310.
- [15] a) P. K. Maity, Q. M. Kainz, S. Faisal, A. Rolfe, T. B. Samarakoon, F. Z. Basha, O. Reiser, P. R. Hanson, *Chem. Commun.* **2011**, 47, 12524–12526; b) P. K. Maity, A. Rolfe, T. B. Samarakoon, S. Faisal, R. D. Kurtz, T. R. Long, A. Schätz, D. L. Flynn, R. N. Grass, W. J. Stark et al., *Org. Lett.* **2011**, 13, 8–10.
- [16] a) S. Brandes, C. Gros, F. Denat, P. Pullumbi, R. Guillard, *Bull. Soc. Chim. Fr.* **1996**, 133, 65–73; b) E. Kimura, S. Aoki, T. Koike, M. Shiro, *J. Am. Chem. Soc.* **1997**, 119, 3068–3076; c) D. S. Turygin, M. Subat, O. A. Raitman, V. V. Arslanov, B. König, M. A. Kalinina, *Angew. Chem.* **2006**, 118, 5466–5470; *Angew. Chem. Int. Ed.* **2006**, 45, 5340–5344.
- [17] A. Schätz, M. Zeltner, T. D. Michl, M. Rossier, R. Fuhrer, W. J. Stark, *Chem. Eur. J.* **2011**, 17, 10566–10573.
- [18] A. K. Tucker-Schwartz, R. L. Garrell, *Chem. Eur. J.* **2010**, 16, 12718–12726.
- [19] See supporting information.

- [20] a) C. W. Tornøe, M. Meldal in *American Peptide Symposium* (Eds.: M. Lebl, Houghten R. A.), American Peptide Society, Kluwer Academic Publishers, San Diego, CA, **2001**; b) V. V. Rostovtsev, L. G. Green, V. V. Fokin, K. B. Sharpless, *Angew. Chem.* **2002**, *114*, 2708–2711; *Angew. Chem. Int. Ed.* **2002**, *41*, 2596–2599; c) C. W. Tornøe, C. Christensen, M. Meldal, *J. Org. Chem.* **2002**, *67*, 3057–3064; d) S. Löber, P. Rodriguez-Loaiza, P. Gmeiner, *Org. Lett.* **2003**, *5*, 1753–1755.
- [21] J. Geduhn, T. Walenzyk, B. König, *Curr. Org. Synth.* **2007**, *4*, 390–412.
- [22] To ensure reliable optical properties the change of the riboflavin spectra in the envisaged pH range between 8 and 3.5 were recorded. The spectra virtually did not change in this range.
- [23] The extraction experiments described were carried out at concentrations of 10 µM flavin. However, lowering the concentration to 1 µM gave identical results.
- [24] A. Schätz, R. N. Grass, W. J. Stark, O. Reiser, *Chem. Eur. J.* **2008**, *14*, 8262–8266.
- [25] S. Adapted from: Ritter, Dissertation, University of Regensburg, **2007**.

### 3. Ring-Opening Metathesis Polymerization-based Recyclable Magnetic Acylation Reagents<sup>i</sup>



An operationally simple method for the acylation of amines utilizing carbon-coated metal nanoparticles as recyclable supports is reported. Highly magnetic carbon-coated cobalt (Co/C) and iron (Fe/C) nanobeads were functionalized with a norbornene tag (Nb-tag) through a “click” reaction followed by surface activation employing Grubbs-II catalyst and subsequent grafting of acylated *N*-hydroxysuccinimide ROMPgels (ROMP = ring-opening metathesis polymerization). The high loading (up to 2.6 mmol/g) hybrid material was applied in the acylation of various primary and secondary amines. The products were isolated in high yields (86–99%) and excellent purities (all >95% by NMR spectroscopy) after rapid magnetic decantation and simple evaporation of the solvents. The spent resins were successfully re-acylated by acid chlorides, anhydrides, and carboxylic acids and reused for up to five consecutive cycles without considerable loss of activity.<sup>ii</sup>

<sup>i</sup> Reproduced with permission from: Q. M. Kainz, R. Linhardt, P. K. Maity, P. R. Hanson, O. Reiser, *ChemSusChem* **2013**, 6, 721–729. Copyright 2013 WILEY-VCH Verlag GmbH & Co. KGaA, Weinheim.

<sup>ii</sup> All experiments and studies were carried out by Q. M. Kainz.

### 3.1 Introduction

Although polymer-supported reagents for organic synthesis have been around for a while, they remain of current interest especially in the field of combinatorial chemistry, with new methods and new supports being continuously developed.<sup>[1]</sup> The main reason for their popularity is the combination of well-established solution-phase chemistry (along with sophisticated analytical techniques) with ease of purification (mostly filtration) and the possibility for automation. Among them, a wide variety of acyl transfer resins have been developed, for example, polymer-supported *ortho*-nitrophenol,<sup>[2]</sup> *para*-(hydroxyphenyl)-sulfone,<sup>[3]</sup> a range of supported mixed anhydrides,<sup>[4]</sup> and, more recently, tetrafluorophenol.<sup>[5]</sup> However, one of the most commonly utilized resins for acylation reactions is supported *N*-hydroxybenzotriazole (HOBt).<sup>[6,7]</sup> Although its reactivity in acylations can be advantageous, it is hampered by poor stability in DMF.<sup>[8]</sup>

Active esters derived from *N*-hydroxysuccinimide (NHS) are considered to be more stable and were frequently applied to the activation of amino acids, the introduction of carbamate protecting groups, and as staining, radiolabeling, or crosslinking agents in various biological systems.<sup>[9]</sup> Several polymer-supported NHS analogues are known, for example, copoly(ethylene-*N*-hydroxymaleimide),<sup>[10]</sup> and copoly(styrene-*N*-hydroxymaleimide).<sup>[11]</sup> In addition, Adamczyk and co-workers demonstrated the immobilization of NHS on commercially available Merrifield and ArgoPore-Cl resins.<sup>[12,13]</sup> We herein report acyl derivatives of a NHS high capacity ROMPgels (ROMP = ring-opening metathesis polymerization) grafted on magnetic Co/C or Fe/C nanobeads as versatile and recyclable active-ester equivalents for the acylation of various primary and secondary amines.

### 3.2 Results and Discussion

Polymers and oligomers derived from ring-opening metathesis polymerization of monomers containing the functionality of the desired reagent and a strained alkene have been developed by the group of Barrett<sup>[14,15]</sup> and by Buchmeiser.<sup>[16]</sup> More recently, Hanson and co-workers contributed to this field with the development of new oligomeric reagents<sup>[17]</sup> as well as scavengers.<sup>[18]</sup> The main advantages of these “designer” polymers (termed as ROMPgels) over conventional polystyrene-based polymers are the high mechanical stability, excellent quality, and quantitative loading because of functionalization performed usually on the monomer stage. Active esters of

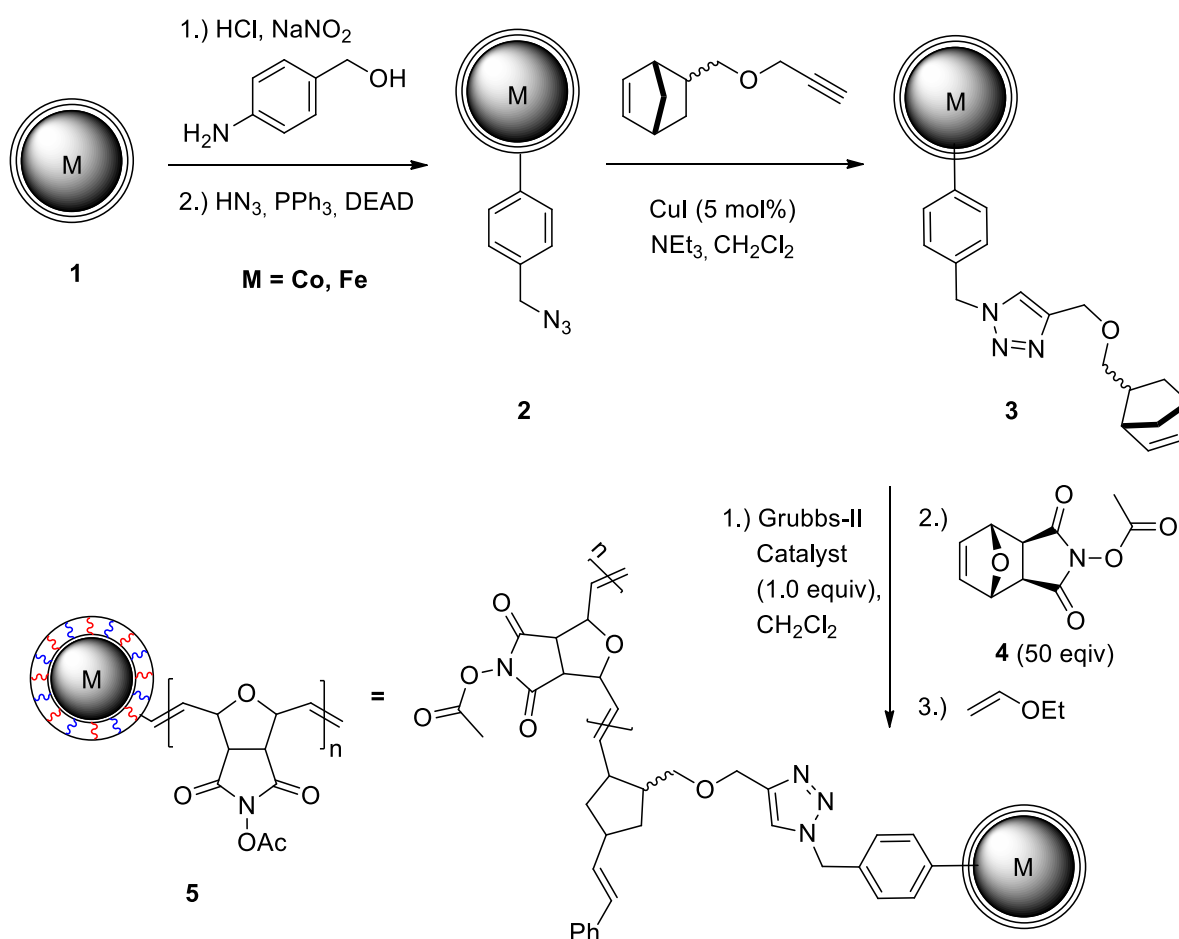
a NHS ROMPgels were successfully utilized by Barrett et al. for the synthesis of various amides, ureas, carbamates,<sup>[19]</sup> and oxadiazoles<sup>[20]</sup> in excellent yields and purities. Recently, Roberts<sup>[21]</sup> reported the grafting of NHS ROMPgels on Wang resins to combine the convenience of a bead format with the high loading of the ROMPgels. Despite the good site accessibility, limitations in the choice of acylating reagents occurred and perfluorinated solvents had to be employed to achieve adequate yields.

Magnetic nanoparticles as supports would even further facilitate the workup process by replacing the energy-intensive pumping to draw solvent through a filter and the tedious recovery of the polymer by an operationally simple magnetic decantation. Furthermore, the magnetic properties of the nanobeads also allow application under continuous-flow conditions by confining them within a magnetic field rather than in a membrane reactor.<sup>[22]</sup> Recently, Stark et al. reported the synthesis of carbon-coated cobalt (Co/C)<sup>[23]</sup> or iron (Fe/C)<sup>[24]</sup> nanoparticles on multigram scale (>30 g/h) from inexpensive metal carboxylates by performing reducing-flame spray pyrolysis. These metal nanoparticles combine excellent thermal and chemical stabilities with high magnetization (up to 158 emu/g). The surface of the nanobeads is accessible by covalent and/or non-covalent functionalization,<sup>[25]</sup> which allows for applications such as extraction of analytes or contaminants from water,<sup>[26,27]</sup> purification of blood,<sup>[28]</sup> or as recyclable support for catalysts.<sup>[22,29,30]</sup>

ROMPgels based on magnetic Co/C nano-supports have previously been reported by our group for the immobilization of a highly active and recyclable palladium complex for Suzuki-Miyaura cross-coupling reactions.<sup>[31]</sup> Furthermore, such nanoparticles were applied for the facile purification of intermolecular<sup>[32]</sup> as well as intramolecular<sup>[33]</sup> Mitsunobu reactions utilizing norbornene-tagged (Nb-tagged) reagents and a surface-initiated sequestration protocol. It has been demonstrated that because of the explicitly high magnetic moment of the cobalt nanobeads the overall magnetization of the resulting hybrid material is significantly higher than that of polymer-coated iron oxide nanoparticles with comparable metal content, thus allowing rapid separation of the ROMPgels from reaction mixtures. The high loadings achieved using this approach make the development of other supported reagents, which can be recycled through rapid and simple magnetic decantation and subsequent regeneration of the reactive groups, desirable.

## Synthesis of magnetic ROMPgels for acylation reactions

To render the magnetic Co/C or Fe/C nanoparticles **1** accessible to the grafting of ROMPgels, a covalent surface-functionalization strategy introducing norbornene groups was utilized. At first, well-established diazonium chemistry followed by hydroxyl azide exchange to **2** via a Mitsunobu reaction with hydrazoic acid as nucleophile was carried out (Scheme 1).<sup>[22,29]</sup> Subsequently, norbornene moieties were introduced through a copper(I)-catalyzed alkyne/azide cycloaddition (click reaction),<sup>[34]</sup> giving rise to **3**, which is a suitable precursor for subsequent ROMP with Nb-tagged catalysts or reagents.



**Scheme 1.** Synthesis of the magnetic ROMPgel. DEAD=diethyl azodicarboxylate.

Loadings of 0.10-0.15 mmol norbornene groups per gram nanoparticle were determined by elemental microanalysis for **3**. Clearly, loadings of this magnitude, limited by the diazonium functionalization step from **1** to **2**, are not very attractive for the

direct immobilization of reagents because of the sheer mass of support needed for considerable amounts of reactive groups.

ROMP using Nb-tagged reagents is an effective method to increase the loading and to control the properties of the polymer shell around the nanobeads by varying the amount of catalyst and monomer used. Thus, the acetylated NHS monomer **4** was synthesized from furan and maleic anhydride in three steps following literature procedures.<sup>[21,35,36]</sup> Applying conditions reported by Roberts<sup>[21]</sup> for ROMP of **4** at room temperature on modified Wang beads pre-activated with Grubbs-I catalyst<sup>[37]</sup> led to no noticeable formation of ROMPgels on the Nb-tagged Co/C nanobeads **3** (Table 1, entry 1), which was confirmed by elemental analysis. A control experiment at 60 °C revealed, that Grubbs-I catalyst is not suitable to conduct surface-initiated ROMP on the magnetic nanobeads. However, oligomers could be precipitated from the solution by addition of MeOH. Grubbs-I catalyst was also not active in the surface-initiated sequestration of Nb-tagged Mitsunobu reagents.<sup>[32,33]</sup>

**Table 1.** Screening of reaction conditions for the synthesis of **5** by ROM polymerization on the magnetic beads.<sup>[a]</sup>

Entry	Particles	Catalyst	T [°C]	Reaction time [h]	Loading (N) [mmol/g] <sup>[b]</sup>
1	Co/C-Nb ( <b>3</b> )	Grubbs 1 <sup>st</sup>	25	24	No gel <sup>[c]</sup>
2	Co/C-Nb ( <b>3</b> )	Grubbs 1 <sup>st</sup>	60	10	No gel <sup>[c]</sup>
3	Co/C-Nb ( <b>3</b> )	Grubbs 2 <sup>nd</sup>	60	1	2.37
4	Fe/C-Nb ( <b>3</b> )	Grubbs 2 <sup>nd</sup>	60	1	1.96
5	Co/C-N <sub>3</sub> ( <b>2</b> )	Grubbs 2 <sup>nd</sup>	60	1	No gel <sup>[c]</sup>

[a] 50 Equiv. of monomer and 1.0 equiv. of catalyst with respect to the norbornene units attached on the nanobeads. [b] Determined by nitrogen microanalysis. [c] Oligomers in solution.

In contrast, Grubbs-II catalyst<sup>[38]</sup> allowed the grafting of the desired ROMPgels on the nanobeads: To initiate ROMP on the surface of the nanobeads, Nb-tagged Co/C nanobeads **3** were dispersed in degassed CH<sub>2</sub>Cl<sub>2</sub> in a sealed vessel under nitrogen atmosphere using a tempered (60 °C) ultrasonic bath. A solution of Grubbs-II catalyst (1.0 equiv. with respect to the loading with norbornene groups of **3**) was injected to generate an active ruthenium carbene species on the surface of the nano-

beads by ring-opening metathesis with the immobilized norbornene moieties. A NHS ROMPgel was grafted onto the nanobeads by subsequent addition of a solution containing monomer **4** (50 equiv.). Immediately, a voluminous black gel was formed, which, after quenching with ethyl vinyl ether (EVE), contracted. The lump was dried well under vacuum and crushed for further use. Based on the gain in mass of magnetic resin **5**, more than 95% of monomer **4** was incorporated into the hybrid material. Combustion analysis revealed 4.21% nitrogen, corresponding to a loading of 2.37 mmol/g (Table 1, entry 3), thus increasing the loading from the initially azide-tagged nanobeads **2** by a factor of more than 20. Images taken by transmission electron microscopy (TEM) confirmed the encapsulation of the Co/C-particles in a polymer matrix, separating the previously densely packed nanoparticle clusters, a characteristic owed to the highly magnetic remanence of the metal nanobeads.<sup>[39]</sup>

Alternatively, ROMPgels supported on Fe/C nanoparticles were successfully synthesized, giving rise to high loading magnetic resins consisting of biologically well acceptable components (Table 1, entry 4). The morphology and performance of the Fe/C ROMPgel was identical with the Co/C analogue, whereas variations in the overall loading arose from slightly different loadings of norbornene moieties from batch to batch. To demonstrate that the ROMPgel was actually covalently bound to the magnetic support and not just encapsulating the nanobeads, a control experiment employing the azide-functionalized nanobeads **2** instead of the Nb-tagged variant **3** was performed. In this case no nanoparticle-supported ROMPgel **5** could be formed and nanoparticles **2** were recovered from the solution, while oligomers remained in solution upon precipitation with MeOH.

The swelling properties of both resins were in line with literature reports for ROMPgels.<sup>[15,21]</sup> The resins exhibited a distinct volume increase in THF, CH<sub>2</sub>Cl<sub>2</sub>, and CHCl<sub>3</sub>, whereas solvents such as MeOH and Et<sub>2</sub>O did not induce such an effect. In DMF, however, the formation of a gummy like mass was observed. Spectroscopic data of the various beads was obtained by infrared spectroscopy using the attenuated total reflectance sampling technique (IR-ATR). The azide-functionalized nanoparticles **2** show a characteristic massive peak at 2100 cm<sup>-1</sup>, which vanished after the click reaction yielded the Nb-tagged beads **3** (Figure 1). After ROMP, the characteristic carbonyl stretches of monomer **4** were present in the spectrum of the magnetic ROMPgel **5** (1822, 1788, and 1731 cm<sup>-1</sup>). A peak broadening, typical for magnetic nanobeads functionalized with organic molecules, was apparent at lower wave-



numbers. For resin **9** bearing hydroxyl groups, the peak at  $1822\text{ cm}^{-1}$  disappeared completely indicating successful cleavage of the acetyl group in **5**.

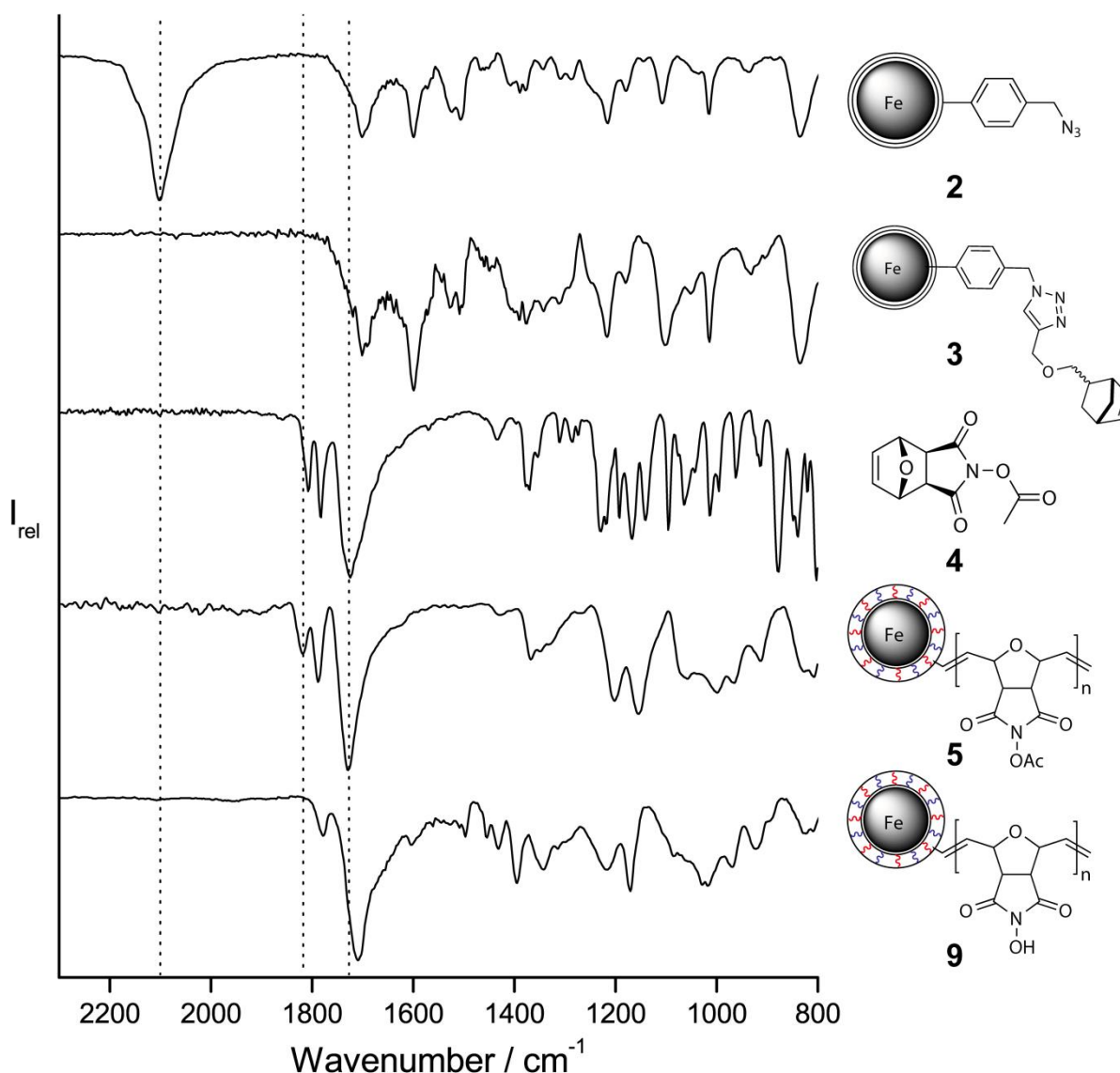


**Figure 1.** IR-ATR spectra of functionalized nanobeads **2** and **3**, the monomer **4**, and the corresponding magnetic ROMPgels **5** and **9**.

To optimize the loading of magnetic ROMPgel **5**, a series of experiments was performed by varying the amount of monomer **4** from 50 to 100 equivalents while keeping the amount of nanobeads **3** and Grubbs-II catalyst constant (Table 2). The particle yields and loadings increased up to 80 equivalents of monomer **4**; however, when using 100 equivalents of **4**, a decrease in loading and yield was observed. Moreover, the gel lump showed to be of inhomogeneous composition with darker (more nanobeads) and lighter areas (more polymer) caused by irregular polymeriza-

tion, which was also confirmed by inconsistent data obtained from multiple elemental analysis. Hence, 80 equivalents of monomer **4** seemed to be optimal with respect to the amount of ROMPgel produced, loading, and sufficient homogeneity.

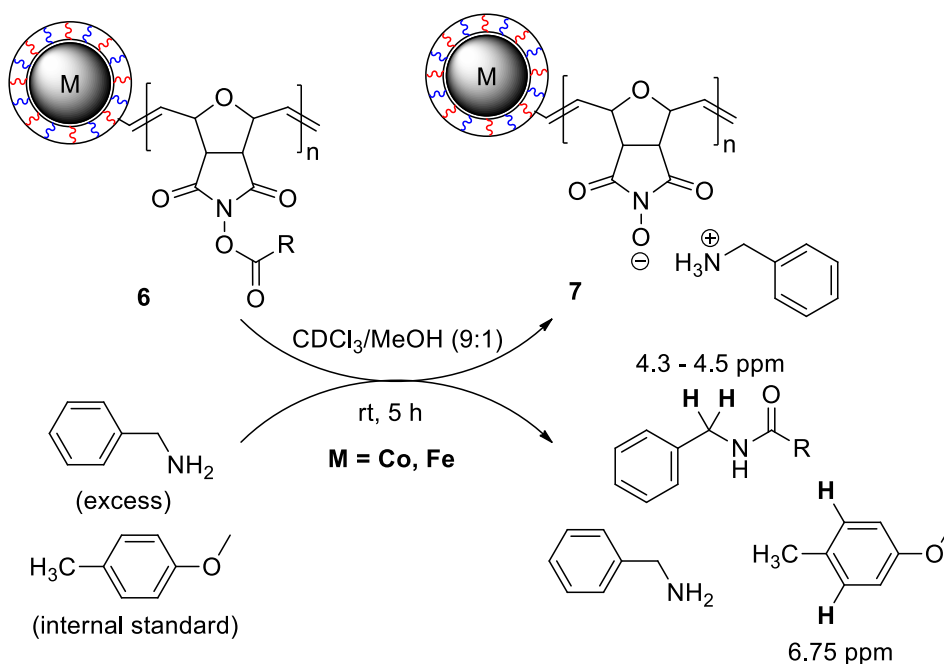
**Table 2.** Tuning of the hybrid material by variation of the amount of monomer.<sup>[a]</sup>

Entry	Equiv. monomer	Yield [mg]	Max calculated loading [mmol/g]	Observed loading (N) [mmol/g] <sup>[b]</sup>	Observed loading NMR assay [mmol/g]
1	50	147	2.31	2.16	2.24
2	60	163	2.50	2.23	2.32
3	80	201	2.79	2.46	2.60
4	100	196	2.99	2.09 <sup>[c]</sup>	2.36

[a] For each reaction 70 mg of Co/C nanobeads and 1.0 equiv. of Grubbs-II catalyst were used. [b] Determined by nitrogen analysis. [c] Inhomogeneous.

### Determination of the loading and stability tests

Although determination of the loading through nitrogen elemental analysis is possible, for higher sample throughput a <sup>1</sup>H NMR assay was developed. An assay for the NMR titration of ROMPgels as described by Roberts<sup>[21]</sup> was adjusted to fit the needs of this project. Briefly, acylated ROMPgel **6** was treated with an excess of benzylamine in a mixture of deuterated chloroform and nondeuterated methanol (9:1). An internal standard was added as accurate determination of the benzylamine remaining in solution is not possible because the liberated *N*-hydroxyl resin **7** can capture amines from the solution (Scheme 2).<sup>[40,41]</sup> We found the internal standard used by Roberts, benzyl methyl ether, not to be ideal because of an overlap with the product in some cases. Therefore, we used 4-methylanisole instead. Owing to its magnetic properties, resin **7** had to be removed from the solution by magnetic decantation before acquiring the <sup>1</sup>H NMR spectrum. To determine the loading, the benzylic CH<sub>2</sub> doublet of the resulting amide was compared with that of the phenylic CH groups of the standard.<sup>[39]</sup> Loadings determined by this method closely matched the values obtained by elemental analysis (Table 2).



**Scheme 2.** Determination of the loading by using an NMR assay (50 mg test reactions).

To examine the long-time stability of the acetylated resin **5**, one batch was stored five months in the fridge and was then analyzed again by elemental microanalysis and <sup>1</sup>H NMR assay (Table 3). NMR analysis revealed a decrease in loading of less than one percent, whereas the data obtained from elemental analysis indicated a slightly higher degree of decomposition (4-7%).

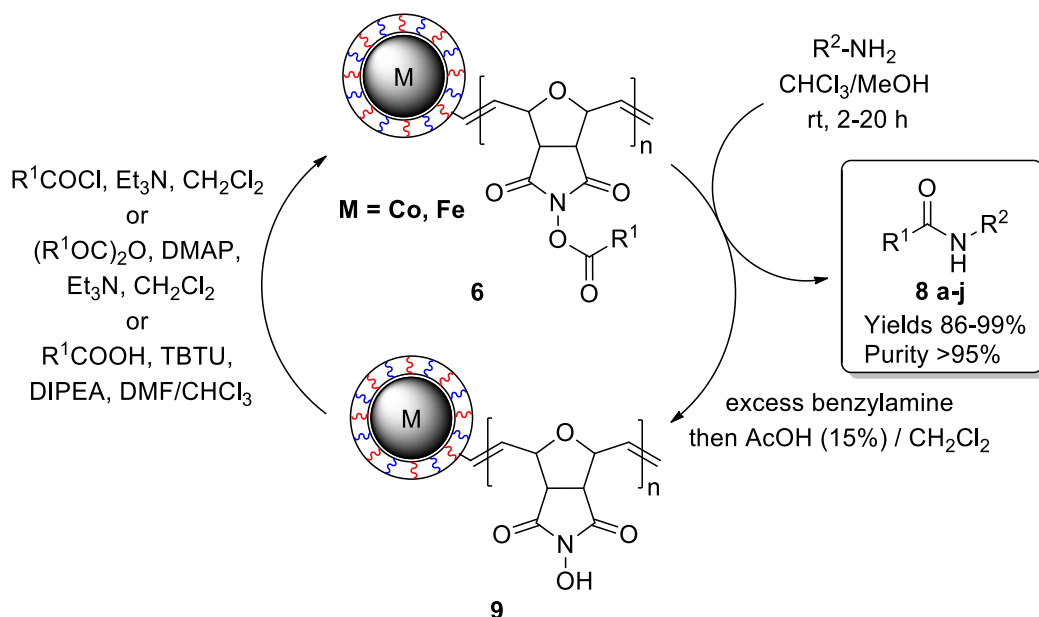
**Table 3.** Stability test of ROMPgel **5** by a comparison of the loading.

Entry	Storage time [month]	Loading (C) [mmol/g] <sup>[a]</sup>	Loading (N) [mmol/g] <sup>[b]</sup>	Loading NMR [mmol/g]
1	0	2.30	2.34	2.28
2	5	2.15	2.24	2.26

[a] Determined by carbon analysis. [b] Determined by nitrogen analysis.

### Acylation of various amines using magnetic ROMPgels

After detailed investigation of the synthesis, loading, and stability of magnetic ROMPgels, the acylation of amines and the recycling of the ROMPgel were examined (Scheme 3). In the first step, benzylamine as an initial test substrate was stirred with a slight excess of the acetylated Fe/C ROMPgel **5**. After completion of the acyl-



**Scheme 3.** Acylation of amines using magnetic ROMPgels and subsequent recycling of the resin.

ation, ROMPgel was fully recovered by using a magnet and benzylamide **8a** was isolated by simple decantation and evaporation of the solvents (Figure 2).

Pure chloroform alone was not the ideal solvent with respect to yield (82%) and product purity, but addition of 10 vol % methanol gave rise to the benzylamide in high yield (93%) and purity (>95% by NMR). The solvent mixture was removed by simple distillation and reused for the next run. Also other, more sustainable, solvents were tested. The yields are slightly lower using EtOAc (89%) or THF (83%) while the product purity remained excellent. However, the solvent range applicable for this reaction is limited as sufficient swelling of the resin has to be ensured during the reaction.

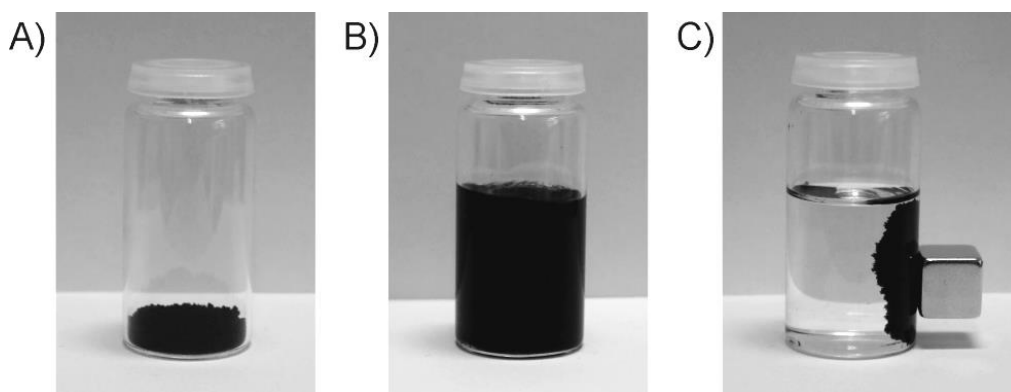


**Figure 2.** Pictures of Fe/C ROMPgel **5**: pristine (A), dispersed in  $CHCl_3/MeOH$  (9:1) by a magnetic stirrer (B), and after recovery by an external magnet (C).

In some cases the product solution was filtered over cotton to remove traces of finely dispersed resin or degraded polymer. An NMR comparison of the product before and after filtration showed slightly better line separation in the spectrum acquired after filtration.<sup>[39]</sup> To quantify the effectiveness of the magnetic decantation, we performed an additional experiment, for which we determined the weight of the product before and after filtration. Only 1 wt% was lost during filtration, which is in line with the marginal weight gain of the filter. The material collected by the filter corresponded to less than 0.3 wt% of the initial resin, which underlines the effectiveness of the magnetic decantation.<sup>[39]</sup>

Keeping in mind our goal to develop a protocol that will allow the use of different types of acyl transfer reagents, the spent resin was stirred with an excess of benzylamine to cleave the remaining acetyl groups. As free N-OH resins are capable of capturing amine from the solution,<sup>[40,41]</sup> a washing step with acetic acid (15 vol%) in CH<sub>2</sub>Cl<sub>2</sub> followed by THF was conducted to regenerate **9**.

To investigate the recycling and reloading potential of the magnetic ROMPgel, a series of reactions was performed. Co/C ROMPgel **5** with an initial loading of 1.52 mmol/g was used to synthesize *N*-benzylacetamide (**8a**) in 91% yield and excellent purity by stirring for 5 h (Table 4). Remaining acyl groups were cleaved and the resin washed with acid as described above. Effective re-acylation (91%, 1.39 mmol/g) of the resin was achieved by stirring with acetyl chloride (3 equiv.) in the presence of an excess of triethylamine. The high product yields (91-99%) and the ability for reloading (82-98%) were maintained for five consecutive cycles (Table 4).

**Table 4.** Consecutive synthesis of *N*-benzylacetamide (**8a**) and subsequent regeneration of the magnetic Co/C acylation reagent.

Entry	Run	Yield (isolated)	Purity <sup>[a]</sup>	Loading after recycling [mmol/g] <sup>[a]</sup>	Regeneration of initial loading <sup>[b]</sup>
1	1	91%	> 95%	1.39	91%
2	2	98%	> 95%	1.49	98%
3	3	99%	> 95%	1.24	82%
4	4	98%	> 95%	1.32	87%
5	5	91%	> 95%	1.41	93%

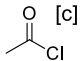
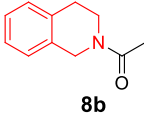
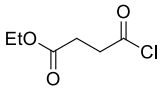
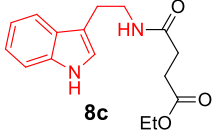
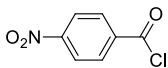
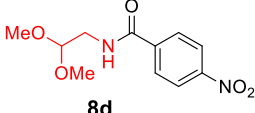
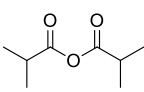
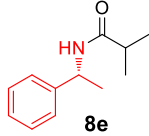
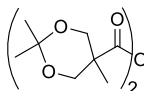
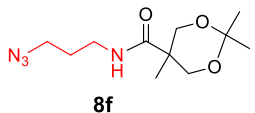
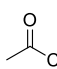
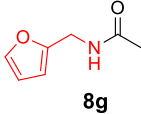
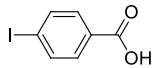
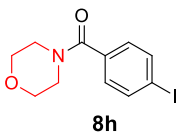
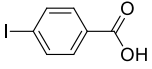
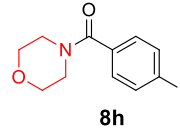
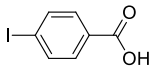
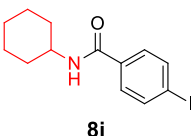
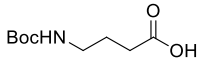
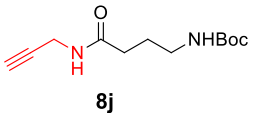
[a] Determined by NMR. [b] Initial loading: 1.52 mmol/g.

Despite the numerous washing steps, 76% of the initial amount of nanobeads was recovered after five runs, but with a slightly lower loading of 1.41 mmol/g. Images acquired by using a TEM revealed no substantial differences between freshly prepared and reisolated (after five cycles) ROMPgels **5**.<sup>[39]</sup>

Different acid chlorides readily reacylated the Fe/C ROMPgels **9** following the procedure described above. Three equivalents of acid chloride were sufficient to reach high loadings (>2 mmol/g), and the subsequent acylation of different primary as well as secondary amines yielded the corresponding amides (**8b-d**) in high purities and yields with no detectable cross-contamination (Table 5). Likewise, anhydrides were able to reload the free N-OH resin **9** on addition of 4-(dimethylamino)-pyridine (DMAP) as a nucleophilic catalyst with slightly decreased efficiency when compared to acid chlorides (Table 5, entries 4 and 5). Notably, no racemization occurred using an enantiomeric pure amine as substrate, demonstrating that the magnetic ROMPgels are very mild acylating agents applicable to sensitive compounds.

However, in some cases acid chlorides or anhydrides are neither readily available nor easily synthesized and their high reactivity might cause stability problems, for example, racemization.<sup>[42]</sup> Therefore, acylation of the magnetic Fe/C ROMPgels **9** by coupling with aryl and alkyl carboxylic acids was investigated (Table 5, entries 7-10). Initially, 1-ethyl-3-(3-dimethylaminopropyl)carbodiimide (EDC; free-base form) was applied as coupling reagent in a mixture of DMF and CH<sub>2</sub>Cl<sub>2</sub> (1:1) leading to a moderate loading (0.74 mmol/g), which corresponded to 47% functionalization with acyl groups taking into account the distinct mass increase; subsequently, the corresponding amide **8h** was formed in high yields and purities. Other coupling reagent and base combinations, such as 2-(1*H*-benzotriazole-1-yl)-1,1,3,3-tetramethylaminium tetrafluoroborate/ethyl-diisopropylamine (TBTU/DIPEA) or diisopropylcarbodiimide/DMAP (DIC/DMAP), showed slightly improved loadings when using the same acid, with the best result (0.89 mmol/g, 56% functionalization) achieved by the most reactive reagent (TBTU; Table 5, entry 8). In all cases three equivalents of acid and three equivalents of coupling reagent were used. The high purities of the product amides underline the successful removal of the spent coupling reagents from the resin in the washing steps, which is sometimes not trivial when using extraction to purify the reaction mixture. Moreover, entries 7 and 8 (Table 5) demonstrate the reproducibility of the acylation when using the same amine.

**Table 5.** Reloading of ROMPgel **9** by acid chlorides, anhydrides, and acids and subsequent synthesis of amides (**8b-j**) recycling the resin after each run.

Entry	Cycle	Acyating agent	Additives for coupling	Loading <sup>[a]</sup> [mmol/g]	Product amide <sup>[b]</sup>	Yield
1	1	 [c]	Et <sub>3</sub> N	2.26	 <b>8b</b>	96 %
2	2		Et <sub>3</sub> N	2.27	 <b>8c</b>	94 %
3	3		Et <sub>3</sub> N	2.18	 <b>8d</b>	86 %
4	4		DMAP, Et <sub>3</sub> N	1.80	 <b>8e</b>	91 %
5	5		DMAP, Et <sub>3</sub> N	1.36	 <b>8f</b>	95 %
6	1	 [c]	Et <sub>3</sub> N	2.14	 <b>8g</b>	95 %
7	2		EDC	0.74	 <b>8h</b>	90 %
8	3		TBTU, DIPEA	0.89	 <b>8h</b>	88 %
9	4		DIC, DMAP	0.80	 <b>8i</b>	87 %
10	5		TBTU, DIPEA	0.67	 <b>8j</b>	97 %

[a] Determined by NMR assay. [b] Purity >95% in all cases based on NMR. [b] Product **8 b-j**. [c] Acylation on monomer stage.

Although the loadings obtained with carboxylic acids cannot compete with the excellent loadings obtained using acid chlorides, they are comparable with other acyl transfer resins.<sup>[7,12,13]</sup> Reasons might be the reduced reactivity of activated esters compared to acid chlorides and the steric demand of the coupling reagents. The loadings might be significantly improved when using more equivalents of acid and coupling reagent or double couplings.<sup>[21]</sup> However, one has to decide for each application, if slightly increased loadings compensate for the need for higher amounts of high molecular weight coupling reagents and potentially laborious acids.

### 3.3 Conclusion

We have demonstrated the successful synthesis of acylated magnetic ROMPgels starting from readily synthesized carbon coated iron or cobalt nanoparticles. Whereas Grubbs-I catalyst failed to initiate the polymerization on the nanoparticle surface, Grubbs-II catalyst efficiently catalyzed the formation of magnetic ROMPgels, which were rapidly recovered from reaction mixtures by magnetic decantation. Further experiments revealed an optimal amount of 80 equivalents of monomer, leading to a high loading (up to 2.6 mmol/g) hybrid material that was stable for more than five months. Furthermore, IR spectra, TEM pictures, and an NMR-assay were applied to thoroughly characterize the ROMPgels.

Synthesis of various amides in excellent yields and purities followed by subsequent regeneration of the magnetic acyl transfer resin was achieved for at least five consecutive cycles. The resin was efficiently recovered by magnetic decantation after each step, dispensing the need of tedious and energy-intensive filtration or even chromatography. No cross-contamination was detected when using different acylation reagents or amines, suggesting the magnetic resins to be reliable and readily recyclable acyl transfer reagents. Although acid chlorides and anhydrides readily reacylated the resin, couplings with carboxylic acids only generated moderate loadings regardless of the coupling reagent or reaction conditions. Further studies, which are currently conducted in our laboratories, include the improvement of these loadings, the use of more sophisticated substrates, and the use of ROMPgels as support for fluorescent labels. Also, the upscaling to multi-gram experiments is planned, for which the advantages of the magnetic resins should even be more apparent.



### 3.4 Experimental Section

#### Materials and methods

The carbon-coated cobalt nanomagnets (Co/C,  $20.5 \text{ m}^2 \text{ g}^{-1}$ , mean particle size  $\approx 25 \text{ nm}$ ) were purchased from Turbobebeads Llc, Switzerland. Prior to use, they were washed five times for 24 h in a concentrated HCl (Merck, puriss.)/deionized water (Millipore) mixture (1:1). Acid residuals were removed by washing with Millipore water (5x), and the particles were dried at  $50^\circ \text{C}$  in a vacuum oven.<sup>[27]</sup> Azide- (**2**)<sup>[22,29]</sup> and norbornene- (**3**)<sup>[31]</sup> functionalized nanobeads were synthesized according to literature procedures. Acetylated monomer **4** was prepared in three steps following literature-known syntheses.<sup>[21,35,36]</sup> All other commercially available compounds were used as received.  $^1\text{H}$  NMR (300 MHz) and  $^{13}\text{C}$  NMR (75.5 MHz) spectra were recorded by using a Bruker AC300 spectrometer with  $\text{CHCl}_3$  (7.26 ppm) as a standard. Magnetic nanobeads were dispersed using an ultrasound bath (Sonorex RK 255 H-R, Bandelin) and recovered with the aid of a neodymium-based magnet (side length 12 mm). They were characterized by using a IR-ATR spectrometer equipped with a Specac Golden Gate Diamond Single Reflection ATR-System and elemental microanalysis (LECO CHN-900).

#### Synthesis of magnetic ROMPgel (**5**)

In a typical experiment, Nb-tagged, carbon-coated iron nanoparticles (400 mg,  $0.12 \text{ mmol/g}$ ) were dispersed in dry  $\text{CH}_2\text{Cl}_2$  (5 mL) by sonication for 15 min in a sealed reaction vessel under nitrogen atmosphere. A solution of Grubbs-II catalyst (40.8 mg,  $48 \text{ }\mu\text{mol}$ , 1.0 equiv. with respect to the loading with Nb) in dry  $\text{CH}_2\text{Cl}_2$  (3 mL) was injected and the dispersion subjected to sonication for 30 min with the ultrasonic bath tempered to  $60^\circ \text{C}$ . Next, a solution of the acetylated *N*-hydroxysuccinimide monomer **4** (672 mg,  $2.88 \text{ mmol}$ , 60 equiv.) in dry  $\text{CH}_2\text{Cl}_2$  (10 mL) was added and the sonication continued for 1 h at  $60^\circ \text{C}$ . The pressure in the reaction vessel was released from time to time to allow formation of ROMPgel **5** after a few minutes. The magnetic gel was separated by an external magnet and washed with  $\text{CH}_2\text{Cl}_2$  ( $3 \times 5 \text{ mL}$ ). To quench the reaction, a  $\text{CH}_2\text{Cl}_2/\text{EVE}$  (1:1; 5 mL) mixture was added followed by sonication at ambient temperature for 20 min. The gel lump was washed with  $\text{CH}_2\text{Cl}_2$  ( $3 \times 5 \text{ mL}$ ), dried under vacuum, and crushed to yield NHS-functionalized magnetic ROMPgel.

**Incorporation of monomer:** >95%; **IR** (ATR,  $\bar{\nu}/\text{cm}^{-1}$ ): 1822, 1788, 1731, 1368, 1200, 1154, 1059, 1002, 967, 914, 809, 729; **elemental microanalysis:** 35.77% C; 2.58% H, 3.84% N.

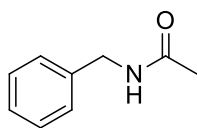
### **<sup>1</sup>H NMR assay for the determination of the loading**

A stock solution was prepared by introducing benzyl amine (1.64 mL, 15 mmol), *p*-methylanisole (378  $\mu\text{L}$ , 3 mmol), and methanol (2.5 mL, nondeuterated) into a 25 mL volumetric flask and filling up with  $\text{CDCl}_3$ . To the Co/C-ROMPgels or Fe/C-ROMPgels **6** (50 mg) in a capped vial, stock solution (1.00 mL) was added and the ROMPgels suspended by magnetic agitation utilizing the intrinsic magnetic properties of the material. After agitation for 5 h at RT, the magnetic beads were separated by using an external magnet and the solution was filtered over cotton. NMR spectra were acquired, and the integration of the benzylic  $\text{CH}_2$  doublet of the product (typically 4.3-4.5 ppm) was compared with that of the phenylic CH groups of the standard (typically 6.75 ppm).

### **General procedure for the acylation of amines using magnetic ROMPgels**

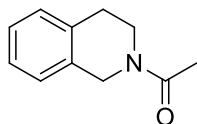
An excess (1.3 equiv. acyl groups) of magnetic ROMPgels **7** was stirred with amine (1.0 equiv) in 5 mL of a  $\text{CHCl}_3/\text{MeOH}$  (9:1) mixture at RT for 2–16 h (TLC monitoring). The nanoparticles were recovered by using a magnet, the solution decanted, and the nanobeads washed three times with a  $\text{CHCl}_3/\text{MeOH}$  (9:1; 5 mL) mixture. The combined solutions were filtered over cotton, the solvents were distilled for reuse in the next cycle, and the crude product was dried under high vacuum.

The recovered particles were subsequently stirred in a solution of  $\text{CH}_2\text{Cl}_2/\text{MeOH}/\text{benzylamine}$  (8:1:1;  $\approx 1$  mL per 100 mg resin) overnight. After decantation of the solution, the particles were washed with 15%  $\text{AcOH}/\text{CH}_2\text{Cl}_2$  (3x), THF (3x), and  $\text{Et}_2\text{O}$  (1x). 1 mL of solvent per 100 mg resin was used in each washing step, and the particles were suspended by stirring for 15 min. The particles were dried under vacuum for 5 h.

***N*-Benzylacetamide (8a)**

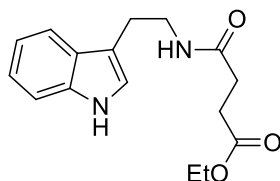
According to the general procedure Fe/C ROMPgel **5** (508 mg, 0.71 mmol, 1.39 mmol/g) loaded with acetyl groups was used to acetylate benzylamine (59  $\mu$ L, 543  $\mu$ mol) while stirring for 5 h. Crude *N*-benzylacetamide **8a** (79.9 mg, 536  $\mu$ mol, 99%) was obtained as a pale brown solid and the resin recycled for the next run.

**<sup>1</sup>H NMR** (300 MHz, CDCl<sub>3</sub>):  $\delta$  = 7.39–7.18 (m, 5H), 6.11 (bs, 1H), 4.39 (d,  $J$ =5.6 Hz, 2H), 1.98 ppm (s, 3H); **<sup>13</sup>C NMR** (75 MHz, CDCl<sub>3</sub>):  $\delta$  = 170.2, 138.3, 128.8, 127.9, 127.6, 43.8, 23.3 ppm; **MS** (ESI-MS):  $m/z$  (%) = 150.1 (50) [ $M^+$ -H], calc. 149.1.

**1-[3,4-Dihydroisoquinolin-2(1*H*)-yl]ethanone (8b)**

Synthesized according to the general procedure. Yield: 96%.

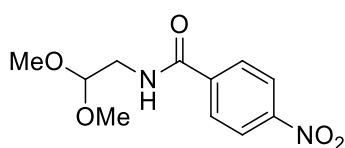
**<sup>1</sup>H NMR** (300 MHz, CDCl<sub>3</sub>, mixture of rotamers):  $\delta$  = 7.24–7.04 (m, 9H,  $r_{\text{maj}}+r_{\text{min}}$ ), 4.73 (s, 3H,  $r_{\text{maj}}$ ), 4.61 (s, 2H,  $r_{\text{min}}$ ), 3.82 (t,  $J$ =6.0 Hz, 2H,  $r_{\text{min}}$ ), 3.67 (t,  $J$ =5.9 Hz, 3H,  $r_{\text{maj}}$ ), 2.90 (t,  $J$ =5.9 Hz, 3H,  $r_{\text{maj}}$ ), 2.85 (t,  $J$ =5.9 Hz, 2H,  $r_{\text{min}}$ ), 2.18 (s, 3H,  $r_{\text{min}}$ ), 2.17 ppm (s, 4H,  $r_{\text{maj}}$ ); **<sup>13</sup>C NMR** (75 MHz, CDCl<sub>3</sub>, mixture of rotamers):  $\delta$  = 169.5, 169.4, 135.1, 134.1, 133.6, 132.6, 129.0, 128.3, 126.9, 126.7, 126.6(4), 126.5(6), 126.4, 126.1, 48.1, 44.1, 44.0, 39.5, 29.5, 28.6, 22.0, 21.7 ppm; **MS** (ESI-MS):  $m/z$  (%) = 351.0 (100) [ $2M^+$ -H], calc. 51.2.

**4-[[2-(1*H*-Indol-3-yl)ethyl]amino]-4-oxobutanoate (8c)**

Synthesized according to the general procedure. Yield: 94%.

**<sup>1</sup>H NMR** (300 MHz, CDCl<sub>3</sub>):  $\delta$  = 8.22 (s, 1H), 7.60 (d,  $J$ =7.8 Hz, 1H), 7.37 (d,  $J$ =8.0 Hz, 1H), 7.20 (t,  $J$ =7.3 Hz, 1H), 7.12 (t,  $J$ =7.3 Hz, 1H), 7.04 (d,  $J$ =1.6 Hz, 1H), 5.73 (s, 1H), 4.11 (q,  $J$ =7.1 Hz, 2H), 3.59 (dd,  $J$ =12.8 Hz, 6.5, 2H), 2.96 (t,  $J$ =6.7 Hz, 2H), 2.64 (t,  $J$ =6.8 Hz, 2H), 2.40 (t,  $J$ =6.8 Hz, 2H), 1.23 ppm (t,  $J$ =7.1 Hz, 3H); **<sup>13</sup>C NMR** (75 MHz, CDCl<sub>3</sub>):  $\delta$  = 173.2, 171.5, 136.5, 127.5, 122.2(8), 122.2(6), 119.6, 118.8, 113.0, 111.4, 60.8, 39.9, 31.2, 29.7, 25.4, 14.3 ppm; **MS** (ESI-MS):  $m/z$  (%) = 288.9 (50) [ $M^+$ -H], calc. 288.2.

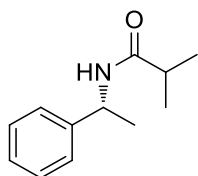
### ***N*-(2,2-Dimethoxyethyl)-4-nitrobenzamide (8d)**



Synthesized according to the general procedure. Yield: 86%.

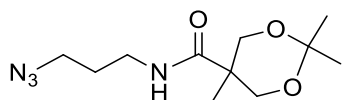
**<sup>1</sup>H NMR** (300 MHz, CDCl<sub>3</sub>):  $\delta$  = 8.32–7.26 (m, 2H), 7.96–7.91 (m, 2H), 6.44 (bs, 1H), 4.50 (t,  $J$ =5.0 Hz, 1H), 3.63 (t,  $J$ =5.4 Hz, 2H), 3.44 ppm (s, 6H); **<sup>13</sup>C NMR** (75 MHz, CDCl<sub>3</sub>):  $\delta$  = 165.7, 149.8, 140.0, 128.3, 124.0, 102.6, 54.9, 41.8 ppm; **MS** (ESI-MS):  $m/z$  (%) = 255.1 (100) [ $M^+$ -H], calc. 255.1.

### ***(R)*-N-(1-Phenylethyl)isobutyramide (8e)**



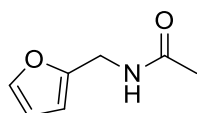
Synthesized according to the general procedure. Yield: 91%.

$[\alpha]_D^{25}$  = +118° (1.0 g per 100 mL in CHCl<sub>3</sub>, 21 °C);  $ee$  > 99%, determined by HPLC analysis using a Chiralpak AS-H column eluting with a 95:5 heptane/2-propanol mixture; **<sup>1</sup>H NMR** (300 MHz, CDCl<sub>3</sub>):  $\delta$  = 7.39–7.27 (m, 5H), 5.65 (bs, 1H), 5.23–5.04 (m, 1H), 2.43–2.24 (m, 1H), 1.49 (d,  $J$ =6.8 Hz, 3H), 1.15 ppm (t,  $J$ =6.7 Hz, 6H); **<sup>13</sup>C NMR** (75 MHz, CDCl<sub>3</sub>):  $\delta$  = 176.1, 143.5, 128.8, 127.4, 126.3, 48.5, 35.8, 21.8, 19.7 ppm; **MS** (ESI-MS):  $m/z$  (%) = 192.2 (100) [ $M^+$ -H], calc. 192.1.

***N*-(3-Azidopropyl)-2,2,5-trimethyl-1,3-dioxane-5-carboxamide (8f)**

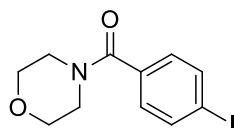
Synthesized according to the general procedure. Yield: 95%.

**<sup>1</sup>H NMR** (300 MHz, CDCl<sub>3</sub>):  $\delta$  = 7.22 (bs, 1H), 3.90 (d,  $J$ =12.4 Hz, 2H), 3.77 (d,  $J$ =12.4 Hz, 2H), 3.46–3.35 (m, 4H), 1.84 (p,  $J$ =6.7 Hz, 2H), 1.48 (s, 3H), 1.43 (s, 3H), 1.00 ppm (s, 3H); **<sup>13</sup>C NMR** (75 MHz, CDCl<sub>3</sub>):  $\delta$  = 175.3, 98.7, 68.4, 67.3, 49.3, 40.3, 37.0, 29.2, 28.9, 18.3, 17.9 ppm; **IR** ( $\bar{\nu}$ /cm<sup>-1</sup>): 3375, 2989, 2937, 2872, 2095, 1650, 1537, 1454, 1375, 1265, 1201, 1082, 828, 637; **MS** (ESI-MS):  $m/z$  (%) = 257.1605 (100) [ $M^+$ -H], calc. 257.1608.

***N*-(Furan-2-ylmethyl)acetamide (8g)**

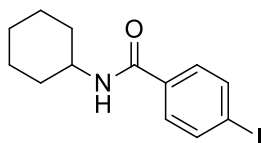
Synthesized according to the general procedure. Yield: 95%.

**<sup>1</sup>H NMR** (300 MHz, CDCl<sub>3</sub>):  $\delta$  = 7.35 (d,  $J$ =1.1 Hz, 1H), 6.32 (dd,  $J$ =3.0 Hz, 1.9, 1H), 6.22 (d,  $J$ =3.0 Hz, 1H), 5.87 (bs, 1H), 4.42 (d,  $J$ =5.4 Hz, 2H), 2.00 ppm (s, 3H); **<sup>13</sup>C NMR** (75 MHz, CDCl<sub>3</sub>):  $\delta$  = 170.0, 151.3, 142.3, 110.6, 107.6, 36.7, 23.6 ppm; **MS** (ESI-MS):  $m/z$  (%) = 157.1 (100) [ $M^+$ -NH<sub>4</sub>], calc. 157.1.

**(4-Iodophenyl)(morpholino)methanone (8h)**

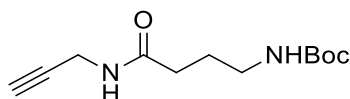
Synthesized according to the general procedure. Yield: 90%.

**<sup>1</sup>H NMR** (300 MHz, CDCl<sub>3</sub>):  $\delta$  = 7.77 (d,  $J$ =8.3 Hz, 2H), 7.15 (d,  $J$ =8.3 Hz, 2H), 3.94–3.31 ppm (m,  $J$ =72.7 Hz, 8H); **<sup>13</sup>C NMR** (75 MHz, CDCl<sub>3</sub>):  $\delta$  = 169.6, 137.9, 134.8, 129.0, 96.3, 67.0 ppm; **MS** (ESI-MS):  $m/z$  (%) = 317.0 (30) [ $M^+$ -H], calc. 317.0.

**N-Cyclohexyl-4-iodobenzamide (8i)**

Synthesized according to the general procedure. Yield: 87%.

**m.p.** 171-173 °C; **IR** (ATR,  $\bar{\nu}/\text{cm}^{-1}$ ): 3296, 2934, 2853, 1715, 1623, 1585, 1537, 1477, 1445, 1330, 1151, 1006, 890, 837, 713, 677;  **$^1\text{H}$  NMR** (300 MHz,  $\text{CDCl}_3$ ):  $\delta$  = 7.77 (d,  $J=8.4$  Hz, 2H), 7.47 (d,  $J=8.3$  Hz, 2H), 5.88 (bs, 1H), 4.03–3.88 (m, 1H), 2.08–1.96 (m, 2H), 1.82–1.52 (m, 4H), 1.53–1.33 (m, 2H), 1.32–1.18 ppm (m, 2H);  **$^{13}\text{C}$  NMR** (75 MHz,  $\text{CDCl}_3$ ):  $\delta$  = 165.9, 137.8, 134.6, 128.6, 98.2, 49.0, 33.3, 25.7, 25.0 ppm; **MS** (ESI-MS):  $m/z$  (%) = 330.0351 (100) [ $M^+-\text{H}$ ], calc. 330.0349.

**tert-Butyl (4-oxo-4-(prop-2-yn-1-ylamino)butyl)carbamate (8j)**

Synthesized according to the general procedure. Yield: 97 %.

**$^1\text{H}$  NMR** (300 MHz,  $\text{CDCl}_3$ ):  $\delta$  = 6.45 (bs, 1H), 4.73 (bs, 1H), 4.05 (dd,  $J=4.8$  Hz, 2.4, 2H), 3.17 (t,  $J=6.4$  Hz, 2H), 2.34–2.15 (m, 3H), 1.90–1.73 (m, 2H), 1.44 ppm (s, 9H);  **$^{13}\text{C}$  NMR** (75 MHz,  $\text{CDCl}_3$ ):  $\delta$  = 172.5, 156.7, 79.8, 79.6, 39.7, 33.5, 29.3, 28.5, 26.6 ppm; **MS** (ESI-MS):  $m/z$  (%) = 241.1 (100) [ $M^+-\text{H}$ ], calc. 241.2.

**General method for the reacylation of magnetic ROMPgels using acid chlorides or anhydrides**

Magnetic ROMPgel resin bearing free *N*-hydroxyl groups (**9**) was dispersed in  $\text{CH}_2\text{Cl}_2$  by stirring for 15 min. After cooling to 0 °C,  $\text{Et}_3\text{N}$  (4.0 equiv.) and acid chloride or anhydride (3.0 equiv., dropwise/in portions) were added. In the case of anhydrides, 0.1 equiv. of DMAP were added as catalyst. The slurry was stirred for 30 min at 0 °C, and the stirring continued for 16 h at RT. Thereafter, the magnetic ROMPgel was collected by using a magnet, and the solution decanted. The particles were subsequently washed with THF (3×5 mL),  $\text{CH}_2\text{Cl}_2$  (3×5 mL), and  $\text{Et}_2\text{O}$  (1×5 mL). After drying under high vacuum, the loading was determined by an NMR assay.

**General method for the reacylation of magnetic ROMPgels using acids**

Resin **9** was predispersed in a DMF/CH<sub>2</sub>Cl<sub>2</sub> mixture (1:1) and cooled to 0 °C. Acid (3.0 equiv.), TBTU (3.0 equiv.), and DIPEA (3.0 equiv.) were stirred together in 3 mL DMF/CH<sub>2</sub>Cl<sub>2</sub> at 0 °C for 15 min before dropwise addition to the resin. The resulting slurry was stirred for 1 h at 0 °C and overnight at RT before the ROMPgels was recovered by using a magnet. The particles were subsequently washed with THF (3×5 mL), CH<sub>2</sub>Cl<sub>2</sub> (3×5 mL), and Et<sub>2</sub>O (1×5 mL). After drying under high vacuum, the loading was again determined by using an NMR assay.

➔ Please find supporting information including additional experimental procedures, TEM pictures, and <sup>1</sup>H- and <sup>13</sup>C-NMR spectra on the enclosed CD.

### 3.5 References

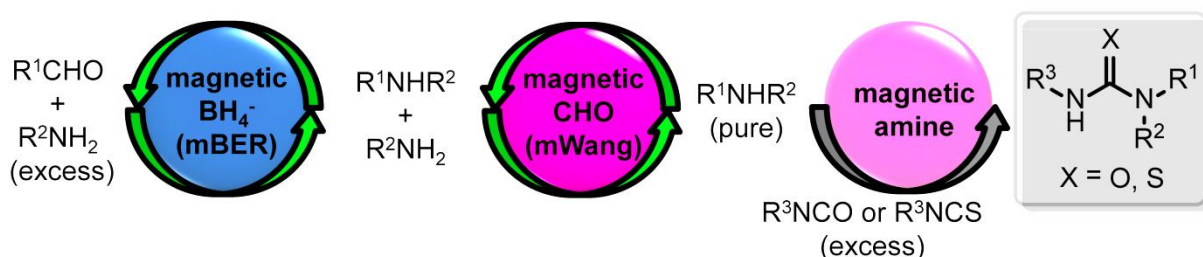
- [1] a) R. J. Booth, J. C. Hodges, *Acc. Chem. Res.* **1999**, *32*, 18–26; b) A. Kirschning, H. Monenschein, R. Wittenberg, *Angew. Chem. Int. Ed.* **2001**, *40*, 650–679; c) A. Loupy (Ed.) *Microwave-Assisted Combinatorial Chemistry*, Wiley-VCH Verlag GmbH & Co. KGaA, Weinheim, **2002**; d) R. E. Dolle, *J. Comb. Chem.* **2005**, *7*, 739–798.
- [2] a) M. Fridkin, A. Patchornik, E. Katchalski, *J. Am. Chem. Soc.* **1965**, *87*, 4646–4648; b) M. Fridkin, A. Patchornik, E. Katchalski, *J. Am. Chem. Soc.* **1966**, *88*, 3164–3165; c) M. Fridkin, A. Patchornik, E. Katchalski, *J. Am. Chem. Soc.* **1968**, *90*, 2953–2957; d) G. T. Panse, D. A. Laufer, *Tetrahedron Lett.* **1970**, *11*, 4181–4184; e) J. W. Lee, Y. Q. Louie, D. P. Walsh, Y.-T. Chang, *J. Comb. Chem.* **2003**, *5*, 330–335.
- [3] a) T. Wieland, C. Birr, *Angew. Chem. Int. Ed.* **1966**, *5*, 310; b) E. Flanigan, G. R. Marshall, *Tetrahedron Lett.* **1970**, *27*, 2403–2406; c) D. L. Marshall, I. E. Liener, *J. Org. Chem.* **1970**, *35*, 867–868.
- [4] a) T. L. Ang, H. J. Harwood, *J. Macromol. Sci., Part A: Pure Appl. Chem.* **1973**, *7*, 1079–1083; b) M. B. Shambhu, G. A. Digenis, *Tetrahedron Lett.* **1973**, *18*, 1627–1629; c) S. Porto, J. Durán, J. M. Seco, E. Quiñoá, R. Riguera, *Org. Lett.* **2003**, *5*, 2979–2982.
- [5] a) J. M. Salvino, B. Gerard, H. F. Ye, B. Sauvagnat, R. E. Dolle, *J. Comb. Chem.* **2003**, *5*, 260–266; b) J. M. Salvino et al., *J. Comb. Chem.* **2000**, *2*, 691–697.
- [6] a) R. Kalir, A. Warshawsky, M. Fridkin, A. Patchornik, *Eur. J. Biochem.* **1975**, *59*, 55–61; b) M. Mokotoff, A. Patchornik, *Int. J. Pept. Protein Res.* **1983**, *21*, 145–154.
- [7] O. W. Gooding, L. Vo, S. Bhattacharyya, J. W. Labadie, *J. Comb. Chem.* **2002**, *4*, 576–583.
- [8] I. E. Pop, B. P. Déprez, A. L. Tartar, *J. Org. Chem.* **1997**, *62*, 2594–2603.
- [9] a) J. V. Staros, *Biochemistry* **1982**, *21*, 3950–3955; b) G. T. Hermanson, *Bioconjugate techniques*, 2nd ed., Academic Press, San Diego, **1996**.
- [10] a) D. A. Laufer, T. M. Chapman, D. I. Marlborough, V. M. Vaidya, E. R. Blout, *J. Am. Chem. Soc.* **1968**, *90*, 2696–2698; b) M. Fridkin, A. Patchornik, E. Katchalski, *Biochemistry* **1972**, *11*, 466–471.
- [11] a) M. Akiyama, M. Narita, M. Okawara, *J. Polym. Sci., Part A: Polym. Chem.* **1969**, *7*, 1299–1306; b) M. Akiyama, Y. Yanagisawa, M. Okawara, *J. Polym. Sci., Part A: Polym. Chem.* **1969**, *7*, 1905–1912; c) M. Akiyama, K. Shimizu, M. Narita, *Tetrahedron Lett.* **1976**, 1015–1016.
- [12] M. Adamczyk, J. R. Fishpau, P. G. Mattingly, *Tetrahedron Lett.* **1999**, *40*, 463–466.
- [13] M. Adamczyk, J. R. Fishpau, P. G. Mattingly, *Bioorg. Med. Chem. Lett.* **1999**, *9*, 217–220.
- [14] A. G. M. Barrett, B. T. Hopkins, J. Köbberling, *Chem. Rev.* **2002**, *102*, 3301–3324.
- [15] A. G. Barrett, B. Bibal, B. T. Hopkins, J. Köbberling, A. C. Love, L. Tedeschi, *Tetrahedron* **2005**, *61*, 12033–12041.
- [16] a) M. R. Buchmeiser, *Chem. Rev.* **2000**, *100*, 1565–1604; b) M. R. Buchmeiser, *Bioorg. Med. Chem. Lett.* **2002**, *12*, 1837–1840.
- [17] a) A. M. Harned, W. Sherill, D. L. Flynn, P. R. Hanson, *Tetrahedron* **2005**, *61*, 12093–12099; b) A. M. Harned, H. S. He, P. H. Toy, D. L. Flynn, P. R. Hanson, *J. Am. Chem. Soc.* **2005**, *127*, 52–53; c) T. R. Long, P. K. Maity, T. B. Samarakoon, P. R. Hanson, *Org. Lett.* **2010**, *12*, 2904–2907.
- [18] a) J. D. Moore, A. M. Harned, J. Henle, D. L. Flynn, P. R. Hanson, *Org. Lett.* **2002**, *4*, 1847–1849; b) J. D. Moore, R. H. Herpel, J. R. Lichtsinn, D. L. Flynn, P. R. Hanson, *Org. Lett.* **2003**, *5*, 105–107; c) A. Rolfe, D. A. Probst, K. A. Volp, I. Omar, D. L. Flynn, P. R. Hanson, *J. Org. Chem.* **2008**, *73*, 8785–8790.
- [19] A. G. M. Barrett, S. M. Cramp, R. S. Roberts, F. J. Zecri, *Org. Lett.* **2000**, *2*, 261–264.
- [20] A. G. Barrett, R. S. Roberts, F. J. Zecri, S. M. Cramp, *Comb. Chem. High Throughput Screen.* **2000**, *3*, 131–138.
- [21] R. S. Roberts, *J. Comb. Chem.* **2005**, *7*, 21–32.
- [22] A. Schätz, R. N. Grass, Q. Kainz, W. J. Stark, O. Reiser, *Chem. Mater.* **2010**, *22*, 305–310.
- [23] R. N. Grass, E. K. Athanassiou, W. J. Stark, *Angew. Chem.* **2007**, *119*, 4996–4999; *Angew. Chem. Int. Ed.* **2007**, *46*, 4909–4912.



- [24] I. K. Herrmann, R. N. Grass, D. Mazunin, W. J. Stark, *Chem. Mater.* **2009**, *21*, 3275–3281.
- [25] Q. M. Kainz, A. Schätz, A. Zöpfl, W. J. Stark, O. Reiser, *Chem. Mater.* **2011**, *23*, 3606–3613.
- [26] a) F. M. Koehler, M. Rossier, M. Waelle, E. K. Athanassiou, L. K. Limbach, R. N. Grass, D. Günther, W. J. Stark, *Chem. Commun.* **2009**, 4862–4864; b) M. Rossier, F. M. Koehler, E. K. Athanassiou, R. N. Grass, M. Waelle, K. Birbaum, D. Günther, W. J. Stark, *Ind. Eng. Chem. Res.* **2010**, *49*, 9355–9362; c) Q. M. Kainz, A. Späth, S. Weiss, T. D. Michl, A. Schätz, W. J. Stark, B. König, O. Reiser, *ChemistryOpen* **2012**, *1*, 125–129.
- [27] M. Rossier, F. M. Koehler, E. K. Athanassiou, R. N. Grass, B. Aeschlimann, D. Günther, W. J. Stark, *J. Mater. Chem.* **2009**, *19*, 8239–8243.
- [28] I. K. Herrmann, M. Urner, F. M. Koehler, M. Hasler, B. Roth-Z'Graggen, R. N. Grass, U. Ziegler, B. Beck-Schimmer, W. J. Stark, *Small* **2010**, *6*, 1388–1392.
- [29] A. Schätz, R. N. Grass, W. J. Stark, O. Reiser, *Chem. Eur. J.* **2008**, *14*, 8262–8266.
- [30] a) A. Schätz, O. Reiser, W. J. Stark, *Chem. Eur. J.* **2010**, *16*, 8950–8967; b) S. Wittmann, A. Schätz, R. N. Grass, W. J. Stark, O. Reiser, *Angew. Chem., Int. Ed.* **2010**, *49*, 1867–1870; *Angew. Chem.* **2010**, *122*, 1911–1914.
- [31] A. Schätz, T. R. Long, R. N. Grass, W. J. Stark, P. R. Hanson, O. Reiser, *Adv. Funct. Mater.* **2010**, *20*, 4323–4328.
- [32] P. K. Maity, A. Rolfe, T. B. Samarakoon, S. Faisal, R. D. Kurtz, T. R. Long, A. Schätz, D. L. Flynn, R. N. Grass, W. J. Stark, O. Reiser, P. R. Hanson, *Org. Lett.* **2011**, *13*, 8–10.
- [33] P. K. Maity, Q. M. Kainz, S. Faisal, A. Rolfe, T. B. Samarakoon, F. Z. Basha, O. Reiser, P. R. Hanson, *Chem. Commun.* **2011**, *47*, 12524–12526.
- [34] a) V. V. Rostovtsev, L. G. Green, V. V. Fokin, K. B. Sharpless, *Angew. Chem. Int. Ed.* **2002**, *41*, 2596–2599; b) C. W. Tornøe, M. Meldal in *American Peptide Symposium* (Eds.: M. Lebl, Houghten R. A.), American Peptide Society, Kluwer Academic Publishers, San Diego, CA, **2001**; c) C. W. Tornøe, C. Christensen, M. Meldal, *J. Org. Chem.* **2002**, *67*, 3057–3064.
- [35] W. H. Heath, F. Palmieri, J. R. Adams, B. K. Long, J. Chute, T. W. Holcombe, S. Zieren, M. J. Truitt, J. L. White, C. G. Willson, *Macromolecules* **2008**, *41*, 719–726.
- [36] N. A. O'Connor, A. J. Berro, J. R. Lancaster, X. Gu, S. Jockusch, T. Nagai, T. Ogata, S. Lee, P. Zimmerman, C. G. Willson et al., *Chem. Mater.* **2008**, *20*, 7374–7376.
- [37] (PCy<sub>3</sub>)<sub>2</sub>(Cl)<sub>2</sub>Ru=CHPh; a) P. Schwab, M. B. France, J. W. Ziller, R. H. Grubbs, *Angew. Chem. Int. Ed.* **1995**, *34*, 2039–2041; *Angew. Chem.* **1995**, *107*, 2179–2181; b) P. Schwab, R. H. Grubbs, J. W. Ziller, *J. Am. Chem. Soc.* **1996**, *118*, 100–110.
- [38] (IMesH<sub>2</sub>)(PCy<sub>3</sub>)(Cl)<sub>2</sub>Ru=CHPh; M. Scholl, S. Ding, C. W. Lee, R. H. Grubbs, *Org. Lett.* **1999**, *1*, 953–956.
- [39] See supporting information.
- [40] C. Somlai, G. Szókán, L. Balásperi, *Synthesis* **1992**, *1992*, 285–287.
- [41] C. Somlai, G. Szókán, B. Penke, *Synthesis* **1995**, *1995*, 683–686.
- [42] a) S. Han, K. Young-Ahn, *Tetrahedron* **2004**, *60*, 2447–2467; b) L. A. Carpino, M. Beyermann, H. Wenschuh, M. Bienert, *Acc. Chem. Res.* **1996**, *29*, 268–274.



#### 4. Synthesis of Trisubstituted Ureas by a Multistep Sequence Utilizing Recyclable Magnetic Reagents and Scavengers<sup>i</sup>



Unprecedented magnetic borohydride exchange (mBER), magnetic Wang aldehyde (mWang), and magnetic amine resins are prepared from highly magnetic polymer-coated cobalt or iron nanoparticles. Microwave irradiation is used to obtain excellent functionalization (> 95%) and loadings (up to 3.0 mmol/g) in short reaction times of 15 minutes or less. A small library of ureas and thioureas is synthesized by the exclusive application of these magnetic resins. As a first step, a reductive amination of aromatic and aliphatic aldehydes is carried out using the mBER. The excess of primary amine needed to complete the reaction is subsequently scavenged selectively by mWang aldehyde. Simple magnetic decantation from the resins resulted in secondary amines in good to excellent yields and purities. The used magnetic resins were efficiently regenerated and reused for the next run. In a second step, the secondary amines are converted to tri-substituted (thio)ureas in excellent yields and purities by stirring with an excess of iso(thio)cyanate, which is scavenged by addition of the magnetic amine resin after completion of the reaction. The whole reaction sequence is carried out without any purification apart from magnetic decantation, moreover, conventional magnetic stirring can be used as opposed to vortexing required for polystyrene resins.<sup>ii</sup>

<sup>i</sup> Reproduced with permission from: Q. M. Kainz, M. Zeltner, M. Rossier, W. J. Stark, O. Reiser, *Chem. Eur. J.* **2013**, *19*, 10038-10045. Copyright 2013 WILEY-VCH Verlag GmbH & Co. KGaA, Weinheim.

<sup>ii</sup> TEM was performed by M. Zeltner and M. Rossier. All other experiments were carried out by Q. M. Kainz.

## 4.1 Introduction

Initiated by the pioneering work of Merrifield<sup>[1]</sup> five decades ago, polymer resins as insoluble supports have been of considerable and steadily growing interest in the field of organic synthesis. Solid-phase organic synthesis (SPOS)<sup>[2]</sup> nothing less than revolutionized the synthesis of polypeptides and polynucleotides by the adaption of established solution phase reactions to solid phase. Driven by the demand of the pharmaceutical industry for high speed parallel synthesis an alternative solution-phase technique utilizing reagents,<sup>[3,4]</sup> catalysts<sup>[5]</sup> and scavengers<sup>[6]</sup> supported on functional polymers evolved recently. In contrast to SPOS this complementary approach is considerably simpler dispensing from the need of linker chemistry and sparing two additional steps for attaching the starting material to the resin and cleavage of the product from the solid support.<sup>[7]</sup> Additional advantages are the facile monitoring of reaction progress by standard analytical techniques like thin layer chromatography (TLC) and the potential reuse of the catalysts and regeneration of the reagents supported on the polymer resins.<sup>[4]</sup> The workup consists of simple filtration and evaporation of the solvents leading to generally very clean and high yielding products and avoiding complex and expensive purification steps that also might generate additional waste.

While a lot of effort was put into the diversification of reagents, catalysts, and scavengers, the resins itself are still dominated largely by simple cross-linked polystyrene. To bring the supports to the next level, we envisaged to introduce highly magnetic cores to the polystyrene beads to enable an even quicker and more convenient separation of the supports from reaction mixtures by rapid magnetic decantation. This would avoid clogging of filters, facilitate recovery and subsequently recycling of the resins, and allow for continuous-flow applications using magnetic fields rather than membranes to contain the supports.<sup>[8]</sup> Recently, Stark *et al.* developed the large scale synthesis (> 30 g/h) of carbon coated cobalt (Co/C)<sup>[9]</sup> and iron (Fe/C)<sup>[10]</sup> nanobeads via reducing flame spray pyrolysis of inexpensive metal carboxylates. The raw materials cost for manufacturing carbon coated nanoparticles by this route can be estimated as < 100 USD/kg.<sup>[11]</sup> These nanoparticles feature an excellent thermal as well as chemical stability due to the graphene-like shell, and the core of pure metal leads to an exceptionally high saturation magnetization (up to 158 emu/g) being five times higher than for common iron oxide (e.g. magnetite) beads.<sup>[12]</sup> Effective covalent and/or non-covalent functionalization of the surface was achieved<sup>[13]</sup> giving rise to the

application in the extraction of organic molecules and metals from aqueous solutions up to the ton per hour scale,<sup>[14]</sup> in the purification of blood,<sup>[15]</sup> or as recyclable support for catalysts.<sup>[16,8]</sup> To increase the loading with functional groups by at least one order of magnitude polymer shells were introduced by either surface initiated ring-opening metathesis polymerization (ROMP)<sup>[17]</sup> or alternatively by radical polymerization on the nanoparticle surface.<sup>[18,19]</sup> ROMP-based scavenger for Mitsunobu reactions as well as recyclable acylation reagents were already established.<sup>[20]</sup>

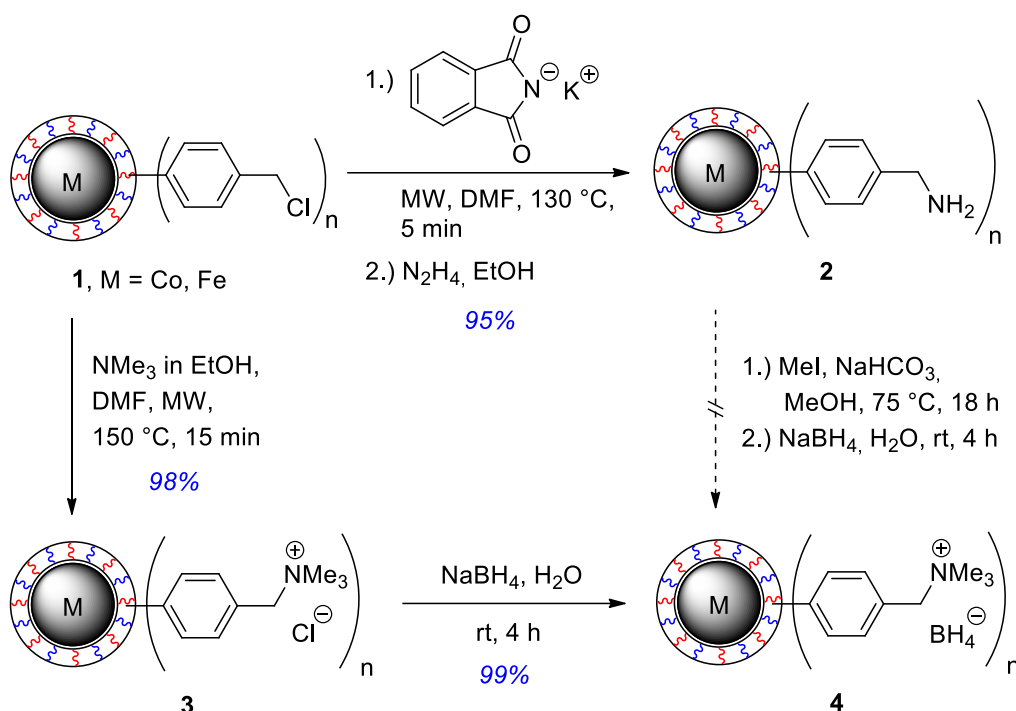
Building on the results of Kaldor *et al.*<sup>[21]</sup> and Guinó *et al.*<sup>[22]</sup> we herein report the - to the best of our knowledge - first multi-step synthesis by exclusively combining magnetic reagents and scavengers. A small library of secondary amines was prepared via reductive amination followed by conversion into tri-substituted ureas or thioureas. All magnetic resins were functionalized by quick and efficient microwave protocols and recycled for several runs whenever possible.

## 4.2 Results and Discussion

### Synthesis of magnetic borohydride resin (mBER)

In order to synthesize a magnetic variant of the borohydride exchange resin (BER)<sup>[23]</sup> carbon-coated cobalt or iron nanoparticles with an additional polystyrene-shell (**1**) were applied as basis (Scheme 1). They were easily prepared on multi-gram scale in three steps starting from pristine Co/C or Fe/C nanobeads.<sup>[19]</sup> High loadings of 3.0-3.5 mmol benzyl chloride moieties per gram magnetic resin are obtained for **1** as determined by chlorine microanalysis. The swelling of the resin is analogous to conventional polystyrene beads and the exceptionally high magnetic moment of the metal core leads to an overall saturation magnetization (>33 emu/g)<sup>[19]</sup> that allows rapid separation of the high loading hybrid material from reaction mixtures (Figure 1). No irreversible aggregation of the nanobeads or limited recovery was observed under the conditions used in this work. Besides magnetic separation, the nanoparticles can be agitated by – internal or external – magnetic stirring, being a distinct advantage to polystyrene resins, which require agitation by vortexing.

The preparation of the mBER **4** the resin-bound benzylamine **2** was envisioned followed by quaternization with methyl iodine and counterion-exchange with an aqueous sodium-borohydride solution (Scheme 1). Thus, a protocol for the Gabriel synthesis described by Rotello *et al.*<sup>[24]</sup> was modified to use a focussed microwave



**Scheme 1.** Microwave-assisted synthesis of a magnetic borohydride exchange resin **4** (mBER).

oven to quickly and efficiently heat the metal nanoparticles being very susceptible to microwave irradiation,<sup>[25]</sup> which allowed to shorten the reaction time for the functionalization to 5 minutes. After cleavage with hydrazine the amino-modified beads **2** were obtained with a loading of 3 mmol/g (95% of benzyl chloride substituted) as determined by elemental microanalysis. Additionally, the reaction was conveniently monitored by infrared spectroscopy using attenuated total reflectance as sampling technique (ATR-IR).<sup>[26]</sup> The functionalized nanobeads **2** can be applied as scavengers for electrophiles as demonstrated later in this paper. However, the planned quaterniza-

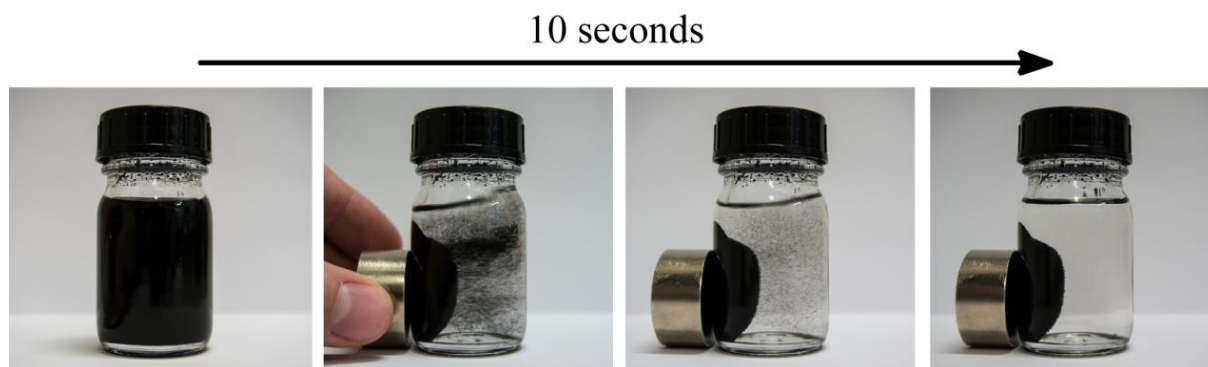


**Figure 1.** Magnetic recovery of polystyrene-coated nanobeads **1** from a CH<sub>2</sub>Cl<sub>2</sub> solution. The golden coloured cylinder is a Neodymium-based magnet.

tion *en route* to mBER **4** using methyl iodide was not exhaustive concluding from elemental analysis data and it was impossible to monitor the reaction progress conclusively by ATR-IR.

Therefore, an alternative synthetic route was developed. The direct conversion of benzyl chloride moieties to quaternary ammonium cations has been reported for the synthesis of water-soluble calix[*n*]arene<sup>[27]</sup> or porphyrins<sup>[28]</sup> using either trimethylamine gas or, more conveniently, aqueous or ethanolic solutions of trimethylamine with the addition of co-solvents. Applying the latter method to benzyl chloride functionalized nanobeads **1**, a 33% ethanolic solution of trimethylamine and DMF as co-solvent ensuring efficient swelling of the polystyrene shell were used to prepare nanobeads loaded with quaternary ammonium cations **3** (Scheme 1). Stirring for two days at room temperature as indicated in the literature<sup>[27,28]</sup> led to a good degree of substitution (91%) concluding from nitrogen elemental analysis (Table 1, Entry 1). Again, microwave irradiation was used to cut down on reaction times (Table 1, Entries 2-6). The higher pressures of up to 15 bar due to the gaseous trimethylamine and temperatures above the boiling point of ethanol were tolerated by the microwave oven and the glassware alike. A control experiment without the co-solvent DMF led to an even higher degree of functionalization (93%, Table 1, Entry 4) compared to the experiment with added DMF (90%, Table 1, Entry 3). At optimized conditions (150 °C, 15 min, no DMF) the benzyl chloride moieties were substituted almost quantitatively regardless if polystyrene-coated Co/C or Fe/C nanoparticles were used.

**Table 1.** Functionalization of polymer coated nanobeads **1** with quaternary ammonium ions applying microwave heating.

Entry	Particles	DMF as co-solvent	T [°C]	t [min]	Degree of functionalization <sup>[a]</sup>
1	Fe/C	yes	25 <sup>[b]</sup>	2 d	91%
2	Fe/C	yes	140	30	95%
3	Co/C	yes	150	10	90%
4	Co/C	no	150	10	93%
5 <sup>[c]</sup>	Co/C	no	150	15	97%
6 <sup>[c]</sup>	Fe/C	no	150	15	98%

[a] Determined by nitrogen elemental analysis. [b] No microwave irradiation applied. [c] Scale: 1g.

The progress of the functionalization was again conveniently monitored by ATR-IR (Figure 2). The characteristic benzyl chloride peak at  $1263\text{ cm}^{-1}$  vanished completely upon nucleophilic substitution by the amine and after stirring with an aqueous solution of sodium borohydride for four hours characteristic peaks for the borohydride counterion ( $2203$  and  $1070\text{ cm}^{-1}$ ) appeared. Elemental microanalysis revealed that 99% of the chlorine was substituted by this ion exchange and the reducing capacity for the novel mBER resin **4** was determined by a  $^1\text{H}$ -NMR-assay utilizing an excess of 4-nitrobenzaldehyde as substrate and 4-methoxyanisole as internal standard. The obtained loadings (up to  $3.3\text{ mmol/g}$ ) are on par or in some cases slightly above the loadings for literature reported<sup>[23]</sup> and commercially available Amberlite® IRA-400 or Amberlyst® A-26 resins functionalized with borohydride ions ( $2.5$ – $3.3\text{ mmol/g}$ ). While pictures obtained from transmission electron microscopy (TEM) for pristine Co/C or Fe/C nanoparticles and polymer-coated nanoparticles **1** obviously differ due to the additional polymer shell around the nanobeads, no substantial chan-

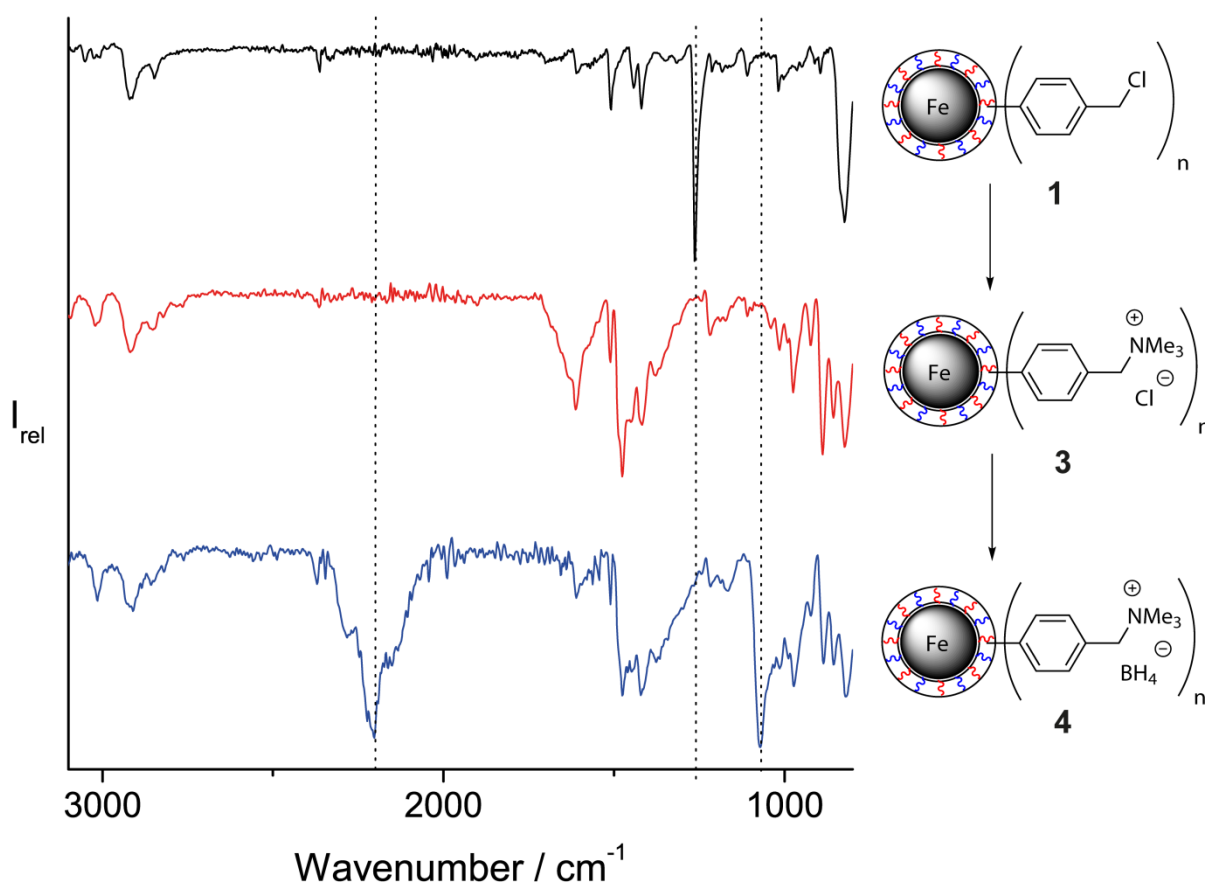


**Figure 2.** IR-ATR spectra of polymer coated Fe/C nanobeads bearing chlorine moieties **1** (top), after conversion to quaternary ammonium ions **3** (middle) and subsequent exchange of the chlorine counterion with borohydride (**4**) (bottom).



ges are apparent when comparing **1** to functionalized mBER resin **4**, demonstrating the stability of the carbon coated nanobeads during the microwave functionalization at elevated temperatures.<sup>[26]</sup>

To demonstrate the versatility, efficiency and recyclability of the novel magnetic borohydride resin, a series of different substrates was reduced by stirring with 1.5 equiv. of mBER **4** in methanol for 2-3 hours (Table 2). Aromatic as well as aliphatic aldehydes were readily reduced to the corresponding alcohols in high yields and purities (Table 2, Entry 1-3), and also ketones are amenable for reduction by **4** (Table 2, Entry 4+5). Notably, when using an  $\alpha,\beta$ -unsaturated ketone the carbonyl group was reduced selectively leaving the double bond untouched (Table 2, Entry 5). The activity and selectivity of **4** is consistent with reports found in literature for polystyrene based borohydride resins.<sup>[23]</sup> However, in contrast to these conventional beads the spent magnetic mBER can be collected by a magnet within seconds (Figure 1). To

**Table 2.** Reduction of aldehydes, ketones, and  $\alpha,\beta$ -unsaturated substrates with Fe/C-mBER (**4**) in methanol.

Entry	Substrate	Product ( <b>5a-e</b> )	t [h]	Yield <sup>[b]</sup>
1			2	88%
2			3	89%
3			2	88%
4			3	98%
5			3	99%

[a] Loading determined by Nitrogen elemental analysis. [b] Isolated yields. Purity > 95% in all cases as determined by NMR spectroscopy.

obtain the pure product in solution the supernatant was conveniently decanted and the particles were washed by re-suspending in methanol. Usually, more than 99.7 wt% of the nanoparticles was recovered after drying under vacuum. To prevent line broadening in the NMR spectrum due to trace amounts of magnetic material, in some cases additional filtration of the product solution was nevertheless necessary.<sup>[26]</sup> The spent resin was washed with aqueous sodium hydroxide followed by aqueous sodium chloride to regenerate the chlorine form **3** of the resin, while stirring with a borohydride solution finally restored the mBER **4**. A NMR-assay of the recycled resin **4** revealed loadings (2.5-3.3 mmol/g) comparable to pristine mBER **4** indicating efficient recharging. The recycled resin **4** was applied for the next run without apparent cross contamination.

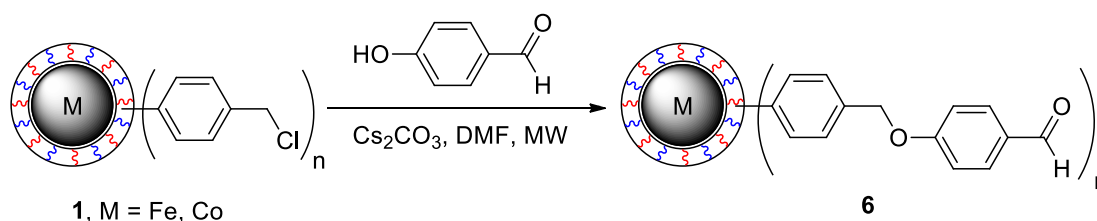
### **Preparation of a magnetic Wang aldehyde resin (mWang)**

Having successfully prepared the mBER resin **4**, a magnetic scavenger for reductive aminations was synthesized next. While there are several polymer-based scavengers for amines known in literature<sup>[29]</sup> the Wang aldehyde resin is arguably one of the most frequently used. It has been successfully employed in the sequestration of primary amines in the presence of secondary amines,<sup>[30,21,22]</sup> in the synthesis of 2,3-dihydro-4-pyridones,<sup>[31]</sup> or, more recently, in the synthesis of  $\alpha,\alpha$ -disubstituted amino acid derivatives.<sup>[32]</sup> This resin is also commercially available nowadays on the multi-gram scale.

For the preparation of the magnetic variant **6** of the Wang-aldehyde resin (mWang), a modified microwave synthesis<sup>[32]</sup> was used to efficiently functionalize the nanobeads **1** (Table 3). A control experiment under thermal conditions using 4-hydroxybenzaldehyde as nucleophile and Cs<sub>2</sub>CO<sub>3</sub> as a base stirring at 80 °C for three days only resulted in a moderate conversion of 73% (Table 3, Entry 1). Microwave irradiation and increasing the temperature to 130 °C drastically speeded up the transformation reaching 89% Cl displacement after only 5 minutes regardless if cobalt or iron nanoparticles were used (Table 3, Entry 2+3). Increasing the temperature to 140 °C and the reaction time to 15 min almost quantitative functionalization was achieved for a batch of 1 g demonstrating the effectiveness of this microwave transformation (Table 3, Entry 4). Taking into account the gain in molecular mass during this functionalization the loadings determined by chlorine elemental analysis (2.5 - 2.7 mmol/g) are excellent and on par with commercially available Wang-aldehyde

resins (up to 3.0 mmol/g) despite the metal core of the hybrid material. TEM analysis revealed no noticeable differences between polystyrene-coated nanoparticles **1**, the mBER variant **4** and the mWang resin **6**.<sup>[26]</sup>

**Table 3.** Introduction of aldehyde functionalities onto magnetic nanoparticles by nucleophilic substitution utilizing microwave heating.

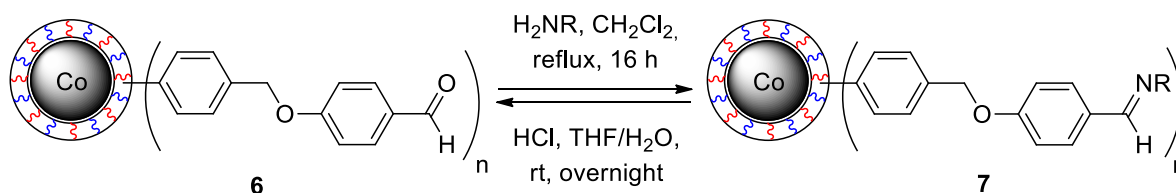


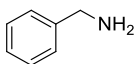
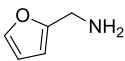
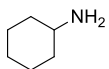
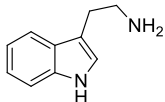
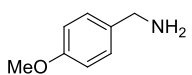
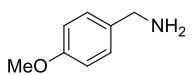
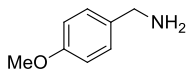
Entry	Particles	T [°C]	Microwave	t [min]	DoF <sup>[a]</sup>
1	Fe/C	80	no	3 d	73%
2	Fe/C	130	yes	5	89%
3	Co/C	130	yes	5	89%
4 <sup>[a]</sup>	Co/C	140	yes	15	98%

[a] Degree of functionalization, determined by chlorine elemental analysis. [b] Scale: 1 g.

To test the scope and effective loading of the new magnetic scavenger an excess of various benzylic and aliphatic primary amines was refluxed with **6** overnight (Table 4). The resin supported imines **7** were generated in high loadings (1.9-2.2 mmol/g) corresponding to yields of 89-99% as determined by nitrogen elemental analysis. These results are considerably better than those for conventional Wang aldehyde polystyrene resin, for which yields of 59-82% are obtained for a comparable series of amines.<sup>[22]</sup> Subsequently, the spent mWang resin **6** was regenerated by stirring **7** with aqueous HCl in a THF/H<sub>2</sub>O mixture over night followed by several washing cycles using water, methanol and acetone. The loadings of residual imine after hydrolysis were at the detection limit of the elemental microanalysis (0.01-0.05 mmol/g), which indicates quantitative cleavage.

In order to demonstrate the recyclability of the mWang **6**, the cycle of immobilization and hydrolysis was repeated trice (Table 4, Entry 5-7). While the loading with imine increased from 94% to 99% in the second cycle, the loadings after hydrolysis remained on a negligible low level. Additional qualitative analysis of the successful

**Table 4.** Reversible scavenging of primary amines by mWang resin **6**.


Entry	Run	Amines	Loading <sup>[a]</sup> [mmol/g]	Yield	Loading after hydrolysis <sup>[a]</sup> [mmol/g]
1	1		1.91	88%	0.01
2	1		1.97	89%	0.03
3	1		1.94	88%	0.01
4	1		2.00	98%	0.05
5	1		2.06	94%	0.02
6	2		2.19	99%	0.03
7	3		2.19	99%	0.04

[a] Loading determined by Nitrogen elemental analysis.

functionalization as well as cleavage was provided by ATR-IR analysis (Figure 3). In the spectrum of the mWang resin **6**, a broad peak at  $1676\text{ cm}^{-1}$  is dominant which can be assigned to the carbonyl group of the immobilized aldehyde. After conversion to the resin bound imine **7**, the aldehyde peak completely vanished and a new peak appeared at  $1636\text{ cm}^{-1}$  corresponding to the resin-bound imine groups. After the aldehyde groups were restored by hydrolysis of the imine, the obtained spectrum (Figure 3, bottom) perfectly matched the spectrum of as-prepared mWang resin **6** (Figure 3, top) perfectly underlining the good recyclability of the resin.

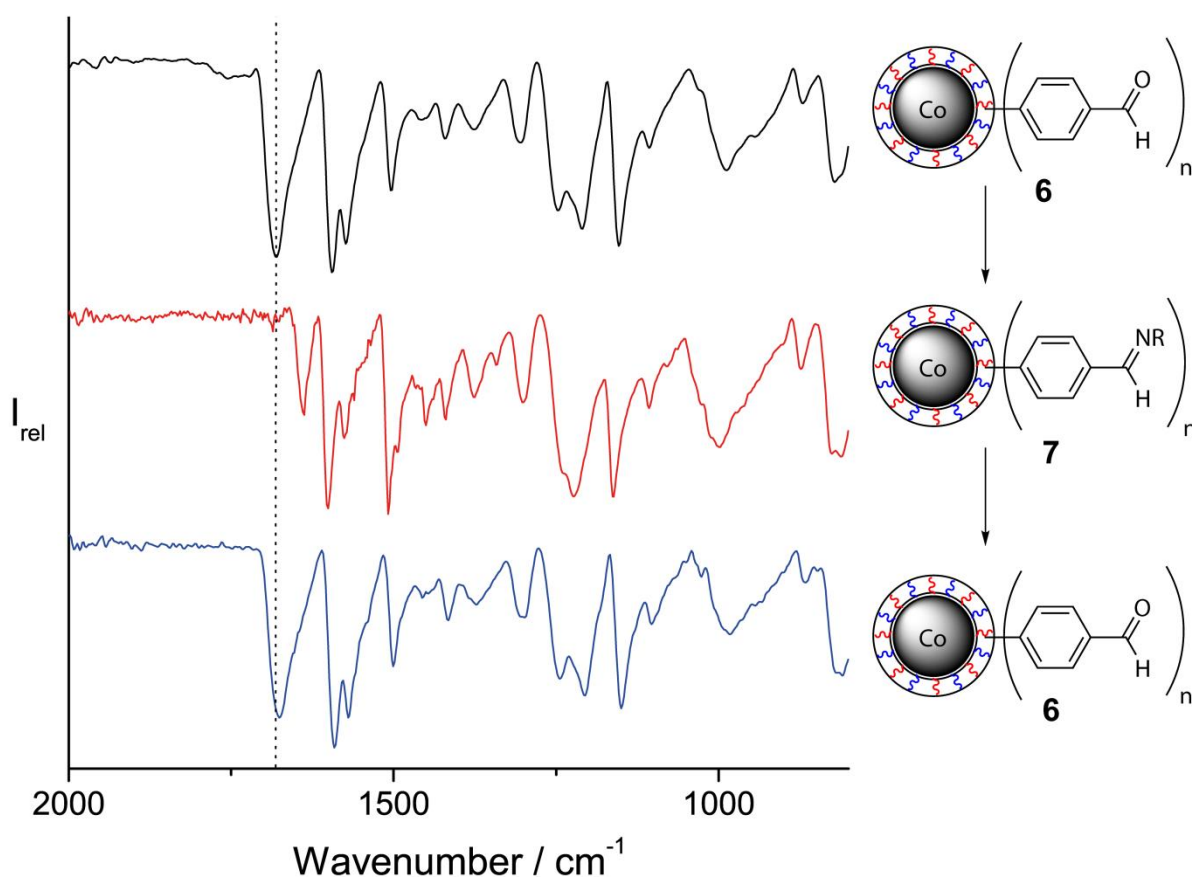
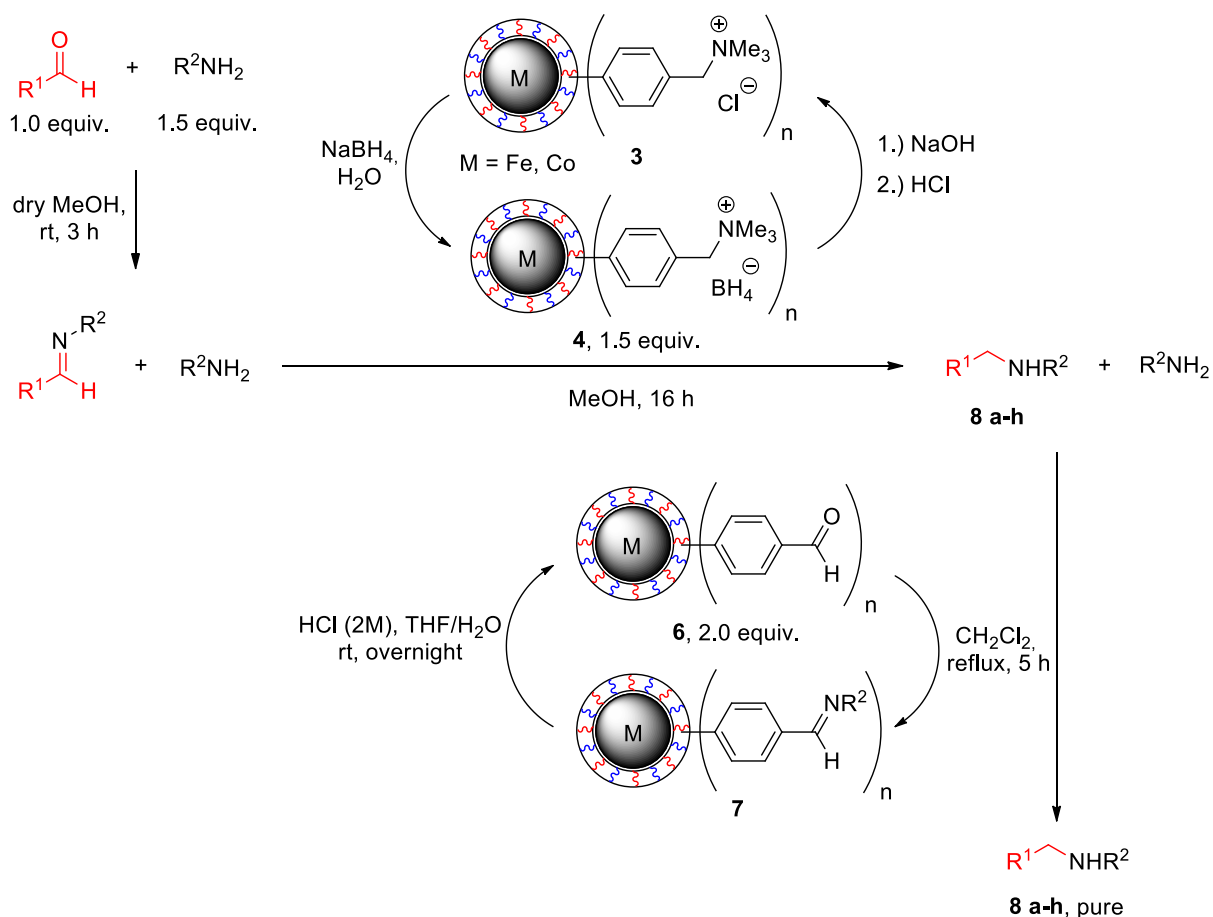


**Figure 3.** IR-ATR spectra of mWang resin **6** (top), after immobilization of benzylamine (middle) and subsequent hydrolysis with aqueous HCl (bottom). The spectra of **6** before and after one cycle coincide perfectly, indicating complete regeneration of the aldehyde scavenger.

### Reductive amination combining mBER and mWang

The combination of these two recyclable resins was probed next in the synthesis of a small library of secondary amines via reductive amination of various aldehydes. To allow complete formation of the intermediary imines, aromatic or aliphatic aldehydes were stirred with an excess (1.5 equiv.) of primary amine in dry MeOH for three hours at room temperature (Scheme 2). The imines were readily reduced to the secondary amines **8a-h** by adding an excess of mBER resin **4** and continuing the stirring overnight. In some literature reports for the reductive amination with conventional polystyrene reagents<sup>[22]</sup> MeOH turned out to be not effective, so a 1:1 mixture of MeOH and CH<sub>2</sub>Cl<sub>2</sub> was applied instead. In our case, however, adding CH<sub>2</sub>Cl<sub>2</sub> slowed down the reduction noticeable and no conversion to the secondary amine **8** was observed when using pure CH<sub>2</sub>Cl<sub>2</sub>. By applying MeOH and the mBER **4** we were able to cut down the excess of reducing reagent from 2.5 equiv. to 1.5 equiv. and the reaction time from 48 h to 16 h. The spent resin was efficiently collected by a magnet, washed



**Scheme 2.** Combination of mBER **4** and mWang resin **6** for the reductive amination of aldehydes leading to the secondary amines **8a-h**.<sup>iii</sup>

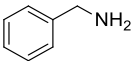
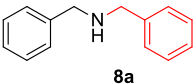
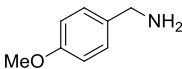
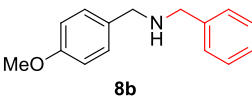
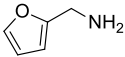
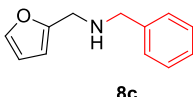
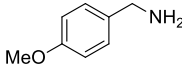
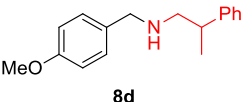
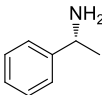
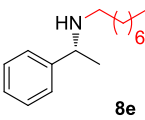
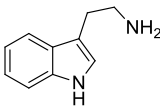
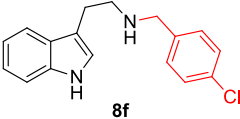
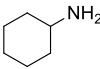
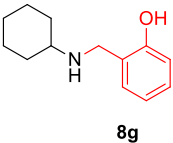
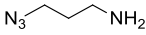
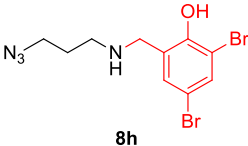
and recycled for the next run as described previously.

In order to attain pure product solutions the initial excess of primary amine had to be removed from the reaction mixtures. Selective and complete sequestration was obtained by refluxing with mWang resin **6** in  $CH_2Cl_2$  for five hours (Scheme 2). After simple magnetic decantation, washing of the particles, and evaporation of the solvent the remaining secondary amines (**8a-h**) were obtained in good yields (49-99%) and purities (all > 95% by NMR) (Table 5). In some cases, however, filtration over cotton was necessary to remove traces of magnetic material before acquiring the NMR-spectrum. The spent mWang scavenger **7** was regenerated by hydrolysis with aqueous HCl as described above and reused in the next run without apparent cross-contamination (Scheme 2).

To demonstrate the broad reaction scope, benzylic (Entry 1-5) as well as aliphatic (Entry 6-8) primary amines were reacted with either aromatic (Entry 1-3, 6-7)

<sup>iii</sup> Scheme was modified to fit on page.

**Table 5.** Small library of secondary amines **8a-h** synthesized by reductive amination of various aldehydes.

Entry	Primary amines	Products ( <b>8a-h</b> )	Yield <sup>[a]</sup>	Purity <sup>[b]</sup>
1		 <b>8a</b>	97%	> 95%
2		 <b>8b</b>	96%	> 95%
3		 <b>8c</b>	91%	> 95%
4		 <b>8d</b>	95%	> 95%
5		 <b>8e</b>	80%	> 95%
6		 <b>8f</b>	97%	> 95%
7 <sup>[c]</sup>		 <b>8g</b>	99%	> 95%
8 <sup>[c]</sup>		 <b>8h</b>	49%	> 95%

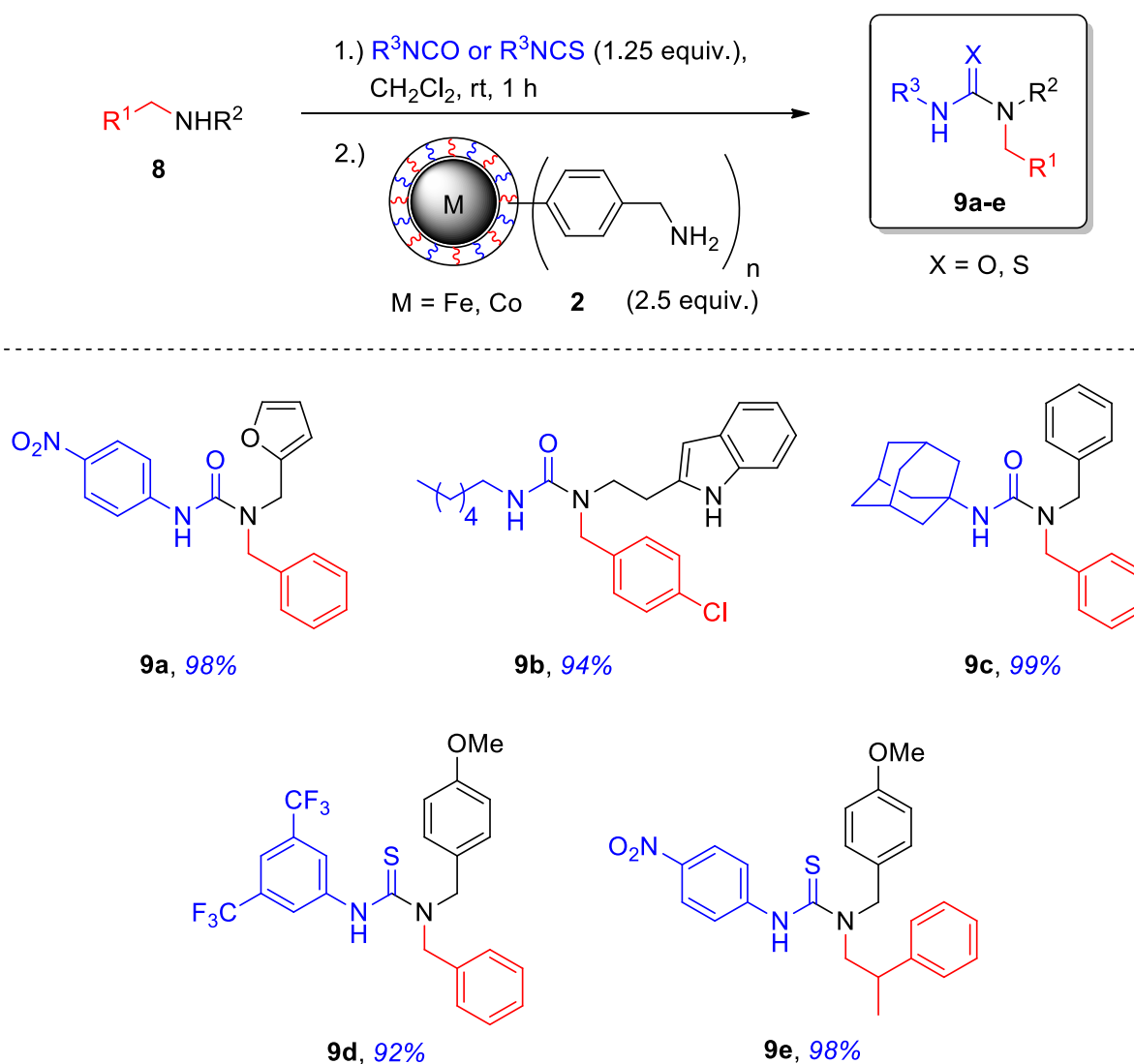
[a] Isolated yields. [b] Determined by NMR spectroscopy. [c] No need of scavenging due to the low boiling point of the amines.

or aliphatic (Entry 4,5) aldehydes. In only two cases the obtained yield was below 90%: When using a long chain aliphatic aldehyde (**8d**, Entry 4), being known to be a difficult substrate in the literature,<sup>[22]</sup> and when using an aldehyde with a strongly acidic group (**8h**, Entry 8), which might result in product loss due to protonation of the

resin and binding via electrostatic interactions. An aromatic alcohol that lacks the electron withdrawing groups (**8g**, Entry 7) was perfectly tolerated. Also, no racemization was observed when using enantiopure primary amines (**8e**, Entry 5). Additionally, upscaling to 1.5 mmol of aldehyde and 2.3 mmol of amine was carried out for **8a** with an equally good yield of 96%.

### Synthesis of tri-substituted (thio)ureas using magnetic resins

As the third step in the sequence the secondary amines **8** were converted to trisubstituted (thio)ureas by stirring with an excess (1.25 equiv.) of either isocyanate or isothiocyanate in  $\text{CH}_2\text{Cl}_2$  for one hour (Scheme 3). In order to remove the excess



**Scheme 3.** Synthesis of a small library of tri-substituted (thio)ureas **9a-e** using magnetic amine **2** as scavenger of excess reagent.



of reagent from the products **9a-e**, a second magnetic scavenger was used. The polymer-coated magnetic nanobeads functionalized with benzylic amine **2**, which are accessible via Gabriel synthesis (Scheme 1), readily sequestered the excess of iso(thio)cyanate upon further stirring for 2 h. By applying an external magnet to the side of the reaction vessel (Figure 1) the entire magnetic scavenger was collected within seconds and the product solution decanted. After several washing steps and evaporation of the solvents, the pure products **9a-e** were isolated in very high yields (92-99%) and excellent purities (> 95% by NMR) without the need for further purification (Scheme 3). Aromatic (**9a**) as well as aliphatic (**9b**, **9c**) iosocyanates were applicable in this transformation including much hindered ones (**9c**) with isothiocyanates (**9d**, **9e**) working equally well (Scheme 3). No limitations arose from the choice of amine regardless if dibenzylic or monobenzylic secondary amines were used and scales of up to 1.4 mmol amine were successfully tested. In contrast to the other two magnetic resins, this scavenger cannot be recycled due to the irreversible formation of resin-bound (thio)urea.

### 4.3 Conclusion

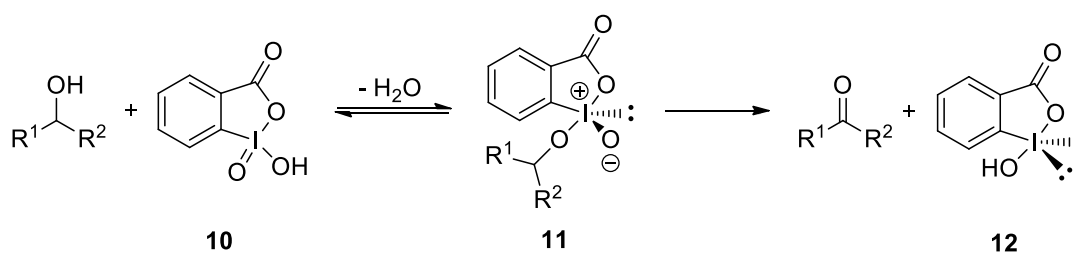
In summary, we demonstrated the efficient synthesis of three novel magnetic reagents and scavengers based on Co/C or Fe/C nanoparticles, which are produced from low cost raw materials and are commercially available on a kilogram scale. The high loading magnetic resins were prepared by surface-initiated polymerization followed by quantitative functionalization utilizing microwave irradiation. The progress of the syntheses was conveniently monitored by ATR-IR spectroscopy while TEM analysis showed no noticeable differences between the various magnetic resins. The highly magnetic core of the hybrid material allowed rapid recovery of the resin from reaction mixtures by an external magnet followed by convenient decantation of the product solution.

The magnetic borohydride exchange resin (mBER) was subsequently tested in the reduction of various aldehydes, ketones, and  $\alpha,\beta$ -unsaturated substrates leading to the corresponding alcohols in excellent yields and purities. The magnetic Wang aldehyde scavenger (mWang) was successfully applied in the reversible sequestration of primary amines. Next, both magnetic resins were applied consecutively in the reductive amination of aldehydes. The imines formed by stirring of aldehydes with an excess of primary amines were readily reduced by mBER and the residual primary

amines selectively scavenged by the mWang resin. A small library of secondary amines was synthesized in good to excellent yields and excellent purities. Apart from magnetic decantation, no additional purification steps were needed and the resins were recycled for eight consecutive runs using different substrates without noticeable cross contamination. Building on these results, the secondary amines were converted to tri-substituted (thio)ureas. The excess of iso(thio) cyanate used was scavenged by a third magnetic resin bearing amino groups, giving rise to excellent yields and purities of ureas and tioureas. The successful demonstration of this multi-step synthesis applying exclusively magnetic reagents and scavengers opens new possibilities for reaction automatization such as magnetic flow reactors, which is under investigation in our laboratories.

## 4.4 Addendum

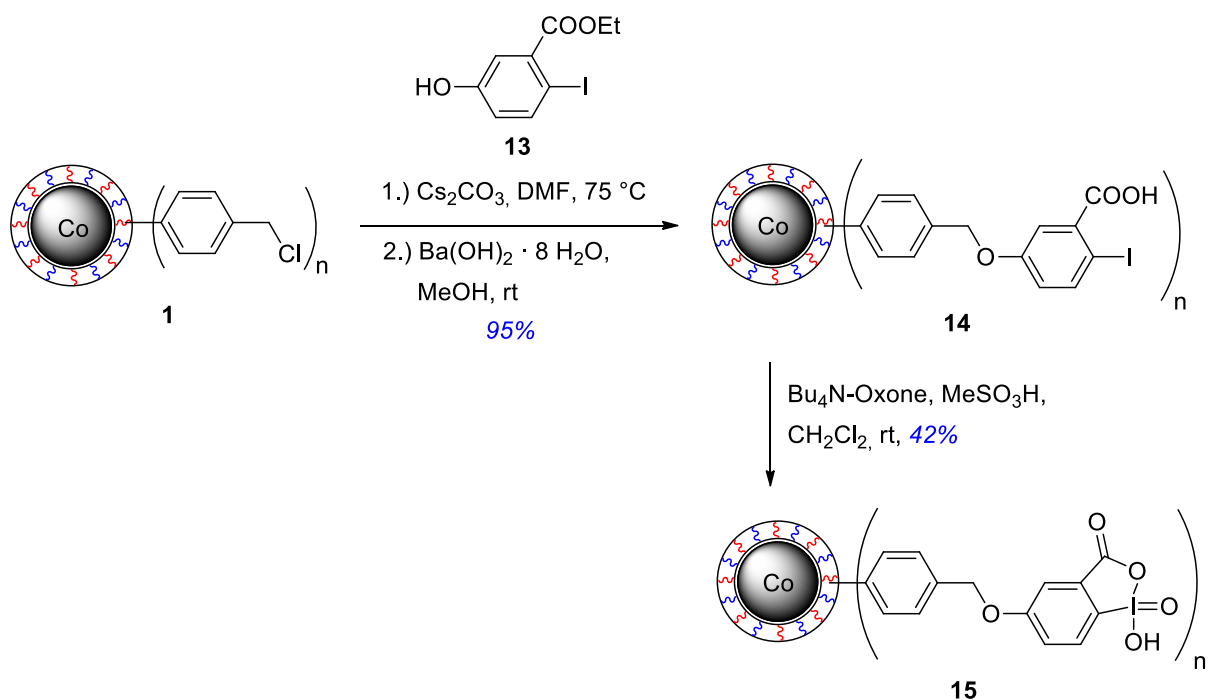
Although it has been known for more than a century, the influence of 1-hydroxy-(1*H*)-benzo-1,2-iodoxol-3-one 1-oxide (2-iodoxybenzoic acid, IBX) on organic synthesis has remained limited largely due to its particular insolubility in most common organic solvents.<sup>[33]</sup> In 1994 Frigerio and Santagostino successfully demonstrated, that IBX can be used as hypervalent reagent for the oxidation of primary and secondary alcohols in DMSO.<sup>[34]</sup> The growing interest in IBX within the last decade is based on its mild and selective oxidizing attributes showing functional group tolerance even towards thioethers and amines.<sup>[35]</sup> The oxidation mechanism involves two steps: The first step is formally a fast ligand exchange on the iodine atom of IBX (**10**) (Scheme 4). The product **11** disproportionates in a second step to the carbonyl derivative and iodosoarene (**12**).<sup>[36]</sup>



**Scheme 4.** Mechanism of the oxidation of alcohols by IBX (**10**).

In order to allow convenient separation and recycling IBX has been immobilized on several resins during the last decade, e.g. cross-linked polystyrene,<sup>[37]</sup> polyethylene glycol,<sup>[38]</sup> and aminopropylsilica gel.<sup>[39]</sup> The resin-bound IBX also facilitated the use of more common solvents like THF and CH<sub>2</sub>Cl<sub>2</sub> for the oxidations and larger scale applications due to a safer handling of the potentially explosive hypervalent iodine reagent. IBX seemed to be ideal to round up the portfolio of magnetic scavengers (magnetic amine and mWang) and magnetic reagents (mBER and magnetic acylation reagents) with a magnetically recyclable oxidizing reagent.

To synthesize the magnetic IBX resin (mIBX) Co/C nanoparticles functionalized with benzyl chloride moieties (**1**) were heated with ethyl 5-hydroxy-2-iodobenzoate (**13**), which is accessible via literature known procedures (Scheme 5).<sup>[38]</sup> Caesium carbonate was used as base in this nucleophilic substitution and the



**Scheme 5.** Synthesis of a magnetic variant of IBX (mlBX).

ester group was subsequently saponified to yield resin-bound iodocarboxylic acid (**14**). Iodine microanalysis revealed a loading of 1.85 mmol/g which corresponds to 95% functionalization. This good yield was also confirmed by the distinct mass increase corresponding to 97% functionalization and the very low amount of residual chlorine (0.4%). In small batch microwave heating ( $140^\circ\text{C}$ , 10 min) instead of conventional heating ( $75^\circ\text{C}$ , 20 h) was tested to lower reaction times, however, a slightly lower loading of 1.78 mmol/g (91 % functionalization) was determined in this case. Moreover, most common laboratory scale microwave ovens are too small to handle several grams of resin in one batch.

In a second step the iodocarboxylic acid (**14**) was oxidized to the final mlBX (**15**) (Scheme 5). Tetrabutylammonium Oxone<sup>[40]</sup> was prepared according to literature procedures, titrated to determine its oxidizing potential, and finally used as oxidizing agent due to its solubility in organic solvents, e.g.  $\text{CH}_2\text{Cl}_2$ , which are necessary to swell the polymer coating of the magnetic resin. Methane sulfonic acid was added for the *in situ* formation of Caro's acid (monoperoxysulfuric acid), which is an stronger oxidant.<sup>[38]</sup> The progress of the functionalization and oxidation was monitored by IR-ATR (Figure 4). The best indication for the successful functionalization with iodocarboxylic acid was the disappearance of the characteristic benzyl chloride peak at  $1263\text{ cm}^{-1}$  and the appearance of a marked carbonyl stretch at  $1717\text{ cm}^{-1}$  derived from the

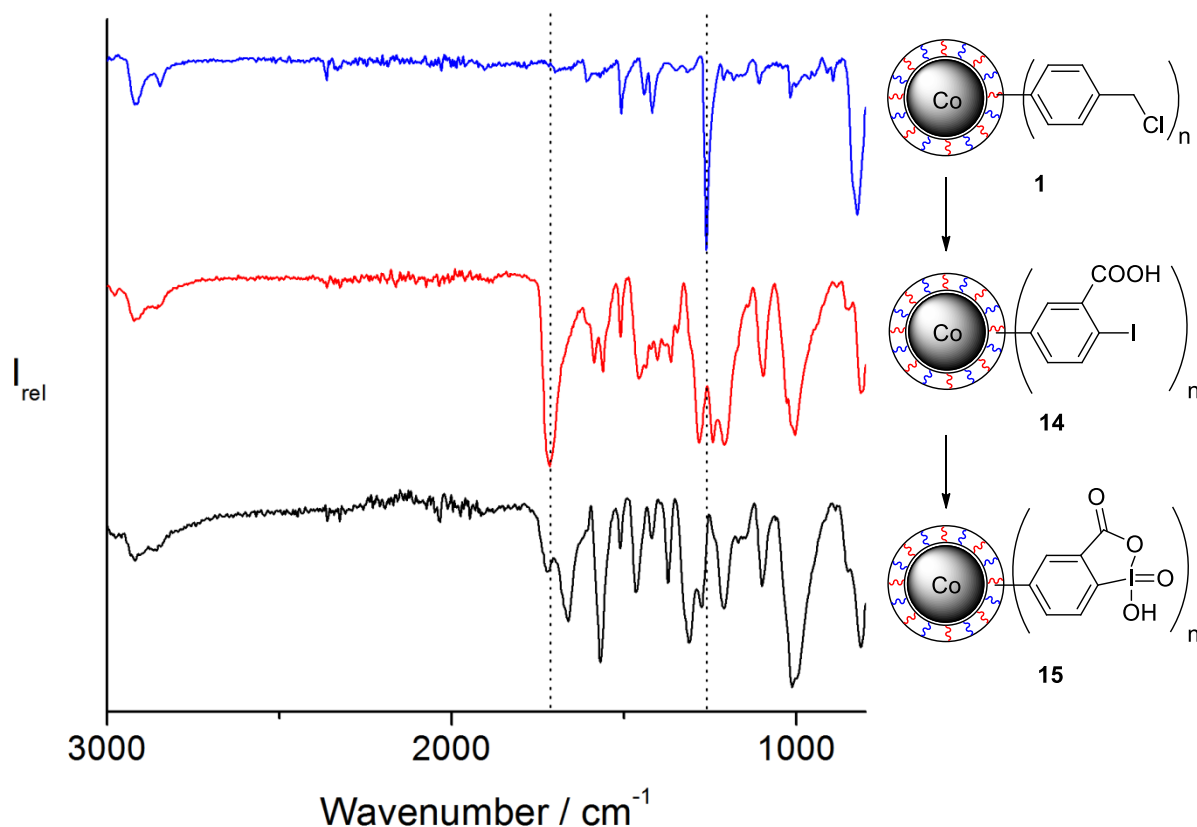
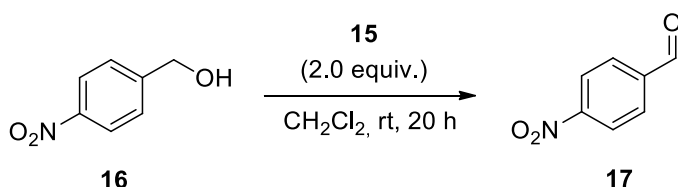


**Figure 4.** IR-ATR spectra of polystyrene-coated Co/C nanobeads **1** (top), after immobilization iodo-benzoic acid **14** (middle), and subsequent oxidation to mIBX **15** (bottom). The spectrum of **15** indicated an incomplete oxidation.

carboxylic acid. Upon oxidation this carbonyl peak shifted to 1663 cm<sup>-1</sup> however, a small peak at 1722 cm<sup>-1</sup> remained indicating incomplete oxidation. A <sup>1</sup>H-NMR-assay was used to determine the oxidizing capacity of the mIBX resin in analogy to the assay used in the case of the mBER resin **4**. An excess of 4-nitrobenzyl alcohol as substrate and 4-methoxyanisole as internal standard were stirred with a portion of the resin for 20 h in CDCl<sub>3</sub>. Evaluation of the integrals revealed a loading of 0.75 mmol/g, which corresponds to only 42 % conversion. However, the loading is in the range of other IBX resins (0.2-1.1 mmol/g).<sup>[37-39]</sup>

In a first test reaction 4-nitrobenzyl alcohol (**16**) was oxidized to 4-nitrobenzaldehyde (**17**) by stirring with two equivalents of mIBX (**15**) in CH<sub>2</sub>Cl<sub>2</sub> for 20 h (Scheme 6). While the educt was completely converted, impurities were detected in the product even after additional filtration as determined by <sup>1</sup>H-NMR.<sup>[26]</sup> One of these impurities was identified as tetrabutylammonium, a component of the oxidizing agent.



**Scheme 6.** Reduction of 4-nitrobenzyl alcohol (**16**) to the corresponding aldehyde (**17**) using mIBX (**15**).

Moreover, a significant amount of sulfur (1.53 %) was detected in the final IBX resin by elemental analysis. This also indicates residual oxidizing agents, i.e. tetrabutylammonium Oxone and/or methane sulfonic acid, after the oxidizing step, despite intensive washing of the particles with THF, CH<sub>2</sub>Cl<sub>2</sub> and Et<sub>2</sub>O. Although identical oxidizing and washing procedures are described in literature for other IBX resins, in none of these reports hints for residual oxidizing agents can be found.<sup>[37,38]</sup> Attempts to wash the particles with other solvents, e.g. DMSO, MeOH, or DMF, led to a gradual decrease of oxidizing potential of mIBX without completely removing the residuals.

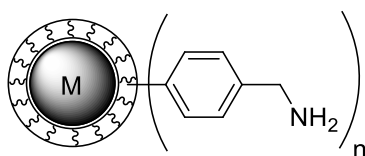
Taking all these results into account the mIBX resin is not competitive at this stage. The nucleophilic substitution to form the resin-bound iodocarboxylic acid was achieved in excellent yields. However, the final loading after oxidation is roughly only one third of mBER and mWang resins and considerable impurities in the product knock out the advantage of a rapid separation via magnetic decantation. More research on alternative, potentially completely different, oxidation protocols is needed in order to advance this project.

## 4.5 Experimental Section

### Materials and methods

Polystyrene-encapsulated nanobeads (**1**) were synthesized according to literature procedures.<sup>[19]</sup> Ethyl 5-hydroxy-2-iodobenzoate (**13**)<sup>[38]</sup> and tetrabutylammonium Oxone<sup>[41]</sup> were prepared according to literature procedures. Amines and aldehydes were distilled under reduced pressure before use. All other commercially available compounds were used as received. <sup>1</sup>H NMR and <sup>13</sup>C NMR spectra were recorded on a Bruker AC 300 or AC 400 spectrometer with CHCl<sub>3</sub> (7.26 ppm) as a standard. Magnetic nanobeads were dispersed using an ultrasound bath (Sonorex RK 255 H-R, Bandelin) and recovered with the aid of a neodymium based magnet (side length 12 mm). They were characterized by IR-ATR spectroscopy equipped with a Specac Golden Gate Diamond Single Reflection ATR-System, transmission electron microscopy (Zeiss, LEO912AB, 100 kV), and elemental microanalysis (LECO CHN-900).

### Synthesis of polymer coated nanobeads bearing amino groups (**2**)

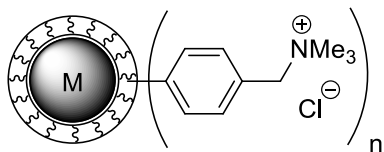


In the first step, polystyrene coated iron nanobeads **1** (1.0 g, 3.0 mmol benzyl chloride moieties) were heated with potassium phthalimide (5.6 g, 30 mmol) in 30 mL dry DMF under nitrogen atmosphere in the microwave to 130 °C for 5 min. After cooling to room temperature the particles were recovered by a magnet, washed with H<sub>2</sub>O (2 x 30 mL), MeOH (2 x 30 mL), acetone (2 x 30 mL), and CH<sub>2</sub>Cl<sub>2</sub> (2 x 30 mL) and dried under vacuum. **IR** (ATR,  $\bar{\nu}$ /cm<sup>-1</sup>): 2918, 2845, 1770, 1705, 1510, 1388, 1325, 1081, 934, 802, 713.

Second, the particles functionalized with phthalimide were stirred in a refluxing mixture of 16 mL hydrazine monohydrate and 64 mL EtOH overnight. After magnetic decantation, the amine particles **2** were washed with H<sub>2</sub>O (3 x 30 mL), MeOH (3 x 30 mL), and CH<sub>2</sub>Cl<sub>2</sub> (3 x 30 mL) and dried under vacuum yielding 952 mg of the product resin **2**.

**IR** (ATR,  $\bar{\nu}$ /cm<sup>-1</sup>): 3347, 3290, 2906, 2845, 1636, 1567, 1506, 1477, 1439, 1417, 1362, 1147, 808; **elemental microanalysis** (%): C 47.95, H 4.65, N 5.72, Cl 0.58%.

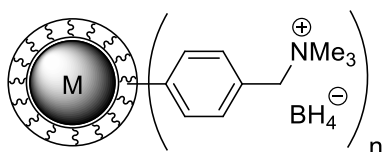
### Preparation of polymer coated nanobeads bearing quaternary ammonium ions (3)



Polystyrene coated iron nanobeads **1** (1.0 g, 3.5 mmol benzyl chloride moieties) were introduced to a microwave vial followed by the addition of 17 mL trimethylamine solution (4.2M in EtOH). The slurry was stirred for 15 min at 150°C under microwave heating. The particles were collected by an external magnet, washed with acetone (3 x 5 mL) and Et<sub>2</sub>O (2 x 5 mL), and dried under vacuum yielding 1.14 g of functionalized beads **3** (loading: 2.9 mmol/g).

**IR** (ATR,  $\bar{\nu}/\text{cm}^{-1}$ ): 3371, 3021, 2919, 2852, 2769, 1612, 1511, 1475, 1418, 1218, 974, 888, 823; **elemental microanalysis** (%): C 53.58, H 6.19, N 4.00, Cl 5.44.

### Preparation of magnetic borohydride resin (mBER) (4)



Polymer coated iron nanobeads bearing quaternary ammonium ions **3** (1.09 g, 3.3 mmol) were dispersed in 15 mL water by stirring for 10 min. Then, a solution of NaBH<sub>4</sub> (372 mg, 9.9 mmol) in 10 mL H<sub>2</sub>O was added dropwise and the stirring continued for 4 h. The particles were recovered by magnetic decantation, washed with H<sub>2</sub>O (3 x 20 mL) and MeOH (20 mL), and dried under vacuum for at least 5 h leading to borohydride functionalized nanobeads **4** with a borohydride loading of 3.0 mmol/g.

**IR** (ATR,  $\bar{\nu}/\text{cm}^{-1}$ ): 3014, 2910, 2280, 2203, 1610, 1510, 1475, 1418, 1376, 1071, 972, 885, 820; **elemental microanalysis** (%): C 55.77, H 6.58, N 4.08, Cl 0.1.

### Determination of the Loading of mBER resin 4 by <sup>1</sup>H-NMR assay

To quickly estimate the loading of freshly prepared magnetic borohydride resins, 50 mg of the mBER **6** were stirred in 1.0 mL of deuterated MeOH with an excess of 4-nitrobenzaldehyde (120.9 mg, 0.8 mmol) as substrate and 4-methylanisole (50.4  $\mu\text{L}$ ,

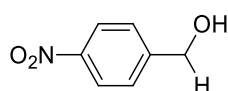


0.4 mmol) as internal standard for three hours at room temperature. The magnetic particles were collected by an external magnet, the supernatant filtered over a plug of cotton into a NMR tube and the  $^1\text{H}$ -NMR spectrum acquired. To calculate the loading the integrations of the aromatic CH doublets of the product at 7.70 ppm were compared to the integration of the aromatic CH doublet of the standard at 7.03 ppm.

### General Procedure A: Reduction of aldehydes and ketones using mBER resin 4

In a typical experiment 33 mg of p-nitrobenzaldehyde (0.2 mmol, 1.0 equiv.) was dissolved in 1 mL MeOH, 100 mg of the mBER resin 4 (3 mmol/g, 0.3 mmol  $\text{BH}_4$ , 1.5 equiv.) added, and the resulting slurry stirred for 2 h at room temperature. Thereafter, the resin was collected by a magnet, the solution decanted, and the particles washed with MeOH (5 x 3 mL). After drying under high vacuum, 99.7 mg (99.7 wt%) of the spent nanoparticles were recovered. The combined decanted solution and washing solutions were evaporated to dryness yielding 33.2 mg of (4-nitrophenyl)methanol (**5a**). To remove traces of finely ground resin, the product was dissolved in  $\text{CH}_2\text{Cl}_2$ , filtered over cotton, and dried under vacuum. 0.3 mg of impurities were collected by the filter and 32.9 mg (0.215 mmol, 99%) of the pure product **5a** reisolated.

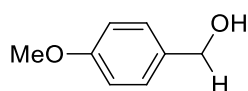
#### (4-Nitrophenyl)methanol (**5a**)



Synthesized according to the general procedure A obtaining the product in 88% yield as a yellow solid.

$^1\text{H}$  NMR (400 MHz,  $\text{CDCl}_3$ ):  $\delta$  = 8.26 – 8.18 (m, 2H), 7.54 (d,  $J$  = 8.8 Hz, 2H), 4.84 (s, 2H), 1.84 (s, 1H);  $^{13}\text{C}$  NMR (101 MHz,  $\text{CDCl}_3$ ):  $\delta$  = 148.2, 147.5, 127.2, 123.9, 64.2.

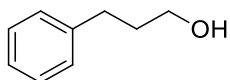
#### (4-Methoxyphenyl)methanol (**5b**)



Synthesized according to the general procedure A obtaining the product in 89% yield as a colorless liquid.

**$^1\text{H}$  NMR** (300 MHz,  $\text{CDCl}_3$ ):  $\delta$  = 7.33 – 7.27 (m, 2H), 6.93 – 6.87 (m, 2H), 4.62 (s, 2H), 3.81 (s, 3H), 1.61 (s, 1H);  **$^{13}\text{C}$  NMR** (75 MHz,  $\text{CDCl}_3$ ):  $\delta$  = 159.4, 133.2, 128.8, 114.1, 65.2, 55.4.

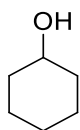
### 3-Phenylpropan-1-ol (5c)



Synthesized according to the general procedure A obtaining the product in 88% yield as a colorless oil.

**$^1\text{H}$  NMR** (300 MHz,  $\text{CDCl}_3$ ):  $\delta$  = 7.35 – 7.26 (m, 2H), 7.24 – 7.15 (m, 3H), 3.68 (t,  $J$  = 6.4 Hz, 2H), 2.76 – 2.68 (m, 2H), 1.96 – 1.85 (m, 2H), 1.51 (s, 1H);  **$^{13}\text{C}$  NMR** (75 MHz,  $\text{CDCl}_3$ ):  $\delta$  = 141.9, 128.5(5), 128.5(3), 126.0, 62.4, 34.3, 32.2.

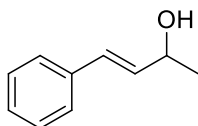
### Cyclohexanol (5d)



Synthesized according to the general procedure A obtaining the product in 98% yield as a colorless, viscous liquid.

**$^1\text{H}$  NMR** (300 MHz,  $\text{CDCl}_3$ ):  $\delta$  = 3.71 – 3.50 (m, 1H), 2.00 – 1.81 (m, 2H), 1.80 – 1.63 (m, 2H), 1.64 – 1.45 (m, 2H), 1.40 – 1.06 (m, 5H);  **$^{13}\text{C}$  NMR** (75 MHz,  $\text{CDCl}_3$ ):  $\delta$  = 70.5, 35.7, 25.6, 24.3.

### (*E*)-4-Phenylbut-3-en-2-ol (5e)



Synthesized according to the general procedure A obtaining the product in 99% yield as a colorless, viscous liquid.

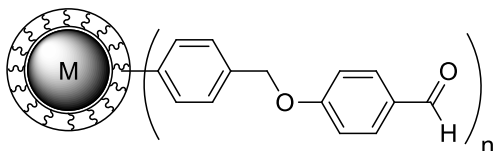
**$^1\text{H}$  NMR** (300 MHz,  $\text{CDCl}_3$ ):  $\delta$  = 7.43 – 7.19 (m, 5H), 6.57 (d,  $J$  = 15.9 Hz, 1H), 6.27 (dd,  $J$  = 15.9, 6.4 Hz, 1H), 4.50 (pd,  $J$  = 6.4, 1.0 Hz, 1H), 1.62 (s, 1H), 1.38 (d,  $J$  = 6.4

Hz, 3H);  $^{13}\text{C}$  NMR (75 MHz,  $\text{CDCl}_3$ ):  $\delta$  = 136.8, 133.7, 129.6, 128.7, 127.8, 126.6, 69.1, 23.6; **MS** (EI-MS):  $m/z$  (%) = 148.1 (90,  $\text{M}^+$ ), calc. 148.1.

#### Regeneration of magnetic borohydride resin **4**

Typically, 0.5 g (1.5 mmol) of used magnetic borohydride resin **4** was regenerated by stirring in MeOH (2 x 5 mL),  $\text{H}_2\text{O}$  (2 x 5 mL), aq. NaOH (1M, 2 x 5 mL),  $\text{H}_2\text{O}$  (2 x 5 mL), aq. HCl (1M, 2 x 5 mL),  $\text{H}_2\text{O}$  (5 x 5 mL), aq.  $\text{NaBH}_4$  (9 mmol, 0.4 M),  $\text{H}_2\text{O}$  (3 x 5 mL), and MeOH (1 x 5 mL). The resin was then dried under vacuum for at least 5 h.

#### Synthesis of magnetic Wang aldehyde (mWang) (**6**)



Polystyrene coated cobalt nanobeads **1** (500 mg, 1.75 mmol benzyl chloride moieties) were stirred in 8 mL of dry DMF under nitrogen atmosphere using a microwave vessel. Subsequently, 4-hydroxybenzaldehyde (427 mg, 3.5 mmol) and  $\text{Cs}_2\text{CO}_3$  (1.71 g, 5.25 mmol) were added and the slurry heated to 140 °C for 15 min in a focused microwave oven. The particles were recovered by magnetic decantation and thoroughly washed with  $\text{H}_2\text{O}$ /MeOH/acetone (1:1:1, 3 x 5 mL), MeOH/acetone (1:1, 3 x 5 mL), acetone (3 x 5 mL),  $\text{CH}_2\text{Cl}_2$  (3 x 5 mL), and  $\text{Et}_2\text{O}$  (1 x 5 mL). After drying under vacuum for 5 h 601 mg of mWang resin **6** with a loading of 2.5 mmol/g was obtained.

**IR** (ATR,  $\bar{\nu}/\text{cm}^{-1}$ ): 2919, 2845, 2726, 1683, 1596, 1506, 1422, 1379, 1249, 1212, 1155, 991, 814; **elemental microanalysis** (%): C 63.55; H 4.90, N 0.05; Cl 0.22.

#### Reversible scavenging experiments of primary amines with mWang resin

In a typical experiment 100 mg (0.3 mmol) of mWang resin **6** were stirred with 195  $\mu\text{L}$  (1.5 mmol) *p*-methoxybenzylamine in 3 mL dry  $\text{CH}_2\text{Cl}_2$  at 50 °C for 16 h under nitrogen atmosphere. The particles were recovered by an external magnet, washed with dry  $\text{CH}_2\text{Cl}_2$  (3 x 3 mL) and  $\text{Et}_2\text{O}$  (2 x 3 mL), and dried under vacuum. 120 mg of imine functionalized nanobeads **7** featuring a loading of 2.06 mmol/g were obtained.

**IR** (ATR,  $\bar{\nu}/\text{cm}^{-1}$ ): 2888, 2833, 1641, 1602, 1507, 1457, 1420, 1241, 1164, 1014, 814; **elemental microanalysis (%)**: C 63.75, H 5.18, N 3.00.

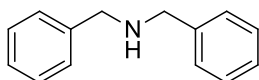
To release the scavenged amine and therefore regenerate the resin 100 mg of **7** were subsequently stirred in a mixture of THF/H<sub>2</sub>O (2:1, 5 mL), aq. HCl (2M, 0.5 mL), and MeOH (0.5 mL) over night at room temperature. After magnetic recovery of the particles they were resuspended for washing in H<sub>2</sub>O/MeOH/acetone (1:1:1, 3 x 5 mL), MeOH/acetone (1:1, 3 x 5 mL), acetone (3 x 5 mL), CH<sub>2</sub>Cl<sub>2</sub> (3 x 5 mL), and Et<sub>2</sub>O (1 x 5 mL) and dried under vacuum.

**IR** (ATR,  $\bar{\nu}/\text{cm}^{-1}$ ): 2912, 1681, 1595, 1573, 1505, 1459, 1420, 1302, 1248, 1209, 1154, 1107, 986, 812; **elemental microanalysis (%)**: C 62.12, H 4.06, N 0.15.

### General Procedure B: Reductive amination of aldehydes applying mBER and mWang resins

Aldehyde (0.5 mmol) and an excess of primary amine (0.75 mmol) were stirred in 2 mL of dry methanol under nitrogen atmosphere for 3 h in a flame-dried Schlenk tube. Then, mBER resin **4** (250 mg, 0.75 mmol) was added to the reaction mixture and the stirring continued for 16 h. The particles were recovered by magnetic decantation, washed with MeOH (3 x 3 mL) and the combined solutions evaporated to dryness. 5 mL of CH<sub>2</sub>Cl<sub>2</sub> and 200 mg (0.5 mmol) of mWang resin **6** were added and the slurry refluxed at 50 °C for 5 h. The product solution was decanted by the aid of a magnet and the resin washed with CH<sub>2</sub>Cl<sub>2</sub> (3 x 5 mL). Evaporation of the solvent resulted in the pure secondary amines **8a-h** in high yields. Before NMR-analysis, some CDCl<sub>3</sub> solutions had to be filtered over cotton. Both magnetic resins were regenerated following the general procedures described above.

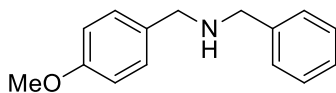
### Dibenzylamine (8a)



Prepared according to the general procedure B obtaining the product in 97% yield as a colorless liquid.

**$^1\text{H}$  NMR** (300 MHz,  $\text{CDCl}_3$ ):  $\delta$  = 7.39 – 7.26 (m, 10H), 3.82 (s, 4H), 1.92 (s, 1H);  **$^{13}\text{C}$  NMR** (75 MHz,  $\text{CDCl}_3$ ):  $\delta$  = 140.1, 128.6, 128.4, 127.2, 53.2; **MS** (EI-MS):  $m/z$  (%) = 197.2 (20,  $\text{M}^+$ ), calc. 197.1.

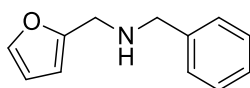
***N*-Benzyl-1-(4-methoxyphenyl)methanamine (8b)**



Prepared according to the general procedure B obtaining the product in 96% yield as a yellow oil.

**$^1\text{H}$  NMR** (300 MHz,  $\text{CDCl}_3$ ):  $\delta$  = 7.37 – 7.23 (m, 7H), 6.91 – 6.85 (m, 2H), 3.80 (d,  $J$  = 1.3 Hz, 5H), 3.75 (s, 2H), 1.78 (s, 1H);  **$^{13}\text{C}$  NMR** (75 MHz,  $\text{CDCl}_3$ ):  $\delta$  = 158.8, 140.4, 132.4, 129.5, 128.5, 128.3, 127.1, 113.9, 55.4, 53.1, 52.6; **MS** (EI-MS):  $m/z$  (%) = 227.2 (30,  $\text{MH}^+$ ), calc. 227.1.

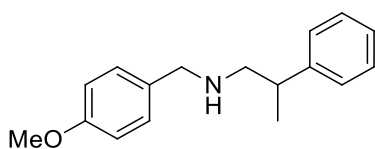
***N*-Benzyl-1-(furan-2-yl)methanamine (8c)**



Prepared according to the general procedure B obtaining the product in 91% yield as a slightly yellow liquid.

**$^1\text{H}$  NMR** (300 MHz,  $\text{CDCl}_3$ ):  $\delta$  = 7.38 (dd,  $J$  = 1.8, 0.8 Hz, 1H), 7.33 (d,  $J$  = 4.4 Hz, 4H), 7.31 – 7.24 (m, 1H), 6.33 (dd,  $J$  = 3.1, 1.9 Hz, 1H), 6.20 (dd,  $J$  = 3.1, 0.5 Hz, 1H), 3.80 (s, 4H), 1.88 (s, 1H);  **$^{13}\text{C}$  NMR** (75 MHz,  $\text{CDCl}_3$ ):  $\delta$  = 153.8, 142.1, 139.9, 128.6, 128.4, 127.2, 110.3, 107.3, 52.9, 45.4; **MS** (EI-MS):  $m/z$  (%) = 187.1 (20,  $\text{M}^+$ ), calc. 187.1.

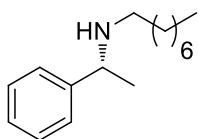
***N*-(4-methoxybenzyl)-2-phenylpropan-1-amine (8d)**



Prepared according to the general procedure B obtaining the product in 95% yield as a yellow oil.

**<sup>1</sup>H NMR** (400 MHz, CDCl<sub>3</sub>):  $\delta$  = 7.34 – 7.28 (m, 2H), 7.24 – 7.18 (m, 3H), 7.16 (d,  $J$  = 8.6 Hz, 2H), 6.87 – 6.80 (m, 2H), 3.79 (s, 3H), 3.69 (q,  $J$  = 13.1 Hz, 2H), 2.97 (h,  $J$  = 7.0 Hz, 1H), 2.78 (dd,  $J$  = 7.2, 1.3 Hz, 2H), 1.41 (d,  $J$  = 6.8 Hz, 1H), 1.26 (d,  $J$  = 6.9 Hz, 3H); **<sup>13</sup>C NMR** (101 MHz, CDCl<sub>3</sub>):  $\delta$  = 158.7, 145.5, 132.6, 129.3, 128.7, 127.4, 126.5, 113.9, 56.4, 55.4, 53.3, 40.1, 20.3; **MS** (ESI-MS):  $m/z$  (%) = 256.16 (100, MH<sup>+</sup>), calc. 256.15.

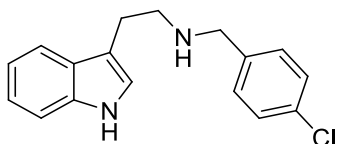
**(*R*)-*N*-(1-Phenylethyl)hexan-1-amine (8e)**



Prepared according to the general procedure B obtaining the product in 80% yield as a yellow liquid.

**<sup>1</sup>H NMR** (400 MHz, CDCl<sub>3</sub>):  $\delta$  = 7.36 – 7.29 (m, 8H), 7.26 – 7.21 (m, 2H), 3.76 (d,  $J$  = 6.6 Hz, 2H), 2.57 – 2.31 (m, 4H), 1.85 (s, 2H), 1.52 – 1.40 (m, 4H), 1.37 (d,  $J$  = 6.6 Hz, 6H), 1.24 (s,  $J$  = 23.2 Hz, 22H), 0.87 (t,  $J$  = 6.8 Hz, 7H); **<sup>13</sup>C NMR** (101 MHz, CDCl<sub>3</sub>):  $\delta$  = 145.8, 128.6, 127.0, 126.7, 58.6, 48.0, 32.0, 30.3, 29.6, 29.4, 27.5, 24.4, 22.8, 14.2; **MS (CI-MS)**:  $m/z$  (%) = 234.2 (100, MH<sup>+</sup>), calc. 233.2;  $[\alpha]_D^{20}$  = + 121° ( $c$  = 3 in CHCl<sub>3</sub>, 21 °C); **ee** > 99%, determined after conversion to the *N*-acetyl derivate by chiral HPLC analysis using a Phenomenex: Lux<sup>®</sup> 3u Cellulose-1 column eluting with a 99:1 heptane/2-propanol mixture.

***N*-(4-Chlorobenzyl)-2-(1*H*-indol-3-yl)ethanamine (8f)**

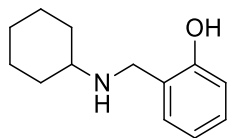


Prepared according to the general procedure B obtaining the product in 97% yield as a slightly yellow oil.

**<sup>1</sup>H NMR** (400 MHz, CDCl<sub>3</sub>):  $\delta$  = 8.13 (s, 1H), 7.62 (d,  $J$  = 7.9 Hz, 1H), 7.35 (d,  $J$  = 8.1 Hz, 1H), 7.29 – 7.17 (m, 5H), 7.13 (t,  $J$  = 7.4 Hz, 1H), 7.01 (d,  $J$  = 1.5 Hz, 1H), 3.78 (s, 2H), 3.08 – 2.88 (m, 4H), 1.67 (s, 1H); **<sup>13</sup>C NMR** (101 MHz, CDCl<sub>3</sub>):  $\delta$  = 138.9,

136.3, 132.7, 129.6, 128.6, 127.6, 122.2, 122.1, 119.4, 119.0, 114.0, 111.3, 53.2, 49.4, 25.9; **MS** (CI-MS):  $m/z$  (%) = 285.1 (100,  $MH^+$ ), calc. 284.1.

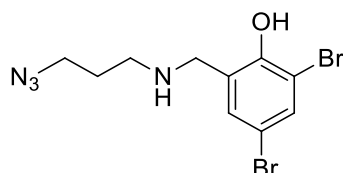
### 2-((Cyclohexylamino)methyl)phenol (**8g**)



Prepared according to the general procedure B obtaining the product in 99% yield as a slightly yellow solid.

**$^1H$  NMR** (400 MHz,  $CDCl_3$ ):  $\delta$  = 7.16 (td,  $J$  = 8.0, 1.6 Hz, 1H), 6.98 (d,  $J$  = 7.0 Hz, 1H), 6.82 (d,  $J$  = 8.1 Hz, 1H), 6.76 (td,  $J$  = 7.4, 1.0 Hz, 1H), 6.34 (bs, 1H), 4.02 (s, 2H), 2.59 – 2.50 (m, 1H), 1.98 (dd,  $J$  = 12.4, 2.8 Hz, 2H), 1.79 – 1.70 (m, 2H), 1.66 – 1.58 (m, 1H), 1.34 – 1.07 (m, 5H);  **$^{13}C$  NMR** (101 MHz,  $CDCl_3$ ):  $\delta$  = 158.6, 128.7, 128.2, 123.2, 119.0, 116.6, 55.7, 49.8, 33.1, 26.0, 24.9; **MS** (CI-MS):  $m/z$  (%) = 206.1 (100,  $MH^+$ ), calc. 205.2.

### 2-(((3-Azidopropyl)amino)methyl)-4,6-dibromophenol (**8h**)



Prepared according to the general procedure B obtaining the product in 49% yield as a brownish solid.

**M.p.:** 135 – 136 °C;  **$^1H$  NMR** (400 MHz,  $CDCl_3$ ):  $\delta$  = 7.55 (d,  $J$  = 2.3 Hz, 1H), 7.07 (d,  $J$  = 2.3 Hz, 1H), 5.64 (bs,  $J$  = 137.0 Hz, 1H), 3.98 (s, 2H), 3.41 (t,  $J$  = 6.5 Hz, 2H), 2.77 (t,  $J$  = 6.9 Hz, 2H), 1.82 (p,  $J$  = 6.7 Hz, 2H);  **$^{13}C$  NMR** (101 MHz,  $CDCl_3$ ):  $\delta$  = 154.5, 134.3, 130.3, 124.7, 111.5, 110.8, 52.3, 49.6, 46.2, 28.6; **IR** (ATR,  $\bar{\nu}/cm^{-1}$ ): 2940, 2878, 2088, 1575, 1435, 1380, 1253, 1167, 902, 859, 826, 749, 683; **HRMS** (ESI-MS):  $m/z$  (%) = 364.9434 (100,  $MH^+$ ), calc. 364.9430.

### Large scale synthesis dibenzylamine (**8a**):

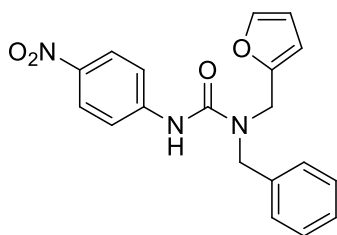
To demonstrate the scalability of the reductive amination 151.6  $\mu L$  (1.5 mmol) benzaldehyde and 246.0  $\mu L$  (2.25 mmol) benzylamine were stirred in 10 mL of dry meth-

anol under nitrogen atmosphere for 3 h at room temperature. Thereafter, 750 mg (2.25 mmol, 3 mmol/g) mBER resin **4** was added to the reaction mixture and the stirring continued for 24 h. The particles were collected by a magnet, the solution decanted, and the magnetic resin washed with MeOH (3 x 3 mL). The combined solutions were evaporated to dryness, 10 mL of CH<sub>2</sub>Cl<sub>2</sub> and 600 mg (1.5 mmol, 2.5 mmol/g) of mWang resin **6** added and the slurry refluxed at 50 °C for 5 h. Magnetic decantation, washing with CH<sub>2</sub>Cl<sub>2</sub> (3 x 5 mL), and evaporation of the combined solutions yielded **8a** (1.44 mmol, 96%) as a slightly yellow, viscous liquid.

### General Procedure C: Synthesis of tri-substituted ureas (9a-e)

In a flame-dried Schlenk tube secondary amine **8** (0.4 mmol) and isocyanate or isothiocyanate (0.5 mmol) were dissolved in 3 mL dry CH<sub>2</sub>Cl<sub>2</sub>. The mixture was stirred at room temperature under nitrogen atmosphere for 2 h. Amine functionalized magnetic polymer beads **2** (83 mg, 0.25 mmol) were added and the stirring continued for 2 h. The resin was collected by an external magnet, the solution decanted, and the beads washed with CH<sub>2</sub>Cl<sub>2</sub> (3 x 5 mL). Evaporation of the combined solutions yielded the trisubstituted ureas **9a-e** in excellent purities.

#### 1-Benzyl-1-(furan-2-ylmethyl)-3-(4-nitrophenyl)urea (9a)

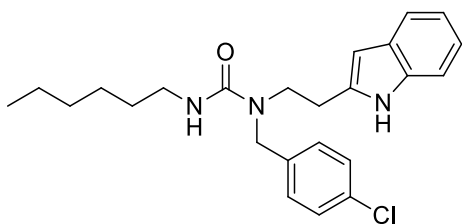


According to the general procedure C the title compound was synthesized as a yellow solid in 98% yield.

**M.p.:** 164 – 168 °C; **<sup>1</sup>H NMR** (400 MHz, CDCl<sub>3</sub>): δ = 8.10 (d, *J* = 9.1 Hz, 2H), 7.44 – 7.24 (m, 8H), 7.08 (s, *J* = 50.4 Hz, 1H), 6.37 – 6.31 (m, 1H), 6.22 (d, *J* = 3.1 Hz, 1H), 4.58 (s, 2H), 4.49 (s, 2H); **<sup>13</sup>C NMR** (101 MHz, CDCl<sub>3</sub>): δ = 154.8, 150.3, 145.4, 143.1, 142.7, 136.7, 129.3, 128.3, 127.6, 125.2, 118.6, 110.9, 109.2, 50.8, 43.9; **IR** (ATR,  $\bar{\nu}$ /cm<sup>-1</sup>): 3337, 1650, 1611, 1545, 1505, 1473, 1421, 1329, 1301, 1221, 1111, 1007, 970, 853, 730, 692; **HRMS** (ESI-MS): *m/z* (%) = 352.1294 (100, MH<sup>+</sup>), calc. 352.1292.



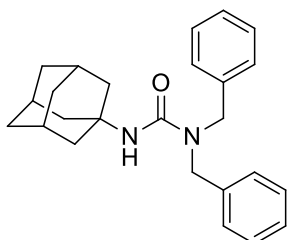
### 1-Benzyl-1-(furan-2-ylmethyl)-3-(4-chlorophenyl)urea (9b)



According to the general procedure C the title compound was synthesized as a pale yellow solid in 94% yield.

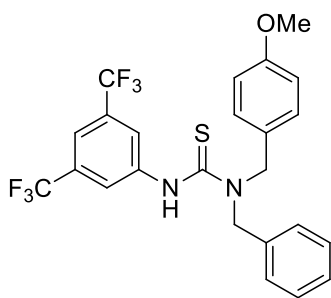
**M.p.:** 130 – 131 °C; **<sup>1</sup>H NMR** (400 MHz, CDCl<sub>3</sub>): δ = 8.39 (d, *J* = 18.2 Hz, 1H), 7.55 (d, *J* = 7.8 Hz, 1H), 7.36 (d, *J* = 8.1 Hz, 1H), 7.30 – 7.24 (m, *J* = 8.4 Hz, 2H), 7.23 – 7.08 (m, 4H), 6.94 (s, 1H), 4.43 (s, 2H), 4.02 (bs, 1H), 3.52 (t, *J* = 6.8 Hz, 2H), 2.97 (t, *J* = 6.6 Hz, 4H), 1.31 – 1.02 (m, 8H), 0.85 (t, *J* = 7.1 Hz, 3H); **<sup>13</sup>C NMR** (101 MHz, CDCl<sub>3</sub>): δ = 158.6, 137.1, 136.6, 133.2, 128.9, 128.9, 127.0, 122.6, 122.4, 119.8, 118.4, 112.7, 111.6, 50.0, 48.1, 41.1, 31.6, 29.8, 26.6, 24.5, 22.7, 14.2; **IR** (ATR,  $\bar{\nu}$ /cm<sup>-1</sup>): 3247, 2925, 2858, 1599, 1537, 1490, 1455, 1404, 1253, 1217, 1089, 1012, 800, 740, 686; **HRMS** (ESI-MS): *m/z* (%) = 412.2156 (100, MH<sup>+</sup>), calc. 412.2150.

### 3-((3s,5s,7s)-adamantan-1-yl)-1,1-dibenzylurea (9c)



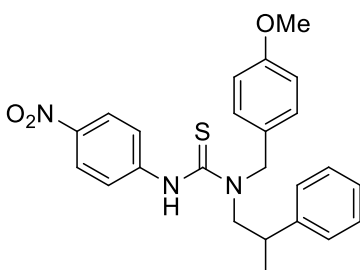
According to the general procedure C the title compound was synthesized as a colorless solid in 99% yield.

**M.p.:** 153 – 155 °C; **<sup>1</sup>H NMR** (400 MHz, CDCl<sub>3</sub>): δ = 7.38 – 7.20 (m, 10H), 4.45 (s, 4H), 4.16 (s, 1H), 2.02 (s, 3H), 1.87 (d, *J* = 2.3 Hz, 6H), 1.62 (s, 6H); **<sup>13</sup>C NMR** (101 MHz, CDCl<sub>3</sub>): δ = 157.4, 138.2, 128.9, 127.5(2), 127.4(5), 51.5, 50.6, 42.4, 36.6, 29.7; **IR** (ATR,  $\bar{\nu}$ /cm<sup>-1</sup>): 3365, 2902, 2848, 1615, 1538, 1454, 1308, 1234, 1170, 1071, 969, 738, 699, 459; **HRMS** (ESI-MS): *m/z* (%) = 375.2431 (100, MH<sup>+</sup>), calc. 375.2431.

**1-Benzyl-3-(3,5-bis(trifluoromethyl)phenyl)-1-(4-methoxybenzyl)thiourea (9d)**

According to the general procedure C the title compound was synthesized as a yellow oil in 92% yield.

**<sup>1</sup>H NMR** (400 MHz, CDCl<sub>3</sub>):  $\delta$  = 7.66 (s, 2H), 7.62 (s, 1H), 7.47 – 7.24 (m, 8H), 6.95 (d,  $J$  = 8.6 Hz, 2H), 5.05 (d,  $J$  = 25.7 Hz, 4H), 3.83 (s, 3H); **<sup>13</sup>C NMR** (101 MHz, CDCl<sub>3</sub>):  $\delta$  = 182.8, 159.9, 141.2, 135.3, 132.3, 132.0, 131.6, 131.3, 129.5, 128.7, 128.6, 127.3, 125.0, 124.5, 121.8, 118.9, 114.9, 55.5, 54.8, 54.4; **IR** (ATR,  $\bar{\nu}$ /cm<sup>-1</sup>): 3361, 2934, 1612, 1512, 1375, 1274, 1170, 1124, 1029, 886, 817, 733, 699, 601, 517; **HRMS** (ESI-MS):  $m/z$  (%) = 499.1279 (60, MH<sup>+</sup>), calc. 499.1273.

**1-(4-Methoxybenzyl)-3-(4-nitrophenyl)-1-(2-phenylpropyl)thiourea (9e)**

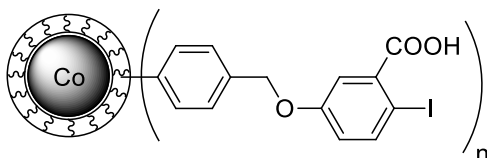
According to the general procedure C the title compound was synthesized as a yellow solid in 98% yield.

**M.p.:** 80 – 82 °C; **<sup>1</sup>H NMR** (400 MHz, CDCl<sub>3</sub>):  $\delta$  = 8.06 (d,  $J$  = 9.0 Hz, 2H), 7.46 – 7.29 (m, 5H), 7.21 (d,  $J$  = 8.2 Hz, 2H), 7.07 (d,  $J$  = 8.8 Hz, 2H), 6.92 (d,  $J$  = 8.5 Hz, 2H), 6.76 (bs, 1H), 4.84 (bs, 1H), 4.62 (d,  $J$  = 15.6 Hz, 1H), 4.00 (bs, 1H), 3.82 (s, 3H), 3.77 (dd,  $J$  = 14.1, 10.0 Hz, 1H), 3.44 (bs, 1H), 1.36 (d,  $J$  = 7.0 Hz, 3H); **<sup>13</sup>C NMR** (101 MHz, CDCl<sub>3</sub>):  $\delta$  = 182.3, 159.8, 145.8, 144.1, 143.7, 129.5, 128.7, 127.7, 127.6, 127.2, 124.4, 122.7, 114.7, 60.0, 55.5, 55.0, 38.3, 19.1; **IR** (ATR,  $\bar{\nu}$ /cm<sup>-1</sup>): 3335, 2962, 2930, 1595, 1506, 1319, 1290, 1247, 1174, 1026, 846, 812, 750, 729, 700; **HRMS** (ESI-MS):  $m/z$  (%) = 436.1698 (100, MH<sup>+</sup>), calc. 436.1689.

### Large scale synthesis dibenzylamine (9c)

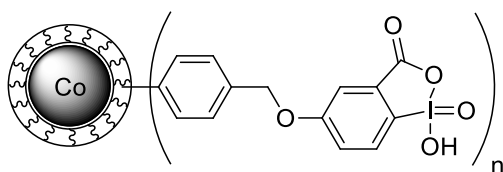
The synthesis of urea **9c** was repeated on a significantly larger scale: 276 mg (1.4 mmol, 1.0) of dibenzylamine (**8a**) and 310 mg (1.75 mmol) of adamantylisocyanate were stirred in 5 ml dry CH<sub>2</sub>Cl<sub>2</sub> for 3 h at room temperature. Magnetic amine **2** (292 mg, 0.88 mmol, 3 mmol/g) was added as a scavenger and the stirring continued for 2 h. The product solution was decanted and the beads washed with CH<sub>2</sub>Cl<sub>2</sub> (3 x 5 mL) according to the general procedure. Evaporation of the solvents yielded 515.1 mg (1.38 mmol, 98%) of **9c** as a colorless solid.

### Immobilization of iodocarboxylic acid to polymer-coated Co/C beads (14)



Benzyl chloride functionalized nanobeads (**1**, 2.87 g, 3.5 mmol/g) were dispersed in 20 ml dry DMF in a Schlenk flask under nitrogen atmosphere using an ultrasonic bath. After adding 7.3 g (25.1 mmol) of ethyl 5-hydroxy-2-iodobenzoate (**13**) and 3.6 g Cs<sub>2</sub>CO<sub>3</sub> (11.1 mmol) the mixture was heated to 75 °C for 20 h. The particles were separated by an external magnet and washed with DMF (3 x 20 mL), acetone (2 x 20 mL), H<sub>2</sub>O (2 x 20 mL), and MeOH (2 x 20 mL). Ba(OH)<sub>2</sub>·8 H<sub>2</sub>O (1.5 g) in 20 ml MeOH was added and the reaction mixture stirred for 12 h at RT. Thereafter, the particles were collected by a magnet, washed with H<sub>2</sub>O (3 x 20 mL), MeOH (3 x 20 mL), and Et<sub>2</sub>O (2 x 20 mL). After drying under vacuum, 5.0 g (97 %) of functionalized particles **14** were yielded.

**IR** (ATR,  $\bar{\nu}$ /cm<sup>-1</sup>): 2922, 2860, 1717, 1587, 1562, 1511, 1458, 1282, 1243, 1210, 1097, 1005, 812; **elemental microanalysis** (%): C, 47.54; H, 3.77; N, 0.01; Cl, 0.35; I, 23.47.

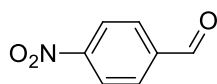
**Oxidation of resin-bound iodocarboxylic acid to the magnetic IBX resin (15)**

To a Schlenk vessel 1 g of resin **14** (1.85 mmol/g, 1.85 mmol) and 10 ml of dry  $\text{CH}_2\text{Cl}_2$  were introduced under nitrogen atmosphere. Tetrabutylammonium Oxone (8.6 g, 1.08 mmol/g, 9.3 mmol) was added followed by the dropwise addition of methanesulfonic acid (601  $\mu\text{l}$ , 9.3 mmol). The slurry was stirred for 3 hours at RT and the oxidized particles washed with  $\text{CH}_2\text{Cl}_2$  (8 x 10 mL), THF (5 x 10 mL),  $\text{CH}_2\text{Cl}_2$  (3 x 10 mL), and  $\text{Et}_2\text{O}$  (2 x 10 mL), before drying under vacuum. Only 806 mg of **15** were recovered.

**IR** (ATR,  $\bar{\nu}/\text{cm}^{-1}$ ): 2921, 1722, 1663, 1570, 1542, 1466, 1420, 1372, 1312, 1211, 1101, 1013, 813; **elemental microanalysis** (%): C, 41.92; H, 3.62; N, 0.01; S, 1.53.

**Determination of the Loading of mIBX resin 15 by  $^1\text{H}$ -NMR assay**

To rapidly estimate the loading of as-prepared magnetic IBX resins, 100 mg of the mIBX **15** were stirred in 2.0 mL of  $\text{CDCl}_3$  with an excess of 4-nitrobenzylalcohol (29.1 mg, 0.19 mmol) as substrate and 4-methylanisole (24  $\mu\text{L}$ , 0.19 mmol) as internal standard for 20 hours at room temperature. The magnetic resin was separated by a magnet, the supernatant filtered over a plug of cotton into a NMR tube and the  $^1\text{H}$ -NMR spectrum acquired. To estimate the loading the integrations of the aromatic CH doublets of the product at 8.40 ppm were compared to the integration of the aromatic CH doublet of the standard at 7.08 ppm.

**Oxidation of 4-nitrobenzyl alcohol using magnetic IBX resin**

4-Nitrobenzyl alcohol (**16**, 30.6 mg, 0.2 mmol) was dissolved in 5 ml of  $\text{CH}_2\text{Cl}_2$ . After the addition of 533 mg (0.75 mmol/g, 0.4 mmol) mIBX **15**, the solution was stirred for 20 hours at room temperature monitoring the reaction progress by TLC. The product

solution was filtered over cotton and the solvent evaporated. 35.8 mg (> 100%) of slightly impure product **17** was isolated after drying under vacuum.

**<sup>1</sup>H NMR** (300 MHz, CDCl<sub>3</sub>): δ = 10.16 (s, 1H), 8.40 (d, *J* = 8.6, 2H), 8.08 (d, *J* = 8.7, 2H).

➔ Please find supporting information including additional IR spectra, TEM pictures, as well as <sup>1</sup>H- and <sup>13</sup>C-NMR spectra on the enclosed CD.

## 4.6 References

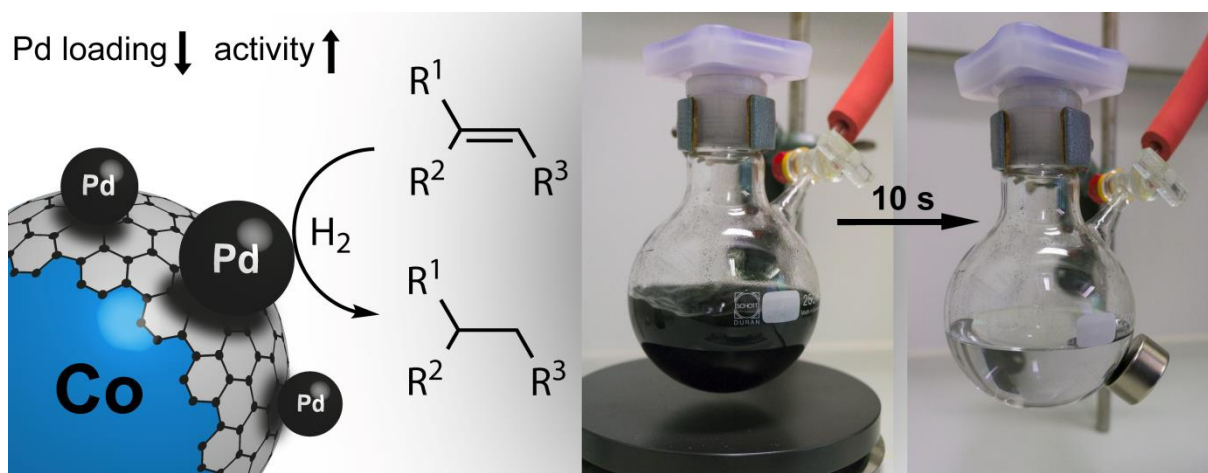
- [1] R. B. Merrifield, *J. Am. Chem. Soc.* **1963**, *85*, 2149–2154.
- [2] a) I. W. James, *Tetrahedron* **1999**, *55*, 4855–4946; b) F. Guillier, D. Orain, M. Bradley, *Chem. Rev.* **2000**, *100*, 2091–2158; c) A. R. Vaino, K. D. Janda, *J. Comb. Chem.* **2000**, *2*, 579–596; d) P. Blaney, R. Grigg, V. Sridharan, *Chem. Rev.* **2002**, *102*, 2607–2624; e) H. E. Blackwell, *Org. Biomol. Chem.* **2003**, *1*, 1251–1255.
- [3] a) S. Kaldor, *Curr. Opin. Chem. Biol.* **1997**, *1*, 101–106; b) A. Chesney, *Green Chem.* **1999**, *1*, 209–219; c) G. Bhalay, A. Dunstan, A. Glen, *Synlett* **2000**, 1846–1859; d) S. V. Ley, I. R. Baxendale, R. N. Bream, P. S. Jackson, A. G. Leach, D. A. Longbottom, M. Nesi, J. S. Scott, R. I. Storer, S. J. Taylor, *J. Chem. Soc., Perkin Trans. 1* **2000**, 3815–4195; e) L. A. Thompson, *Curr. Opin. Chem. Biol.* **2000**, *4*, 324–337; f) S. V. Ley, I. R. Baxendale, *Nat. Rev. Drug. Discov.* **2002**, *1*, 573–586; g) A. Solinas, M. Taddei, *Synthesis* **2007**, 2409–2453.
- [4] A. Kirschning, H. Monenschein, R. Wittenberg, *Angew. Chem. Int. Ed.* **2001**, *40*, 650–679.
- [5] a) S. Kobayashi, *Curr. Opin. Chem. Biol.* **2000**, *4*, 338–345; b) B. Clapham, T. S. Reger, K. D. Janda, *Tetrahedron* **2001**, *57*, 4637–4662; c) Y. R. de Miguel, E. Brulé, R. G. Margue, *J. Chem. Soc., Perkin Trans. 1* **2001**, 3085–3094.
- [6] a) R. John Booth, John C. Hodges, *J. Am. Chem. Soc.* **1997**, *119*, 4882–4886; b) J. J. Parlow, R. V. Devraj, M. S. South, *Curr. Opin. Chem. Biol.* **1999**, *3*, 320–336; c) S. J. Shuttleworth, S. M. Allin, R. D. Wilson, D. Nasturica, *Synthesis* **2000**, 1035–1074; d) J. Eames, M. Watkinson, *Eur. J. Org. Chem.* **2001**, 1213–1224; e) S. Ley, I. R. Baxendale, G. Brusotti, M. Caldarelli, A. Massi, M. Nesi, *Il Farmaco* **2002**, *57*, 321–330.
- [7] D. H. Drewry, D. M. Coe, S. Poon, *Med. Res. Rev.* **1999**, *19*, 97–148.
- [8] A. Schätz, R. N. Grass, Q. Kainz, W. J. Stark, O. Reiser, *Chem. Mater.* **2010**, *22*, 305–310.
- [9] R. N. Grass, E. K. Athanassiou, W. J. Stark, *Angew. Chem. Int. Ed.* **2007**, *46*, 4909–4912; *Angew. Chem.* **2007**, *119*, 4996–4999.
- [10] I. K. Herrmann, R. N. Grass, D. Mazunin, W. J. Stark, *Chem. Mater.* **2009**, *21*, 3275–3281.
- [11] N. Osterwalder, C. Capello, K. Hungerbühler, W. J. Stark, *J. Nanopart. Res.* **2006**, *8*, 1–9.
- [12] A. K. Tucker-Schwartz, R. L. Garrell, *Chem. Eur. J.* **2010**, *16*, 12718–12726.
- [13] Q. M. Kainz, A. Schätz, A. Zöpfl, W. J. Stark, O. Reiser, *Chem. Mater.* **2011**, *23*, 3606–3613.
- [14] a) F. M. Koehler, M. Rossier, M. Waelle, E. K. Athanassiou, L. K. Limbach, R. N. Grass, D. Günther, W. J. Stark, *Chem. Commun.* **2009**, 4862–4864; b) M. Rossier, F. M. Koehler, E. K. Athanassiou, R. N. Grass, M. Waelle, K. Birbaum, D. Günther, W. J. Stark, *Ind. Eng. Chem. Res.* **2010**, *49*, 9355–9362; c) R. Fuhrer, I. K. Herrmann, E. K. Athanassiou, R. N. Grass, W. J. Stark, *Langmuir* **2011**, *27*, 1924–1929; d) M. Rossier, A. Schaetz, E. K. Athanassiou, R. N. Grass, W. J. Stark, *Chem. Eng. J.* **2011**, *175*, 244–250; e) Q. M. Kainz, A. Späth, S. Weiss, T. D. Michl, A. Schätz, W. J. Stark, B. König, O. Reiser, *ChemistryOpen* **2012**, *1*, 125–129; f) M. Rossier, M. Schreier, U. Krebs, B. Aeschlimann, R. Fuhrer, M. Zeltner, R. N. Grass, D. Günther, W. J. Stark, *Sep. Pur. Technol.* **2012**, *96*, 68–74.
- [15] a) I. K. Herrmann, M. Urner, F. M. Koehler, M. Hasler, B. Roth-Z'Graggen, R. N. Grass, U. Ziegler, B. Beck-Schimmer, W. J. Stark, *Small* **2010**, *6*, 1388–1392; b) I. K. Herrmann, R. E. Bernabei, M. Urner, R. N. Grass, B. Beck-Schimmer, W. J. Stark, *Nephrol. Dial. Transpl.* **2011**, *26*, 2948–2954.
- [16] a) A. Schätz, R. N. Grass, W. J. Stark, O. Reiser, *Chem. Eur. J.* **2008**, *14*, 8262–8266; b) A. Schätz, O. Reiser, W. J. Stark, *Chem. Eur. J.* **2010**, *16*, 8950–8967; c) S. Wittmann, A. Schätz, R. N. Grass, W. J. Stark, O. Reiser, *Angew. Chem. Int. Ed.* **2010**, *49*, 1867–1870; *Angew. Chem.* **2010**, *122*, 1911–1914.
- [17] A. Schätz, T. R. Long, R. N. Grass, W. J. Stark, P. R. Hanson, O. Reiser, *Adv. Funct. Mater.* **2010**, *20*, 4323–4328.
- [18] a) M. Zeltner, A. Schätz, M. L. Hefti, W. J. Stark, *J. Mat. Chem.* **2011**, *21*, 2991; b) M. Zeltner, R. N. Grass, A. Schaetz, S. B. Bubenhofer, N. A. Luechinger, W. J. Stark, *J. Mater. Chem.* **2012**, *22*, 12064.

- [19] A. Schätz, M. Zeltner, T. D. Michl, M. Rossier, R. Fuhrer, W. J. Stark, *Chem. Eur. J.* **2011**, *17*, 10566–10573.
- [20] a) P. K. Maity, Q. M. Kainz, S. Faisal, A. Rolfe, T. B. Samarakoon, F. Z. Basha, O. Reiser, P. R. Hanson, *Chem. Commun.* **2011**, *47*, 12524–12526; b) P. K. Maity, A. Rolfe, T. B. Samarakoon, S. Faisal, R. D. Kurtz, T. R. Long, A. Schätz, D. L. Flynn, R. N. Grass, W. J. Stark, O. Reiser, P. R. Hanson, *Org. Lett.* **2011**, *13*, 8–10; c) Q. M. Kainz, *ChemSusChem* **2013**, *6*, 721–729.
- [21] S. W. Kaldor, M. G. Siegel, J. E. Fritz, B. A. Dressman, P. J. Hahn, *Tetrahedron Lett.* **1996**, *37*, 7193–7196.
- [22] M. Guinó, E. Brulé, Y. R. de Miguel, *J. Comb. Chem.* **2003**, *5*, 161–165.
- [23] a) H. W. Gibson, F. C. Bailey, *J. Chem. Soc., Chem. Commun.* **1977**, 815; b) N. M. Yoon, K. B. Park, Y. S. Gyoung, *Tetrahedron Lett.* **1983**, *24*, 5367–5370; c) A. R. Sande, *Tetrahedron Lett.* **1984**, *25*, 3501–3504; d) N. M. Yoon, E. G. Kim, H. S. Son, J. Choi, *Synth. Commun.* **1993**, *23*, 1595–1599.
- [24] A. K. Boal, T. H. Galow, F. Ilhan, V. M. Rotello, *Adv. Funct. Mater.* **2001**, *11*, 461–465.
- [25] S. Wittmann, J.-P. Majoral, R. N. Grass, W. J. Stark, O. Reiser, *Green Proc. Synth.* **2012**, *1*, 275–279.
- [26] See supporting information.
- [27] a) S. Shimizu, T. Suzuki, S. Shirakawa, Y. Sasaki, C. Hirai, *Adv. Synth. Catal.* **2002**, *344*, 370–378; b) M. Wang, V. Janout, S. L. Regen, *Langmuir* **2010**, *26*, 12988–12993; c) A. D'Urso, D. A. Cristaldi, M. E. Fragalà, G. Gattuso, A. Pappalardo, V. Villari, N. Micali, S. Pappalardo, M. F. Parisi, R. Purrello, *Chem. Eur. J.* **2010**, *16*, 10439–10446.
- [28] J. P. Collman, Y.-L. Yan, T. Eberspacher, X. Xie, E. I. Solomon, *Inorg. Chem.* **2005**, *44*, 9628–9630.
- [29] a) G. M. Coppola, *Tetrahedron Lett.* **1998**, *39*, 8233–8236; b) A. S. Kiselyov, C. Dominguez, *Tetrahedron Lett.* **1999**, *40*, 5111–5114; c) T. Arnould, A. G. M. Barrett, S. M. Cramp, R. S. Roberts, F. J. Zécari, *Org. Lett.* **2000**, *2*, 2663–2666; d) Z. Yu, S. Alesso, D. Pears, P. A. Worthington, R. W. A. Luke, M. Bradley, *J. Chem. Soc., Perkin Trans. 1* **2001**, 1947–1952; e) Zhanru Yu, Sonia Alesso, David Pears, Paul A. Worthington, Richard W. A. Luke, Mark Bradley, *Tetrahedron Lett.* **2000**, *41*, 8963–8967.
- [30] a) M. Creswell, G. L. Bolton, J. C. Hodges, M. Meppen, *Tetrahedron* **1998**, *54*, 3983–3998; b) S. V. Ley, A. Massi, *J. Chem. Soc., Perkin Trans. 1* **2000**, 3645–3654.
- [31] Y. Wang, S. R. Wilson, *Tetrahedron Lett.* **1997**, *38*, 4021–4024.
- [32] M. Guinó, K. Kuok Hii, *Org. Biomol. Chem.* **2005**, *3*, 3188.
- [33] a) C. Hartmann, V. Meyer, *Ber. Dtsch. Chem. Ges.* **1893**, *26*, 1727–1732; b) M. Frigerio, M. Santagostino, S. Sputore, *J. Org. Chem.* **1999**, *64*, 4537–4538.
- [34] M. Frigero, M. Santagostino, *Tetrahedron Lett.* **1994**, *35*, 8019–8022.
- [35] M. Frigerio, M. Santagostino, S. Sputore, G. Palmisano, *J. Org. Chem.* **1995**, *60*, 7272–7276.
- [36] T. Wirth, *Angew. Chem. Int. Ed.* **2001**, *40*, 2812–2814.
- [37] a) G. Sorg, A. Mengel, G. Jung, J. Rademann, *Angew. Chem. Int. Ed.* **2001**, *40*, 4395–4397; b) Z. Lei, C. Denecker, S. Jegasothy, D. C. Sherrington, N. K. Slater, A. J. Sutherland, *Tetrahedron Lett.* **2003**, *44*, 1635–1637; c) W. J. Chung, D. K. Kim, Y. S. Lee, *Tetrahedron Lett.* **2003**, *44*, 9251–9254.
- [38] N. N. Reed, M. Delgado, K. Hereford, B. Clapham, K. D. Janda, *Bioorg. Med. Chem. Lett.* **2002**, *12*, 2047–2049.
- [39] M. Mülbaier, A. Giannis, *Angew. Chem. Int. Ed.* **2001**, *40*, 4393–4394.
- [40] B. M. Trost, R. Braslau, *J. Org. Chem.* **1988**, *53*, 532–537.





## 5. Palladium Nanoparticles Supported on Magnetic Carbon-Coated Cobalt Nanobeads – Highly Active and Recyclable Catalysts for Alkene Hydrogenation<sup>i</sup>



Palladium nanoparticles have been synthesized on the surface of highly magnetic carbon-coated cobalt nanoparticles. In contrast to the established synthesis of Pd nanoparticles via reduction of Pd(II) precursors, the microwave decomposition of a Pd(0) source leads to a more efficient Pd deposition, resulting in a material with considerably higher activity in the hydrogenation of alkenes. Systematic variation of the Pd loading on the carbon-coated cobalt nanoparticle surface reveals a distinct trend to higher activities with decreased loading of Pd. The Pd nanoparticles can be stabilized by the introduction of functional groups on the surface of the Co/C support, and the activity of the catalysts is further improved by the addition of 10 vol% Et<sub>2</sub>O to isopropanol that was found to be the solvent of choice. With respect to activity (TOFs up to 11095 h<sup>-1</sup>), handling, recyclability through magnetic decantation, and leaching of Pd ( $\leq 6$  ppm/cycle), this novel magnetic hybrid material compares favorably to conventional Pd/C or Pd@CNT catalysts.<sup>ii</sup>

<sup>i</sup> This chapter includes parts from a manuscript which has been prepared in collaboration with R. Linhardt, R. Grass, G. Vilé, J. Pérez-Ramírez, W. J. Stark, and O. Reiser and submitted to *Adv. Funct. Mat.* for publication.

<sup>ii</sup> TEM as well as EDX was conducted by R. Grass. CO pulse chemisorption and additional TEM (SI) was carried out by G. Vilé. XRD measurements were performed by F. Pielhofer and ICP-OES by J. Rewitzer. All other syntheses and experiments were carried out by Q. M. Kainz.

## 5.1 Introduction

Catalytic hydrogenations are among the most important and widely accessed transformations in chemical industry. If molecular hydrogen is used and the catalyst is recyclable, this method is atom economic and arguably the cleanest possible way to reduce an organic compound.<sup>[1]</sup> The recovery and recycling of catalysts comes more and more into focus not only from an economical but also from an ecological perspective driven by the rise of green and sustainable chemistry.<sup>[2]</sup>

Generally, homogeneous catalysts feature high levels of activity and selectivity since they are uniform on a molecular level and readily dissolved in the reaction medium. However, especially on large scale it is often tedious and expensive to efficiently separate these catalysts from reaction mixtures, which is important due to the high costs of catalysts and to avoid heavy metal contamination of the final products, a key issue in pharmaceutical industry.<sup>[3]</sup> In fact, in about 80 % of the industrially relevant catalytic transformations heterogeneous catalyst systems are applied.<sup>[4]</sup> Despite considerable research efforts, predominantly the sites on the surface of the porous supports are catalytically active, reducing the overall activity of such heterogeneous systems.<sup>[5]</sup>

Due to their high surface-to-volume ratio, nanocatalysts, e.g. transition-metal nanoparticles, nicely bridge the gap between both worlds by featuring attributes of homogeneous (high activity and selectivity) and heterogeneous (easy separation and recycling) systems. However, quite expensive ultracentrifugation has to be used to separate nano-sized particles instead of simple filtration. In addition, such particles tend to agglomerate to the bulk material without the addition of stabilizers, which hampers their activity by shielding the surface.<sup>[5,6]</sup> Therefore, many attempts have been made to stabilize nanoparticles by immobilization on various functionalized and unfunctionalized supports, such as polymers,<sup>[7]</sup> silica,<sup>[8]</sup> zeolites,<sup>[9]</sup> carbon,<sup>[10]</sup> graphene,<sup>[11]</sup> and CNTs.<sup>[12–14]</sup> However, most of these supports have serious drawbacks like a complicated synthesis, hampered diffusion kinetics, or tedious separation via centrifugation. An elegant way of merging high surface-area with convenient recovery via magnetic decantation is the application of magnetic nanoparticles as supports. Recent examples demonstrate the successful synthesis of palladium nanoparticles on the surface of magnetic substrates, e.g. polymer/silica /carbon-coated magnetite particles,<sup>[15,16]</sup> magnetite-graphene composites,<sup>[17,18]</sup> carbon-coated FeNi nanoparticles,<sup>[19]</sup> and ordered mesoporous carbon doped with Co/C nanoparticles.<sup>[20]</sup>

We report here a novel nanoparticle-on-nanoparticle hybrid system, which consists of three components: (i) a nano-sized cobalt core, which provides higher magnetization than conventional metal oxides allowing separation of the catalyst within seconds; (ii) several carbon shells, which protect the core and stabilize attached catalysts; (iii) palladium nanoparticles immobilized on the surface of the carbon shells showing exceptionally high catalytic activity in hydrogenation reactions. Key features of this study include the evaluation of different palladium sources and conditions for the synthesis of the Pd nanoparticles, investigation of the influence of various palladium loadings on the catalytic activity, leaching and recycling tests, and the additional introduction of stabilizing groups on the carbon surface.

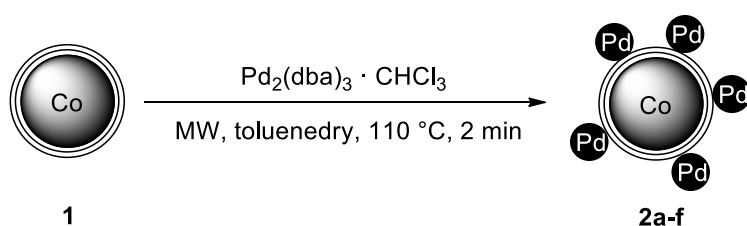
## 5.2 Results and Discussion

Carbon-coated cobalt nanoparticles (Co/C) were used as magnetic supports. The large scale synthesis (> 30 g/h) of these magnetic beads via reducing flame spray pyrolysis was recently reported by Stark *et al.*<sup>[21]</sup> Unique features are a remarkably high chemical and thermal stability due to the graphene-like shell and a saturation magnetization (158 emu/g) equivalent to that of bulk cobalt, exceeding common iron oxide (e.g. magnetite) beads by a factor of five.<sup>[22]</sup> Furthermore, the raw material costs (cobalt carboxylate and acetylene) for manufacturing Co/C nanoparticles following this route can be estimated as <100 USD/kg.<sup>[23]</sup> We successfully functionalized the carbon surface of the Co/C beads by covalent and/or non-covalent methods<sup>[24]</sup> leading to various applications, e.g. to recyclable supports for catalysts,<sup>[25],[26]</sup> for the extraction of vitamins and contaminants from aqueous solutions,<sup>[27,28]</sup> or for the purification of blood.<sup>[29]</sup> The high magnetization of the beads allows continuous-flow applications using external magnetic fields rather than membranes to contain the catalyst.<sup>[30]</sup> High loading magnetic reagents and scavengers are also accessible after the introduction of polymer shells to the Co/C nanoparticles.<sup>[31]</sup>

### Synthesis of Pd nanoparticles on the surface of Co/C beads

Since carbon materials are reported to provide significant stabilization to Pd nanoparticles, presumably through strong  $\pi$ -interactions with  $sp^2$  carbon atoms,<sup>[17,32]</sup>

the highly magnetic Co/C nanoparticles seem to be an ideal support for the deposition of such nanoparticles. A procedure described by Urriolabeitia *et al.*<sup>[14]</sup> was modified to synthesize Pd nanoparticles on the surface of Co/C nanobeads **1**: Pd<sub>2</sub>(dba)<sub>3</sub>·CHCl<sub>3</sub> as stable Pd(0) source and Co/C nanoparticles, which are very susceptible to microwave irradiation,<sup>[33]</sup> were heated in a focused microwave oven, (Scheme 1), leading to the formation of Pd nanoparticles on the carbon surface of the Co/C support in only 2 min (Pd@Co/C **2a**).



**Scheme 1.** Microwave-synthesis of Pd@Co/C nanocomposites.

In order to determine the effects of different loadings and dispersions of Pd nanoparticles on the surface of the Co/C supports, Pd@Co/C hybrid material, **2a-f** was synthesized with Pd contents ranging from 14.3 wt% to 0.2 wt% (Table 1, entry 1-6). In all cases, the incorporation of Pd was nearly quantitative (92-100%, Figure 1A) as determined by inductively coupled plasma optical emission spectrometry (ICP-OES). Pd<sub>2</sub>(dba)<sub>3</sub> lacking the chloroform adduct was additionally tested as Pd(0) source under identical conditions in the microwave synthesis (Table 1, entry 7+8). However, at two different concentrations, a palladium incorporation of only 62 and 71% was measured (Figure 1A). These results indicate a beneficial influence of the chloroform adduct in the formation of Pd(0) clusters and nanoparticles. Furthermore, Na<sub>2</sub>PdCl<sub>4</sub>, a Pd(II) source commonly used for the synthesis of Pd nanoparticles, was also tested. A dispersion of **1** in an aqueous solution of Na<sub>2</sub>PdCl<sub>4</sub> was treated with either NaBH<sub>4</sub> (**2i**) or stirred under H<sub>2</sub> atmosphere (**2j**) to reduce the Pd(II) salt to Pd(0) nanoparticles (Table 1, entry 9+10). Analysis of the resulting nanocomposites resulted in 87% Pd deposition in the case of NaBH<sub>4</sub> reduction and 81% in the case of H<sub>2</sub> reduction. Due to their unpolar nature the particles **1** are less dispersible in an aqueous solution rather than in toluene as used in the microwave synthesis starting from Pd(0), which might account for the inferior results obtained by the reductive method starting from Pd(II).

**Table 1.** Synthesis of Pd@Co/C nanoparticles with varying Pd loadings.

Entry	Index	Pd source	Method of synthesis <sup>[a]</sup>	Pd incorporated [%] <sup>[b]</sup>	Pd loading [mmol/g] <sup>[b]</sup>	Pd content [wt%] <sup>[b]</sup>	Pd dispersion [%] <sup>[c]</sup>	$d_{Pd}$ [nm] <sup>[c]</sup>	$S_{Pd}$ [m <sup>2</sup> /g] <sup>[c]</sup>
1	<b>2a</b>	Pd <sub>2</sub> (dba) <sub>3</sub> ·CHCl <sub>3</sub>	A	92	1.34	14.3			
2	<b>2b</b>	Pd <sub>2</sub> (dba) <sub>3</sub> ·CHCl <sub>3</sub>	A	100	0.83	8.8	4	30.4	8
3	<b>2c</b>	Pd <sub>2</sub> (dba) <sub>3</sub> ·CHCl <sub>3</sub>	A	98	0.41	4.4		5–10 <sup>d</sup>	
4	<b>2d</b>	Pd <sub>2</sub> (dba) <sub>3</sub> ·CHCl <sub>3</sub>	A	100	0.15	1.6	22	6.3	54
5	<b>2e</b>	Pd <sub>2</sub> (dba) <sub>3</sub> ·CHCl <sub>3</sub>	A	96	0.073	0.8	35	3.8	95
6	<b>2f</b>	Pd <sub>2</sub> (dba) <sub>3</sub> ·CHCl <sub>3</sub>	A	100	0.015	0.2	47	2.7	113
7	<b>2g</b>	Pd <sub>2</sub> (dba) <sub>3</sub>	A	62	0.042	0.4			
8	<b>2h</b>	Pd <sub>2</sub> (dba) <sub>3</sub>	A	71	0.012	0.1			
9	<b>2i</b>	Na <sub>2</sub> PdCl <sub>4</sub>	B	87	0.013	0.1			
10	<b>2j</b>	Na <sub>2</sub> PdCl <sub>4</sub>	C	81	0.012	0.1			

[a] Method A: heating under microwave irradiation; method B: reduction with NaBH<sub>4</sub>; method C: reduction with H<sub>2</sub>. [b] Determined by ICP-OES analysis. [c] Determined by CO pulse chemisorption. [d] Determined by transmission electron microscopy.

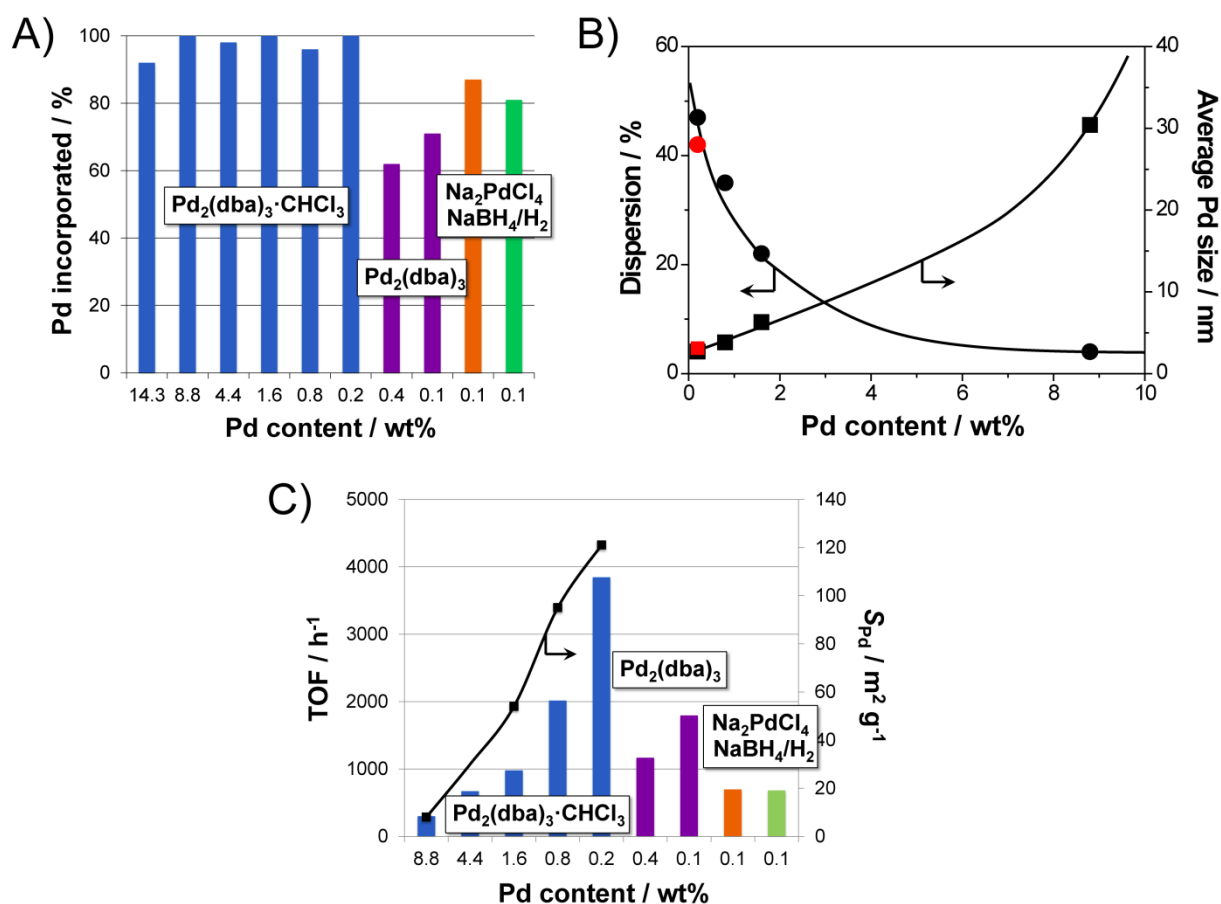


**Figure 1.** (A) Synthesis of Pd nanoparticles on the surface of Co/C nanobeads varying the Pd source and the Pd concentration. (B) Dispersion and size of Pd nanoparticles (**2b,d,e,f**) determined by CO pulse chemisorption measurements. The red marks indicate a sample after six runs of catalysis. (C) Hydrogenation tests of *trans*-stilbene at a Pd loading of 0.1 mol%. The best results were obtained for Pd@Co/C particles with a low Pd content of 0.2 wt% (**2f**) synthesized by MW decomposition of  $\text{Pd}_2(\text{dba})_3 \cdot \text{CHCl}_3$ .

### Characterization of Pd@Co/C nanoparticles

The so synthesized Pd@Co/C hybrid materials were subsequently characterized by a series of techniques. The Pd dispersion and the average size of the Pd nanoparticles were determined by CO pulse chemisorption (Figure 1B). A reference sample of **1** did not show any adsorption of CO, strongly suggesting that all Co particles were well coated by carbon. The smallest nanoparticles (2.7 nm) and highest Pd dispersion (47%) were determined for the nanocomposite **2f** with the lowest Pd loading (Table 1, entry 6). Further studies nicely showed a trend to larger Pd nanoparticles as well as a decreased dispersion by increasing the Pd content in the nanocomposite (Figure 1B). At 8.8 wt% Pd nanoparticles with a large mean size of 30.3 nm and a very low dispersion of 4% were observed (Table 1, Entry 2). Consequently, the ex-

posed surface of the Pd nanoparticles, a key factor for catalytic activity, decreases with higher Pd loadings. Transmission electron microscopy of nanoparticles **2c** with 4.4 wt% Pd indeed showed deposition of Pd nanoparticles with a size of about 5–10 nm on the surface of the larger Co/C supports, which have an average diameter of 25 nm (Figure 2).<sup>21</sup> An unambiguous assignment of the particle size distribution, however, was not possible due to the rather broad size distribution of the Co/C supports. Especially for nanocomposites with low Pd loadings, a clear determination of the very small Pd nanoparticles was difficult.<sup>[34]</sup> Energy-dispersive X-ray spectroscopy (EDX) confirmed, that the nanocomposites comprise of the elements Co, C, and Pd, which are derived from cobalt core, carbon shell, and Pd deposited on the surface.<sup>[34]</sup>

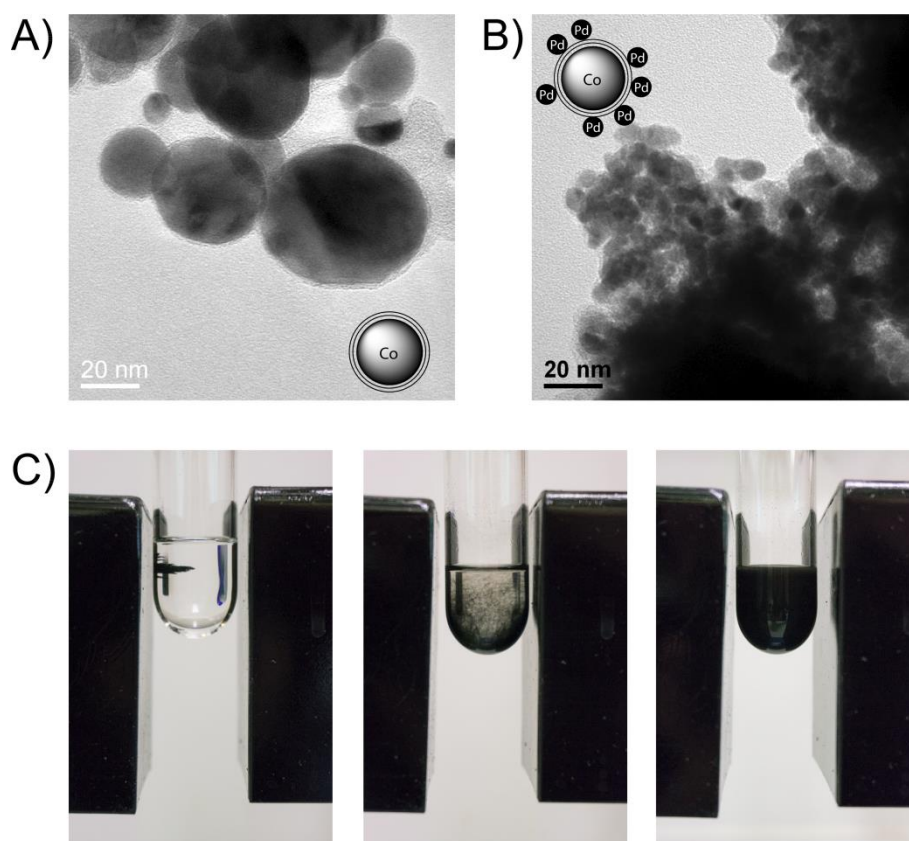


**Figure 2.** (A) TEM pictures of pristine Co/C nanobeads **1** (A) and Pd@Co/C **2c** (B, 4.4 wt% Pd). (C) shows the dispersion of the nanoparticles without a stirring bar. The black boxes contain contrarily rotating permanent magnets.

Additionally, X-ray powder diffraction (XRD) was performed. With Pd loadings ranging from 0.2 to 8.8 wt% only the characteristic diffraction peaks at  $2\theta$  of  $44.2^\circ$ ,  $51.5^\circ$ , and  $75.8^\circ$  corresponding to the diffraction of (111), (200), and (220) of the co-

balt core were observed.<sup>[34]</sup> Only for **2a**, featuring a high loading of 14.3 wt% Pd one broad peak at  $2\theta$  of  $39.9^\circ$  was detected in addition to the cobalt peaks, which can be indexed as the diffraction (111) of crystalline Pd(0) indicating that Pd exists in the reduced form Pd(0) instead of Pd(II).<sup>[34]</sup>

### Application of Pd@Co/C in the hydrogenation of *trans*-stilbene

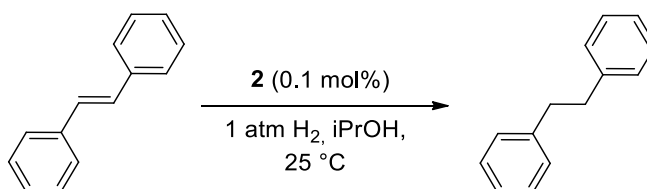
The nanocomposites were subsequently tested as catalysts for the hydrogenation of alkenes using molecular hydrogen. As a first test substrate *trans*-stilbene was hydrogenated using particles **2b-j** having different Pd contents (Table 2, entry 1-5). The total amount of particles was adjusted to obtain the same low Pd content of 0.1 mol% for each reaction. *i*PrOH turned out to be the ideal solvent for this transformation, since the particles disperse much worse in more polar solvents like MeOH or H<sub>2</sub>O. Tests also showed that the conversion in *i*PrOH is much higher as in more unpolar solvents, e.g. in CHCl<sub>3</sub>. Comparing the turn over frequencies (TOF), a clear trend of increasing activity with decreasing Pd content of the nanocomposites **2b-f** is observable (Figure 1C). The data from the activity tests nicely fit the data for the exposed Pd surface obtained from CO pulse chemisorption. The very high TOF (3845 h<sup>-1</sup>) of the particles with 0.2 wt% Pd (Table 2, entry 5) by far exceeds the TOFs for the same reaction catalyzed by palladium nanoparticles immobilized on magnetite beads (46-49 h<sup>-1</sup>)<sup>[16]</sup> and Pd nanoparticles deposited on the surface of CNTs (2820 h<sup>-1</sup>).<sup>[13]</sup> Due to the high saturation magnetization of the cobalt core dispersing and stirring of the nanocatalyst **2** was also possible by the application of an external rotating magnetic field (Figure 2C), dispensing from the need of an ultrasonic bath and an internal stirring bar. However, the conversion drops by two third compared to the reaction with stirring bar (Table 2, entry 6). This can be attributed to the possibility of more vigorous convection using an internal stirring bar, which is an important factor since the contact area with the hydrogen atmosphere is crucial in this reaction. Lowering the catalyst loading to 0.01 mol% full conversion was obtained after only one hour by raising the hydrogen pressure to 10 bar. This low loading results in an extremely high TOF of 11095 h<sup>-1</sup> (Table 2, entry 7), which, to the best of our knowledge, exceeds all reported TOFs of supported Pd catalysts for the hydrogenation of this particular substrate.

When nanocatalysts **2g** and **2h** were applied, which were synthesized by the decomposition of Pd<sub>2</sub>(dba)<sub>3</sub>, considerably smaller TOFs were obtained compared to



**2f** (Figure 1C, Table 2), showing again the beneficial influence of the Pd<sub>2</sub>(dba)<sub>3</sub>-chloroform adduct as the Pd source. However, the same trend of higher catalytic activity at lower Pd content is also observable in this case (Table 2, entry 8+9). The nanocomposites **2b** and **2c** exhibit even lower catalytic activities regardless of the

**Table 2.** Hydrogenation of *trans*-stilbene using Pd@Co/C.<sup>[a]</sup>



Entry	Particles	Pd [wt %]	t [min]	Conversion [%] <sup>[b]</sup>	TOF [h <sup>-1</sup> ] <sup>[c]</sup>
1	<b>2b</b>	8.8	60	30	300
2	<b>2c</b>	4.4	60	67	670
3	<b>2d</b>	1.6	60	98	980
4	<b>2e</b>	0.8	40	96	2015
5	<b>2f</b>	0.2	10	64	3845
6 <sup>[d]</sup>	<b>2f</b>	0.2	10	18	1060
7 <sup>[e]</sup>	<b>2f</b>	0.2	60	100	11095
8	<b>2g</b>	0.4	40	78	1166
9	<b>2h</b>	0.1	20	60	1793
10	<b>2i</b>	0.1	60	70	697
11	<b>2j</b>	0.1	60	68	681
12	-	-	240	0.5	n.d.
13	<b>1</b>	-	240	0.6	n.d.
14	Pd/C	1.8 <sup>[f]</sup>	60	59	585

[a] Stilbene (0.5 mmol) in *i*PrOH (5 mL) was hydrogenated by 0.5 μmol **2** (0.1 mol% Pd) adding dodecane as GC standard. [b] Conversion determined by GC analysis using internal standard. [c] Mol of substrate transformed per mol of catalyst per hour. [d] No stirring bar. [e] 0.01 mol% catalyst loading, 10 bar H<sub>2</sub> pressure. [f] Equivalent to 0.2 wt% on the magnetic nanoparticles.

method of reduction (Table 2, entry 10+11). These results might be reasoned by the reduced dispersability in water of **1** during the synthesis, which seems to be essential for the deposition of active Pd nanoparticles on the surface of these supports. Concluding from all the above results,  $\text{Pd}_2(\text{dba})_3 \cdot \text{CHCl}_3$  is by far the optimal Pd source regarding efficiency of Pd incorporation and catalytic activity.

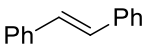
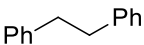
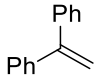
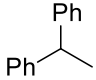
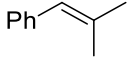
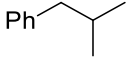
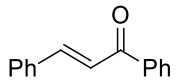
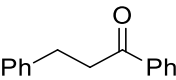
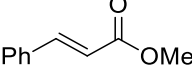
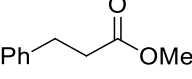
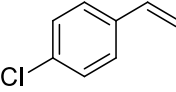
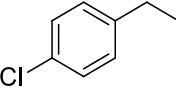
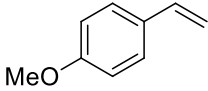
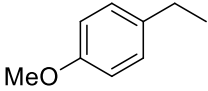
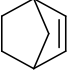
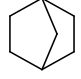
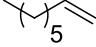
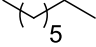
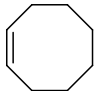
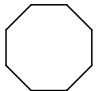
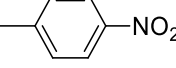
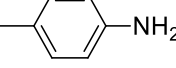
Additionally, a series of control experiments was conducted. In the absence of nanocatalyst a negligible background conversion of 0.5% after 4 h of reaction time was observed (Table 2, entry 12). Almost the same value was obtained using Co/C nanoparticles **1**, excluding any relevant catalytic activity by the support itself (Table 2, entry 13). In another experiment, applying particles **2f**, the catalyst was collected by a magnet after 15 min of reaction time and the supernatant decanted into a fresh reaction tube. The conversion at this time was 72.3%. Stirring the decanted solution for two more hours under hydrogen atmosphere led to an additional conversion of only 0.2%, which correlates very well with the background activity. This experiment shows that indeed the Pd nanoparticles catalyze the reaction and not Pd that is dissolved in the reaction mixture. Finally, to probe the influence of the support on the catalytic activity, Pd was deposited on activated charcoal (Merck) using the exact same conditions used for the synthesis of the most active particles **2f**. The amount of palladium was adjusted to ensure the same Pd to C ratio as in the nanocatalyst. The temperature ramping in the microwave, however, was considerably longer to reach the final temperature of 110 °C and the incorporation efficiency of Pd into the activated charcoal was only 86% in comparison to 100% in the case of **2f**. Moreover, the catalytic activity measured for this freshly prepared Pd/C catalyst (Table 2, entry 14) is only 15% of the activity of **2f** under identical conditions. The better accessibility of active sites on the nano-globular particles **2f** and/or an activating electronic effect of the cobalt core might account for this result.

### Evaluation of the substrate scope and additives

In order to test the substrate scope and to classify the results obtained for *trans*-stilbene with respect to other substrates various olefins and a nitro compound were evaluated under the same conditions applying nanocatalyst **2f**. Di- or tri-substituted olefins were successfully hydrogenated in reactions times similar to that of *trans*-stilbene (Table 3, entry 1-3). In  $\alpha,\beta$ -unsaturated compounds (Table 3, entry 4+5) the alkene moiety was reduced selectively. Chalcone (Table 3, entry 4) was hydrogenat-

ed ten times slower than methyl cinnamate (Table 3, entry 5), which might be reasoned by the stronger electron withdrawing effect of the neighboring keto group compared to the ester group in methyl cinnamate. Styrene-derivatives reacted in a very short reaction time of only ten minutes regardless if donor or acceptor substituents are present on the arene ring (Table 3, entry 6+7), as well as norbornene (Table 3, entry 8). In the case of octane the starting material was consumed after 5 minutes

**Table 3.** Hydrogenation of olefins and a nitro compound by Pd@Co/C catalyst **2f**.<sup>[a]</sup>

Entry	Substrate	Product	t [min]	Conversion [%] <sup>[b]</sup>
1			20	100
2			15	100
3			20	100
4			150	100
5			15	100
6			10	100
7			10	100
8			10	100
9 <sup>[c]</sup>			45	100
10			240	100
11			20	100

[a] Substrate (0.5 mmol) in *i*PrOH (5 mL) was hydrogenated by 0.5  $\mu$ mol **2f** (0.2 wt% Pd) adding dodecane as GC standard. [b] Determined by GC analysis using internal standard. [c] Initial isomerization to (*E*)-oct-2-ene detectable.

according to GC measurements, however, a partial isomerization to (*E*)-oct-2-ene was detected and additional 40 min were needed to complete the hydrogenation to octane (Table 3, entry 9). The cyclic analogue (*Z*)-cyclooctane turned out to be a more difficult substrate needing 4 h for full conversion. Finally, 4-nitrotoluene was readily converted to the corresponding amine demonstrating that nitro compounds are also feasible substrates for nanocatalyst **2f**.

To further enhance the activity of the nanocatalyst by activation of the Pd surface, the use of additives was evaluated in a series of experiments. Initial tests with different solvents revealed that the addition of ethers activate the nanocatalyst **2**. For more detailed studies of this effect, diethyl ether was chosen as additive since it is conveniently available and the low boiling allows easy removal from the product. Indeed, diethyl ether enhanced the TOF in the hydrogenation of *trans*-stilbene using catalyst **2f** up to 30% (Figure 3A). The optimum ratio seems to be 10 vol% of diethyl ether in <sup>i</sup>PrOH leading to an extraordinary high TOF of 5507 h<sup>-1</sup>. Higher amounts of ether reduced the activity again, which could be explained with a lower ability of dissolving hydrogen. The activating effect of diethyl ether might be a general phenomenon for Pd nanoparticles, which will be further explored by us in other catalyzed reactions.

### Recycling and leaching tests

Having determined the most active catalyst, the substrate scope, and the best conditions, the recovery and recycling of the catalyst remained of prevalent interest. A large-scale hydrogenation of *trans*-stilbene applying 0.1 mol% catalyst **2f** was set up, recycling the nanocatalyst after each run (Figure 3B). After a reaction time of 15 min, a permanent magnet was added to the side of the reaction flask, allowing the complete separation of the magnetic catalyst within seconds (Figure 3C), which is of great advantage compared to supports with inferior magnetization levels, e.g. iron oxide based nanoparticles. The product solution was simply decanted, which is arguably more convenient than removal of conventional polymer, silica, or carbon supports by filtration or CNTs by centrifugation. After washing the magnetically recovered particles thoroughly, they were reused directly for the next run. In the first run, full conversion was reached after only 15 min at a high TOF of 3722 h<sup>-1</sup> (Table 4). While in the second run the conversion remained at a high level of 96% it constantly decreased in the following runs reaching 55% in the 6<sup>th</sup> run (Figure 3B).

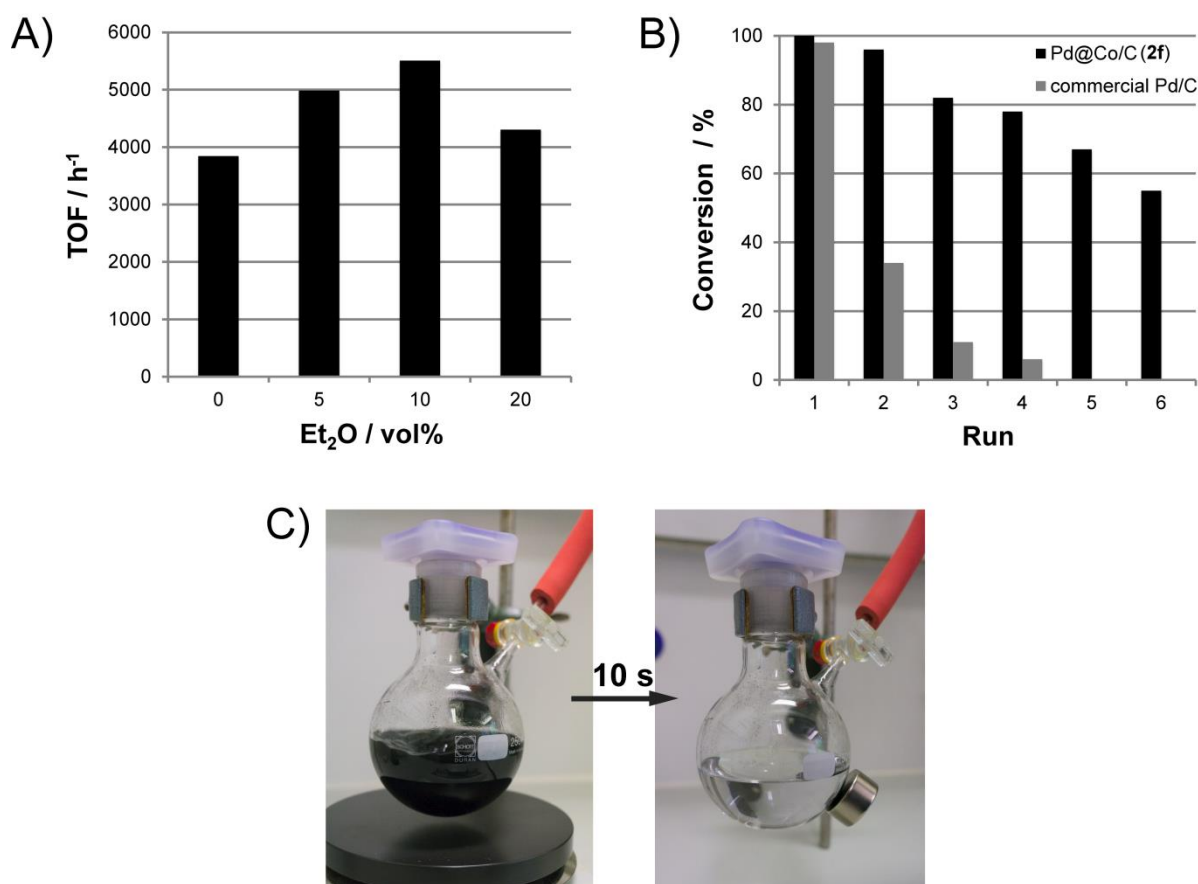


**Figure 3.** (A) Effects of the addition of Et<sub>2</sub>O on the catalytic activity of catalyst **2f** (0.1 mol%) in the hydrogenation of *trans*-stilbene. (B) Repetitive hydrogenation of *trans*-stilbene using 0.1 mol% of Pd catalyst. The conversion of **2f** was determined after 15 min for six consecutive runs and the conversion of commercial Pd/C (1 wt%) after 270 min for four consecutive runs. (C) The magnetic catalyst **2f** can be recovered by an external magnet (silver colored cylinder) within seconds.

In order to compare the results with a common hydrogenation catalyst, commercially available Pd on activated charcoal (Acros, 1 wt% Pd) was also tested. The Pd loading was determined by ICP-EOS as 0.086 mmol/g and the values obtained by CO adsorption ( $d_{\text{Pd}} = 4.7 \text{ nm}$ ,  $S_{\text{Pd}} = 68 \text{ m}^2 \text{ g}^{-1}$ ,  $D_{\text{Pd}} = 29 \%$ ) are in the range of Pd@Co/C nanocatalysts with similar loadings (Table 1). Applying the commercial Pd/C in the hydrogenation of stilbene, however, the reaction time had to be raised to 4.5 h to reach nearly full conversion (98 %) in the first run at a catalyst loading of 0.1 mol%. The resulting TOF ( $241 \text{ h}^{-1}$ ) is more than ten times lower as for the nanocatalyst **2f** and even lower as Pd/C synthesized by microwave deposition of Pd nanoparticles on activated charcoal (Table 2, entry 14). In order to recycle the Pd/C catalyst, the solution was filtered from the insoluble catalyst and the catalyst was recovered from the filter. Inevitably, some catalyst material was lost during this tedious proce-

ture, so, in contrast to the magnetic catalysts, the amount of substrate was adjusted for each run to compensate the loss of catalyst. The activity of the Pd/C system, however, dropped by 65% after the first run and after four runs, only 6 % conversion was determined resulting in a very low TOF of 14 h<sup>-1</sup> (Figure 3B). Due to this greatly reduced activity no further runs were carried out.

There are three possible explanations for the decrease of activity upon recycling of the Pd@Co/C nanocatalyst: (i) passivation of the surface, presumably via oxidation to Pd(II); (ii) leaching of the Pd from the support; (iii) agglomeration of the Pd nanoparticles on the carbon surface of the support. Oxidation of the surface, however, is unlikely since a reducing environment is prevalent throughout the course of reaction. Leaching of Pd from the supports or loss of the entire Pd@Co/C nanocatalyst was investigated also in view of the low limits for heavy metal impurities in products set by the pharmaceutical industry.<sup>3</sup> While the decantation test discussed above already indicated a low leaching of active Pd species, the Pd and Co contamination in the final product was more precisely determined by ICP-OES measurements. To quantify the metal content a second batch of *trans*-stilbene was hydrogenated, this time letting the reaction run to full conversion in each run.<sup>[34]</sup> The detected Pd content in the isolated product was always below the detection limit of our equip-

**Table 4.** Consecutive large scale hydrogenation and determination of the leaching.<sup>[a]</sup>

Run	Batch 1		Batch 2 <sup>[b]</sup>		
	Conversion after 15 min [%] <sup>[c]</sup>	TOF [h <sup>-1</sup> ]	Time to full conversion [min]	Leaching Pd [ppm] <sup>[d]</sup>	Leaching Co [ppm] <sup>[d]</sup>
1	100	3722	15	n.d.	n.d.
2	96	3668	20	< 2	6
3	82	3279	35	< 2	< 2
4	78	3116	50	6	4
5	67	2681	90	< 2	< 2
6	55	2203	120	< 2	17

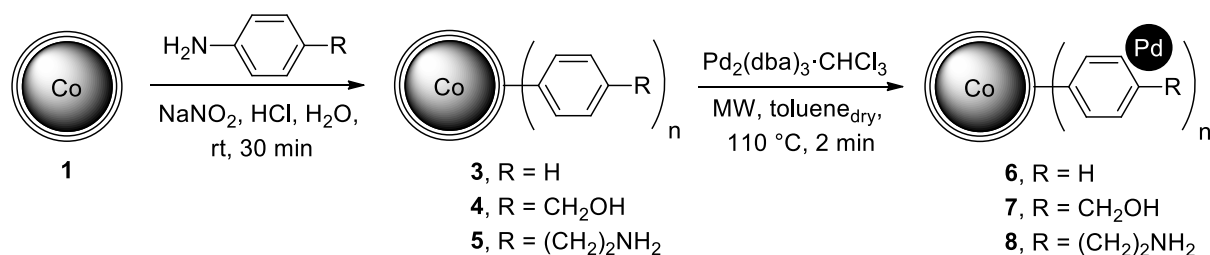
[a] Stilbene (7.3 mmol) in <sup>i</sup>PrOH/Et<sub>2</sub>O (9:1) was hydrogenated by 7.3 μmol **2f** (0.2 wt% Pd) adding dodecane as GC standard. [b] Each run was stopped at 100% conversion. No standard was added after run 1. [c] Conversion determined by GC analysis using internal standard. [d] In μg per g of product. Determined by ICP-OES.

ment (2 ppm) except of one run (Table 4). The contamination with cobalt was also in almost all runs at the threshold of the detection limit and only in one case a slightly higher Co contamination was measured probably due to the loss of a small amount of supports during magnetic separation. With one exception, however, the heavy metal concentrations are below the 10 ppm limit set by the industry.<sup>[3]</sup> Moreover, the remaining Pd on the supports was determined for batch 1 (6 runs, each run 15 min) as 100% of the initial loading and for batch 2 (6 runs, each run to full conversion) as 95%. The particularly bad results in the recycling of Pd/C were underlined by the ICP-OES measurements where only 10% of the initial Pd was detected in the Pd/C catalyst after four runs of catalysis, explaining the massive drop in activity. Even after filtering the solution twice, a contamination of 40 ppm Pd was found in the hydrogenation product, which is way above the levels reached by the magnetic catalyst (Table 4).

Since these results exclude excessive leaching as the cause for the constant drop of activity from run to run for nanocatalyst **2f**, the possible agglomeration of the Pd nanoparticles on the graphene surface of the support was investigated next. Comparing measurements of pulsed CO adsorption of pristine catalyst **2f** and the same catalyst after six runs reveal a slight increase in particle size from 2.7 nm to 3.1 nm and as a consequence thereof a drop in exposed surface from 121 to 113 m<sup>2</sup> g<sup>-1</sup> (Figure 1B). Also the dispersion of Pd declined from 47% to 42%. Although all these values are conclusive with an aggregation of the nanoparticles the differences seem to be too small to regard aggregation as the exclusive reason for the observed drop of activity. We therefore reason that a combination of deactivation modes such as aggregation of the Pd nanoparticles, small losses of entire nanocomposites, marginal leaching of Pd, and passivation of the surface by oxidation and/or substrate or product inhibition could be responsible, nevertheless, it should be noted that the activity of the catalyst at run 6 with a TOF of >2000/h is still impressively high.

### Additional surface functionalization

Apart from using additives like diethyl ether or coordinating ligands, functionalizing the carbon surface of the magnetic beads with coordinating groups could also stabilize the deposited Pd nanoparticles. Covalent functionalization of the Co/C particles **1** has been realized via diazonium chemistry.<sup>[21,25]</sup> Following this route phenyl (**3**), phenyl methanol (**4**), or 4-(2-aminoethyl)phenyl groups (**5**) were introduced to the carbon



**Scheme 2.** Surface functionalization of Co/C nanobeads and subsequent Pd deposition.

surface (Scheme 2). Although for each synthesis the same conditions and ratios of nanoparticles to reactants were used, the loading with functional groups was quite different in each case. By elemental microanalysis 0.05 mmol/g were determined for **3**, 0.1 mmol/g for **4**, and 0.015 mmol/g for **5** (Table 5). The subsequent deposition of Pd nanoparticles on the surface of the functionalized beads was again achieved by decomposition of Pd<sub>2</sub>(dba)<sub>3</sub>·CHCl<sub>3</sub> using microwave heating. The incorporation of Pd during synthesis was determined by ICP-OES. While for the unfunctionalized particles **2e** 96 % of the Pd was deposited on the magnetic supports, for Pd@Co/C-Ph (**6**) only 91 % and for Pd@Co/C-NH<sub>2</sub> (**8**) 88 % were detected. In the case of Pd@Co/C-OH (**7**), however, 100 % of the introduced Pd was found in the nanocomposites (Table 5).

**Table 5.** Surface functionalization of Co/C beads, subsequent Pd deposition, and application in the hydrogenation of *trans*-stilbene.

Entry	Particles	Loading FGs [mmol/g]	Pd incorporated [%] <sup>[b]</sup>	Loading Pd [mmol/g] <sup>[b]</sup>	TOF 1 <sup>st</sup> run [h <sup>-1</sup> ]	Pd retained after 4 runs [%] <sup>[b]</sup>
1	Pd@Co/C ( <b>2e</b> )	-	96	0.073	2015	92
2	Pd@Co/C-Ph ( <b>6</b> )	0.05	91	0.068	1120	91
3	Pd@Co/C-OH ( <b>7</b> )	0.1	100	0.075	345	100
4	Pd@Co/C-NH <sub>2</sub> ( <b>8</b> )	0.15	88	0.066	720	83

[a] Determined by elemental analysis. [b] Determined by ICP-OES analysis. [c] Determined by GC calibrated using internal standard.

These novel hybrid materials were then tested in the hydrogenation of *trans*-stilbene in <sup>i</sup>PrOH instead of an <sup>i</sup>PrOH/Et<sub>2</sub>O mixture to exclude competing stabilizing effects. The TOF in the first run dropped almost by half when using the phenyl-



functionalized nanobeads **6** instead of un-functionalized beads **2e**, both at 0.1 mol% Pd (Table 5). This might be caused by a blocking of the surface due to the additional covalent functionalization influencing the dispersion of the Pd nanobeads. Another drastic drop in activity was noticeable when changing to phenyl methanol instead of phenyl groups on the surface. The doubled loading as well as the additional coordinating groups apparently drastically influenced the catalytic activity of the deposited Pd nanoparticles. The nanoparticles with strong coordinating amine groups **8** showed an intermediate reactivity despite the even increased amount of functional groups on the surface.

Next, the recycling of each catalyst system was tested running each reaction for 40 min and determining the activity by GC measurements (Figure 4). For the un-functionalized nanoparticles **2e** the activity decreased slightly after the second run, similar as shown above for the same particles with a lower Pd content (**2f**, Figure 3B). The phenyl-modified particles **6** showed the same trend, however, at an overall reduced level of activity (Figure 4). Therefore, the additional Phenyl groups seem not to stabilize the Pd nanoparticles during the hydrogenation reaction and the washing steps. Similar effects were observed for amine-functionalized nanobeads **8**. The amine groups apparently do also not affect the stabilization of the Pd nanoparticles considerably. Interestingly, the Pd@Co/C-OH (**7**) nanoparticles showed a completely different trend, starting from a comparably low initial activity, which increased slightly from run to run indicating successful stabilization of the Pd nanoparticles by the hydroxyl groups. Also, 100 % of the initial Pd was measured for **7** after four runs, while for the other functionalized (**6**, **8**) and un-functionalized particles (**2e**) slightly reduced loadings were detected after four runs (Table 5). However, it might depend on the application if perfect stabilization overcompensates a drastically reduced initial activity. Pd@Co/C particles show after four runs still a higher activity as all nanoparticles with additional functionalization in the first run.

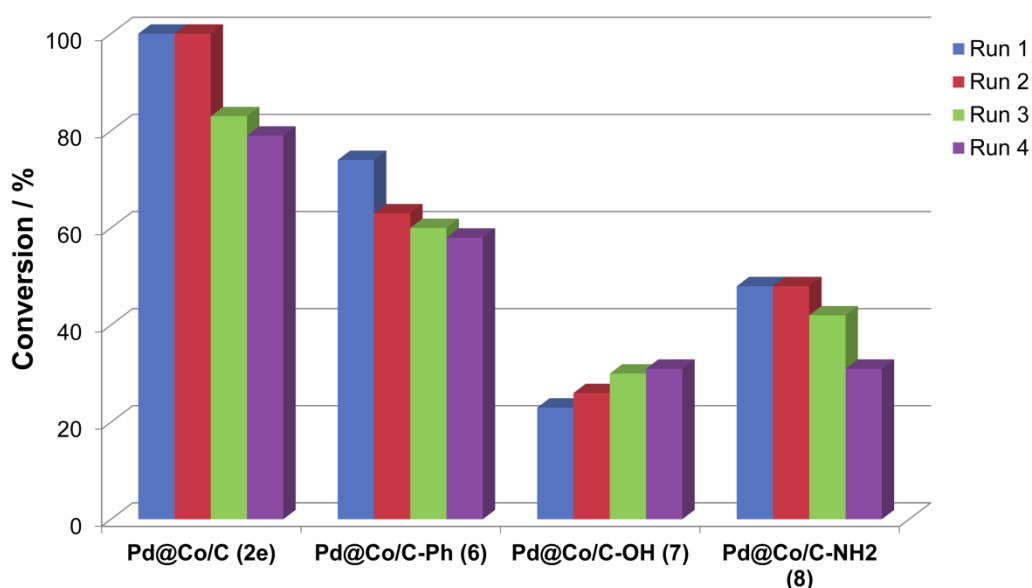


**Figure 4.** The conversion in the hydrogenation of *trans*-stilbene with Pd supported on functionalized and unfunctionalized Co/C nanoparticles was determined after 40 min reaction time. Each sample was tested in four consecutive runs.

### 5.3 Conclusion

We described the efficient and rapid microwave deposition of Pd nanoparticles on the surface of highly magnetic Co/C nanobeads starting from  $\text{Pd}_2(\text{dba})_3\cdot\text{CHCl}_3$  and the extensive characterization of the resulting hybrid material. This method proved to be superior to established routes which proceed via reduction of Pd(II) sources. We were able to demonstrate that the catalytic activity of the nanocomposites rises considerably with decreasing Pd loading. Extraordinary high turnover frequencies ( $3845\text{ h}^{-1}$ ) were achieved for the hydrogenation of *trans*-stilbene exceeding not only all literature reports for supported Pd nanoparticles, but also comparable Pd/C catalysts by far.

Furthermore, the catalytic activity was significantly enhanced adding 10 vol%  $\text{Et}_2\text{O}$ . The particles were rapidly separated by applying an external magnet and re-used for six consecutive runs. A noticeable loss of activity was observed after the second run with only marginal leaching of Pd and Co detectable. However, slight agglomeration of the Pd nanoparticles on the supports was determined by pulsed CO adsorption measurements. In order to stabilize the Pd nanobeads, various functional groups were introduced to the carbon surface of the Co/C supports. Phenyl methanol groups helped to preserve the activity over several runs with 100% Pd incorporation during synthesis and no loss of Pd during catalysis, however, with the drawback of decreased initial activity.

All these novel magnetic nanocatalysts are superior to the industry standard Pd/C in every relevant aspect. They feature a way higher initial activity, a much more convenient separation, better recycling, and less contamination of the products. On-going studies in our laboratory deal with the application of these nanocatalysts in cross coupling reactions, stabilization of the Pd nanoparticles by supported ionic liquids, and further scale up of the procedures.

## 5.4 Experimental Section

### Materials and methods

Carbon coated cobalt nanoparticles (Co/C, 20.5 m<sup>2</sup>/g, mean particle size  $\approx$  25 nm) were obtained from Turbobebeads Llc, Switzerland. Prior to use, they were washed five times for 24 h in a concentrated HCl (Merck, puriss) / deionized water (Millipore) mixture (1:1). Acid residuals were removed by washing with millipore water (5x) and the particles were dried at 50°C in a vacuum oven.<sup>[28]</sup> All other commercially available compounds were used as received. Magnetic nanobeads were dispersed using an ultrasound bath (Sonorex RK 255 H-R, Bandelin) and recovered with the aid of a neodymium based magnet (side length 12 mm). They were characterized by transmission electron microscopy (CM30 ST-Philips, LaB<sub>6</sub> cathode, operated at 300 kV point resolution  $\sim$  4 Å), energy-dispersive X-ray spectroscopy (EDAX / AMETEK GmbH, Apollo XL), X-ray powder diffraction (Huber G670 X-ray diffractometer, operated at Ge-monochromatized Cu-K $\alpha$  radiation,  $\lambda$  = 1.5406 Å), and inductively coupled plasma optical emission spectrometry (Spectro Analytical Instruments ICP Modula EOP,  $\lambda$  = 340 nm).

Metal dispersion was determined by CO pulse chemisorption technique on a Thermo TPDRO 1100 set-up equipped with a thermal conductivity detector. Prior to analyses, the samples (50-100 mg) were pretreated at 393 K under flowing He (20 cm<sup>3</sup> STP min<sup>-1</sup>) for 60 min, and reduced at 348 K under flowing 5 vol% H<sub>2</sub>/He (20 cm<sup>3</sup> STP min<sup>-1</sup>) for 30 min. Thereafter, 0.344 cm<sup>3</sup> of 1 vol% CO/He were pulsed over the catalyst bed every 4 min at 308 K. The interval between successive pulses was kept as short as possible to avoid desorption of CO. The palladium dispersion was calculated from the amount of CO chemisorbed, using an atomic surface density of 1.26 $\times$ 10<sup>19</sup> atoms m<sup>-2</sup> and an adsorption stoichiometry of Pd/CO = 2.<sup>[35]</sup>

<sup>1</sup>H NMR (400 MHz) spectra were recorded on a Bruker AC 400 spectrometer with CHCl<sub>3</sub> (7.26 ppm) as a standard. Gas chromatography was performed on a Fisons Instruments GC8000 equipped with a capillary (30 m x 250  $\mu$ m x 0.25  $\mu$ m) and flame ionization detector.

## Nomenclature

For the nanoparticles the nomenclature used in this chapter is as follows: Co/C for magnetic nanoparticles with cobalt core and carbon shell, Pd@Co/C for Pd nanoparticles deposited on the surface of Co/C nanobeads. Co/C-Ph for phenyl-functionalized Co/C beads, Co/C-OH for phenyl methanol-tagged Co/C nanoparticles, and Co/C-NH<sub>2</sub> for 4-(2-aminoethyl)phenyl groups introduced to the surface of Co/C beads. Pd@Co/C-Ph, Pd@Co/C-OH, and Pd@Co/C-NH<sub>2</sub> abbreviate the respective hybrid material with deposited Pd nanoparticles on the surface.

## Representative procedure for the microwave synthesis of Pd@Co/C catalyst (2f)

Co/C nanoparticles **1** (1.0 g, 7.8 wt% C), Pd<sub>2</sub>(dba)<sub>3</sub>·CHCl<sub>3</sub> (7.8 mg, 15 mmol) and dry toluene (5 mL) were introduced to a microwave vial under nitrogen atmosphere. The reaction mixture was sonicated in an ultrasonic bath for 10 min and then heated in a focused microwave oven to 110 °C for 2 min. The magnetic catalyst was recovered by an external magnet, the solution decanted, and the particles washed with CH<sub>2</sub>Cl<sub>2</sub> (5 x 5 mL). After drying under vacuum a loading of 14.6 μmol/g (97 %) was determined by ICP-OES.

## Synthesis of Pd@Co/C particles (2i) by reduction with sodium borohydride

Co/C nanoparticles **1** (100 mg, 7.8 wt% C) were introduced to a reaction tube, 1.0 ml of a freshly prepared Na<sub>2</sub>PdCl<sub>4</sub> solution (1.5 mM PdCl<sub>2</sub>, 3 mM NaCl) added, and the slurry sonicated for 10 min. Subsequently, NaBH<sub>4</sub> dissolved in 1.0 mL of H<sub>2</sub>O was added dropwise and the sonication continued for 10 min. The magnetic particles were separated with the aid of a magnet, washed with H<sub>2</sub>O (3 x 3 mL), MeOH (3 x 3 mL), and CH<sub>2</sub>Cl<sub>2</sub> (2 x 3 mL), and dried for several hours under vacuum. ICP-OES revealed a loading of 13 μmol/g (87%).

## Synthesis of Pd@Co/C particles (2j) by reduction with hydrogen

To a schlenk tube were introduced Co/C nanoparticles **1** (100 mg, 7.8 wt% C), 1.0 ml H<sub>2</sub>O, and 1.0 ml of a freshly prepared Na<sub>2</sub>PdCl<sub>4</sub> solution (1.5 mM PdCl<sub>2</sub>, 3 mM NaCl). The reaction mixture was stirred vigorously under 1 atm H<sub>2</sub> (balloon) for 30 min. The magnetic catalyst was collected with a magnet, the solution decanted, and the parti-

cles washed with H<sub>2</sub>O (3 x 3 mL), MeOH (3 x 3 mL), and CH<sub>2</sub>Cl<sub>2</sub> (2 x 3 mL). A loading of 12 µmol/g (81%) was measured by ICP-OES.

### General procedure for the hydrogenation using Pd@Co/C

To a schlenk tube Pd@Co/C nanoparticles **2** (0.1 mol% Pd, 0.5 µmol), substrate (0.5 mmol) and *i*PrOH (5 mL) were introduced. Dodecane (0.5 mmol) was added as internal standard and the slurry sonicated in an ultrasonic bath for 10 min. The tube was evaporated and flushed with H<sub>2</sub> several times followed by vigorous stirring under 1 atm H<sub>2</sub> (balloon). The progress of the reaction was monitored by GC separating the magnetic material by an external magnet before sampling. GC conditions:

**1,2-Diphenylethane:** 3 min at 140 °C, 20 °C/min to 300 °C; Retention time: Dodecane (3.53 min), 1,2-diphenylethane (7.70 min), trans-stilbene (9.42 min).

**Ethane-1,1-diylidibenzene:** 3 min at 140 °C, 16 °C/min to 300 °C; Retention time: Dodecane (3.50 min), ethane-1,1-diylidibenzene (6.24 min), ethene-1,1-diylidibenzene (6.45 min).

**Isobutylbenzene:** 3 min at 60 °C, 24 °C/min to 300 °C; Retention time: Isobutylbenzene (6.02 min), (2-methylprop-1-en-1-yl)benzene (6.70 min), Dodecane (7.81 min).

**Diphenylpropan-1-one:** 3min at 140 °C, 16 °C/min to 300; Retention time: Dodecane (3.43 min), 1,3-diphenylpropan-1-one (9.26 min), chalcone (10.30 min). The selective hydrogenation of the C=C double bond was checked by <sup>1</sup>H-NMR (400 MHz, CDCl<sub>3</sub>): δ = 8.00-7.95 (m, 2H), 7.59-7.54 (m, 1H), 7.50-7.43 (m, 2H), 7.39-7.18 (m, 5H), 3.34-3.29 (m, 2H), 3.12-3.06 (m, 2H).

**Methyl 3-phenylpropanoate:** 3 min at 100 °C, 20 °C/min to 300 °C; Retention time: Dodecane (5.92 min), methyl 3-phenylpropanoate (6.43 min), methyl cinnamate (7.39 min).

**1-Chloro-4-ethylbenzene:** 5 min at 100 °C, 25 °C/min to 300 °C; Retention time: 1-Chloro-4-ethylbenzene (4.51 min), 1-chloro-4-vinylbenzene (4.83 min), dodecane (7.09 min).

**1-Methoxy-4-ethylbenzene:** 5 min at 100 °C, 25 °C/min to 300 °C; Retention time: 1-Methoxy-4-ethylbenzene (5.62 min), 1-methoxy-4-vinylbenzene (6.18 min), dodecane (7.17 min).

**Bicyclo[2.2.1]heptane:** 3 min at 60 °C, 30 °C/min to 300 °C; Retention time: Norbornene (2.53 min), bicyclo[2.2.1]heptane (2.83 min), dodecane (7.19 min).

**Octane:** 8 min at 40 °C, 32 °C/min to 200 °C; Retention time: Oct-1-ene (5.95 min), (*E*)-oct-2-ene (6.73 min), octane (6.58 min), dodecane (12.76 min).

**Cyclooctane:** 3 min at 60 °C, 20 °C/min to 300 °C; Retention time: Cyclooctene (4.67 min), cyclooctane (4.92 min), dodecane (7.26 min).

**4-Aminotoluene:** 3 min at 70 °C, 13 °C/min to 200 °C; Retention time: 4-Aminotoluene (6.80 min), 4-nitrotoluene (8.69 min), dodecane (8.89 min).

### Large scale hydrogenation of *trans*-stilbene (Batch 1)

Pd@Co/C nanoparticles **2f** (500 mg, 0.2 wt% Pd, 14.6 mmol Pd/g), *trans*-stilbene (1.31 g, 7.28 mmol), and an *i*PrOH/Et<sub>2</sub>O mixture (73 mL, 9:1) were added to a 250 mL schlenk flask. Dodecane (826  $\mu$ L, 3.64 mmol) was added as internal standard, the slurry sonicated for 10 min, and then vigorously stirred under 1 atm H<sub>2</sub> (balloon) for 15 min until full conversion was detected by GC-analysis (TOF = 3722 h<sup>-1</sup>). The particles were separated by the addition of an external magnet, the solution decanted, and the particles re-dispersed in 70 mL of an *i*PrOH/Et<sub>2</sub>O mixture (9:1). After having repeated this procedure twice and washing once with CH<sub>2</sub>Cl<sub>2</sub>, the nanocatalyst was dried under vacuum for several hours and reused for the next run. Each consecutive run was stopped after 15 min and the conversion determined for this reaction time.

### Large scale hydrogenation of *trans*-stilbene (Batch 2)

A second batch was prepared using the exact same conditions and particles as for batch 1. Full conversion was detected after 15 min and the TOF (3801 h<sup>-1</sup>) was comparable to batch 1. In contrast to batch 1, however, the cycles 2-6 were also run to full conversion (no educt detected in the GC) omitting the internal standard. This allowed the determination of the Pd and Co contamination directly in the final products by ICE-OES after magnetic decantation and evaporation of the solvents.

### Hydrogenation of *trans*-stilbene using commercial Pd/C

To a 100 mL schlenk flask were added 34.9 mg of commercial Pd/C catalyst (Acros 1 wt%, 0.086 mmol/g, 3  $\mu$ mol), 540.8 mg *trans*-stilbene (3 mmol), 681  $\mu$ L dodecane (3 mmol), and 30 mL of *i*PrOH. The slurry was sonicated for 10 min and then stirred for 270 min at 1 atm H<sub>2</sub> (balloon). The conversion was detected by GC and the solution

filtered over a frit to separate the catalyst. The Pd/C was washed thoroughly with  $\text{CH}_2\text{Cl}_2$ , recovered from the frit, and dried under vacuum for several hours. The Pd/C was then reused for the next run adjusting the amount of substrate to compensate the loss of catalyst. After four runs only 19.4 mg (56%) of Pd/C was re-isolated.

### General procedure for the surface functionalization of the Co/C nanobeads

Covalent functionalization of the Co/C nanoparticles **1** was obtained by sonication of **1** (1.0 g), the respective aniline (1 mmol), and  $\text{HCl}_{\text{conc}}$  (1.0 mL) in 15 mL  $\text{H}_2\text{O}$  for 10 min. The dispersion was cooled in an ice bath before generation of the diazonium species *in situ* by the addition of a cooled solution of  $\text{NaNO}_2$  (104 mg, 1.5 mmol). To ensure complete conversion the slurry was further sonicated for 30 min at room temperature. The particles were collected by a magnet, the supernatant decanted, and the particles washed with  $\text{H}_2\text{O}$  (3 x 15 mL), acetone (3 x 15 mL), and  $\text{Et}_2\text{O}$  (2 x 15 mL).

### Phenyl functionalized Co/C nanoparticles (3)

Nanoparticles **3** were prepared according to the general procedure using 500 mg of Co/C beads **1**, 46  $\mu\text{L}$  (0.5 mmol) of aniline, 0.3 mL of  $\text{HCl}_{\text{conc}}$ , and 52 mg (0.75 mmol)  $\text{NaNO}_2$ .

**Elemental analysis:** C, 7.45; H, 0.10; N, 0.01. **Loading:** 0.05 mmol/g.

### Phenylmethanol functionalized Co/C nanoparticles (4)<sup>[25]</sup>

Nanoparticles **4** were prepared according to the general procedure using 1.5 g of Co/C beads **1**, 277.1 mg (2.25 mmol) of (4-aminophenyl)methanol, 0.9 mL of  $\text{HCl}_{\text{conc}}$ , and 238 mg (3.45 mmol)  $\text{NaNO}_2$ .

**Elemental analysis:** C, 7.96; H, 0.11; N, 0.19. **Loading:** 0.1 mmol/g.

### 4-(2-Aminoethyl)phenyl functionalized Co/C nanoparticles (5)

Nanoparticles **5** were prepared according to the general procedure using 1 g of Co/C beads **1**, 132  $\mu\text{L}$  (1 mmol) of 4-(2-aminoethyl)aniline, 1.0 mL of  $\text{HCl}_{\text{conc}}$ , and 104 mg (1.5 mmol)  $\text{NaNO}_2$ .

**Elemental analysis:** C, 9.02; H, 0.22; N, 0.23. **Loading:** 0.15 mmol/g.



### **Deposition of Pd onto functionalized nanoparticles**

Pd@Co/C-Ph (**6**), Pd@Co/C-PhOH (**7**), and Pd@Co/C-PhNH<sub>2</sub> (**8**) particles were prepared by Pd deposition in the microwave on **3**, **4**, or **5** according to the procedure for un-functionalized particles **2**.

➔ Please find supporting information including TEM pictures, EDX measurements, and XRD spectra on the enclosed CD.

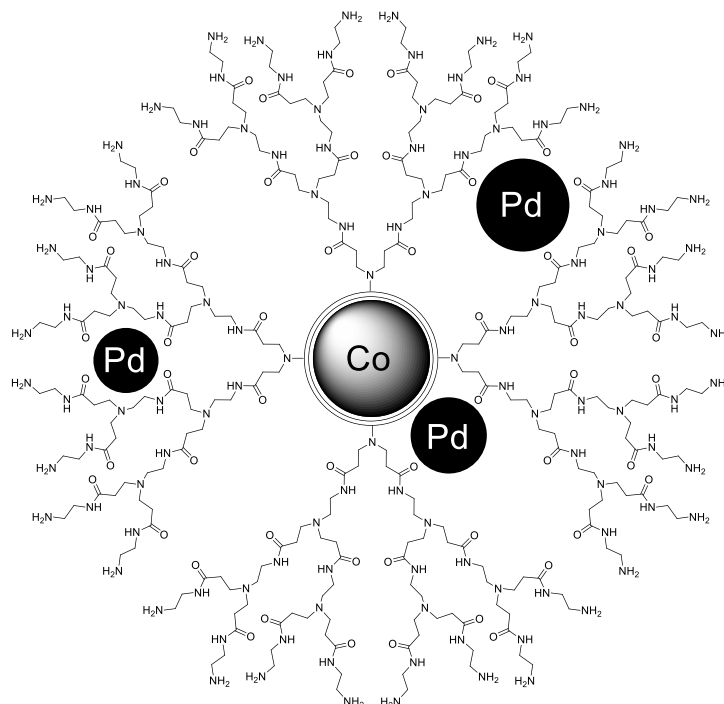
## 5.5 References

- [1] W. Bonrath, J. Medlock, J. Schutz, B. Wustenberg, T. Netscher in *Hydrogenation* (Ed.: I. Karam), InTech, **2012**.
- [2] a) P. T. Anastas, J. C. Warner, *Green chemistry. Theory and practice*, Oxford University Press, Oxford, New York, **1998**; b) P. T. Anastas, M. M. Kirchhoff, *Acc. Chem. Res.* **2002**, *35*, 686–694; c) R. A. Sheldon, *Chem. Commun.* **2008**, 3352.
- [3] a) C. E. Garrett, K. Prasad, *Adv. Synth. Catal.* **2004**, *346*, 889–900; b) V. L. Budarin, P. S. Shuttleworth, J. H. Clark, R. Luque, *Curr. Org. Synth.* **2010**, *7*, 614–627.
- [4] a) R. A. Sheldon, H. van Bekkum, *Fine chemicals through heterogeneous catalysis*, Wiley-VCH, Weinheim, New York, **2001**; c) K. V. S. Ranganath, F. Glorius, *Catal. Sci. Technol.* **2011**, *1*, 13–22; b) R. A. Sheldon, *J. Environ. Monit.* **2008**, *10*, 406.
- [5] V. Polshettiwar, R. Luque, A. Fihri, H. Zhu, M. Bouhrara, J.-M. Basset, *Chem. Rev.* **2011**, *111*, 3036–3075.
- [6] a) S. Shylesh, V. Schünemann, W. R. Thiel, *Angew. Chem., Int. Ed.* **2010**, *49*, 3428–3459; b) L. N. Lewis, *Chem. Rev.* **1993**, *93*, 2693–2730; c) A. Roucoux, J. Schulz, H. Patin, *Chem. Rev.* **2002**, *102*, 3757–3778.
- [7] a) Y. Li, X. M. Hong, D. M. Collard, M. A. El-Sayed, *Org. Lett.* **2000**, *2*, 2385–2388; b) R. Narayanan, M. A. El-Sayed, *J. Am. Chem. Soc.* **2003**, *125*, 8340–8347; c) B. J. Gallon, R. W. Kojima, R. B. Kaner, P. L. Diaconescu, *Angew. Chem. Int. Ed.* **2007**, *46*, 7251–7254; d) Y. Mei, Y. Lu, F. Polzer, M. Ballauff, M. Drechsler, *Chem. Mater.* **2007**, *19*, 1062–1069; e) K. Mennecke, A. Kirschning, *Beilstein J. Org. Chem.* **2009**, *5*.
- [8] a) R. B. Bedford, U. G. Singh, R. I. Walton, R. T. Williams, S. A. Davis, *Chem. Mater.* **2005**, *17*, 701–707; b) C.-H. Tu, A.-Q. Wang, M.-Y. Zheng, X.-D. Wang, T. Zhang, *Appl. Catal. A-Gen.* **2006**, *297*, 40–47; c) N. Erathodiyil, S. Ooi, A. M. Seayad, Y. Han, S. S. Lee, J. Y. Ying, *Chem. Eur. J.* **2008**, *14*, 3118–3125; d) S. Jana, B. Dutta, R. Bera, S. Koner, *Inorg. Chem.* **2008**, *47*, 5512–5520.
- [9] a) L. Djakovitch, K. Koehler, *J. Am. Chem. Soc.* **2001**, *123*, 5990–5999; b) M. Dams, *J. Catal.* **2002**, *209*, 225–236; c) S. Mandal, D. Roy, R. V. Chaudhari, M. Sastry, *Chem. Mater.* **2004**, *16*, 3714–3724.
- [10] a) G. Marck, A. Villiger, R. Buchecker, *Tetrahedron Lett.* **1994**, *35*, 3277–3280; b) S. H. Joo, S. J. Choi, I. Oh, J. Kwak, Z. Liu, O. Terasaki, R. Ryoo, *Nature* **2001**, *412*, 169–172; c) K. Köhler, R. G. Heidenreich, J. G. E. Krauter, J. Pietsch, *Chem. Eur. J.* **2002**, *8*, 622–631; d) J. Huang, D. Wang, H. Hou, T. You, *Adv. Funct. Mater.* **2008**, *18*, 441–448; e) N. N. Kariuki, X. Wang, J. R. Mawdsley, M. S. Ferrandon, S. G. Niyogi, J. T. Vaughey, D. J. Myers, *Chem. Mater.* **2010**, *22*, 4144–4152.
- [11] a) G. M. Scheuermann, L. Rumi, P. Steurer, W. Bannwarth, R. Mülhaupt, *J. Am. Chem. Soc.* **2009**, *131*, 8262–8270; d) Y. Li, X. Fan, J. Qi, J. Ji, S. Wang, G. Zhang, F. Zhang, *Nano Res.* **2010**, *3*, 429–437; c) N. Li, Z. Wang, K. Zhao, Z. Shi, S. Xu, Z. Gu, *J. Nanosci. Nanotech.* **2010**, *10*, 6748–6751; d) A. R. Siamaki, Khder, Abd El Rahman S., V. Abdelsayed, M. S. El-Shall, B. F. Gupton, *J. Catal.* **2011**, *279*, 1–11;.
- [12] a) X. Pan, Z. Fan, W. Chen, Y. Ding, H. Luo, X. Bao, *Nat Mater* **2007**, *6*, 507–511; b) M. Rueping, R. M. Koenigs, R. Borrmann, J. Zoller, T. E. Weirich, J. Mayer, *Chem. Mater.* **2011**, *23*, 2008–2010.
- [13] Y. S. Chun, J. Y. Shin, C. E. Song, S.-g. Lee, *Chem. Commun.* **2008**, 942.
- [14] M. Cano, A. Benito, W. K. Maser, E. P. Urriolabeitia, *Carbon* **2011**, *49*, 652–658.
- [15] a) V. S. Coker, J. A. Bennett, N. D. Telling, T. Henkel, J. M. Charnock, G. van der Laan, R. A. D. Patrick, C. I. Pearce, R. S. Cutting, I. J. Shannon, J. Wood, E. Arenholz, I. C. Lyon, J. R. Lloyd, *ACS Nano* **2010**, *4*, 2577–2584; b) M. Zhu, G. Diao, *J. Phys. Chem. C* **2011**, *115*, 24743–24749; c) Q. Du, W. Zhang, H. Ma, J. Zheng, B. Zhou, Y. Li, *Tetrahedron* **2012**, *68*, 3577–3584.
- [16] a) A. J. Amali, R. K. Rana, *Green Chem.* **2009**, *11*, 1781; b) J.-Y. Shin, Y.-R. Jung, S.-J. Kim, S.-g. Lee, *Bull. Korean Chem. Soc.* **2011**, *32*, 3105–3108.

- [17] S. Chandra, S. Bag, P. Das, D. Bhattacharya, P. Pramanik, *Chem. Phys. Lett.* **2012**, 519–520, 59–63.
- [18] J. Hu, Y. Wang, M. Han, Y. Zhou, X. Jiang, P. Sun, *Catal. Sci. Technol.* **2012**, 2, 2332.
- [19] S. C. Tsang, V. Caps, I. Paraskevas, D. Chadwick, D. Thompson, *Angew. Chem. Int. Ed.* **2004**, 43, 5645–5649.
- [20] A.-H. Lu, W. Schmidt, N. Matoussevitch, H. Bönemann, B. Spliethoff, B. Tesche, E. Bill, W. Kiefer, F. Schüth, *Angew. Chem. Int. Ed.* **2004**, 43, 4303–4306.
- [21] R. N. Grass, E. K. Athanassiou, W. J. Stark, *Angew. Chem. Int. Ed.* **2007**, 46, 4909–4912.
- [22] A. K. Tucker-Schwartz, R. L. Garrell, *Chem. Eur. J.* **2010**, 16, 12718–12726.
- [23] N. Osterwalder, C. Capello, K. Hungerbühler, W. J. Stark, *J. Nanopart. Res.* **2006**, 8, 1–9.
- [24] Q. M. Kainz, A. Schätz, A. Zöpfl, W. J. Stark, O. Reiser, *Chem. Mater.* **2011**, 23, 3606–3613.
- [25] A. Schätz, R. N. Grass, W. J. Stark, O. Reiser, *Chem. Eur. J.* **2008**, 14, 8262–8266.
- [26] a) A. Schätz, O. Reiser, W. J. Stark, *Chem. Eur. J.* **2010**, 16, 8950–8967; b) S. Wittmann, A. Schätz, R. N. Grass, W. J. Stark, O. Reiser, *Angew. Chem. Int. Ed.* **2010**, 49, 1867–1870; c) M. Keller, V. Collière, O. Reiser, A.-M. Caminade, J.-P. Majoral, A. Ouali, *Angew. Chem.* **2013**, 125, 3714–3717; d) M. Keller, A. Perrier, R. Linhardt, L. Travers, S. Wittmann, A.-M. Caminade, J.-P. Majoral, O. Reiser, A. Ouali, *Adv. Synth. Catal.* **2013**, 355, 1748–1754.
- [27] a) F. M. Koehler, M. Rossier, M. Waelle, E. K. Athanassiou, L. K. Limbach, R. N. Grass, D. Günther, W. J. Stark, *Chem. Commun.* **2009**, 4862–4864; b) M. Rossier, F. M. Koehler, E. K. Athanassiou, R. N. Grass, M. Waelle, K. Birbaum, D. Günther, W. J. Stark, *Ind. Eng. Chem. Res.* **2010**, 49, 9355–9362; c) M. Rossier, A. Schätz, E. K. Athanassiou, R. N. Grass, W. J. Stark, *Chem. Eng. J.* **2011**, 175, 244–250; d) R. Fuhrer, I. K. Herrmann, E. K. Athanassiou, R. N. Grass, W. J. Stark, *Langmuir* **2011**, 27, 1924–1929; e) M. Rossier, M. Schreier, U. Krebs, B. Aeschlimann, R. Fuhrer, M. Zeltner, R. N. Grass, D. Günther, W. J. Stark, *Sep. Purif. Technol.* **2012**, 96, 68–74; f) Q. M. Kainz, A. Späth, S. Weiss, T. D. Michl, A. Schätz, W. J. Stark, B. König, O. Reiser, *ChemistryOpen* **2012**, 1, 125–129.
- [28] M. Rossier, F. M. Koehler, E. K. Athanassiou, R. N. Grass, B. Aeschlimann, D. Günther, W. J. Stark, *J. Mater. Chem.* **2009**, 19, 8239–8243.
- [29] a) I. K. Herrmann, M. Urner, F. M. Koehler, M. Hasler, B. Roth-Z'Graggen, R. N. Grass, U. Ziegler, B. Beck-Schimmer, W. J. Stark, *Small* **2010**, 6, 1388–1392; b) I. K. Herrmann, R. E. Bernabei, M. Urner, R. N. Grass, B. Beck-Schimmer, W. J. Stark, *Nephrol. Dial. Transpl.* **2011**, 26, 2948–2954.
- [30] A. Schätz, R. N. Grass, Q. Kainz, W. J. Stark, O. Reiser, *Chem. Mater.* **2010**, 22, 305–310.
- [31] a) A. Schätz, T. R. Long, R. N. Grass, W. J. Stark, P. R. Hanson, O. Reiser, *Adv. Funct. Mater.* **2010**, 20, 4323–4328; b) P. K. Maity, A. Rolfe, T. B. Samarakoon, S. Faisal, R. D. Kurtz, T. R. Long, A. Schätz, D. L. Flynn, R. N. Grass, W. J. Stark, O. Reiser, P. R. Hanson, *Org. Lett.* **2011**, 13, 8–10; c) P. K. Maity, Q. M. Kainz, S. Faisal, A. Rolfe, T. B. Samarakoon, F. Z. Basha, O. Reiser, P. R. Hanson, *Chem. Commun.* **2011**, 47, 12524–12526; d) A. Schätz, M. Zeltner, T. D. Michl, M. Rossier, R. Fuhrer, W. J. Stark, *Chem. Eur. J.* **2011**, 17, 10566–10573; e) Q. M. Kainz, R. Linhardt, P. K. Maity, P. R. Hanson, O. Reiser, *ChemSusChem* **2013**, 6, 721–729; f) Q. M. Kainz, M. Zeltner, M. Rossier, W. J. Stark, O. Reiser, *Chem. Eur. J.* **2013**, 19, 10038–10045.
- [32] a) D. Kim, S. Hu, P. Tarakeshwar, K. S. Kim, J. M. Lisy, *J. Phys. Chem. A* **2003**, 107, 1228–1238; b) A. Balanta, C. Godard, C. Claver, *Chem. Soc. Rev.* **2011**, 40, 4973.
- [33] S. Wittmann, J.-P. Majoral, R. N. Grass, W. J. Stark, O. Reiser, *Green Proc. Synth.* **2012**, 1, 275–279.
- [34] See supporting information.
- [35] G. Fagherazzi, P. Canton, P. Riello, N. Pernicone, F. Pinna, M. Battagliarin, *Langmuir* **2000**, 16, 4539–4546.



## 6. Towards Magnetic Dendrimer- and Polymer-Encapsulated Palladium Nanoparticles



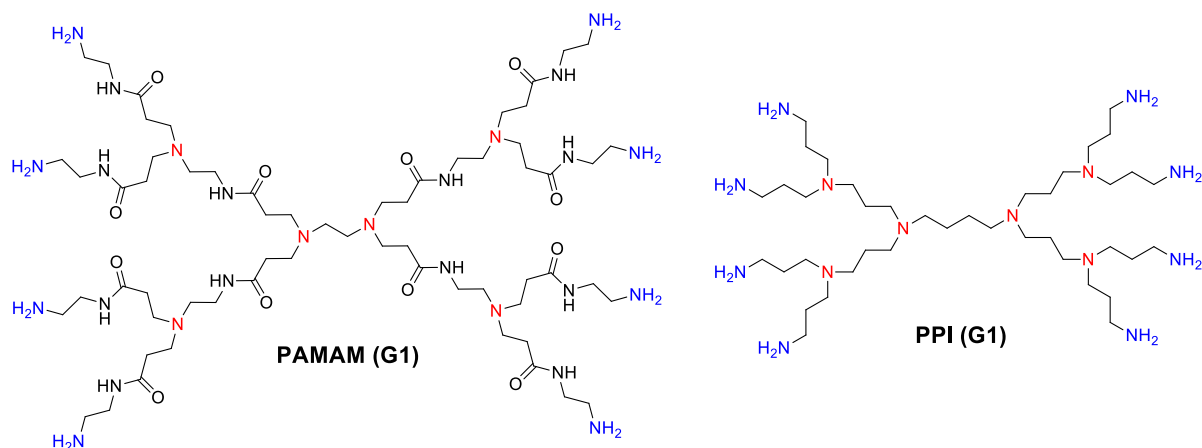
Dendrimers and polymers are covalently or non-covalently attached to the surface of highly magnetic carbon-coated cobalt (Co/C) nanoparticles by surface-initiated synthesis or physisorption. The organic coatings promote the dispersion stability of the magnetic nanoparticles in polar solvents due to their high content of amines. The loading of the particles with dendrimers and polymers is assessed by thermogravimetric analysis and elemental microanalysis. The magnetic hybrid materials are furthermore tested as templates for the synthesis of stabilized Pd nanoparticles. However, the catalytic activity in the hydrogenation reaction still needs to be improved to be competitive.

## 6.1 Introduction

The synthesis of small (1-10 nm) and monodisperse transition-metal nanoparticles is of high importance for a plethora of applications, especially in the field of catalysis.<sup>[1]</sup> Since metal nanoparticles tend to aggregate stabilizing agents like polymers, surfactants, or ionic liquids, have to be used to preserve the geometry and activity of the nanoparticles. Another strategy to prevent their aggregation is the synthesis of metal nanoparticles on inorganic supports, e.g. carbon materials, silica, or alumina.<sup>[2]</sup> In most cases, however, stabilizers and supports passivate extended parts of the surface of the metal nanoparticles through strong surface interactions. Therefore, ideal stabilizing agents would cage the metal nanoparticles to control their size and prevent agglomeration and at the same time be sufficiently porous to allow access to the surface of the metal nanobeads.<sup>[3]</sup>

Initiated by the first reports of Crooks<sup>[4]</sup> and Thomalia<sup>[5]</sup> in 1998, dendrimers gained rising attention as advantageous templates for the synthesis of metal nanoparticles. Dendrimer-encapsulated nanoparticles (DENs) have been extensively reviewed in the last decade.<sup>[3,6,7]</sup> There are several benefits arising from the unique structure of the dendrimers: (1) due to advanced methods the host dendrimers can be synthesized in a nearly uniform structure and composition, resulting in likewise well-defined nanoparticle guests; (2) the size of the nanoparticle replicas can be easily tuned by varying the generation of the dendrimer template; (3) the nanoparticles generated in the cavities of the dendrimers are mainly stabilized by steric effects leaving a large extent of the their surface unpassivated and therefore available for catalytic reactions; (4) the terminal groups of the dendrimers can be functionalized to tailor the solubility of the nanocomposites, or used as handles in order to tether the nanocomposites to inorganic or polymeric supports; (5) reports have shown,<sup>[8]</sup> that the pores within the dendrimers can be tuned to enable a size selective catalysis by controlling the access of substrates to the encaged nanoparticles.

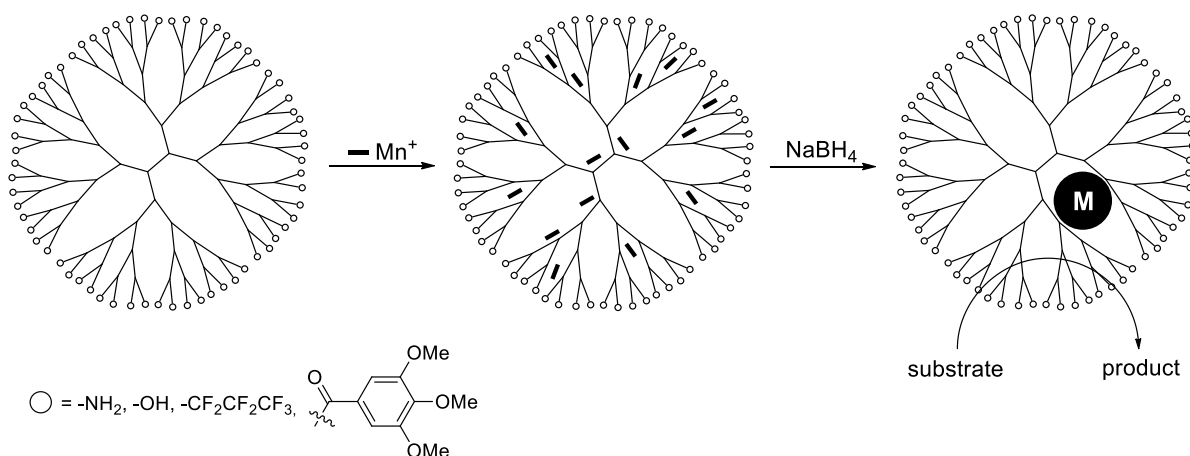
Usually, commercially available poly(amidoamine) (PAMAM)<sup>[9]</sup> or poly(propylene imine) (PPI)<sup>[10]</sup> dendrimers (Figure 1) are applied as templates for the synthesis DENs. The number of functional groups on the surface of the dendrimers grows exponentially as a function of the dendrimer generation. Likewise, the steric crowding increases with the generation leading to drastic geometrical alterations: While generation one (G1) PAMAM dendrimers exhibit an expanded “open” configuration, G4 can be regarded as a sponge-like spheroid, and G8 as an impermeable ball.<sup>[6]</sup>



**Scheme 1.** The first generation of PAMAM and PPI dendrimers, each featuring 8 terminal primary amines (blue) and 6 internal tertiary amines (red).

There are some inherent differences between PAMAM and PPI dendrimers which have to be considered to select the appropriate dendrimer template. PAMAM dendrimers are considerably larger than PPI dendrimers at the same generation (4.5 vs. 2.8 nm for G4, respectively),<sup>[11]</sup> which also influences the size of the particular cavities inside the dendrimers. Also, both dendrimers show quite different thermal stabilities. PAMAM dendrimers undergo retro-Michael additions at temperatures higher than about 100 °C, while G4 PPI dendrimers are stable up to 470 °C.<sup>[12]</sup> At higher generations, both dendrimers can entrap nanoscopic guest molecules due to their three dimensional structure and their various internal and external functional groups.<sup>[13]</sup> Driving forces for the internalization of the guest molecules are usually based on complexation reactions, electrostatic interactions, covalent bond formation, or a combination of those.

In order to synthesize DENs, metal ions are internalized into the dendrimers forming *intradendrimer* complexes (Scheme 2). To exclude *interdendrimer* complexes,<sup>[14]</sup> the primary amines of amine-terminated dendrimers can be exclusively protonated since they are more basic than the interior tertiary amines ( $pK_a = 9.5$  and  $5.5$  for PAMAM dendrimers, respectively). Subsequent reduction by stirring with an aqueous borohydride solution yielded Pd nanoparticles templated by G4 PAMAM dendrimers.<sup>[15]</sup> Spectroscopic studies by Crooks et al.<sup>[16]</sup> revealed that the applied  $K_2PdCl_4$  complex is hydrolyzed to  $PdCl_3(H_2O)^-$  followed by covalent attachment to tertiary amines within the dendrimers. Alternatively, different end group functionalities can be introduced, e.g. hydroxyl groups,<sup>[4]</sup> per-fluorinated chains,<sup>[17,18]</sup> or triethoxybenzoic acid moieties,<sup>[19]</sup> to not only passivate the surface of the dendrimers, but



**Scheme 2.** Synthesis of dendrimer-encapsulated nanoparticles (DENs) by impregnation of dendrimers with metal ions and subsequent reduction to zerovalent nanoparticles.

to tune the solubility of the final nanocomposite in diverse solvents. Palladium DENs were successfully applied for hydrogenation reactions<sup>[20]</sup> as well as Heck-<sup>[18,21]</sup> and Suzuki-couplings<sup>[22]</sup> at high TOFs. Also, the size-selective conversion of the substrates was achieved depending on the dendrimer generation and type of end group, taking advantage of both, the unique characteristics of the dendrimers and the high catalytic activity of metal nanoparticles.<sup>[8,23]</sup>

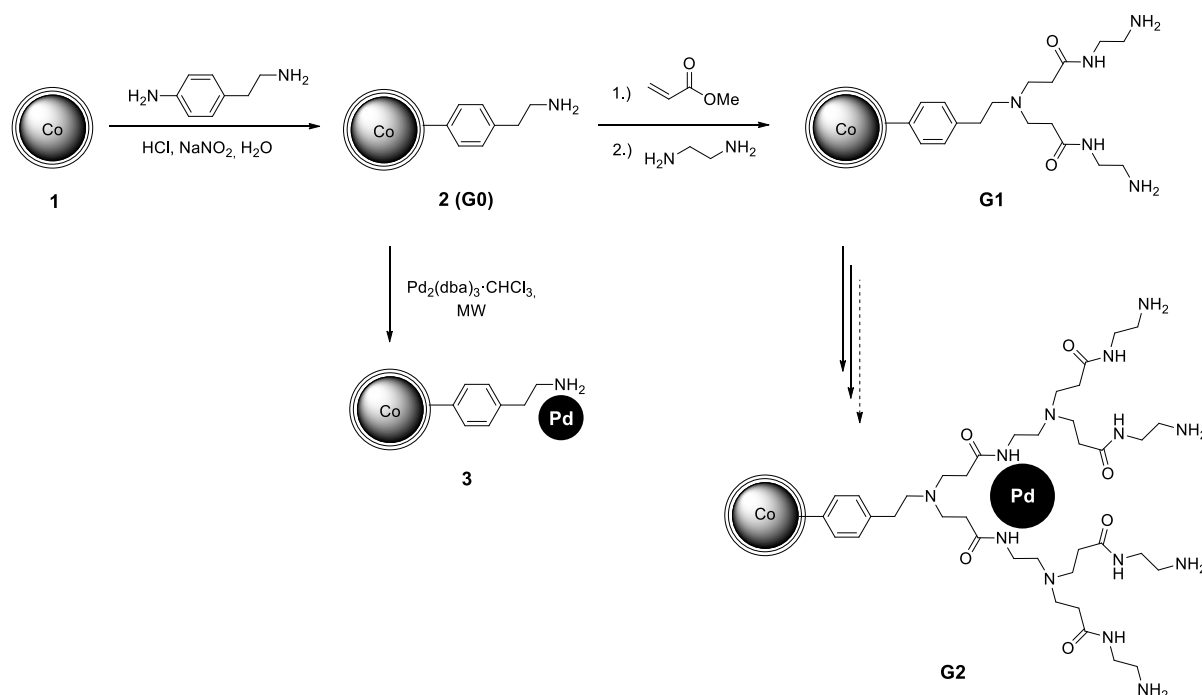
It has been shown, that Pd nanoparticles can be synthesized on the surface of carbon-coated cobalt (Co/C) or iron (Fe/C) nanoparticles (Chapter 5). The introduction of PAMAM dendrons to the surface and subsequent synthesis of Pd nanoparticles in the supported dendrons would lead to a powerful hybrid nanomaterial with all the advantages inherited from its components. The highly magnetic core would allow for rapid removal of the nanocomposite from reaction mixtures even at high loadings. The dendrimer would provide efficient stabilization of Co/C dispersions and additionally stabilize the Pd nanoparticles without surface passivation. Also, the Pd nanoparticles enable a high catalytic activity due to their small size accompanied with a high surface to volume ratio. Moreover, the dendrimer, in synergy with the incorporated Pd nanoparticles, could make a size-selective synthesis possible. Having the PAMAM-coated magnetic nanoparticles in hand would also open possibilities for the application as magnetic drug carriers, since PAMAM dendrimers are known to reversibly internalize acidic drug molecules.<sup>[24]</sup>



## 6.2 Magnetic Dendrimer-Encapsulated Nanoparticles

There are basically two feasible pathways to introduce PAMAM dendrimers to Co/C nanoparticles: the immobilization of linker groups followed by a stepwise growing of PAMAM dendrons or the grafting of entire dendrons. The step-wise synthesis of PAMAM dendrons on magnetic particles has the advantage of easy purification after each step by operationally simple magnetic decantation. Silica-coated magnetite (Si@Fe<sub>3</sub>O<sub>4</sub>) particles primed with (3-aminopropyl)triethoxysilane (APTMS) have already been reported in the literature as scaffolds for the surface-initiated PAMAM synthesis.<sup>[25]</sup> However, a high excess of reagents (up to 125 equiv.) and very long reaction times of 5 days for each step were needed. This is especially problematic since two steps are necessary for each dendrimer generation and only high generations provide internal cavities necessary to template metal nanoparticles.

In order to establish a similar coating on the highly magnetic Co/C beads, we first covalently attached linkers bearing amine groups to the surface. Therefore, 4-(2-aminoethyl)aniline was converted to the corresponding diazonium salt, which subsequently reacted with the carbon surface of pristine Co/C nanobeads (**1**) upon sonification in an ultrasonic bath (Scheme 3).<sup>[26]</sup> The loading with amino groups was determined by elemental microanalysis as 0.15 mmol/g. Back titration, however, indica-

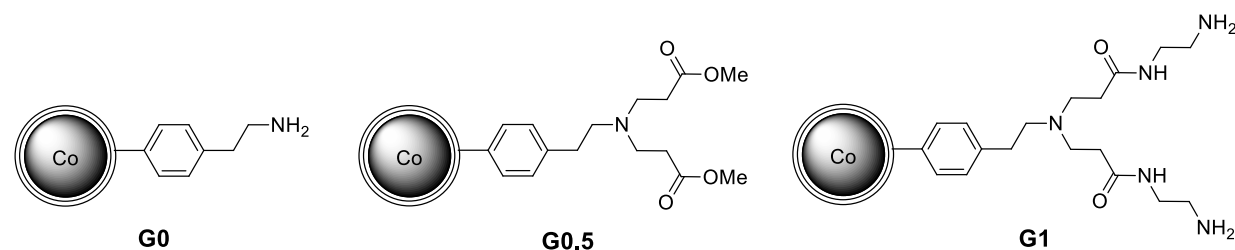


**Scheme 3.** Synthesis of PAMAM dendrons on the surface of Co/C nanobeads and the proposed precipitation of Pd nanoparticles in the hybrid material.

ted a slightly higher content of amino groups of 0.22 mmol/g. For the Si@Fe<sub>3</sub>O<sub>4</sub> particles a slightly higher amine loading of 0.26 mmol/g is reported.<sup>[25]</sup>

The amino-functionalized nanoparticles **2** (G0) have already been used as stabilizers for Pd nanoparticles with moderate success (Chapter 5). The Pd@Co/C-NH<sub>2</sub> particles (**3**) exhibited a lower activity when compared to Pd@Co/C nanobeads without noticeable improvements in the stabilization of the Pd nanobeads. Hence, higher generations were synthesized on the amino-primed surface by Michael-addition of methyl acrylate followed by amidation of the resulting ester groups by stirring with ethylenediamine (Scheme 3). Five days of reaction time for each step, as reported in the literature,<sup>[25]</sup> would be unacceptable for the buildup of high dendrimer generations. Fortunately preliminary results showed, that the loading is not improved upon heating for three days instead of 20 h. Therefore, both reactions were carried out by stirring at 50 °C for 20 h. Dendrons up to generation two were synthesized on the particles by repetition of these two steps and the loading quantitatively analyzed by a combination of elemental analysis, back titration of amino-groups,<sup>[27]</sup> and thermogravimetric analysis (TGA) under nitrogen atmosphere (Table 1).

**Table 1.** Quantitative analysis of PAMAM dendrons (G0-G2) synthesized on Co/C nanoparticles.



Dendrimer generation	Max loading [mmol/g]	Elemental analysis [mmol/g]	Titration <sup>[a]</sup> [mmol/g]	TGA <sup>[b]</sup> [Δ wt%]	TGA [mmol/g]
G0	0.1 - 0.15 <sup>[c]</sup>	0.15	0.22	0.7	0.06
G0.5	0.29 <sup>[d]</sup>	0.10	-	1.4	0.09
G1	0.29 <sup>[d]</sup>	n.d.	0.18	1.2	-
G2	0.54 <sup>[d]</sup>	n.d.	0.22	2.1	-

[a] Back titration of basic groups within the hybrid material. [b] Weight loss under nitrogen at 500 °C in relation to unmodified Co/C nanoparticles **1**. [c] Variations from batch to batch. [d] Calculated on a loading of 0.15 mmol/g at G0.

Already at G0 the three analysis methods produced completely different results. The maximum loading is based on reference values obtained for the functionalization of the carbon-coated metal nanobeads with various diazonium salts.<sup>[28,29]</sup> In this respect, the value obtained from elemental analysis (0.15 mmol/g) seems to be reasonable, while the slightly higher value measured by back titration, which corresponds to a higher amount of basic groups, might be distorted by the influence of the carbon surface and functionalities thereon. A second titration confirmed the result of the first one. The data obtained from TGA, however, only shows a marginal difference in weight-loss upon heating between the reference particles **1** and the amino-functionalized beads **2**, which results in a correspondingly low loading.<sup>[30]</sup>

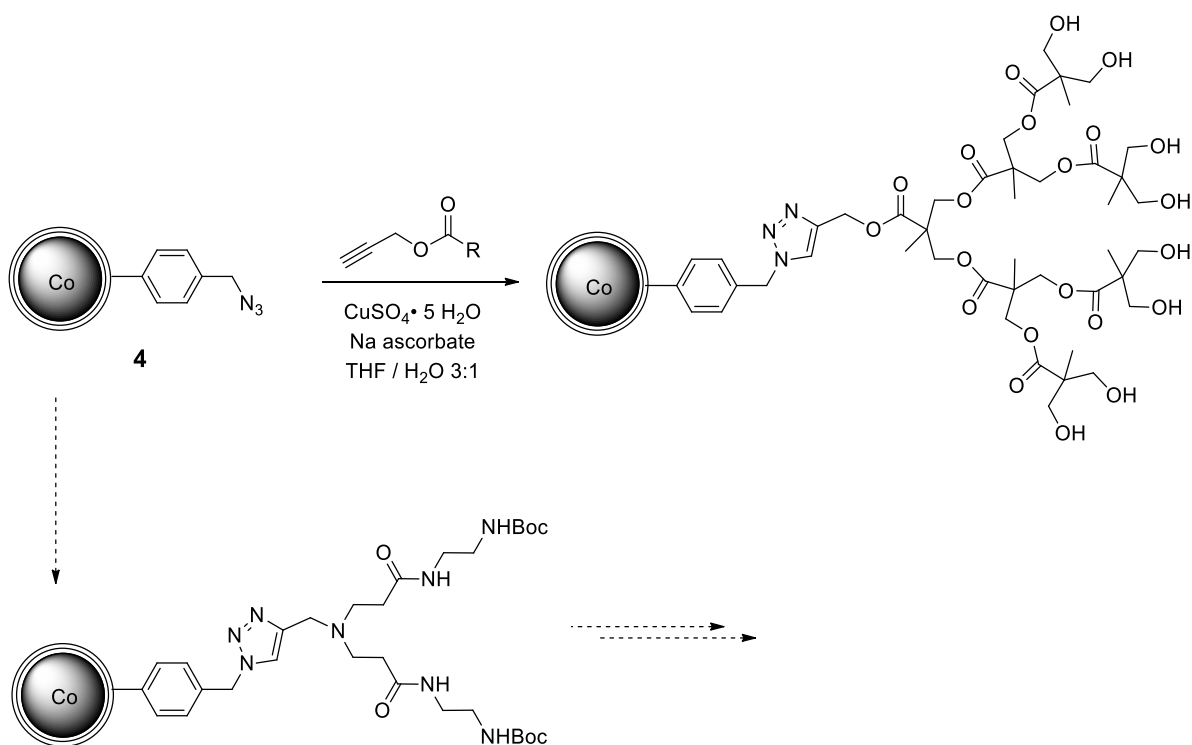
For G0.5 carbon analysis (0.1 mmol/g) revealed, that only one third of the potential methoxy ester terminated branches were introduced. This implies that a large proportion of amino groups has not reacted at all. In this case, however, the data obtained from TGA (0.09 mmol/g) is conclusively indicating an increase of organic material on the surface of the Co/C beads.<sup>[30]</sup> Titration of G0.5 was not carried out, since only primary amino groups were converted into secondary and tertiary amines, while no additional amino groups were introduced.

For G1 and G2 conclusive examination by elemental microanalysis was not viable any longer due to the plethora of synthetic steps and functional groups present. Titration revealed a content of basic groups (amines) of 0.18 mmol/g for G1 and 0.22 mmol/g for G2. However, also internal tertiary amines and secondary amines resulting from incomplete reactions are protonated under the strongly acidic conditions of the titration. Therefore, the number of end groups (primary amines) cannot conclusively be derived from these measurements. Moreover, the values obtained by titration of G1 and G2 only marginally differ from G0. The TGA indicated a lower loading with organic content for G1 when compared with G0.5, which would indicate a loss of branches instead of the addition of the next half-generation.<sup>[30]</sup> While the data for G2 indicates again an increase in organic coating, the unexpected variation of the data for G1 renders unambiguous calculations of the loading impossible.

All in all, the controlled synthesis of PAMAM dendrimers on the surface of Co/C nanoparticles failed to produce satisfying results. Despite the massive excess of methyl acrylate (50 equiv.) and ethylenediamine (125 equiv.) used, only low yields of 30% and below were determined for each step. Additionally, the data obtained from the analytical methods was not conclusive at all. This prevented a controlled

synthesis of high generation dendrons (G4-G6), which would have been necessary for templating metal nanoparticles.

An alternative synthetic approach would be the grafting of complete dendrons synthesized in solution. This strategy would allow the use of established solution phase analytical techniques, e.g. NMR and mass spectrometric analysis. The grafting of alkyne-tagged dendrons via copper-catalyzed cycloaddition ("click"-reaction)<sup>[31]</sup> could be a feasible way to introduce higher generation dendrons to the surface of azide-tagged Co/C nanoparticles (**4**), which are accessible in a two-step synthesis.<sup>[28]</sup> A similar strategy has been successfully applied by our group for the immobilization of ester-based dendrimers up to generation three (Scheme 4).<sup>[32]</sup> PAMAM dendrimers bearing an alkyne moiety at the focal point are known from literature up to generation two.<sup>[33]</sup> However, during the click reaction, the primary amines at the periphery have to be protected by *tert*-butyloxycarbonyl (Boc) groups to prevent complexation of the catalytic copper. Moreover, the synthesis of higher generation dendrimers, their subsequent immobilization, and un-protection requires many synthetic steps (11 steps for G4) including potential purification from monomers and dendrimers with defects after each step. Generally, the grafting of large molecules also suffers from reduced yields due to steric repulsion, which can also be an issue for the immobilization of tree-shaped dendrons.

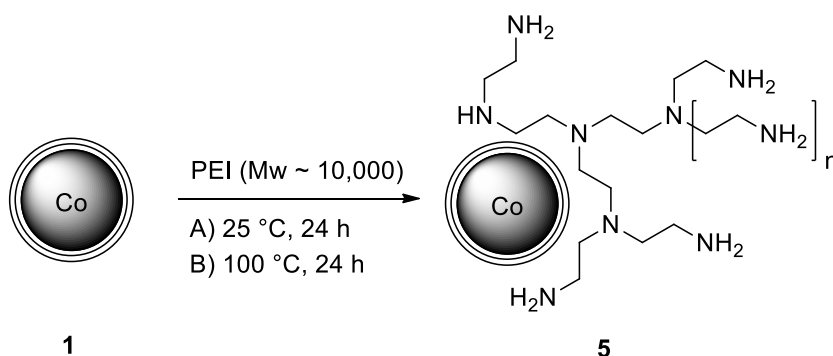


**Scheme 4.** Grafting of ester-based or Boc-protected dendrons on azide-modified Co/C nanoparticles.

### 6.3 Magnetic Polymer-Encapsulated Nanoparticles

A potentially more straightforward alternative to the grafting of complex dendrimers to the surface of magnetic nanoparticles is the grafting of polymers to the surface of magnetic nanoparticles or the surface-initiated polymerization. One polymer, which resembles the nature of the PAMAM and PPI dendrimers in respect to functional groups and polarity, is polyethylene imine (PEI). It contains primary, secondary, and tertiary amine groups in a ratio of 25/50/25 and is commercially available in various molecular weights. Moreover, it is known from literature, that Pd nanoparticles can be synthesized in PEI and are efficiently stabilized by the polymer branches.<sup>[34,35]</sup> In 2009 Stark et al. demonstrated the adsorption of PEI on Fe/C nanoparticles (**1**) with the aim of introducing a high amount of free amine groups to the surface for the attachment of various ligands and chelators.<sup>[36]</sup> It was also demonstrated, that the physisorption of the water soluble polymer is irreversible even in acidic aqueous solutions due to the fact that the simultaneous disruption of all the binding interactions is energetically unfavored.

The procedure was transferred to the synthesis of PEI@Co/C hybrid material (**5**) and studied in more detail in order to synthesize materials for the subsequent deposition of Pd nanoparticles (Scheme 5). PEI with a molecular weight of approximately 10,000 was dissolved in DMF and stirred with the Co/C particles (**1**) for 24 h at room temperature. A second batch was heated to 100 °C for the same period to potentially induce the formation of covalent bonds with the carbon surface, which would further improve the stability of the nanocomposite. However, elemental microanalysis revealed a higher amount of carbon, hydrogen, and nitrogen for the nanocomposite **5a** synthesized at room temperature indicating a higher loading with poly-

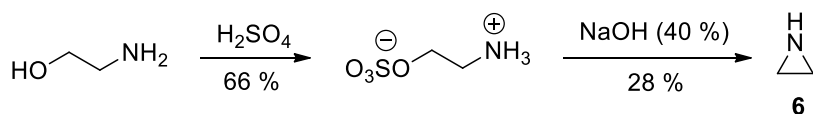


**Scheme 5.** Grafting of polyethylene imine (PEI) on Co/C nanobeads.

mer. This result was confirmed by TGA measurements.<sup>[30]</sup> For **5a** 2.7 wt% of polymer were determined and for **5b**, which was synthesized at 100 °C, 1.9 wt%, respectively.

Additional PEI desorption experiments were carried out stirring the hybrid material **5** in an acetate buffer (pH 3.5) for several hours in order to determine the stability of the PEI layers on the Co/C nanoparticles. While for **5a** a slight loss of polymer was detected, for **5b** only changes within the error margin were determined by nitrogen elemental analysis. Interestingly, after stirring with acetate buffer, both hybrid materials show almost the same polymer loading.

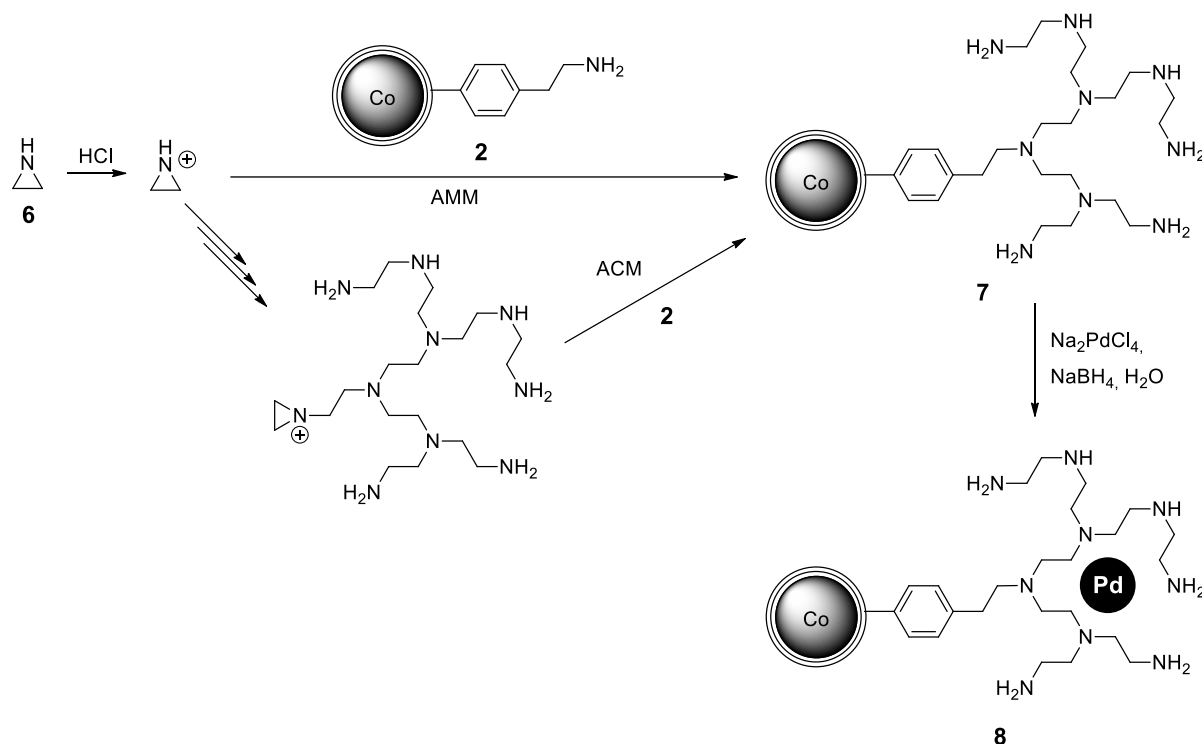
In parallel, the surface-initiated cationic polymerization of aziridine on amino-modified Co/C particles for the covalent attachment of PEI was investigated. Aziridine was prepared following a synthesis published in 1935 by Wenker (Scheme 6).<sup>[37]</sup> First,  $\beta$ -aminoethyl sulfuric acid was prepared by heating ethanolamine with an equimolar amount of sulfuric acid. In a second step distillation with a sodium hydroxide solution gave aziridine (**6**) in moderate yields.



1. **Scheme 6.** Wenker synthesis of aziridine (**6**).<sup>[37]</sup>

The as prepared aziridine was subsequently polymerized on the surface of Co/C particles functionalized with primary amines **2** (Scheme 7) adapting a procedure reported by Liu et al. for the grafting of PEI on amine-modified multiwalled carbon nanotubes (MWCTs).<sup>[38]</sup> Upon addition of catalytic amounts of HCl two mechanisms are feasible for the cationic polymerization, the activated monomer mechanism (AMM) or the activated chain mechanism (ACM).<sup>[39]</sup> Depending on the mechanism either protonated aziridine monomers or iminium ions generated at the terminus of propagation chains are transferred to the amino-groups on the surface of the magnetic nanobeads **2** (Scheme 7). Two batches of hybrid material (**7**) were synthesized by this pathway using 250 (**7a**) and 1000 (**7b**) equivalents of aziridine, respectively. 16.8 wt% polymer for **7a** and 59.7 wt% polymer for **7b** were determined by TGA analysis of the hybrid materials.<sup>[30]</sup> These observations were also underlined by the relative mass increase and the data obtained from elemental microanalysis. Both nanocomposites covalently functionalized with PEI by far exceed the hybrid materials

derived from PEI adsorption when it comes to polymer content, and the dendrimer-coated nanoparticles when it comes to organic content.



**Scheme 7.** Polymerization of aziridine (**6**) on amino-functionalized nanoparticles (**2**) and subsequent synthesis of Pd nanoparticles in the polymer layer. AMM = activated monomer mechanism, ACM = activated chain mechanism.

Therefore, the nanocomposite **7b** was chosen for the first tests of Pd incorporation and subsequent reduction to Pd nanoparticles. Particles **7b**, which are well dispersible in aqueous solutions, were stirred in water and the pH was adjusted to 6 in order to protonate the primary amines on the surface.<sup>[35]</sup> Next, an aqueous solution of sodium tetrachloropalladate ( $\text{Na}_2\text{PdCl}_4$ ) was added and the internalized Pd ions were subsequently reduced to Pd nanoparticles by addition of a sodium borohydride solution (Scheme 7). The resulting nanocatalyst **8** was readily separated from the reaction mixture by an external magnet due to the highly magnetic core, which overcompensates the high loading with polymer. Inductively coupled plasma optical emission spectrometry (ICP-OES) of **8** revealed a Pd loading of 0.67 mmol/g, which is in the range of Pd@Co/C nanoparticles (Chapter 5), but considerably lower than for similar Pd@Fe<sub>3</sub>O<sub>4</sub>-PEI particles (8 - 13 wt% Pd).<sup>[35]</sup>

The nanobeads **8** were successively applied for the hydrogenation of *trans*-stilbene, which has been proven to be a viable test reaction to probe the catalytic ac-

tivity of Pd nanoparticles (Chapter 5). At a catalyst loading of 0.5 mol%, which is rather high for Pd catalyzed hydrogenation reactions, only 26% conversion was determined by gas chromatographic analysis (GC) after two hours of reaction time using dodecane as internal standard. This results in a turn over frequency of  $26\text{ h}^{-1}$ , which is considerably lower than reported for Pd@Fe<sub>3</sub>O<sub>4</sub>-PEI particles ( $49\text{ h}^{-1}$ )<sup>[35]</sup> and more than a hundred times lower than the values obtained for Pd@Co/C catalysts (up to  $3845\text{ h}^{-1}$ , Chapter 5).

## 6.4 Conclusion and Outlook

The aim of this project was to coat Co/C nanoparticles with dendrimers or polymers to provide magnetic templates for the synthesis of highly active and well-stabilized Pd nanoparticles and their application in catalysis. In order to achieve this, several different methods and techniques were screened, all of them having specific advantages and disadvantages.

The stepwise synthesis of PAMAM dendrons on the surface of amino-functionalized Co/C nanoparticles allowed for easy purification after each coupling step by magnetic decantation and subsequent washing of the nanoparticles. However, it was not possible to generate a high loading of dendrimer on the nanoparticles and to unambiguously determine the loading. A higher loading might be achieved by using an even higher excess of reagents and reaction times of several days, however, this would drastically restrict the applicability of this functionalization strategy. An alternative could be the tethering of entire dendrons or even commercially available dendrimers to the nanoparticle surface. Problems associated with this method would be a potentially low loading due to steric repulsion and copper contamination when applying the “click”-reaction as ligation method.

The tethering of polymers to the surface seems to be a more straightforward and operationally simple method to achieve high loadings of organic material capable of stabilizing Pd nanoparticles. However, polymers lack the exactly defined structure of dendrimers and an exact characterization of the hybrid material is also challenging. In a first test, polyethylene imine was adsorbed onto the carbon surface of Co/C nanoparticles. Thermo gravimetric analysis revealed that a higher loading can be obtained when stirring at room temperature and desorption tests underlined the stability of the adsorbed PEI layer. A covalent attachment of PEI was also realized by cationic polymerization of aziridine on amino-functionalized Co/C beads. By varying the



amount of monomer the loading with polymer can be tuned and hybrid materials with 60 wt% polymer are amenable while the physisorption only allowed for a maximum of 3 wt% polymer. Subsequently, Pd nanoparticles were deposited in the hybrid material with the highest polymer content and applied in the hydrogenation of *trans*-stilbene showing only a moderate activity.

However, more tests are needed to determine the ideal hybrid material, which provides sufficient stabilization of deposited Pd nanoparticles without pronounced surface passivation. Additional tuning could be realized by modifying the end groups of the dendrimers and polymers, which also obsoletes the exact control of pH for the internalization of the Pd ions. Furthermore, the synthesized Pd nanoparticles have to be characterized in detail and the leaching of Pd has to be assessed to determine differences to Pd@Co/C particles lacking the dendrimer or polymer. Also, extended recycling studies are needed to evaluate the applicability of the novel hybrid materials.

## 6.5 Experimental Section

### Materials and methods

Co/C nanomagnets (**1**) were purchased from Turbobeats Llc, Switzerland. Prior to use, they were washed five times for 24 h in a concentrated HCl (Merck, puriss.)/deionized water (Millipore) mixture (1:1). Acid residuals were removed by washing with Millipore water (5x).<sup>[27]</sup> The magnetic nanobeads were dispersed using an ultrasound bath (Sonorex RK 255 H-R, Bandelin) and recovered with the aid of a 1.2 T neodymium-based permanent magnet (N42, S-30-15-N, Webcraft GmbH). They were characterized by elemental microanalysis (LECO CHN-900, ETH Zürich), thermogravimetric analysis (TGA, Perkin Elmer TGA7), ATR-IR spectroscopy (Biorad Excalibur FTS 3000, Specac Golden Gate), and inductively coupled plasma optical emission spectrometry (Spectro Analytical Instruments ICP Modula EOP,  $\lambda = 340$  nm).

<sup>1</sup>H NMR (400 MHz) spectra were recorded on a Bruker AC 400 spectrometer with CHCl<sub>3</sub> (7.26 ppm) as a standard. Gas chromatography was performed on a Fisons Instruments GC8000 equipped with a capillary (30 m x 250  $\mu$ m x 0.25  $\mu$ m) and flame ionization detector.

Polyethyleneimine (branched, 99 %, Mw 10000) was purchased from Polysciences Inc. Amino-modified Co/C nanoparticles (**2**)<sup>[26]</sup> and aziridine (**6**)<sup>[37]</sup> were prepared according to literature procedures. All other chemicals are commercially available and were used as received.

### General procedure for the titration of amino-modified Co/C nanoparticles<sup>[27]</sup>

The content of amino groups on the synthesized particles was quantitatively determined by back titration: In a typical example 20 mg of particles were stirred for 3 h in 2.0 mL of 0.01 M HCl aqueous solution using a 5 mL flask. The magnetic particles were separated by an external magnet, the solution filtered (syringe filter, pore size = 0.2  $\mu$ m) and 1.0 mL of the filtrate titrated with 0.01 M NaOH aqueous solution using phenolphthalein as a pH indicator.

**General procedure for the synthesis of PAMAM dendrons on the surface of magnetic Co/C nanoparticles**

In a flame-dried Schlenk flask 400 mg (0.15 mmol/g, 60  $\mu$ mol) of amino-modified Co/C nanoparticles (G0, **1**) were suspended in 3.3 mL of dry MeOH by sonication in an ultrasonic bath for 30 min. Methyl acrylate (272  $\mu$ L, 3 mmol) was added and the slurry heated at 50 °C for 20 h. After cooling to room temperature, the particles were separated by an external magnet. To wash the particles, they were re-suspended in 10 mL dry MeOH, stirred for 10 min, and collected again by a magnet. This procedure was repeated five times and the particles subsequently dried under vacuum to obtain 392 mg of Co/C nanoparticles functionalized with methyl ester moieties (G0.5).

**Elemental microanalysis** (%): C 9.45, H 0.24, N 0.18; 0.09 mmol/g;

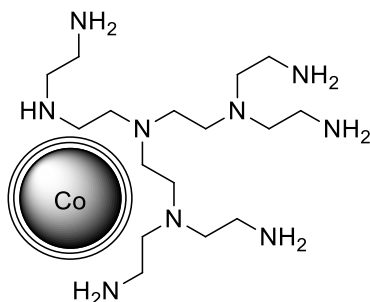
**IR** (ATR,  $\bar{\nu}$ /cm<sup>-1</sup>): 1738, 1591, 1499, 1433, 1368, 1200, 839; **TGA** (N<sub>2</sub>): 0.09 mmol/g.

In a second step, 367 mg of the dried material was suspended in dry MeOH by sonication for 30 min followed by the dropwise addition of ethylenediamine (461  $\mu$ L, 4.1 mmol). Thereafter, the mixture was heated at 50 °C for 20 h. The magnetic particles were recovered at room temperature by magnetic decantation, washed with dry MeOH (5 x 10 mL), and dried under vacuum to yield 373 mg of PAMAM-modified nanobeads (G1).

**Elemental microanalysis** (%): C 9.18, H 0.29, N 0.43.

The second generation of Co/C-PAMAM was prepared following the same manner, using a 50-fold excess of methyl acrylate and a 125-fold excess of ethylenediamine with respect to the amount of calculated amino groups.

## General procedure for grafting of PEI on the surface of Co/C nanoparticles



A solution of 6.66 g polyethylenimine (PEI, Mw 10000) in 100 mL dry DMF was prepared. Washed Co/C beads (**1**, 0.5 g) and 10 mL of dry DMF were introduced to a 100 mL flask and the slurry sonicated for 10 min. 50 mL of the PEI solution was added and the mixture stirred for 20 h at different temperatures. The particles were then collected by a magnet, washed with DMF (3 x 50 mL) and dried under vacuum for 5 h at 50 °C.

### PEI@Co/C (**5a**)

The general procedure for the grafting of PEI was applied stirring at room temperature for 20 h. 514 mg of functionalized particles **5a** were isolated.

**Elemental microanalysis (%)**: C 8.76, H 0.48, N 1.14; **TGA** (N<sub>2</sub>): 2.7 wt% polymer.

### PEI@Co/C (**5b**)

The general procedure for the grafting of PEI was applied stirring at 100 °C for 20 h. After drying, 512 mg of particles **5b** were obtained.

**Elemental microanalysis (%)**: C 8.74, H 0.39, N 1.05; **TGA** (N<sub>2</sub>): 1.9 wt% polymer.

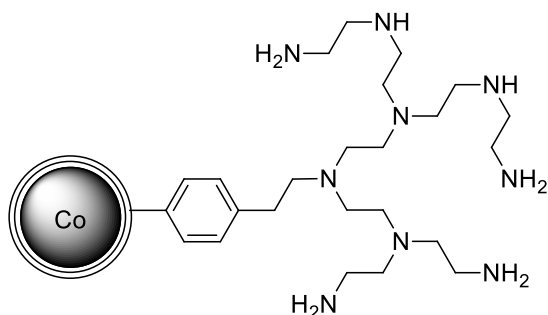
### PEI desorption experiments

The desorption of PEI was tested by adding 50 mg of PEI@Co/C particles and 50 mL of an acetate buffer (pH 3.5) to a 100 mL flask. The mixture was sonicated for 10 min and then vigorously stirred for 3 h. The particles were removed by a magnet, washed by re-suspending in H<sub>2</sub>O (3 x 20 mL) and acetone (3 x 20 mL), and subsequently dried at 50 °C for 6 h.

**PEI@Co/C (**5a**): elemental microanalysis (%)**: C 9.07, H 0.45, N 1.00;  $\Delta N = -0.14$ .

**PEI@Co/C (**5b**): elemental microanalysis (%)**: C 9.03, H 0.41, N 0.99;  $\Delta N = -0.06$ .

### General procedure for the polymerization of aziridine on the surface of amino-modified Co/C particles (**7**)



Co/C-NH<sub>2</sub> nanoparticles (**2**) were pre-dispersed in 10 mL of CH<sub>2</sub>Cl<sub>2</sub> in a 25 mL flask using an ultrasonic bath. Varying amounts of freshly distilled aziridine (250 – 1000 equiv.) were added to the slurry under stirring followed by HCl as catalyst. The mixture was heated to 80 °C for 24 h to form the Co/C-PEI **7**. The magnetic hybrid material was cooled to room temperature, separated by a magnet, and thoroughly washed with CH<sub>2</sub>Cl<sub>2</sub> (5 x 10 mL), water (3 x 10 mL), and CH<sub>2</sub>Cl<sub>2</sub> (3 x 10 mL). The particles were then dried for 8 h at 50 °C.

#### Co/C-PEI (**7a**)

PEI was polymerized on Co/C particles (100 mg, 0.15 mmol/g) according to the general procedure using 195 µL (3.75 mmol, 250 equiv.) of distilled aziridine and 4 µL HCl (12 M). After drying 112 mg of functionalized particles **7a** were isolated.

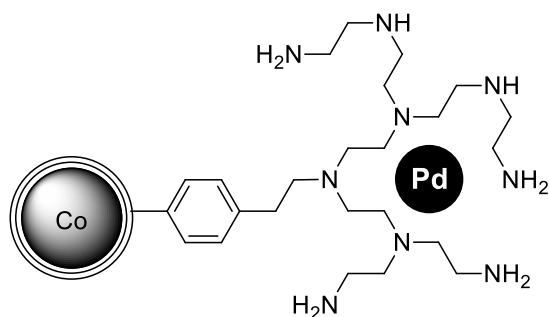
**Elemental microanalysis** (%): C 14.52, H 2.00, N 4.06; **TGA** (N<sub>2</sub>): 16.8 wt% polymer.

#### Co/C-PEI (**7b**)

The general procedure was repeated using 100 mg of Co/C particles (0.15 mmol/g), 778 µL (15 mmol, 1000 equiv.) of distilled aziridine, and 15 µL HCl (12 M). After drying 284 mg of functionalized particles **7b** were isolated.

**Elemental microanalysis** (%): C 28.69, H 5.30, N 13.27; **TGA** (N<sub>2</sub>): 59.7 wt% polymer.

## Synthesis of Pd nanoparticles in the cavities of Co/C-PEI beads (**8**)



Co/C-PEI beads (**7b**, 50 mg) were introduced to a 10 mL flask followed by 2 mL H<sub>2</sub>O. Upon stirring the pH was adjusted to 6 by the dropwise addition of an aqueous solution of HCl (1 M, ~ 50  $\mu$ L). An aqueous solution of Na<sub>2</sub>PdCl<sub>4</sub> (5 mL, 9.4 mM) was added and the slurry stirred for 1 h allowing the incorporation of the Pd ions into the polymer. The particles were then collected by a magnet and washed with H<sub>2</sub>O (3 x 5 mL) to remove excessive Na<sub>2</sub>PdCl<sub>4</sub>. To generate the Pd nanoparticles, a solution of 8.9 mg (0.24 mmol) NaBH<sub>4</sub> in 2.5 mL H<sub>2</sub>O was added dropwise upon vigorous stirring to control foaming. The reaction mixture was thereafter stirred for 30 min, the particles separated with the use of an external magnet and washed with H<sub>2</sub>O (5 x 5 mL), *i*PrOH (2 x 5 mL), and Et<sub>2</sub>O (3 x 5 mL). Drying under vacuum yielded 42 mg of magnetic catalyst **8**.

**ICP-OES:** 0.67 mmol Pd/g.

### Hydrogenation of *trans*-stilbene using Pd@Co/C-PEI

To a schlenk tube Pd@Co/C-PEI nanoparticles **8** (3.4 mg, 0.5 mol% Pd, 2.3  $\mu$ mol), *trans*-stilbene (90.1 mg, 0.5 mmol) and *i*PrOH (5 mL) were introduced. Dodecane (114  $\mu$ L, 0.5 mmol) was added as internal standard and the mixture sonicated in an ultrasonic bath for 10 min. The tube was evaporated and flushed with H<sub>2</sub> several times followed by vigorous stirring under 1 atm H<sub>2</sub> (balloon). The progress of the reaction was monitored by GC at the following conditions: 3 min at 140 °C, then 20 °C/min to 300 °C; Retention time: Dodecane (3.53 min), 1,2-diphenylethane (7.70 min), *trans*-stilbene (9.42 min).

➔ Please find supporting information including TGA data on the enclosed CD.

## 6.5 References

- [1] a) A. Roucoux, J. Schulz, H. Patin, *Chem. Rev.* **2002**, *102*, 3757–3778; b) D. L. Feldheim, C. A. Foss, *Metal nanoparticles. Synthesis, characterization, and applications*, Marcel Dekker, New York, **2002**.
- [2] D. Astruc, F. Lu, J. R. Aranzaes, *Angew. Chem. Int. Ed.* **2005**, *44*, 7852–7872.
- [3] R. Andrés, E. de Jesús, J. C. Flores, *New J. Chem.* **2007**, *31*, 1161.
- [4] M. Zhao, L. Sun, R. M. Crooks, *J. Am. Chem. Soc.* **1998**, *120*, 4877–4878.
- [5] L. Balogh, D. A. Tomalia, *J. Am. Chem. Soc.* **1998**, *120*, 7355–7356.
- [6] R. M. Crooks, M. Zhao, L. Sun, V. Chechik, L. K. Yeung, *Acc. Chem. Res.* **2001**, *34*, 181–190.
- [7] a) R. W. J. Scott, O. M. Wilson, R. M. Crooks, *J. Phys. Chem. B* **2005**, *109*, 692–704; b) V. S. Myers, M. G. Weir, E. V. Carino, D. F. Yancey, S. Pande, R. M. Crooks, *Chem. Sci.* **2011**, *2*, 1632; c) L. M. Bronstein, Z. B. Shifrina, *Chem. Rev.* **2011**, *111*, 5301–5344.
- [8] Y. Niu, L. K. Yeung, R. M. Crooks, *J. Am. Chem. Soc.* **2001**, *123*, 6840–6846.
- [9] G. R. Newkome, Z. Yao, G. R. Baker, V. K. Gupta, *J. Org. Chem.* **1985**, *50*, 2003–2004.
- [10] E. Buhleier, W. Wehner, F. Vögtle, *Synthesis* **1978**, *1978*, 155–158.
- [11] R. M. Crooks, B. I. Lemon, L. Sun, L. K. Yeung, M. Zhao in *Topics in Current Chemistry* (Ed.: F. Vögtle), Springer Berlin Heidelberg, Berlin, Heidelberg, **2001**.
- [12] M. Zhao, Y. Liu, R. M. Crooks, D. E. Bergbreiter, *J. Am. Chem. Soc.* **1999**, *121*, 923–930.
- [13] a) Jansen, J. F. G. A., de Brabander-van den Berg, E. M. M., E. W. Meijer, *Science* **1994**, *266*, 1226–1229; b) A. W. Bosman, H. M. Janssen, E. W. Meijer, *Chem. Rev.* **1999**, *99*, 1665–1688.
- [14] a) K. Esumi, A. Suzuki, N. Aihara, K. Usui, K. Torigoe, *Langmuir* **1998**, *14*, 3157–3159; b) L. H. Hanus, K. Sooklal, C. J. Murphy, H. J. Ploehn, *Langmuir* **2000**, *16*, 2621–2626; c) K. Esumi, A. Suzuki, A. Yamahira, K. Torigoe, *Langmuir* **2000**, *16*, 2604–2608.
- [15] V. Chechik, M. Zhao, R. M. Crooks, *J. Am. Chem. Soc.* **1999**, *121*, 4910–4911.
- [16] R. W. J. Scott, H. Ye, R. R. Henriquez, R. M. Crooks, *Chem. Mater.* **2003**, *15*, 3873–3878.
- [17] V. Chechik, R. M. Crooks, *J. Am. Chem. Soc.* **2000**, *122*, 1243–1244.
- [18] E. H. Rahim, F. S. Kamounah, J. Frederiksen, J. B. Christensen, *Nano Lett.* **2001**, *1*, 499–501.
- [19] M. Ooe, M. Murata, T. Mizugaki, K. Ebitani, K. Kaneda, *Nano Lett.* **2002**, *2*, 999–1002.
- [20] M. Zhao, R. M. Crooks, *Angew. Chem. Int. Ed.* **1999**, *38*, 364–366.
- [21] a) L. K. Yeung, C. T. Lee Jr., K. P. Johnston, R. M. Crooks, *Chem. Commun.* **2001**, 2290–2291; b) L. K. Yeung, R. M. Crooks, *Nano Lett.* **2001**, *1*, 14–17.
- [22] Y. Li, M. A. El-Sayed, *J. Phys. Chem. B* **2001**, *105*, 8938–8943.
- [23] S.-K. Oh, Y. Niu, R. M. Crooks, *Langmuir* **2005**, *21*, 10209–10213.
- [24] a) A. Beezer, A. King, I. Martin, J. Mitchel, L. Twyman, C. Wain, *Tetrahedron* **2003**, *59*, 3873–3880; b) L. Han, R. Huang, S. Liu, S. Huang, C. Jiang, *Mol. Pharmaceutics* **2010**, *7*, 2156–2165.
- [25] R. Abu-Reziq, H. Alper, D. Wang, M. L. Post, *J. Am. Chem. Soc.* **2006**, *128*, 5279–5282.
- [26] M. Zeltner, R. N. Grass, A. Schaetz, S. B. Bubenhofer, N. A. Luechinger, W. J. Stark, *J. Mater. Chem.* **2012**, *22*, 12064–12071.
- [27] a) N. Tsubokawa, K. Kobayashi, Y. Sone, *Polym. J.* **1987**, *19*, 1147–1155; b) N. Tsubokawa, T. Iida, T. Takayama, *J. Appl. Polym. Sci.* **2000**, *75*, 515–522.
- [28] A. Schätz, R. N. Grass, W. J. Stark, O. Reiser, *Chem. Eur. J.* **2008**, *14*, 8262–8266.
- [29] Q. M. Kainz, R. Linhardt, P. K. Maity, P. R. Hanson, O. Reiser, *ChemSusChem* **2013**, *6*, 721–729.
- [30] See supporting information.
- [31] a) C. W. Tornøe, M. Meldal in *American Peptide Symposium* (Eds.: M. Lebl, Houghten R. A.), American Peptide Society, Kluwer Academic Publishers, San Diego, CA, **2001**; b) C. W. Tornøe, C. Christensen, M. Meldal, *J. Org. Chem.* **2002**, *67*, 3057–3064; c) V. V. Rostovtsev, L. G. Green, V. V. Fokin, K. B. Sharpless, *Angew. Chem. Int. Ed.* **2002**, *41*, 2596–2599.
- [32] Q. M. Kainz, A. Schätz, A. Zöpfl, W. J. Stark, O. Reiser, *Chem. Mater.* **2011**, *23*, 3606–3613.
- [33] Y.-J. Lin, B.-K. Tsai, C.-J. Tu, J. Jeng, C.-C. Chu, *Tetrahedron* **2013**, *69*, 1801–1807.
- [34] M. V. Vasylyev, G. Maayan, Y. Hovav, A. Haimov, R. Neumann, *Org. Lett.* **2006**, *8*, 5445–5448.

- [35] A. J. Amali, R. K. Rana, *Green Chem.* **2009**, *11*, 1781.
- [36] a) R. Fuhrer, I. K. Herrmann, E. K. Athanassiou, R. N. Grass, W. J. Stark, *Langmuir* **2011**, *27*, 1924–1929; b) F. M. Koehler, M. Rossier, M. Waelle, E. K. Athanassiou, L. K. Limbach, R. N. Grass, D. Günther, W. J. Stark, *Chem. Commun.* **2009**, 4862–4864.
- [37] H. Wenker, *J. Am. Chem. Soc.* **1935**, *57*, 2328.
- [38] Y. Liu, D.-C. Wu, W.-D. Zhang, X. Jiang, C.-B. He, T. S. Chung, S. H. Goh, K. W. Leong, *Angew. Chem. Int. Ed.* **2005**, *44*, 4782–4785.
- [39] a) Y. Liu, H. Wang, C. Pan, *Macromol. Chem. Phys.* **1997**, *198*, 2613–2622; b) H. Petersen, A. L. Martin, S. Stolnik, C. J. Roberts, M. C. Davies, T. Kissel, *Macromolecules* **2002**, *35*, 9854–9856.



## E List of Abbreviations

AES	atomic emission spectroscopy	FT	fourier transformation
AIBN	azobisisobutyronitrile	h	hour
APTMS	(3-aminopropyl)triethoxysilane	HEPES	2-[4-(2-hydroxyethyl)piperazin-1-yl]ethanesulfonic acid
ATR	attenuated total reflection	HOBt	1-hydroxybenzo-triazole
Boc	<i>tert</i> -butoxycarbonyl	HRMS	high-resolution mass spectrometry
BODIPY	boradiazaindacene	IBX	2-iodoxybenzoic acid
cat	catalyst	ICP	inductively coupled plasma
CNT	carbon nano tube	IR	infrared spectroscopy
Co/C	carbon coated cobalt nanoparticles	mAmine	magnetic amine resin
CuAAC	copper-catalyzed azide/alkyne cycloaddition	mBER	magnetic borohydride exchange resin
CVD	chemical vapor deposition	Me	methyl
d	day, diameter	mIBX	magnetic IBX resin
DEAD	diethyl azodicarboxylate	min	minute
DIAD	diisopropyl azodicarboxylate	MNP	magnetic nanoparticle
DIPEA	<i>N,N</i> -diisopropylethyl-amine	MoM	monomer-on-monomer
DMAP	4-dimethylaminopyridine	MS	mass spectroscopy
DMF	dimethylformamide	MW	microwave
DMSO	dimethylsulfoxide	mWang	magnetic Wang aldehyde resin
DVB	1,4-divinylbenzene	Nb	norbornyl
EDC	1-ethyl-3-(3-dimethylaminopropyl)carbodiimide	NHC	<i>N</i> -heterocyclic carbene
EDTA	ethylenediaminetetraacetic acid	NHS	<i>N</i> -hydroxysuccinimide
EDX	energy-dispersive X-ray spectroscopy	NIPAM	<i>N</i> -isopropylacrylamide
EtOAc	ethylacetate	NMDG	<i>N</i> -methyl-d-glucamine
Emu	electromagnetic unit	NMR	nuclear magnetic resonance
ESI	electrospray ionization	NP	nanoparticle
equiv.	equivalent	OBEAD	oligomeric benzylethyl azodicarboxylate
Et	ethyl	OES	optical emission spectroscopy
FAD	flavin adenine dinucleotide	OTPP	oligomeric triphenylphosphine
Fe/C	carbon coated iron nanoparticles	Oxone	2KHSO <sub>5</sub> ·KHSO <sub>4</sub> ·K <sub>2</sub> SO <sub>4</sub>
		PAMAM	poly(amidoamine)

PEI	polyethylene imine	T	temperature
Ph	phenyl	TBTU	O-(benzotriazol-1-yl)- <i>N,N,N'</i> , <i>N'</i> -tetramethyluronium tetra fluoroborate
PoP	polymer-on-polymer	TEM	transmission electron micros copy
ppb	parts per billion	TEMPO	2,2,6,6-Tetramethyl piperi- dine-1-oxyl
PPh	triphenyl-phosphine	TEOS	tetraethoxysilane
PS	polystyrene	TFA	trifluoroacetic acid
quant.	quantitative	THF	tetrahydrofurane
R	arbitrary rest	TLC	thin layer chromatography
RT	room temperature	TOF	turn over frequency
ROMP	ring-opening metathesis polymerization	UV	ultra violet
s	second	VBC	vinylbenzene chloride
SN <sub>Ar</sub>	nucleophilic aromatic substitu tion	Vis	visible (light)
SPE	solid phase extraction	X	arbitrary anion
SPION	superparamagnetic iron oxide nanoparticles	XRD	X-ray powder diffraction
SPOS	solid-phase organic synthesis		
<sup>t</sup> Bu	tert-butyl		

## F Curriculum Vitae

### Quirin Kainz

University of Regensburg  
Institute of Organic Chemistry  
Universitätsstrasse 31  
93053 Regensburg  
Phone: +49 170 5450643  
E-Mail: quirin.kainz@chemie.uni-regensburg.de

### Personal Data

---

Date and place of birth	August 23, 1985, Dachau
Nationality	German

### Education

---

since 10/2010	Doctoral studies in the group of Prof. Dr. Oliver Reiser, University of Regensburg, as a fellow of the German National Academic Foundation (Studienstiftung des Deutschen Volkes e.V.)
10/2011 – 12/2011	Research stay at the <i>Functional Materials Laboratory (FML)</i> in the group of Prof. W. J. Stark at ETH Zürich, Switzerland
10/2010 – 12/2010	Research stay in the group of Prof. P. R. Hanson at the University of Kansas, Lawrence, USA
09/2010	Master of Science (M.Sc.) in chemistry
01/2010 – 09/2010	Master thesis in the research group of Prof. Dr. Oliver Reiser: “ <i>Covalent and non-covalent coating of magnetic nanoparticles for biological applications</i> ”
09/2008	Bachelor of Science (B.Sc.) in chemistry

03/2008 – 06/2008	Bachelor thesis in organic chemistry on: <i>“Julia-Kocienski olefination of <math>\gamma</math>-butyrolactone derivatives”</i>
10/2005 – 09/2010	Studies in chemistry at the University of Regensburg, Germany
06/2005	Abitur (University entrance diploma), Schyren-Gymnasium Pfaffenhofen, Germany

### Professional Experience

---

since 10/2010	Research Assistant, Institute of Organic Chemistry, University of Regensburg Supervision of undergraduate students in advanced lab courses
06/2008 – 09/2009	Scientific assistant, supervisor of internships and lecturer in organic chemistry for medical students at the Department of Analytical Chemistry, University of Regensburg, Germany
03/2007 – 04/2007	Industrial placement: <i>“Development and validation of a new photochemical method for multi-component analysis”</i> , Daiichi Sankyo Europe GmbH, Pfaffenhofen, Germany

## List of Publications

---

- Q. M. Kainz, O. Reiser, *Acc. Chem. Res.* **2013**, *submitted*:  
*“Polymer and Dendrimer-Coated Magnetic Nanoparticles as Versatile Supports for Catalysts, Scavengers, and Reagents”*
- Q. M. Kainz, R. Linhardt, R. Grass, G. Vilé, J. Pérez-Ramírez, W. J. Stark, O. Reiser, *Adv. Funct. Mat.* **2013**, *submitted*:  
*“Palladium Nanoparticles Supported on Magnetic Carbon-Coated Cobalt Nanobeads – Highly Active and Recyclable Catalysts for Alkene Hydrogenation”*
- Q. M. Kainz, M. Zeltner, M. Rossier, W. J. Stark, O. Reiser, *Chem. Eur. J.* **2013**, *19*, 10038–10045:  
*“Do it Magnetic: Synthesis of Tri-substituted Ureas by a Multi-step Sequence Utilizing Recyclable Magnetic Reagents and Scavengers”*
- Q. M. Kainz, R. Linhardt, P. K. Maity, P. R. Hanson, O. Reiser, *ChemSusChem* **2013**, *6*, 721-729:  
*“Ring-Opening Metathesis Polymerization-based Recyclable Magnetic Acylation Reagents”*
- Q. M. Kainz, A. Späth, S. Weiss, A. Schätz, W. J. Stark, B. König, O. Reiser, *Chem. Open* **2012**, *1*, 125–129:  
*“Magnetic Nanobeads as Support for Zinc(II)-Cyclen Complexes: Selective and Reversible Extraction of Riboflavin”*
- P. K. Maity, Q. M. Kainz, S. Faisal, A. Rolfe, T. B. Samarakoon, F. Z. Basha, O. Reiser, P. R. Hanson, *Chem. Commun.* **2011**, *47*, 12524-12526:  
*“Intramolecular Monomer-on-Monomer (MoM) Mitsunobu cyclization for the Synthesis of Thiadiazepine-dioxides”*

- Q. M. Kainz, A. Schätz, A. Zöpfl, W. J. Stark, O. Reiser, *Chem. Mater.* **2011**, 23, 3606-3613:

*“Combined Covalent and Noncovalent Functionalization of Nanomagnetic Carbon-Surfaces with Dendrimers and BODIPY Fluorescent Dye”*

- Schätz, R. N. Grass, Q. Kainz, W. J. Stark, O. Reiser, *Chem. Mater.* **2010**, 22, 305-310:

*“Cu(II)-Azabis(oxazoline) Complexes Immobilized on Magnetic Co/C Nanoparticles: Kinetic Resolution of 1,2-Diphenylethane-1,2-diol under Batch and Continuous-Flow Conditions”*

## Oral Contributions

---

- Bayer Alumni Meeting, Berlin (Germany), March 06 2013: *“Magnetische Nanopartikel als Trägermaterialien für Katalysatoren und Reagenzien”*
- Falling Walls Lab & Conference, Berlin (Germany), November 08-09 2012: *“Breaking the Wall of Contamination”*
- GDCh-Wissenschaftsforum Chemie, Bremen (Germany), September 04-07 2011: *“Magnetic Scavengers and Reagents”*
- 5<sup>th</sup> Annual Workshop of the International Research Training Group CCROS, Freiburg (Germany), April 7-8 2011: *“Magnetic Catalysts”*

## Poster Contributions

---

- 126<sup>th</sup> International Summer Course at BASF, Ludwigshafen (Germany), August 2013: *“Polymer-Coated Magnetic Nanoparticles as Recyclable Tools for Organic Synthesis”*
- 18<sup>th</sup> European Symposium on Organic Chemistry, Marseille (France), July 08-09 2013: *“Synthesis of Tri-substituted Ureas by a Multi-step Sequence Utilizing Recyclable Magnetic Reagents and Scavengers”*
- ORCHEM, Weimar (Germany), September 24–26 2012: *„Recyclable Polymer Coated Magnetic Nanobeads”* → Poster prize
- 4<sup>th</sup> EuCheMS Chemistry Congress, Prague (Czech Republic), August 26–30 2012: *„Magnetic Nanoparticles as Recyclable Supports for Scavengers and Reagents”*
- Gordon Green Chemistry Conference, Lucca (Italy), July 22-27 2012: *“Recyclable Polymer Coated Magnetic Nanobeads”*; → Highlighted in: Q. Kainz, C. de Salas, S. Wesselbaum, H. Büttner, G. Wienhöfer, D. Munz, F. Stempfle, H. Kayser, *Nachrichten aus der Chemie* **2012**, 60, 1045–1046.
- 17<sup>th</sup> European Symposium on Organic Chemistry, Hersonissos (Greece), July 10-15 2011: *“Intramolecular Mitsunobu Reaction: Facile Purification Utilizing Magnetic Nanoparticles”*
- Heidelberg Forum of Molecular Catalysis, Heidelberg (Germany), July 22 2011: *“Utilizing ROMP on the Surface of Magnetic Nanoparticles”*
- 15<sup>th</sup> Annual Green Chemistry & Engineering Conference, Washington D.C. (USA), June 21-23 2011: *“Intramolecular Mitsunobu Reaction: Facile Purification Utilizing Magnetic Nanoparticles”*

## Academic References

---

### **Prof. Dr. Oliver Reiser**

Institut für Organische Chemie

Universität Regensburg, Universitätsstr. 31

93053 Regensburg, Germany

Phone: +49 - 941 - 9434631

Email: [oliver.reiser@chemie.uni-regensburg.de](mailto:oliver.reiser@chemie.uni-regensburg.de)

### **Prof. Dr. Paul Hanson**

Department of Chemistry

University of Kansas, 1251 Wescoe Hall Drive

Lawrence, KS 66045-7572, USA

Phone: +1 - 785 - 864 - 3094

Email: [phanson@ku.edu](mailto:phanson@ku.edu)

### **Prof. Dr. Wendelin J. Stark**

Institut für Chemie- und Bioingenieurwissenschaften

Department Chemie und Angewandte Biowissenschaften

ETH Zürich, Wolfgang-Pauli-Strasse 10

8093 Zürich, Switzerland

Phone: +41 - 44 - 6320980

E-mail: [wkstark@ethz.ch](mailto:wkstark@ethz.ch)



## G Acknowledgements

### University of Regensburg

First of all I would like to thank **Prof. Dr. Oliver Reiser** for offering me the possibility to work on this fascinating topic, for his guidance and continuous support, and for the interesting and fruitful talks during this study.

I am very grateful for the technical support provided by **Dr. Peter Kreitmeier**, **Georg Adolin**, **Klaus Döring**, **Helena Konkel** and **Roxane Harteis**. They did all kinds of jobs that made everyday life much easier. The same is true for our secretaries **Young Rotermund**, **Hedwig Ohli**, and **Antje Weigert**.

I am also obliged for the support of the central analytic department of the University of Regensburg.

Furthermore, I am especially grateful for the TGA-measurements performed by **Rainer Müller** (Kunz group), the XRD measurements conducted by **Florian Pielhofer** (Weihrich group), and the countless ICP-OES measurements carried out by **Joa-chim Rewitzer** (Wolfbeis group).

For the productive and homelike environment in the institute I have to thank all current and former members of the Reiser group. My special thanks to **Paul Kohls**, **Matthias Knorn**, **Sebastian Wittmann**, **Corinna Eichenseer**, **Andreas Kreuzer**, **Ludwig Pilsl**, **Karin Ulbrich**, **Andreas Okun**, **Daniel Rackl**, **Andreas Bergmann**, **Victor Kais** and **Soraia Fernandes** for their help with all kinds of daily problems and stimulating discussions.

I would like to thank my interns and Bachelor students **Thomas Bartelmann**, **Andreas Meyer**, **Christian Kaiser**, and **Martin Hofmann** for their engaged work in the lab and their fruitful input.

I am also grateful for the continuous support of my close friends from outside of the group **Dennis Kühbeck**, **Stefan Balk**, **Steffen Pockes**, and **Christian Wellner**.

My labmate **Roland Linhardt** deserves sincere thanks for his companionship and the good atmosphere in the lab during the three years.

## University of Kansas

Sincere thanks go to **Prof. Dr. Paul Hanson** for the admission to his group and for his enduring support with reference letters. Also, I would like to thank all group members of the Hanson group for their nice reception. Especially, the kindful help of **Moon Young Hur**, **Alan Rolfe**, **Pradip Maity**, and **Joanna Loh** has to be acknowledged.

## ETH Zürich

I have to thank **Dr. Alexander Schätz** for his continuous support, for the monthly advice on the telephone, for his hospitality in Zürich, for helping with the syntheses of the nanoparticles as well with their characterization and for proof-reading this thesis.

I also have to acknowledge the help of **Prof. Dr. Wendelin J. Stark** and **Dr. Robert N. Grass** as well as their generous donation of nanoparticles.

Furthermore, I am very grateful to **Martin Zeltner**, **Michael Rossier**, and **Roland Fuhrer** for the great time in Zurich and their continuous support. Also, I owe many thanks to Gianvito Vilé (Pérez-Ramírez group) and the analytical department of the ETH Zürich for their help with all kinds of special measurements and analyses.

## Financial Support

I truly appreciate the financial support provided by **Prof. Dr. Oliver Reiser** and the **German National Academic Foundation** (Studienstiftung des Deutschen Volkes e.V.) throughout the PhD period. Additional financial support was provided by the **Bayer Science & Education Foundation**, by the **German Chemical Society** (GDCh), and the **German Academic Exchange Service** (DAAD), which is also gratefully acknowledged.

*Den größten Dank schulde ich jedoch meiner Familie, besonders meinen Eltern und meiner Frau Ulla. Ohne Eure anhaltende Unterstützung in guten sowie schlechten Zeiten wären weder mein Studium noch diese Arbeit möglich gewesen.*